EXTENSIONAL FLOW BEHAVIOR OF TURBULENT
DRAG REDUCING POLYMER SOLUTIONS

BY

JAY ANDERSON SHANDS

A DISSERTATION PRESENTED TO THE GRADUATE
COUNCIL OF THE UNIVERSITY OF FLORIDA
IN PARTIAL FULFILLMENT OF THE REQUIREMENTS
FOR THE DEGREE OF DOCTOR OF PHILOSOPHY

UNIVERSITY OF FLORIDA

1985

ACKNOWLEDGEMENTS

TABLE OF CONTENTS

LIST OF TABLES

LIST OF FIGURES

viii

x

NOMENCLATURE

Symbol	Meaning	Page Number at First Usage in Text
a	radius of viscometer sphere	77
a_i	extensional deformation rates	40
A	constant, logarithmic velocity profile	14
$\hat{A}$	constant, friction law	104
b	particle radius	203
B	constant, logarithmic velocity profile	14
$\hat{B}$	constant, friction law	10
C	constant, conical channel head-discharge relation	65
d	annular width, viscometer	77
d_m	maximum annular width, viscometer	78
D	diameter of main experiment pipe	57
D_{ij}	components of deformation rate tensor	151
e	energy per unit mass	163
e_k	kinetic energy per unit mass	163
e_p	potential energy per unit mass	163
e_u	internal energy per unit mass	163
E	energy	161
f	friction factor	95
$\underline{\underline{F}}_t(s')$	relative deformation gradient tensor	197

xii

Symbol	Meaning	Page Number at First Usage in Text
ρ	mass density	14
τ	shear stress	78
τ_w	wall shear stress	14
τ_{ij}	components of deviatoric stress tensor	165
φ	angular coordinate	150
ϕ	volume concentration	203

Subscripts:

p	pertaining to polymer solution flow (with the exception of r_p and e_p)
w	pertaining to water flow (with the exception of τ_w)
s	pertaining to solvent values
a	actual measured values
i	inviscid flow values

Abstract of Dissertation Presented to the Graduate Council
of the University of Florida in Partial Fulfillment of the
Requirements for the Degree of Doctor of Philosophy

EXTENSIONAL FLOW BEHAVIOR OF TURBULENT
DRAG REDUCING POLYMER SOLUTIONS

By

Jay Anderson Shands

May 1985

Chairman: E.Rune Lindgren
Major Department: Engineering Sciences

Turbulent drag reduction by polymer addition may be
defined as the phenomenon by which drag in a turbulent
shear flow is reduced to below that for the solvent alone.
A popular hypothesis for this phenomenon is that polymer
addition leads to the suppression of turbulence production
by increasing fluid resistance to extensional deformations.
Large resistances to extensional deformations have been
observed in drag-reducing solutions; however, it is not yet
clear whether or not such viscoelastic effects are
essential to drag reduction. The purpose of this
investigation has been to further examine the extensional
behavior of such solutions and to determine if their

extensional characteristics are related to their drag-reducing abilities.

Conical channel rheometers, designed to conduct nearly shear-free flow at high extensional deformation rates (of the order of 1000-10,000 l/s), have been used to examine extensional flow behavior. Drag reduction has been measured using a pipe flow apparatus. Results are reported for aqueous polyacrylamide and polyethylene oxide solutions ranging in concentration from 1 to 45 ppm.

For the conical channel flows, head-discharge measurements have been expressed in terms of first normal stress differences and extensional strain rates. Comparisons are made with related experimental and theoretical results. Using conservation of energy principles, the energy transfer that occurs in a channel has been examined and an expression has been derived that relates first normal stress difference in a channel to the excess pressure drop (relative to solvent flow) occurring over the entire channel. Good agreement has been found with experiment. Two distinct types of non-Newtonian behavior have been observed: for the polyacrylamide solutions, pressure heads in the conical channels were lower than for corresponding water flows, while the polyethylene oxide solutions induced greater pressure heads. However, without regard to additive type, molecular weight grade, concentration, and mixing conditions, the solutions which exhibited the greater non-Newtonian effects

were found to be the more effective drag-reducers. Evidence that molecular interaction can play a significant role in both the drag reduction mechanism and in the generation of non-Newtonian effects in extensional flows is also reported.

CHAPTER I
INTRODUCTION

Turbulent drag reduction by polymer addition may be defined as the phenomenon by which drag in a turbulent shear flow is reduced to below that for the solvent alone. This lowering of turbulent resistance can often be considerable and may be achieved with very small amounts of polymer additive. For example, drag in turbulent shear flow can be reduced by as much as 80% through the addition of just a few parts per million of the more effective polymers.

Motivated in part by the enormous potential for industrial applications, this phenomenon has been extensively investigated during the past two decades. Even though many aspects of this phenomenon have been elucidated, the basic mechanism that is involved is still not well understood. Presently, the most widely accepted explanation attributes this phenomenon to the viscoelastic properties imparted to the fluid by the additives. In particular, many investigators have suggested that polymer addition leads to the suppression of turbulence production by increasing fluid resistance to extensional deformations. It has been established

1

that large resistances to extensional deformations can occur in drag-reducing solutions. However, it is not yet clear whether or not such viscoelastic effects are essential to drag reduction. To date, the experimental evidence has been inconclusive and seemingly contradictory in nature. The inability of investigators to establish conclusive results has arisen, in part, from experimental difficulties in adequately characterizing the extensional behavior of low concentration polymer solutions.

The goal of this dissertation is to further examine the extensional behavior of low concentration polymer solutions and to determine whether their extensional characteristics are related to their drag-reducing abilities.

Summary of Dissertation

In the remaining section of this chapter, the commercial and theoretical significance of drag reduction and polymer additive technology is discussed.

Background information pertinent to this dissertation is presented in Chapter II. First, the general features of drag reduction are briefly reviewed and possible explanations for this phenomenon are mentioned. The general characteristics of viscoelastic liquids are then discussed and the results of previous

investigations where both the viscoelastic and drag-reducing characteristics of polymer solutions have been measured are reviewed. Next, the general aspects of the extensional flow of viscoelastic liquids are discussed and the experimental techniques that have been used to examine such flows are briefly described. Lastly, some comments on the various techniques for measurement of the extensional characteristics of low concentration polymer solutions are made.

The approach used in this work was to conduct shear viscosity, extensional flow, and drag reduction measurements and then to examine the results for correlations. A series of polymer solutions subject to varied conditions of additive type, molecular weight grade, concentration, and mixing were used as the test solutions. The shear viscosity measurements were made using a sliding ball viscometer; the extensional behavior of the polymer solutions was characterized using conical channel rheometers; and drag reduction was determined using a pipe flow apparatus.

In Chapter III, the experimental apparatus and the additives used are described. Solution preparation procedures are also discussed.

The experimental results are presented in Chapters IV, V, and VI for the shear viscosity, drag reduction, and extensional flow measurements, respectively. The

general   format of these chapters is to first present   the
reasons   for selection of the experimental apparatus.   The
goals   and   scope of the measurements are then   presented
and   the   experimental and analytical procedures that   are
used   are discussed.   Lastly, the experimental results are
reported   and   where possible are compared   with   previous
theoretical and experimental results.

In Chapter VII, the correlations between the results
of   the   shear viscosity, drag reduction, and   extensional
flow measurements are examined.

In Chapter VIII, the results of this investigation
are   summarized and recommendations are made for continued
work.

Significance of the Problem

The phenomenon of drag reduction and the use of
polymer   additives have been of interest to   investigators
from both commercial and theoretical standpoints.

Commercially, the use of drag-reducing polymer
additives has been looked at for

1.   More economic transport of liquids over long
distances, e.g.   crude oil transport (Burger   et
al., 1982);

2.   Increasing the capacity of existing pipelines,
e.g.   handling peak storm sewer runoff (Sellin et
al., 1982);

3. Irrigation and firefighting applications (Union Carbide Corp., 1966; Fabula, 1971);

4. Reducing the hydrodynamic drag for marine vessels (Hoyt, 1972).

Polymer additives have also been examined for usage in non-drag-reducing applications. These include use in the hydraulic fracturing of oil fields (Melton and Malone, 1964), in high pressure jet cutting operations (duPlessis and Hashish, 1978), in hydraulic machines (Bilgen and Vasseur, 1977), in jet fuels as anti-misting agents (Peng and Landel, 1983), and in reducing atherosclerosis (Greene et al., 1980).

Theoretically, understanding drag reduction has proven to be a difficult task because both the nature of turbulence and the behavior of macromolecules in a solution are not well understood. Research on the interaction between the polymer molecules and the turbulence should not only produce information concerning drag reduction, but may also provide further insights into turbulence and into the rheology of polymer solutions.

CHAPTER II
LITERATURE REVIEW

Drag Reduction

Turbulent drag reduction by polymer additives may be defined as the phenomenon by which drag in turbulent shear flow of a polymer-additive solution is reduced to below that for the solvent alone. For the more effective additives, drag in turbulent shear flow may be reduced by as much as 80% through the addition of just a few parts per million of polymer. Drag reduction can also be observed in solutions containing fibrous substances and in some soap solutions; however, the most effective drag-reducing solutions result from the use of polymer additives.

One of the earliest reports of drag reduction may be attributed to Forest and Grierson, who in 1931 observed such an effect in wood pulp fiber suspensions (Zakin and Hunston, 1980a). However, it was not until 1949, through the work of Toms, that drag reduction was brought to the general attention of scientists. In his paper, Toms (1949) reported that unusually low friction coefficients could be obtained for pipe flow of polymethyl methacrylate in monochlorobenzene. Early

6

recognition of this phenomenon was also made by K.J. Mysels, who observed drag reduction in gasoline thickened with aluminum soaps during World War II (Agoston et al., 1954). Further recognition of the drag reduction phenomenon continued in the 1950's, when both Shaver and Merrill (1959) and Dodge and Metzner (1959) found during the study of non-Newtonian turbulent pipe flow, that anomalously low friction factors occurred for some of the liquids that they were using. Despite recognition of the phenomenon, research in the field did not really get started until the early 1960's, when the United States Office of Naval Research created a program to fund drag reduction work. Since that time, research in the field has flourished and much has been learned about the phenomenon. In the remainder of this section, some of the main features of drag reduction that have been elucidated will be briefly reviewed.

Main Features of Drag Reduction

Relevant polymer-solvent characteristics. The most effective drag-reducing additives are high molecular weight polymers which have a linear structure or are only moderately branched. Typically, macromolecules with molecular weights of greater than about 10^5 need to be present in a solution before it

becomes drag reducing. Further, in solutions prepared
with polymer samples having wide molecular weight
ranges (as is usually the case), Berman (1977a) and
Hunston and Reischman (1975) have demonstrated that the
primary contribution to drag reduction will be that
from the small percentage of the molecules having the
highest molecular weights.

Another important factor in drag reduction is
polymer conformation. Depending on the type of
solvent, polymer molecules will assume different
conformations. Generally, polymer molecules in
solutions at rest tend to form tangled coils. In good
solvents polymer-solvent interactions will be favored
over polymer-polymer interactions, while in poor
solvents, the opposite will be true. As a result,
polymer molecules in good solvents tend to be more
extended than in poorer solvents. Investigators have
found that the use of good solvents produces more
effective drag-reducing solutions than use of poor
solvents. For example, Hershey and Zakin (1967)
observed that polyisobutylene in a good solvent
(cyclohexane) could exhibit twice as much drag
reduction as when in a poorer solvent (benzene).

This effect is also commonly observed in poly-
electrolytes (charged polymers), whose conformations
will change in response to changes in their ionic

environment. An acidic environment causes them to be highly coiled, while they can be more extended in a alkaline environment. By varying pH levels, Parker and Hedley (1972), Kim et al. (1973), and Banijamali et al. (1974) have found increases in drag reduction in solvents of increasing alkalinity. Thus, it appears that extended polymer conformations are more suitable to drag reduction than more compact structures.

Mechanical properties of drag-reducing solutions. First, almost all macromolecular solutions exhibit a strain-rate-dependent shear viscosity. Usually, at low strain rates, the shear viscosity is constant, then as strain rates are increased, it decreases until sufficiently high strain rates are reached, at which point, it again approaches a constant (but lower) value. The magnitude of decrease of the shear viscosity can often be dramatic (of several orders of magnitude), even for solutions of low additive concentrations (e.g., see Darby, 1970). However, shear-thinning effects are generally not considered as being responsible for drag reduction. Drag reduction has been observed in many solutions whose shear viscosities (at the strain rates corresponding to the drag-reducing flow conditions) were nearly identical to that of their solvents.

Next, viscoelastic characteristics are often observed in concentrated macromolecular solutions. However, such characteristics have been difficult to observe in the less-concentrated solutions of interest in drag reduction. In fact, it has not been until recently (Morgan and Pannell, 1972; Balakrishnan, 1976) that viscoelastic effects could be measured at all for solutions at concentrations relevant to drag reduction. Viscoelasticity now seems to be a concomitant property of drag-reducing solutions; however, whether or not it plays a major role in the drag reduction mechanism is not known. In the following sections, viscoelasticity will be discussed in more detail.

Drag-reducing solutions also often have the ability to form thread-like filaments (Gordon et al., 1973) and they typically exhibit a "slippery to the touch" consistency. The exact mechanisms involved in these last two effects are also not well understood.

Gross aspects of drag reduction. Some of the gross aspects of drag-reducing behavior include the existence of threshold conditions for onset of the phenomenon, saturation effects, maximum drag reduction limits, and degradation effects. In the onset phenomenon, a certain flow condition must occur before drag reduction will become apparent. This onset often occurs after the flow is fully turbulent, although for

certain polymers (e.g., extended polyelectrolytes) at
sufficiently high concentrations, there will not be an
onset in the turbulent regime. Instead, there will be
some sort of direct transition from laminar to
turbulent drag-reducing flow. In the former case,
investigators have recognized that the threshold
condition for onset represents the start of some
significant interaction between the macromolecules and
the turbulent motions of the flow. This interaction
should occur when some certain turbulence scales are of
the same order of magnitude as some corresponding
molecular scales. Length scales, time scales, and
energy scales have been examined, and presently, most
investigators favor the time scaling hypothesis (Tulin,
1980). An example of the experimental support for this
hypothesis may be found in the work by Berman (1977b).
By the addition of various amounts of glycerine to
polyethylene oxide-water and polyacrylamide-water
solutions, he was able to create solutions whose
macomolecules experienced different degrees of coiling,
and hence, different characteristic time scales. It
was found that that increased amounts of glycerine
delayed the onset of drag reduction to larger time
scales and that these results correlated well with
predictions of increased molecular relaxation times
using molecular (Zimm-Rouse) theory. Although the time

scaling hypothesis is widely accepted, it should also be noted that predictions of characteristic molecular time scales do not always correlate well with experimentally measured onset flow time scales. In a recent study of onset conditions for samples of polystyrene in different solvents, Zakin and Hunston (1980b) found that the molecular time scales correlated differently with the flow time scales, depending on the solvent type. In poor solvents, the ratios of molecular to flow time scales at onset were nearly constant for over a wide range of concentrations for several different solvents. However, in good solvents, this same ratio was significantly larger and exhibited a concentration dependence. Zakin and Hunston attributed these deviations, in part, to failure of rheological theories to correctly predict molecular relaxation times.

In another gross feature of the drag reduction phenomenon, limits exist as to the extent of drag reduction that a given polymer solution can attain. First, drag reduction will increase with concentration, until at some point a saturation level is reached, after which further increases in concentration will not result in increases in drag reduction. The concentration required to reach this saturation level will depend on the properties of the polymer solution

and on the flow geometry. Secondly, a maximum drag reduction limit exists, which is independent of polymer solution properties. At this second limit, the flow will consist primarily of large motions and will barely resemble turbulent flow at all (Rollin and Seyer, 1972). The level of drag reduction at this limit will correspond to about 80% of that which could be achieved if the flow were completely laminar (Hoyt, 1972).

Another important feature of the drag reduction phenomenon is the break-up (degradation) of the long chain polymer molecules into chains of shorter lengths. The primary form of such degradation is due to shearing forces, although both chemical and thermal degradation can also occur. As a result of scission of the macromolecules, the molecular weight distribution will change. The main effect appears to be a shift of this distribution to lower molecular weight values with the shape of the distribution undergoing relatively little change (Zakin and Hunston, 1980b). Typically, with increasing shear degradation, drag reducing ability will decrease. This is due to the decrease of the number of molecules having sufficient molecular weight to contribute to drag reduction. However, it should be noted that increased degradation does not always decrease drag reduction, but sometimes can lead to increased drag reduction (e.g., see Chang and Darby,

1983).   In   such   cases, it is   postulated   that   even
though the drag reduction contribution from the highest
molecular weight molecules is diminished, increased
drag   reduction   results   from   lowered   viscous   losses
resulting from the scission of the lower molecular
weight molecules (which leads to lower levels of shear
viscosity).

      Turbulent Flow Structure. The flow structure of a
turbulent   drag-reducing   flow   will   often   vary
substantially from that of a non-drag-reducing flow.
Mean velocity profiles, turbulence intensities, and
organized turbulent motions in the flow are all
altered.   In   fully developed wall-bounded turbulent
flows of   non-drag-reducing   liquids,   a   universal
nondimensional velocity is observed. Near the wall,
this profile is composed of three regions: a viscous
sublayer, where $u^+ = y^+$ for $0 < y^+ < 7$;   a   turbulent
region, where u^+ = A $\log(y^+)$ + B, for $30 < y^+$ and
$y/\delta < 0.15$; and an interactive or buffer region between
them.   In   the   above   equations, u^+ is   the
dimensionless   velocity $(u^+ = U/u_*)$, y^+ is   the
dimensionless distance from the wall $(y^+ = yu_*/\nu)$,
U is the average flow velocity at a distance y from the
wall, u_* is the friction velocity $(u_* = ((\tau_w/\rho)^{1/2})$,
τ_w is the wall shear stress, δ is the boundary layer
thickness, ρ is the mass density, and ν is the

kinematic viscosity. For Newtonian liquids, A and B are constants having values of 2.5 and 5.6, respectively. In a drag-reducing flow, the viscous sublayer profile remains unchanged. The logarithmic region is also observed; however, it is usually displaced to higher velocity levels, causing a thickening of the buffer region. Generally, investigators have found that the logarithmic profile in the drag-reducing flows may be expressed as $u^+ = A \log(y^+) + B + \Delta B$, where ΔB is an additional constant representing the thickening of the buffer region and where the original constants A and B remain unchanged. Such behavior indicates that the observed differences between drag-reducing and Newtonian flow are contained in the buffer region. With increases in drag reduction, the buffer layer also increases. For pipe flow, it has been suggested that the condition of maximum drag reduction corresponds to the point where the expanding buffer layer reaches the middle of the pipe (Berman, 1978).

As a measure of the intensity of turbulence, investigators determine the root-mean-square values of the fluctuations of the flow velocity components. In a wall-bounded turbulent flow of a Newtonian liquid, streamwise turbulent intensities are found to increase with distance from the wall, reach a peak in the buffer region at about $y^+ = 15$, and then decrease as the

middle of the pipe is approached. The transverse intensities are found to gradually increase from the wall to the middle of the pipe without passing through a peak and they are of a lower magnitude than the streamwise intensities. For drag-reducing flows, the peak of intensities in the streamwise direction still exists, but occurs further away from the wall. Some measurements (see Virk, 1975) indicate that these intensities can reach larger values than in Newtonian flows; however, Berman (1978) notes that this is uncertain. Measurements of transverse intensities indicate similar behavior as for Newtonian flows (with the magnitudes being slightly lower); but again, it has been stated that the measurements have not been sufficiently accurate to determine any trends (Berman, 1978).

In a turbulent boundary layer, the flow has been observed to be composed of highly organized motions. These motions, often called coherent structures, can be significantly altered in drag-reducing flows, particularly in the near wall region. For a detailed summary of the general characteristics of these motions in Newtonian flows, the reader is referred to the review by Cantwell (1981). Briefly, for a Newtonian flow, the dominant structures in the viscous sublayer are fluctuating, counter-rotating pairs of vortices.

These vortices densely cover all parts of the wall and average about $1000u_*/\nu$ in streamwise length with their width being about $100u_*/\nu$. Interaction between these structures and motions in the outer region away from the wall occurs through a sequence of events called bursting. In this sequence, a gradual outflow of liquid occurs as low momentum fluid is swept up into streaks between the counter-rotating vortices. This is then followed by lift-up of the streaks, sudden oscillation, and break-up into intense small scale motions, which are ejected into the outer regions of the flow. An inrush of liquid, of velocity greater than the mean, then occurs and the retarded flow left by the ejection event is swept away. It has been suggested that this higher speed liquid has a vortex ring like structure (Falco and Wiggert, 1980). As this vortex ring approaches and interacts with the wall, counter-rotating vortices in the sublayer will again appear and the entire process will continue. Now, for a drag-reducing flow, this same sequence of events is observed, but the frequency of events is diminished and the spacing of the streaks is increased when compared to that for a Newtonian liquid at similar mass flow rates. Further, when the comparison is made after non-dimensionalization with the wall parameters (u_*, ν), the streak spacing is found to increase with increasing

drag reduction; streak streamwise lengths are found to be longer, but bursting periods appear to remain the same as for Newtonian flow. In general, the structure in a drag-reducing flow is one of supressed small scale motions and enhanced large scale motions. For more specific results, the reader is referred to the research papers by Eckelman et al. (1972), Donohue et al. (1972), Reischman and Tiederman (1975), Achia and Thompson (1974), Oldaker and Tiederman (1977), Mizushina and Usui (1977), and Falco and Wiggert (1980).

Polymer Interactions. Whether the combined effects of isolated molecules cause drag reduction, or whether multimolecular structures are responsible for drag reduction is a controversial topic. As support for the belief that isolated molecules are responsible for drag reduction, it has been pointed out that drag reduction can occur at very low concentrations (of less than a ppm), where the distances between individual macromolecules would be so great as to make it unlikely that molecular interaction would occur. To determine whether a solution is dilute enough so that interactions are not likely to occur, investigators have made calculations of the volume occupied by the polymer molecules by replacing each molecule with an equivalent hydrodynamic sphere, having a radius equal

to the rms radius of gyration of the molecule. Now if the volume fraction occupied by these spheres is larger than unity, then molecular interactions are expected to occur, and conversely, for volume fractions significantly less than one, the occurence of interactions is less likely. Early investigators found that drag reduction could occur for solutions having polymer volume fractions as low as 0.01 (Merrill et al., 1966), which therefore led to the assumption that the effects of interactions were negligibly small. However, Fabula and co-workers (1966) noted that such low volume concentrations do not necessarily mean that coil entanglement is unimportant. In a turbulent shear flow, the polymer molecules should be expected to be tumbling and elongated, thus, still possibly allowing frequent contact and interactions to occur. Further, Fabula et al. suggested that the individual macromolecular coils are too small to interfere with the turbulent structure in a particulate manner. For example, Virk et al. (1966), in a summary of available data for various polymer-solvent combinations, found that at onset to drag reduction, the ratios of the rms end to end lengths of the macromolecular coils to the turbulent length scales (u^*/ν) ranged from 0.0015 to 0.1145. That is, the turbulent motions were some 200 to 600 times larger than the molecular dimensions at

onset. Such a large size discrepancy between the molecules and the turbulent length scales led Fabula to suggest that macromolecular entanglements are an essential feature of drag reduction. However, more evidence arose that seemed to justify the consideration of the hypothesis that isolated molecules are responsible for drag reduction, when both Virk (1966) and Paterson and Abernathy (1970) reported measurements which indicated the possible existence of intrinsic levels of drag reduction. They observed that for decreasing concentration (at low concentrations), that the amount of drag reduction divided by the concentration (the specific drag reduction) approached a constant value. Such a result has two implications. First, it implies that drag reduction exists at infinite dilutions, and secondly, it implies that molecular interactions are insignificant. If molecular interaction were to be significant, then one would expect, for example, that a doubling of the concentration (at low concentrations) would more than double the amount of drag reduction (Lumley, 1973). In this case, the specific drag reduction would decrease with concentration, not approach a constant value as Virk (1966) and Paterson and Abernathy (1970) found. However, Paterson and Abernathy note that large errors can occur in the measurements of low values of drag

reduction and they caution that further experiments are necessary to firmly establish this result.

More recently, experimentalists have found evidence of interaction, by observing the existence of multimolecular structures. Stenborg, Lagerstedt, and Lindgren (1977b) have directly observed polymer agglomerations in drag-reducing flows through both a Schlieren set-up and a microscope. Ouibrahim (1977) has presented photographs, showing network structures for solutions having additive concentration as low as 10 ppm. Through use of electron microscopes, Dunlop and Cox (1977) and James and Saringer (1980) have also presented photographs of multimolecular structures. However, such direct evidence of molecular interaction does not necessarily mean that they are essential for drag reduction.

More recently, experimental evidence indicating that interactions can affect the mechanism of drag reduction has been reported (Berman, 1978, 1980). Of particular interest, is the fact that Berman (1978) reports that specific drag reduction can decrease with concentration and not approach a constant value, in contrast to the earlier work of Virk (1966) and Paterson and Abernathy (1970). This would be expected if interactions were to affect drag reduction. In summary, it is now clear that clusters of

macromolecules exist in drag reducing solutions; however, whether or not molecular interactions play an essential role in drag reduction has not yet been clearly determined.

In this section, some of the main features of the drag reduction phenomenon have been briefly discussed. As mentioned earlier, research in this field has been extensive and the discussion presented here represents only a few of the highlights of such endeavors. For more extensive reviews of the work in this field, the reader is referred to the reviews by Lumley (1969, 1973), Patterson et al. (1969), Hoyt (1972, 1974, 1977), Virk (1975), Little et al. (1975), Berman (1978), and Sellin et al. (1982). Literature surveys of work in this field have also been published by Granville (1976, 1979, 1980, 1981).

Theories of Drag Reduction

The earliest explanation of drag reduction is attributed to Oldroyd (1949), who suggested that this phenomenon is the result of wall effects. He envisoned that the wall would constrain the rotation of the polymer molecules, which would somehow lead to an abnormally mobile laminar sublayer, and hence, slip would effectively occur at the wall. Other early explanations of the phenomenon are that drag reduction results from

shear-thinning effects (Shaver and Merrill, 1959); delay
of laminar to turbulent transition (Savins, 1964);
anisotropic viscosity effects (Merrill et al., 1966),
where polymer molecules near the wall, which are
elongated and oriented by the flow, would spatially
hinder momentum transport normal to the direction of the
mean flow; and from possible flow interaction effects
from absorbed layers of molecules on the wall (Davies and
Ponter, 1966; Bryson et al., 1971). Up to now, these
explanations have not been substantiated experimentally,
and generally, they are no longer being considered as
possible drag-reducing mechanisms.

That viscoelastic effects are responsible for drag
reduction was probably first suggested by Dodge and
Metzner (1959). Presently, this remains as the most
popular hypothesis for drag reduction, although the
specific mechanisms involved are still not yet clear.

Viscoelastic mechanisms for the explanation of drag
reduction have been suggested for several reasons.
First, nearly all polymer-solvent combinations that are
drag-reducing at low additive concentrations, exhibit
measurable viscoelastic effects at high additive
concentrations. Secondly, large viscoelastic effects
have been measured in low concentration polymer
solutions, while other solution properties (such as shear
viscosity and mass density) remain very close to solvent

values. That drag reduction and viscoelasticity are the only two large macroscopic effects induced by polymer addition at low additive concentrations suggests that they are related. Further, experimental evidence indicates that the onset of drag reduction occurs when turbulent time scales match polymer time scales. This would suggest that some viscoelastic mechanism involving the stretching of polymer molecules plays a role in drag reduction.

Possible viscoelastic effects that may be of importance in drag reduction are effects resulting from resistance to extensional deformations; stabilization effects due to stress modifications in transient shear deformations; and/or energy storage effects of elastic deformations. As a general mechanism for drag reduction, most investigators suggest that the polymer molecules must interfere with the turbulence bursting process; this would lead to a lower rate of turbulence production, and hence, lower drag. However, exactly what part of the bursting process that is involved is not known.

As an example of how viscoelasticity may interfere with the bursting process, a mechanism proposed by Falco and Wiggert (1980) will be described. In this proposed mechanism, it is assumed that streak formation is initiated by ring-like vortices interacting with the wall. These vortices approach the wall at an angle and

as they intersect the wall, they are bent parallel to the wall and stretched. According to these investigators, the molecules inside these vortices will inhibit the stretching of the vortices by increasing the resistance to these motions. As a result, the ring-like vortices will be stretched less, with the stretching process taking a longer period of time. Due to this reduced stretching, the intensities of the vortices will be lower and they will exhibit lower self-induction effects. Hence, the vortices will approach the wall at a lower velocity and the velocity of the fluid picked up from the wall will also be lower. As a consequence of these effects, less streak build up will occur, and with the inhibition of streak formation, the spatially averaged bursting rate will decrease, turbulence production will decrease, and drag reduction will result.

Since the ring-like vortices would remain in contact with the wall for a longer period of time, this mechanism would explain the observed increase in streak lengths. Also, with the reduced stretching of the vortices, their cross-sectional areas should not decrease as much; this would account for increases in streak spacing. Finally, because of reduced self-induction effects, these vortices would not be expected to get as close to the wall and this would lead to the observed lowering of turbulent intensities in the region closest to the wall.

General Characteristics of Viscoelastic Liquids

Materials may be rheologically classified according to their reactions to applied loads. The equations which describe such material response behavior are called constitutive equations, or rheological equations of state. Materials which can be described by a constitutive equation where the internal stresses are only a function of the instantaneous magnitudes of the deformations are defined as being purely elastic. On the other hand, materials in which the internal stresses are only a function of the instantaneous deformation rates are labeled as being purely viscous. Materials which can exhibit both elastic and viscous characteristics are classified as being viscoelastic. Of interest here are viscoelastic liquids, which are primarily viscous, but are also capable of exhibiting elastic characteristics.

For engineers, probably the most significant characteristic of a viscoelastic liquid is that its shear viscosity is often highly dependent on the deformation rate. For example, polymer solutions (the viscoelastic liquids of interest in this dissertation) are typically shear-thinning. They exhibit a constant viscosity region (i.e., Newtonian behavior) at low strain rates, a region where the viscosity decreases with strain rate at intermediate strain rates, and then they exhibit another Newtonian region at high strain rates. As mentioned

previously, these shear-thinning effects can often be dramatic; viscosities can decrease to 1/100 - 1/10,000 of their zero shear rate values (Bird et al., 1974).

A variety of elastic effects can also be generated in viscoelastic liquids. Typically, the responses of these fluids are dependent not only on the instantaneous deformation conditions, but also on the past history of deformation. As a result, they often show transient responses to oscillating and other unsteady flows. Further, in steady as well as in unsteady flows, viscoelastic liquids can exhibit elastic effects as a result of their abilities to sustain anisotropic normal stresses. Some examples of the effects which can be caused by anisotropic stresses are the Weissenberg effect, where liquid climbs a rotating shaft; extrudate swell, where a jet of a viscoelastic liquid will expand upon emerging from a tube or die; the development of unequal pressures on the inner and outer walls in laminar annular pipe flow; and the tubeless siphon effect, where a siphon can continue to operate after the upstream end of the siphon has been withdrawn from the liquid. For further examples of elastic effects, the reader is referred to Lodge (1964).

Elastic effects can be generated in both shearing and extensional flows. For instance, the first three of the above mentioned examples occur in shearing flows

(flows with transverse velocity gradients), while the last example describes an extensional flow situation (flow with a longitudinal velocity gradient). In general, extensional flows are more capable of generating stronger elastic effects than shearing flows. To qualitatively distinguish extensional flows from shearing flows, consider an idealistic stretching of a dilute macromolecular solution. In simple shear flow, the macromolecules will tend to rotate and stretch until they are aligned with the streamlines. At this point, the ends of each molecule will be moving at similar velocities and the stretching will cease. The molecules will then relax (i.e., return to an unstretched state) until some force perturbs the molecule out of alignment with the streamlines, at which point, the stretching process will start over again. In an extensional flow, the molecules will also tend to align themselves with the streamlines; however, the ends of each molecule will now be in fluid of increasingly different velocity and each molecule will continue to be stretched (with no periods of relaxation). Further, if a molecule is disturbed from such an alignment, the hydrodynamic restoring force will tend to direct the molecule straight back to the aligned position. In contrast, if a molecule is perturbed in a shearing flow so that it rotates in the original direction of rotation, it will likely continue to keep

rotating until it has shifted position by 180 degrees. Consequently, the molecules in a shearing flow are likely to follow a tumbling motion, and at any one time, more molecules are likely to be out of alignment than for an extensional flow. Thus, molecules in extensional flows are more likely to attain greater extensions with a greater percentage of molecules being stretched than in shearing flows. For further discussions on the differences between shearing and extensional motions, the reader is referred to Pipkin and Tanner (1972), Pipkin (1977), and Petrie (1979). Lastly, one important point is that it is not possible to predict behavior in elongation from behavior in shear (Petrie, 1979).

Experimental Correlations of Viscoelastic Characteristics with Drag-Reducing Ability

Over the past two decades, investigators have been attempting to determine whether or not the drag-reducing abilities of polymer solutions are directly related to their viscoelastic characteristics. In this section, the experimental attempts at such correlations will be briefly reviewed.

In 1964, Metzner and Park measured both first normal stress differences[1] generated in a shearing flow and

---

[1]The first and second normal stress differences in simple shear flow may be defined as $(T_{11}-T_{22})$ and

drag reduction characteristics for a 0.3% aqueous polyacrylamide solution (J-100, Dow Chemical Co.). The normal stress differences were determined from measurements of the reductions in thrust (from that for solvent flow at similar flow rates) of jets issuing from a smooth cylindrical tube in which laminar shear flow existed. Drag reduction was determined from measurements of flow rate and pressure drop in a pipe flow. Their results indicate that drag reduction may be a function of the ratio of the elastic to viscous forces developed in the pipe flow; however, no definite conclusions were reached due to the lack of sufficiently extensive data.

In 1966, Gadd reported measurements of the pressure difference between the outer and inner surfaces of an annular pipe flow for several drag reducing solutions. These pressure differences were used as a measure of second normal stress differences. Aqueous solutions, each being supposedly of the same drag reducing ability, of 40 ppm Polyox WSR-301 (Union Carbide), of 72 ppm Separan AP-30 (Dow Chemical Co.), and of 120 ppm Guar gum were studied. Substantial pressure differences were observed for the Polyox solutions, but not for the other

---

$(T_{22}-T_{33})$, where T_{11}, T_{22}, T_{33} are the components of stress in the direction of flow, in the direction of the displacement gradient, and in a "neutral" direction, respectively.

two solutions. Gadd (1966) concluded that there was no obvious correlation between turbulent drag reduction and normal stress differences in laminar shear flow. In a follow-up experiment with similar solutions, Brennen and Gadd (1967) demonstrated that both the level of second normal stress differences and the differences in pitot tube pressure between corresponding polymer solution and solvent flows (also thought to be a viscoelastic effect (Metzner and Astarita, 1967)) could be significantly diminished without apparently impairing their drag-reducing abilities. This would further seem to indicate that drag reduction does not correlate with solution viscoelasticity.

Correlations of Deborah number with drag reduction have also been examined. The Deborah number may be defined as the ratio of a characteristic time parameter of the fluid to that of the flow and a correlation of it with the level of drag reduction would indicate that fluid elasticity would be likely to play a role in drag reduction. Seyer and Metzner (1967) have examined such a possible correlation for pipe flow of several aqueous polyacrylamide solutions ranging in concentration from 0.2% to 0.6% for Reynolds numbers ranging from 5000 to 60,000. In their determination of the Deborah numbers, the characteristic time of the flow was taken as the reciprocal of an estimate of the dissipative frequency of

the turbulence and the characteristic solution time was taken as a molecular relaxation time of a Maxwell fluid. These investigators found that for a given Reynolds number, the level of drag reduction when plotted as a function of the Deborah number was independent of concentration. However, this relationship was found to vary with Reynolds number. These results would seem to indicate that fluid elasticity may be involved in the drag reduction mechanism; however, the lack of a complete correlation does not allow any definite conclusions. Other investigators (e.g., Elata et al., 1966; Rodriguez et al., 1967) have also examined the correlation of drag reduction with fluid elasticity through examination of the Deborah number. Generally, these correlations, which have utilized different formulations of the Deborah number, have shown fair agreement between drag reduction and Deborah number; however, no complete correlations have been found. It should also be noted here that theoretical attempts to explain drag reduction using viscoelastic models have also been tried (e.g., Patterson and Zakin, 1968; Ruckstein, 1971, 1973; Ting, 1972; Hinch and Elata, 1979); however, no one model has proven entirely satisfactory.

In the early 1970's, investigators found the first indications that very large viscoelastic effects could occur in relatively low concentration polymer solutions

(of the order of 100 ppm). In studying extensional flow through orifices, Metzner and Metzner (1970) and Oliver and Bragg (1973) estimated that extensional viscosities (defined as the first normal stress difference divided by the deformation rate in the direction of the flow) as large as 1000 to 10,000 times their corresponding shear viscosities could occur. In both sets of experiments, aqueous polyacrylamide solutions of greater than 100 ppm were studied at deformation rates of the order of 10,000 l/s. The normal stresses were determined using momentum balance analyses and measurements of the reduction in thrust of the jets issuing from the orifices. The extensional deformation rates were determined from estimates of the geometry of the flow entering the orifices. No correlations of extensional viscosity with drag-reducing ability were made; however, just the existence of such large values of extensional viscosity has led many investigators to suggest that drag reduction somehow arises from such large increases in resistance to extensional deformations.

The first viscoelastic measurements for very low concentration (as low as 1 ppm) polymer solutions were reported by Morgan and Pannell (1972). The reductions in jet thrust were measured for laminar shear flow exiting from capillary tubes. Drag reduction measurements were also made in capillary tubes at similar wall shear rates

as experienced in the jet thrust measurements. The measured values of the reduction in jet thrust were compared at three different wall shear rates for solutions containing just enough polymer to give maximum drag reduction. Several aqueous polyethylene oxide and polyacrylamide solutions were examined and the measurements were conducted at wall strain rates of 64,000, 100,000, and 178,000 l/s. The concentrations that yielded maximum drag reduction ranged from 1 to 220 ppm. These investigators found that, regardless of the polymer type or concentration, that at each particular wall shear rate, the reductions in jet thrust in each of these solutions were roughly equal. As a result, they concluded that a general relationship exists between the level of first normal stress difference and drag reducing ability.

Gordon, Balakrishnan, and Pahwa (1975) investigated the importance of filament formation in drag reduction. The ability of many drag reducing solutions to form filamentary structures, called pituity, is thought to be a viscoelastic effect arising from the high extensional viscosity of such solutions (Chang and Lodge, 1971). Gordon et al. devised a pituity test in which a rod was suddenly removed from a beaker of polymer solution. This caused a thread of solution to be formed between the rod and beaker. The time it took for the thread to break was

then taken as a measure of pituity. They examined aqueous solutions made with several different molecular weight grades of a polyethylene oxide and of a polyacrylamide. They found that filament forming ability loosely correlated with drag-reducing ability for each series of these two polymers, however, but not between them. They tentatively concluded that drag reduction and filament formation are not manifestations of the same mechanism. However, one drawback to their correlations was that their pituity tests were conducted at additive concentrations of 0.825% (the high concentrations were necessary to observe any pituity), while the drag-reducing tests were run at much lower concentrations (0.01%).

In his doctoral dissertation, Balakrishnan (1976) examined the freely converging flow of several aqueous polyacrylamide solutions. Extensional viscosities were calculated using a momentum balance with measurements of orifice pressure drop, flow rate, and the angle of convergence of the upstream flow into the orifice. Various conditions of polymer molecular weight, concentration, and conformation were studied. Generally, the more effective drag reducing solutions were found to have the higher extensional viscosities. Balakrishnan concluded that drag reduction was a manifestation of the large extensional viscosities that dilute polymer

solutions can possess. In this investigation, extensional viscosities as large as 3000 times their corresponding shear viscosities were calculated for additive concentrations as low as 10 ppm.

Further measurements of normal stress differences generated in laminar shearing flows were reported by Hasegawa in 1978. Several polyethylene oxide and polyacrylamide solutions ranging in concentrations from 2 to 80 ppm were examined. First normal stress differences were determined using a jet thrust technique for wall shear strain rates ranging from 1000 to 100,000 l/s. In general, the polymer solution flow behaved in nearly the same manner as for water flow through the apparatus. Hasegawa concluded that normal stress effects were not responsible for drag reduction.

Scrivener et al. (1979) report an investigation in which both the extensional and drag reducing behavior were measured for several aqueous polyethylene oxide and polyacrylamide solutions. The extensional behavior of these solutions was examined using birefringence measurements for flow through a cross cell, with the presence of flow birefringence being taken as evidence of macromolecular stretching. Drag reduction was measured using a separate pipe flow apparatus. In particular, the influence of polymer molecular weight was examined. Both drag reduction and the intensity of birefringence were

found to increase with molecular weight. Further, it was determined that the birefringence effects were caused by the highest molecular fraction of the polymer, as has previously been found in drag reduction. The drag reduction experiments were run for concentrations ranging from 10 to 80 ppm, while the phenomenon of flow birefringence could only be observed above a certain minimum additive concentration (500 ppm) and molecular weight (450,000). Despite these concentration differences, Scrivener and co-workers concluded that drag reduction is strongly related to the elastic properties of the macromolecules having the longest chain lengths.

Chang and Darby (1983) report an investigation where the effects of shear degradation on both the drag-reducing and rheological properties of several aqueous polyacrylamide solutions were studied. Drag reduction was measured using a pipe flow apparatus and first normal stress differences were determined using a cone and plate shear flow apparatus. Additive concentrations ranging from 100 to 500 ppm were examined in both set-ups; and in the cone and plate apparatus, shear strain rates were varied from 1 to 100 1/s. Shear viscosity measurements were also reported for strain rates ranging from 0.01 to 10,000 1/s. As a result of the applied shear degradation, the magnitudes of both the elastic and viscous properties of the test solutions were found to be

reduced. However, the degree of drag reduction was found to increase with degradation. Since the fluid elasticity was found to decrease in solutions of increasing drag-reducing ability, it would appear that these results indicate that fluid elasticity does not play an important role in drag reduction. However, Chang and Darby offer an explanation for these results which still supports the viscoelastic hypothesis for drag reduction. They note that a decrease in shear viscosity will tend to increase the apparent level of drag reduction and they argue that the effect of lowered shear viscosity was relatively more significant in their experiments than decreased drag reduction effects due to lowered fluid elasticity. Thus, fluid elasticity may still be responsible for drag reduction, even though drag reduction was found to increase with degradation in these experiments.

In summary, no direct experimental evidence exists which conclusively shows whether or not the drag-reducing abilities of polymer solutions are related to their viscoelastic characteristics. The results of the investigations of Metzner and Park (1964), Seyer and Metzner (1967), Morgan and Pannell (1972), Balakrishnan (1976), and Scrivener et al. (1979) suggest that such a correlation exists, while Gadd (1966), Brennen and Gadd (1967), Gordon et al. (1975) and Hasegawa (1978) present contrary evidence.

These investigations have established that viscoelastic effects can occur in solutions of the low additive concentrations (of the order of just a few ppm) of interest in drag reduction. However, whether the viscoelasticity measured in these instances is merely a concomitant property of the solution, or an essential element of drag reduction is not yet known.

Further, it may be noted from these experiments that the extra normal stresses generated in the extensional flows were generally larger and occurred at lower deformation rates than in shearing flows. For example, Balakrishnan reported a normal stress difference of 250,000 dynes/cm^2 at an extensional deformation rate of 5000 1/s for a 20 ppm Separan AP-30 solution. While, Morgan and Pannell reported normal stress differences of only 5400 dynes/cm^2 at a shear deformation rate of 100,000 1/s for a 17 ppm Separan AP-30 solution. (In general, results from different investigations should not be directly compared due to the many variables that can affect additive behavior; however, this comparison is used only as an example of the general trend that extensional flow effects can be much larger than shearing effects.) Thus, it would seem likely that extensional effects, instead of shearing effects, would play a more significant role in drag reduction, if viscoelasticity were to indeed be be responsible for the phenomenon.

Extensional Flow of Viscoelastic Liquids

In this section, the experimental methods that have been used to examine extensional flow behavior are examined. First, however, the kinematics of such flows are described.

Kinematics of Extensional Flows

A flow is extensional if a fixed Cartesian coordinate system exists where the velocity field may be expressed as

$$u_i = a_i x_i + U_{o_i}$$

where u_i are the components of velocity at a material point x_i, a_i are extensional deformation rates, and U_{o_i} are constants. (The summation convention is not applied in this equation.) For steady flow, a_i are constants and if the flow is incompressible, then

$$a_1 + a_2 + a_3 = 0$$

Now, if there is positive extension in only a single principal direction (e.g., $(a_1, a_2, a_3) = (\Gamma, -\Gamma/2, -\Gamma/2)$), then the flow is classified as uniaxial extension. Another possible type of extension is equal biaxial extension, where there is equal positive

extension in two principal directions (e.g., $(a_1, a_2, a_3) = (\Gamma, \Gamma, -2\Gamma)$). If a flow is two dimensional and extensional, then the flow is classified as strip biaxial (or also called planar, pure shear, or hyperbolic) extension. An example of this type of flow is $(a_1, a_2, a_3) = (\Gamma, -\Gamma, 0)$. For further details concerning the possible types of extensional flows, the reader is referred to Dealy (1971), Tanner and Huilgol (1975), Tanner (1976), and Powell (1983).

Experimental Methods

To describe the extensional behavior of viscoelastic liquids, investigators typically determine the stress-strain rate response for a liquid in an extensional flow and then they express their results as an extensional (or elongational) viscosity, which is then recorded as a function of either the stress or extensional strain rate. These extensional viscosities are defined as a ratio of a normal stress difference to the extensional strain rate. For example, the extensional viscosity, η_e, may be defined for uniaxial sink flow as

$$\eta_e = (T_{11} - T_{22})/\Gamma$$

where T_{11} and T_{22} are components of the stress tensor in the directions of flow and orthogonal to the flow and

where Γ is the magnitude of the strain rate in the direction of the flow.

The first measurement of extensional viscosity was made by Trouton (1906). He placed rods of pitch, pitch-tar mixtures, and wax under constant loads and measured their velocities of extension. He computed coefficients of viscous traction (extensional viscosities) for these substances and found them to be three times greater than their corresponding shear viscosities. This behavior is now known as Trouton´s rule and is followed in most cases by Newtonian fluids (Reiner, pp.172,175-178, 1949).

For viscoelastic liquids, the types of experimental methods which can be used to determine extensional viscosities are dependent on the level of mobility of the test liquid. For highly viscous liquids (having shear viscosities of order 10^4-10^9 Ns/m^2), investigators have conducted extension tests by stretching cylindrical rods of test liquid in uniaxial extensions and by using bubble inflation techniques to obtain equal biaxial and strip biaxial extensions. Typically, a uniaxial extension test consists of clamping a test sample at one end and then extending it in some programmed manner, usually to yield a constant strain rate. The bubble inflation techniques involve clamping a strip of test material between two flat plates, in which a hole has been cut (circular for equal biaxial extension or

rectangular for strip biaxial extension) and then applying a differential pressure across the sample to produce an expansion. The rates of strain that can be obtained in these and the uniaxial tests range from about 0.001-1 1/s and the uses of these techniques are restricted to materials having zero strain rate shear viscosities of greater than about 10^4 Ns/m^2. Due to commercial interest in synthetic polymers, an extensive amount of research has been conducted with polymer melts using such techniques. For reviews of the experimental work conducted in this area, the reader is referred to Dealy (1971, 1978) and Petrie (1979).

For liquids of more moderate shear viscosities, investigators have studied extensional behavior using controlled fiber spinning and related techniques, film blowing processes, stagnation flows, converging flows, and some various unsteady flows. First, in controlled fiber spinning tests, the test liquid is usually extruded downward through a die and is taken up on a rotating spool. In order to stretch the liquid, the take-up speed is set higher than that which the liquid would naturally attain as a result of gravity alone. Deformation rates are calculated from measurements of the change in diameter along the thread, usually being determined from photographs. Stresses are calculated using measurements of the take-up force and applying force balances along

the thread. Fiber spinning can be used for both polymer melts and solutions, with the least viscous liquids that have been spun having zero strain rate shear viscosities of about 0.1 Ns/m^2. The extensional strain rates that have been obtained using such techniques range from about 1 to 100 1/s. For a detailed review of spinning experiments, the reader is referred to the monograph by Petrie (1979).

In another technique closely related to fiber spinning, investigators have examined tubeless siphon flow (or sometimes called Fano flow, named for the investigator for whom its discovery is attributed). In this flow, a siphon is set up with its inlet being positioned above the surface of the material being siphoned. The resulting flow is a rising column of liquid, which has a decreasing cross-sectional diameter as column height increases. The kinematics and dynamics of the flow are determined, in a manner similar to spinning flows, through the use of photographs and measurements of the force required to support the siphon. Tubeless siphon flow has been examined for extensional strain rates ranging from 0.1-100 1/s for liquids having zero strain rate shear viscosities as low as 0.02 Ns/m^2. For more information concerning such flow, the reader is referred to Astarita and Nicodemo (1970), Acierno et al. (1971), and Nicodemo et al. (1975).

Still another technique related to fiber spinning is the triple-jet method developed by Oliver and co-workers (Oliver and Bragg, 1974; Oliver and Ashton, 1976a). Here, a jet of liquid issues from a capillary tube with another set of higher speed jets of the same liquid set to impinge on the central jet at some downstream location. The result of the impingement of the higher speed jets is to stretch the central jet. Stresses are determined by measuring the reduction in thrust on the capillary tube and extensional strain rates are determined using photographs. Oliver and co-workers used this method to examine liquids having shear viscosities of the order of 0.03 Ns/m^2 for extensional strain rates ranging from $100-800$ $1/s$. Strain rates of greater than 1000 $1/s$ could not be attained due to slip developing at the jet impingement point.

The extensional behavior of viscoelastic liquids in film blowing processes has also been experimentally examined (Farber and Dealy, 1974; Han and Park, 1975; Gupta et al., 1982). In such processes, molten polymer is extruded from an annular die and is drawn upward by a take-up device. At the bottom of the die, air can be introduced to inflate the tube of polymer film into a bubble. If the air pressure is set so that there is no pressure difference across the film, then the tube will not inflate and the result will be a uniaxial extensional

flow. By increasing the air pressure in the tube, the extruded film will also be stretched in the transverse direction to the fluid motion and biaxial extensions can be obtained. The kinematics of such flows may be determined from the geometry of the film, which is usually determined using photographs, and from measurements of mass flow rate and film thickness. Stresses may be calculated using force balances with measurements of the take-up force and pressure differential across the film. In such flows, extensional deformation rates ranging from about 0.005 to 5 1/s have been attained.

At this point, it should be noted that the fiber spinning and related techniques and the film blowing processes are materially unsteady flows. In these flow geometries, a fluid element will experience changing deformation rates as it moves and, in general, the stress that it experiences will not have sufficient time to reach a constant level. As a result, the extensional viscosities determined for such flows are not only dependent on the rate of deformation, but also on the entire strain history of that element. Therefore, while often being a convenient comparative parameter, extensional viscosities measured in materially unsteady flows should not be interpreted as representing material properties.

To try to attain constant deformation rates for over the entire flow field, investigators have examined a class of flows called stagnation flows. In such flows, extensional flow fields may be set up by forcing streams of liquid to collide. The stagnation flows that have been examined have been generated through use of opposed coaxial jets (Frank et al., 1971; Mackley and Keller, 1973), through the use of counter rotating cylindrical rollers (Taylor, 1934; Peterlin, 1966, Frank and Mackley, 1976; Crowley et al., 1976; Mackley, 1978; Leal et al., 1980) and through the use of cross flow cells (Scrivener et al., 1979; Lyazid et al., 1980; Cressely and Hocquart, 1980). To obtain stagnation flow in the roller experiments, symmetrically placed rollers are rotated in a reservoir of liquid at equal rates, with each roller being rotated in an opposite sense to the adjacent rollers. The resulting flow, for example, if using four rollers, will have liquid being pumped into the region between the rollers from two opposing directions, with the flow exiting in the other two directions. The flow pattern in a cross flow cell is similar. Here, a chamber is formed by the meeting of four channels, each at right angles to the adjacent channels. The flow enters the chamber from two opposing channels and exits through the other two channels. The kinematics of such flows have been determined through photography of trace particles

and through use of Laser Doppler anemometry. To date, a primary goal of experiments using such flow geometries has been to examine the degree of stretching that macromolecules may attain; and this stretching has been determined through birefringence measurements. Stress measurements, however, have not been made in such set-ups and hence extensional viscosities have not be determined using such flow geometries. For a further discussion of the kinematics and dynamics of stagnation flows and the experiments that may be run to realize such flows, the reader is referred to the report by Winter et al. (1979).

Another class of flows that investigators have used for the examination of the extensional behavior of viscoelastic liquids is that of converging flows. The investigations in this area have utilized two types of flows: one, where the flow is conducted from a reservoir through an abrupt contraction (free convergence), and secondly, where the flow is conducted through converging channels (constrained convergence). In the first case, investigators have utilized the fact that some polymer melts and solutions will exhibit dramatically different flow through a contraction than Newtonian liquids. For a Newtonian liquid, flow will enter a contraction from almost all angles; while for some viscoelastic liquids, flow entering a contraction is restricted to a conical region resembling a wine-glass-stem (Tordella, p.72,

1969; Metzner et al., 1969). This wine-glass-stem shaped region is surrounded by a large torroidal region of slowly recirculating flow. Within the conical region, the flow is almost purely extensional and may be approximated by the irrotational sink flow equations (Metzner et al., 1969). In the experiments conducted by Metzner and co-workers (1969), it was determined that the sink flow equations applied to about 70% of all fluid entering their contraction. After assuming sink flow conditions, the deformation rates can easily be determined from measurements of the angle of flow convergence and of the mass flow rate. To determine normal stress differences, investigators have applied momentum balance analyses which have utilized three types of measurements: measurements of the thrust exerted by the viscoelastic jets emerging from the contractions (Metzner and Metzner, 1970; Oliver and Bragg, 1973), measurements of total pressure drop across the contractions (Balakrishnan, 1976), and measurements of the difference in pressure drop between the flow of the polymer solution and its solvent at a similar flow rate (Fruman and Barigah, 1982). These flows are also materially unsteady, and hence, the extensional viscosities determined using such techniques will again not represent true material properties. These techniques are still valuable, however, as they provide information

about the elasticity of the liquids at higher strain rates (of the order of 10,000 1/s) than can be attained by using any of the previously discussed methods. Generally, liquids of any level of shear viscosity can be used in such techniques; however, this method is restricted to liquids which exhibit wine-glass-stem shaped flow and not all polymer solutions are capable of exhibiting such flow (especially solutions of low additive concentrations).

In constrained convergence, investigators have examined flows through channels of conical and wedge shaped geometries and also for channels profiled to give constant average extensional deformation rates. Liquids ranging from viscous polymer melts to low viscosity polymer solutions have been studied using such channels. The major difference between free and constrained convergence is that shearing effects can be more prominent for flow constrained by channel walls. To avoid such effects, lubricated dies have been used with viscous polymer melts and channels with dimensions designed to minimize viscous losses have been used for lower viscosity polymer solutions. If viscous losses are negligible, then the irrotational sink flow equations may again be used to evaluate the deformation rates. As for the free convergence flows, normal stress differences have been evaluated by using jet thrust techniques. In

addition, normal stresses (and hence, normal stress differences) can now also be determined from pressure measurements obtained from taps positioned along the channel walls (James and Saringer, 1980; Winter et al., 1979). For a review on such flows, with an emphasis on polymer melts, the reader is referred to the paper by Cogswell (1978). For work using less viscous polymer solutions, the reader is referred to reports by James and Saringer (1980, 1982), where both conical and planar wedge flow have been examined, and to a paper by Oliver and Ashton (1976b), where flow through channels, which were designed to yield constant average deformation rates throughout the flow, was examined.

Investigators have also developed techniques for examining the extensional behavior of viscoelastic liquids which make use of unsteady flows. One such technique developed by Pearson and Middleman (1977) utilizes the collapse of a gas bubble in a reservoir of a viscoelastic liquid. In this method, a bubble is brought to rest on top of a capillary tube situated in the reservoir; a rapid change in pressure is then applied to the bubble through the tube which causes the bubble to collapse. As a result, uniaxial extensional flow is set up in the surrounding liquid. Kinematics of the flow are determined from high speed photography. Pearson and Middleman were able to obtain nearly constant strain

rates ranging from 0.1-10 l/s for liquids having shear viscosities of about 100 Ns/m^2. Another technique utilizing an unsteady flow is the method of controlled jet instabilities developed by Schummer and Tebel (1983). This method is based on the behavior of viscoelastic jets emerging from a harmonically vibrating cylindrical nozzle. The resulting jet consists of alternating filament and drop regions. Due to higher surface tensions in the filaments, a mass flow is set up from the filaments to the adjacent drop regions. The result is an extensional deformation of the filaments, with the diameter of each filament decreasing until the filament breaks away from the adjacent drops. The kinematics of the flow are again determined using photographs. Schummer and Tebel examined solutions having zero strain rate shear viscosities as low as 0.074 Ns/m^2 for extensional strain rates ranging from about 10-150 l/s. In both of these set-ups, the investigators have found that nearly constant deformation rates could be attained; however, the flows were maintained for only a short period of time and it is doubtful that constant levels of stress were attained. Recent measurements indicate that this was probably the case, as extensional viscosities determined using the bubble collapse method were less than those determined by the stretching of a cylindrical rod of the same material (Middleman and Munstedt, 1982).

Comments on the Use of Conical Channels to Examine Extensional Flow Behavior

In the present investigation, conical channels have been used to examine the extensional characteristics of the polymer test solutions. This type of flow geometry was selected for several reasons. First, conical channels can be designed to conduct flow at the high extensional deformation rates (of the order of 1000-10,000 1/s) of interest in this investigation.

Secondly, measurements could be conducted at very low additive concentrations for almost all types of solutions. This is an advantage compared to the techniques which utilize freely converging flow, which are restricted to fluids exhibiting wine-glass-stem shaped flow. At the low additive concentrations (of a few ppm) of interest in this investigation, most drag-reducing solutions do not exhibit this type of flow.

A further advantage of the use of conical flow geometry is that only the gross flow measurements of flow rate and pressure drop are needed to estimate viscoelastic parameters. Since such measurements can be quickly and easily made, extensional flow experiments can be easily conducted in conjunction with the drag reduction experiments.

In addition to these advantages, some drawbacks also exist in the use of conical channels as rheometers. The

principal disadvantage is that the flow is materially unsteady. Thus, any viscoelastic parameters that may be determined from the flow measurements in general will not represent material properties. Now, channels can be constructed to yield constant average extensional strain rates (i.e., materially steady flow) and still retain some of the advantages of conical channel flow. However, the use of such channels would also introduce some further complications. In such channels the walls are no longer aligned with a principal plane of stress (as in conical channel flow). As a result, any pressure measurements made using taps situated along the channel wall would include effects from more than one principal stress and measurements from more than one location would be needed to extract the magnitudes of the principle stresses (and hence, normal stress differences). More difficulties and uncertainities would arise in the interpretation of pressure measurements in terms of first normal stress differences than for conical channel flow.

For the purposes of the present investigation, the use of conical channels was selected as the best possible method for characterization of the extensional behavior of the polymer test solutions. This technique will produce viscoelastic parameters that will be useful for comparative purposes; however, due to the materially

unsteady flow conditions, these parameters will not be able to be interpreted as representing material properties.

.

The experimental arrangement consists of set-ups to measure the drag-reducing abilities, the extensional flow behavior, and the shear flow characteristics of highly dilute polymer solutions. These set-ups include a pipe flow apparatus to record drag reduction, conical channel rheometers for examination of extensional flow behavior, and a sliding ball viscometer for characterization of shear behavior. In this chapter, descriptions of each of these set-ups, of the polymer additives used, and of the polymer solution preparation procedures are presented.

Drag Reduction Apparatus

In this investigation, drag reduction was determined from measurements of gross-flow rate and pressure drop in turbulent pipe flow. The polymer test solutions, which were used on a single-pass basis, were prepared "on-the-fly" by the injection of a concentrated master solution into the pipe flow.

In the experimental arrangement, shown in Fig. 3.1, filtered tap water (the solvent in all cases) was delivered to a constant head overflow tank. The excess water was passed directly to the drain, while the

56
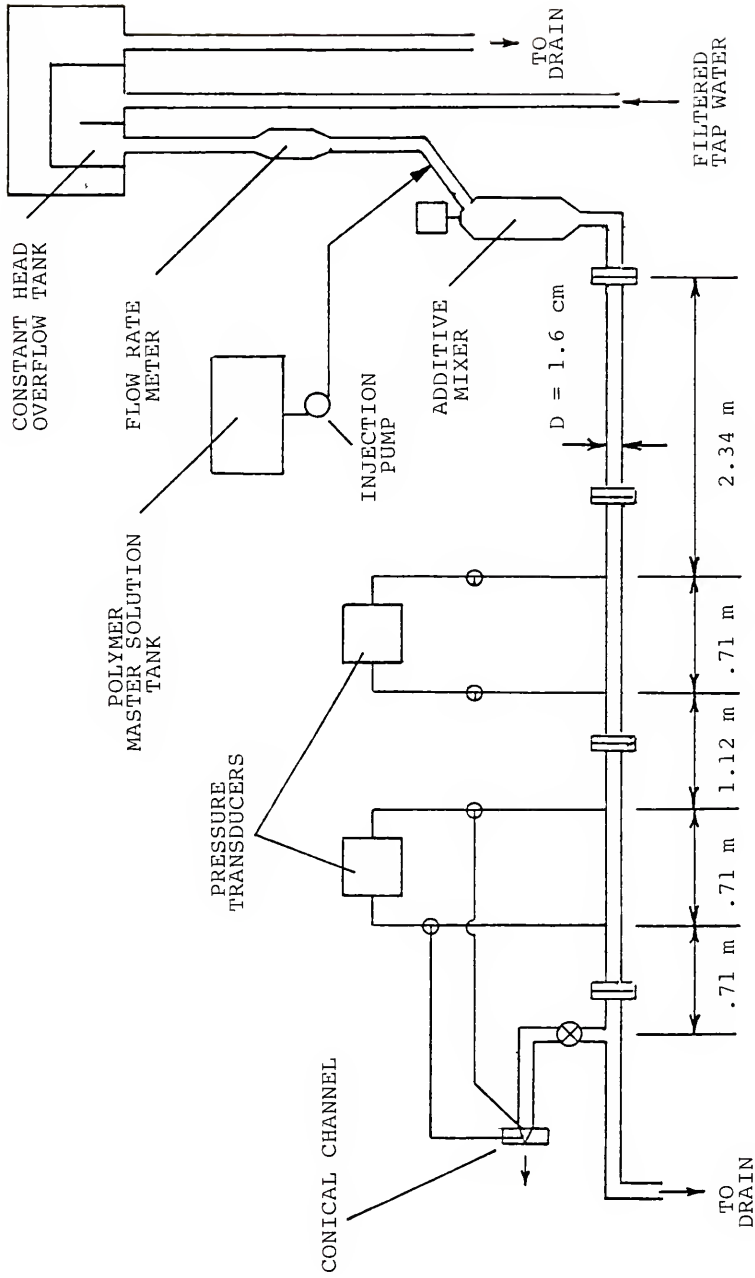
Fig. 3.1. Drag reduction apparatus.

regulated flow was conducted to the experiment pipe via a strain gage flow rate meter. The desired polymer additive, in the form of a concentrated master solution, was injected into the flow at a mixer located just upstream of the experiment pipe. Flow pressure drop was measured at two locations along the experiment pipe using separate strain gage differential pressure transducers. Both pressure transducers and the flow rate meter were connected to potentiometer recorders. The flow rate was adjusted by means of two valves downstream of the experiment pipe. These valves were connected in parallel and both conducted the flow into calibrated compartments of known volume in a storage tank. From the storage tank, the fluid was passed directly to the drain.

The experiment pipe was 5.5 m long with a nominal diameter of 16 mm. It consisted of three equal lengths of acrlyic tubing joined together by flanges. A 6 mm diameter orifice was located at the pipe inlet to provide high entry disturbance levels. The upstream pressure taps for the two pressure transducers were located 147 and 261 diameters downstream of the pipe inlet. The distance between taps for each transducer was 44 diameters. Prior to the drilling of the taps, the mean diameters of the pipe sections were determined from volumetric measurements of their interiors. Each pipe section was mounted vertically, filled with water, and

then a portion of it of measured length was drained, with the water being collected and weighed. Several measurements were made for each pipe section by draining the entire section at a time, and then, additional measurements were conducted by draining the pipes in 10 cm increments. The results of these measurements are presented in Table 3.1. The average diameters, based on measurements where the entire pipe sections were drained at once, were found to be 1.5920 ± 0.0009, 1.5964 ± 0.0006, and 1.5981 ± 0.0011 cm for the upstream, middle, and downstream sections, respectively. These averages were each based on four separate measurements and the $\pm$ values indicate the maximum observed deviation of the measured values from the corresponding average value. Average pipe diameters for each section were also determined by taking a weighted average of the diameters determined from the incremental measurements. These values were found to agree within 0.2% of the previous results. It may also be noticed that from either set of diameter values, the average diameters between pipe sections could vary by 0.4%. Further, based on the incremental measurements, it was found that the diameter could vary along a pipe section by up to about $\pm1\%$ of the mean diameter of that section. The average diameters associated with the upstream and downstream test sections, as determined from the incremental

Table 3.1. Experiment pipe diameters based on volumetric measurements of the pipe sections' interiors. The ± values indicate the maximum observed deviation of measured values from the corresponding listed average diameter.

Pipe Section	Average of Pipe Diameters Determined from Measurements Over Entire Pipe Section (cm)	Weighted Average of Incrementally Determined Pipe Diameters (cm)
Upstream	1.5920±0.0009	1.5934±0.0226
Middle	1.5964±0.0006	1.5933±0.0112
Downstream	1.5981±0.0011	1.5979±0.0149

measurements, were found to be 1.592 and 1.597 cm respectively. These values are used in all following calculations requiring diameter measures.

A peristaltic pump was used to inject the concentrated polymer master solution into the main flow. In this pump, flexible tubing was encased in a housing where rollers, driven by a variable speed motor, rotated to squeeze the fluid through the tubing. In the present investigation, two pump heads which used tubing of 0.8 and 1.7 mm in internal diameter were used. Approximately, 20 cm of 6 mm diameter flexible tubing was used to connect the master solution container to the pump and another equal length of similar tubing was used to connect the pump to the main flow set-up.

The polymer solution was injected into the main flow at the upstream side of an in-line rotational mixer. This mixer, shown in Fig. 3.3, consisted of a Plexiglass housing, 25 cm in length and 4 cm in diameter, in which three sets of impeller blades were mounted on a drive shaft. This shaft was aligned so that the blades rotated in a plane perpendicular to the flow. A variable speed motor was used to rotate the shaft and impellers, with rotation rates of up to 50 revolutions per second (rps) being attainable. To prevent a general swirl of the flow and to assist in the break-up of the polymer additive solution, honeycomb sections were affixed to the
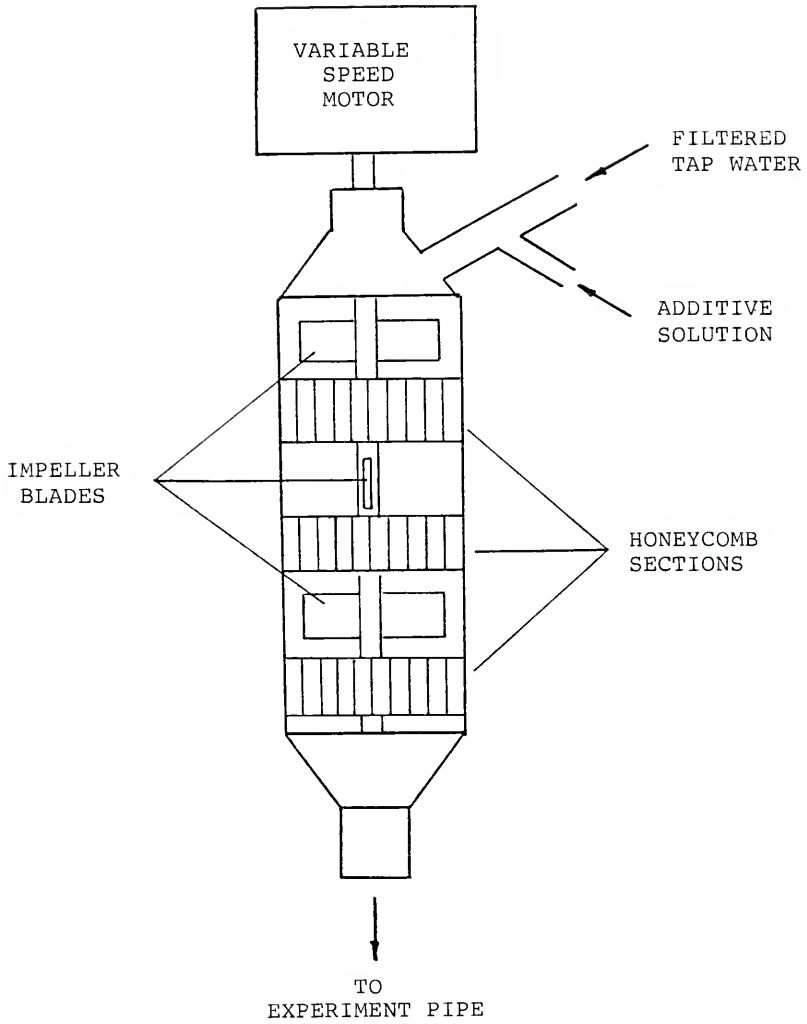
Fig. 3.2.   Schematic of in-line mixer.

mixer housing following each set of impeller blades. These sections, made of 0.1 mm sheet aluminum, were 5 cm long with individual cross dimensions of about 5 mm.

The differential pressure transducers used in this set-up had adjustable measuring spans, ranging from 10 to 125 cm of water. For the drag reduction measurements, the spans were set at 25 cm of water. From calibration by using a manometer set-up, the accuracy of the transducers (defined as being the maximum amount by which the measured values differed from those of the calibration curve) was determined as being better than $\pm 0.3\%$ of full span values. The flow rate meter used in this investigation had a flow range of 20 to 600 cm^3/s. Flow rates (during calibration) were determined by measuring the time for the flow to fill compartments of known volume in the storage tank. The accuracy of the flow rate readings was also determined as being better than $\pm 0.3\%$ of full span. For further detail on these measuring instruments and on the other commercially available equipment used in the drag reduction apparatus, the reader is referred to the manufacturers' literature. A list of the commercially available equipment used in this set-up and their manufacturers is presented in Appendix A.

For further discussion on the use of the drag reduction apparatus, the reader is referred to Chapter V.

Conical Channel Rheometers

General Arrangement

The conical channel rheometers were connected to the drag reduction apparatus (cf. Fig. 3.1) in such a manner so that the fluid that passed through the drag reduction experiment pipe could also be conducted through the conical channels. The conical channel set-up was attached to the main flow set-up at a point immediately following the main experiment pipe. The set-up consisted of a needle valve for flow rate control, followed by about 10 cm of 2.5 cm diameter tubing onto which the various channels could be attached (at one at a time). After passing through a channel, the flow exited to the open atmosphere.

Flow rates and pressure heads at points just upstream of the channel exits were the measured variables in this set-up. The flow rates were determined by using a catch and weigh technique, while pressure heads were measured using the same transducer that was used to measure the downstream pressure drops in the main experiment pipe. Three-way valves, located in the pressure lines, allowed connection to either set-up as desired.

For some preliminary polymer solution measurements, an additional separate conical channel set-up was also employed. In this separate set-up, the conical channels

were connected to a small cylindrical reservoir (10 cm in diameter) by a vertical section of flexible tubing (2.5 cm in diameter). Various lengths of tubing were used, ranging from 0 to 2 m in length. For the experiments conducted with this set-up, the polymer test solutions were supplied to it by manual transfer of solutions from the main flow apparatus. Pressure heads and flow rates were measured in the same manner as in the other channel set-up.

Design Considerations

Present usage of conical channels to measure normal stress effects in dilute polymer solutions is limited; hence, some mention should be given to the basic considerations involved in their design. First, it is desirable to achieve a velocity distribution as near to a frictionless flow as possible. Secondly, the deformation rate in the flow needs to be high enough to create measurable non-Newtonian effects. Lastly, the pressure decrease in a channel due to inertial forces should not be so large as to mask the pressure change due to the non-Newtonian effects.

First, to determine the level of frictional effects in the flow, consider the head-discharge relationship

$$Q_a = Q_i \{1 - \frac{C}{R^{1/2}}\}$$

which has been developed from the boundary layer solution for flow of a Newtonian fluid through a conical channel (cf. Appendix F). Here, Q_a is the actual flow rate through the channel, Q_i is the corresponding flow rate if the flow were frictionless, C is a constant depending on channel geometry, and R is a Reynolds number which may be defined as $R=Ur/\nu$, where $U=(2gh)^{1/2}$, h is the pressure head at a distance r from the imaginary apex of the channel, g is the gravitational constant, and ν is the solution kinematic viscosity. Thus, to diminish the effects of friction, the channels should be designed to conduct flows at high Reynolds numbers. Since the constant C is of the of the order of unity, a Reynolds number of $Ur/\nu \sim 1000$ was selected as being sufficiently large to minimize the influence of frictional effects upon the present investigation.

In conical sink flow, the deformation rate in the direction of flow is $2U/r$. For laminar flow of polymer solutions, the onset of non-Newtonian behavior often occurs at a deformation rate of ~1000 l/s (e.g., see James and Saringer, 1980). Thus, to satisfy the second design requirement, $2U/r$ should be of the order of 1000 l/s.

The appropriate channel dimensions in terms of r, can now be determined by combining the first two design requirements. For the present design, r is found to be

$r \sim (2/\nu)^{1/2}$ and with $\nu \sim 0.01$ cm^2/s, the desired dimensions attain a value of some 0.1 cm.

The flow of dilute polymer solutions through a channel of such designed dimensions should exhibit non-Newtonian effects. However, they may be masked by pressure changes due to inertial forces. The pressure decrease along a channel will be $\sim \rho U^2/2$, and if the pressure change due to non-Newtonian stresses is small compared to this inertial pressure change, difficulties will be encountered in observing and determining the non-Newtonian effects. Therefore, the designed channel dimensions should be checked to see if such masking can be avoided. For the presently designed channel dimensions of ~ 0.1 cm and Reynolds number of ~ 1000, the inertial pressure change should be of the magnitude of 1000 N/m^2. Since dilute polymer solutions can exhibit widely varying non-Newtonian behavior, it is difficult a priori to determine whether or not the inertial pressure effects will dominate the non-Newtonian effects. For example, Balakrishnan (1976) found that a 20 ppm polyacrylamide solution exhibited extra stresses of about 35,000 N/m^2 at strain rates of 5000 1/s, while James and Saringer (1980) measured non-Newtonian stresses of some 100 N/m^2 for a 20 ppm polyethylene oxide solution at similar strain rates. Based on these reported observations, it seems that the non-Newtonian effects

should easily be observable and should not be masked by inertial pressure drops for the presently designed channels. However, if it is found that only very weak non-Newtonian effects are generated, then the channels will have to be re-designed to smaller dimensions (at the sacrifice of introducing more frictional effects). Conversely, if very strong non-Newtonian effects are generated, then larger channels may be needed to avoid possible secondary flows.

Conical Channel Details

A series of channels, 4 mm long with exit dimensions of the order of 0.1 cm, were constructed for use in this investigation. Two sets of channels, one with conical half-angles of 29° and the other of 44°, were cut with a lathe into 6 mm thick Plexiglass sheets. Downstream pressure taps were located just upstream of the channel exits and the upstream taps were placed on the face of the Plexiglas sheet (facing the oncoming flow). The exact dimensions and pressure tap locations for the channels used in this investigation are presented in Fig. 3.3. After drilling the pressure taps, the interior channel walls were manually polished to remove burrs and then were inspected for smoothness using a microscope. Lastly, 10 cm long, 2.5 cm diameter rigid tubing was fastened to the upstream face of the
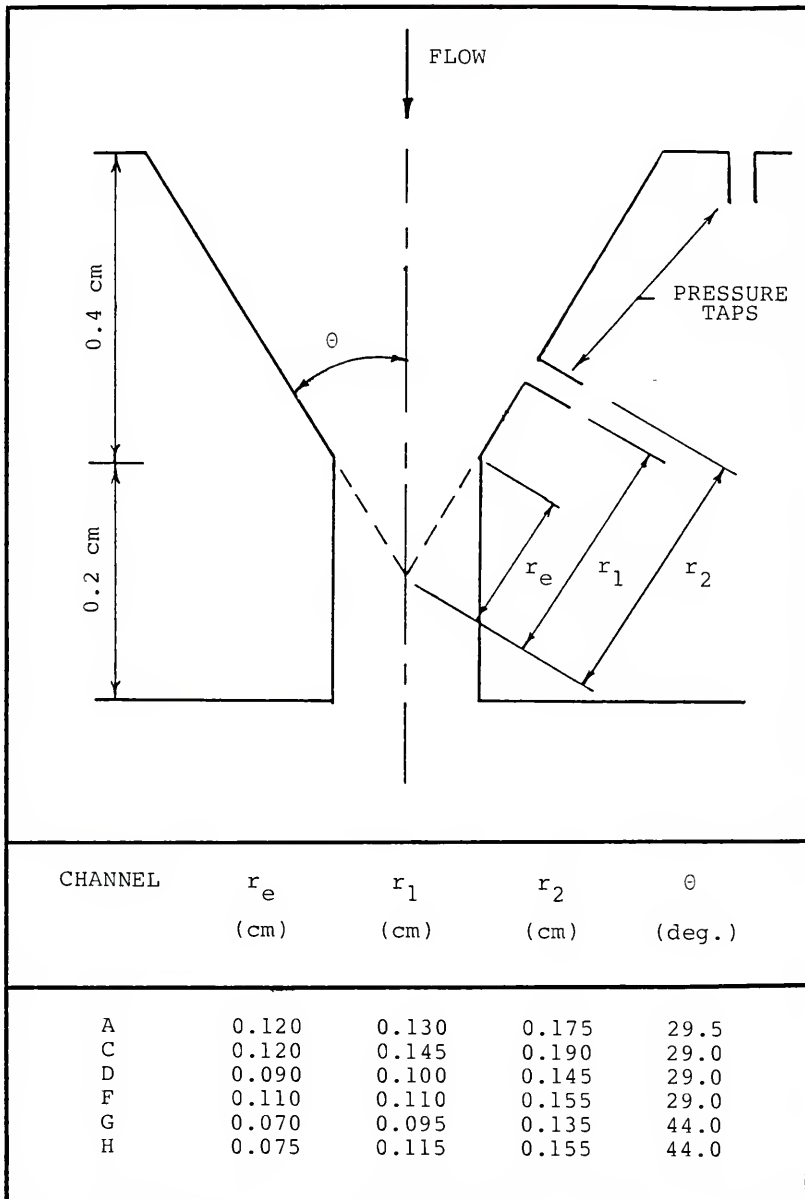
Fig. 3.3.   Dimensions of conical channels.

Plexiglass sheets, with the channels being centered with respect to these tubes. At this point, the channels were ready for attachment to the main flow set-up.

Sliding Ball Viscometer

The shear viscosity measurements were conducted using a Hoppler Rheo-Viscometer. A schematic of this viscometer is shown in Fig. 3.4. This instrument consists of a vertical cylindrical glass container, within which a closely fitted glass sphere is driven downward (without rotation) through the liquid by a known force. This force is transmitted to the sphere via a rigid shaft, which is attached to the sphere at one end and fastened to the balance arm assembly at the other. Various weights were loaded on to the balance arm to provide the driving force. The viscometer measurements consisted of measuring the time required for the sphere to travel a set distance (usually 3 cm) for a given loading. The distance the sphere traveled was monitored using a gage connected to the balance arm. Temperature control during the measurements was maintained by a Haake constant temperature circulator (model F, number 423). For further discussion on the use of this viscometer, including flow analysis, procedures for calculating shear viscosities, and instrument calibration, the reader is referred to Chapter IV and Appendix B.
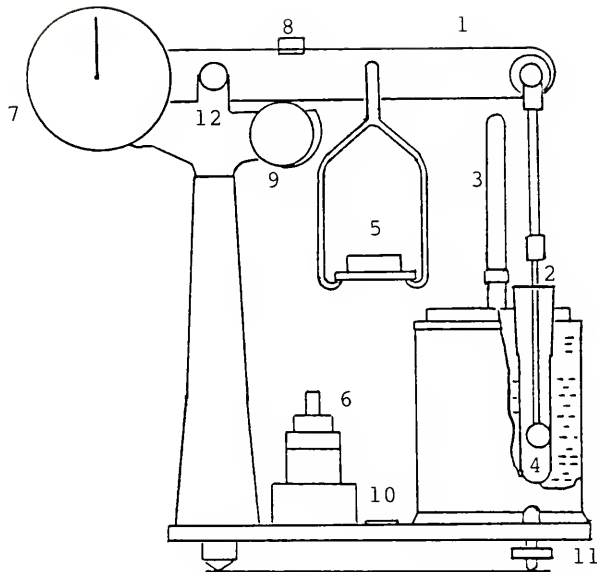
(1)   Balance Arm
(2)   Sphere Rod
(3)   Precision Thermometer
(4)   Measuring Vessel
(5)   Saucer for Weights
(6)   Set of Weights
(7)   Gage Indicating Sphere
        Travel Distance
(8)   Movable Weight for
        Buoyancy Compensation
(9)   Eccentric Cam for Adjustment of
        Sphere Location in Measuring Vessel
(10)   Box Level
(11)   Level Adjustment Screws
(12)   Balance Arm Pivot Point

Fig. 3.4.   Schematic of Hoppler viscometer.

Polymer Additives

General Structural Characteristics

Two molecular weight grades of a polyacrylamide,
Separan AP-30 and Separan AP-273 (Dow Chemical Co.), and
a polyethylene oxide, Polyox WSR-301 (Union Carbide
Corporation), were selected as the polymer additives to
be used in the present investigation. These additives,
which are widely used by investigators studying drag
reduction, are water soluble, linear, high molecular
weight polymers which can be used to produce very
effective drag-reducing solutions. Diagrams illustrating
their chemical compositions are shown in Fig. 3.5. It
should be noted that unmodified polyacrylamide molecules
are essentially non-ionic; however, typically some of the
amide groups $(-NH_2)$ are hydrolyzed to anionic carboxyl
groups $(-COO^-Na^+)$ (Dow Chemical Co., 1975). Thus,
such polymers in neutral solutions may be classified as
anionic polyelectrolytes.

In a state of rest, polyethylene oxide molecules are
thought to form randomly coiled spherical structures.
The polyacrylamide molecules are also thought to be
coiled, but instead of being spherical, they are thought
to be more elongated due to their ionic character
(Berman, 1978).

Due to the polymerization process and to
manufacturer's blending procedures, each additive

$$- [\ CH_2-CH_2-O \ ] -$$

Polyethylene Oxide

$$- [\ (\ CH_2-CH \ )_x - CH_2-CH \ ] -$$
$$\quad\quad\quad | \quad\quad\quad\quad\quad | $$
$$\quad\quad\quad C=O \quad\quad\quad\quad C=O$$
$$\quad\quad\quad | \quad\quad\quad\quad\quad | $$
$$\quad\quad\quad NH_2 \quad\quad\quad\quad O^-Na^+$$
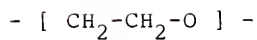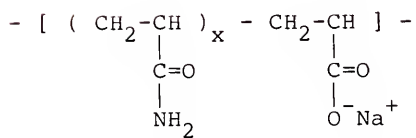
Partially Hydrolyzed Polyacrylamide

Fig. 3.5.   Chemical structure of polymer additives.

contains a broad molecular weight spectrum. Typically listed values for average molecular weights of these additives are 4×10^6 for Polyox WSR-301 (Berman, 1980), 4×10^6 for Separan AP-30 (Berman, 1980), and 5×10^6 for Separan AP-273 (Lagerstedt, 1979).

Solution Preparation

Polymer solutions used in this investigation were prepared "on-the-fly" by injection of a concentrated master polymer solution into the main flow. The master solutions, containing 1% additive by weight, were prepared in about 10 kg quantities by sifting the additives into tap water and manually stirring. Thereafter, solutions were stirred a few minutes at a time on a daily basis. This continued until the additives were dissolved and the solutions visually appeared homogeneous, which required about 2 weeks. The solutions were then stored in covered containers until use.

CHAPTER IV
SHEAR VISCOSITY MEASUREMENTS

Shear viscosities were measured using the Hoppler Rheo-Viscometer (cf. Chapter III). The reasons for the selection of this instrument include speed and simplicity of operation, use of small sample sizes (less than 20 ml), and excellent reproducibilty of results. Thus, the shear viscosity measurements could easily be conducted as supplementary measurements to the primary experiments involving drag reduction and extensional flow. A further advantage of this instrument is that it is capable of measuring fluid responses at high shear strain rates (of the order of 10,000 1/s). For the present investigation, this was desirable from a comparative standpoint, since the results from the extensional flow experiments were also conducted at similar high deformation rates.

The principal disadvantage of this instrument is that neither the shear stresses nor the shear rates are constant within the viscometer. As a result, while the sliding ball viscometer has been used to determine shear viscosities of Newtonian liquids, it has generally not been deemed an appropriate instrument for the determination of the rheological properties of non-

Newtonian liquids. However, recent analysis of such viscometer flow by Schonblom (1974) now allows the determination of shear stress-strain rate relationships for non-Newtonian, as well as for Newtonian liquids.

Goal

The goal of the shear viscosity measurements was to provide a quantitative measure of the shear behavior of the polymer test solutions for comparison with their drag-reducing and extensional flow behavior.

Scope

Shear viscosity measurements were conducted for the same polymer test solutions as used in the drag reduction and extensional flow experiments. Specifically, results are reported for Separan AP-273 solutions of additive concentrations of 5, 15, 20, 30, and 45 ppm; for 5, 10, and 20 ppm Separan AP-30 solutions; and for 20 and 30 ppm Polyox WSR-301 solutions.

Viscometer Flow Analysis

The Hoppler Rheo-Viscometer was developed in Germany at the onset of World War II for the measurement of shear viscosities of Newtonian liquids. According to the manufacturer (VEB Prufgerate-Werk Medingen, Sitz Freital, D.D.R.), the viscosity of a Newtonian liquid, μ, may

be obtained using the expression

$$\mu = K\hat{P}t \tag{4.1}$$

where K is a calibration constant, $\hat{P}$ is the force applied to the viscometer sphere divided by the sphere's cross-sectional area, and t is the time required for the ball to travel a set distance (usually 3.00 cm).

In 1974, Schonblom analyzed the flow in such a viscometer and developed procedures to determine shear viscosities for non-Newtonian liquids. In the remainder of this section, Schonblom's analysis will be briefly reviewed. First, the main assumptions in his analysis were that (1) the speed of the falling sphere was negligible when compared to the flow of the liquid and that (2) the flow was steady and parallel to the outer cylinder walls. In other words, the flow was effectively modeled as steady fluid flow through an eccentric annulus. With these assumptions and the application of conservation of mass and momentum equations across an annular fluid element, Schonblom derived the viscometer equation

$$1/t = \frac{4L^2}{\pi\, a^2 l_t \hat{P}^2} \int_0^\pi (a+\frac{d}{2}) \int_0^{\tau_w} \tau \gamma(\tau) d\tau d\alpha \tag{4.2}$$

where τ is the shear stress with τ_w being its value at the wall, γ is the shear strain rate, a is radius of the viscometer sphere, d is the annular width at angular location α, l_t is the distance through which the sphere travels in time t, and $\hat{P}$ is again the force applied to the viscometer sphere divided by its cross-sectional area. A definition sketch for the geometrical parameters a, d, and α is presented in Fig. 4.1. In arriving at eq. (4.2), Schonblom set the pressure gradient in the direction of the flow equal to the load, $\hat{P}$, on the sphere divided by an effective sphere length, L. This effective length, which has to be determined experimentally, was assumed to be a constant.

For a Newtonian fluid, the viscometer response may now be determined by substituting $\gamma(\tau)=\tau/\mu$ into the viscometer eq. (4.2), and integrating. After assuming the half annular width, d/2, was negligible when compared to the sphere radius, a, and after the wall shear stress was written in terms of the applied load, $\hat{P}$, Schonblom found the Newtonian viscometer response to be
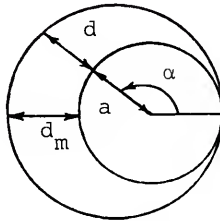
Fig. 4.1 Geometry of eccentric annulus.

$$\mu = (5d_m^3 \hat{P}t)/(96al_t L) \tag{4.3}$$

where d_m is the maximum annular width and the other variables are as previously defined. In comparison with eq. (4.1), we see that the flow response predicted by Schonblom is identical to the manufacturer's supplied expression for the shear viscosity when the ratio $(5d_m^3/96al_t L)$ is replaced by the manufacturer's constant K.

In his dissertation, Schonblom also presents evaluations of viscometer equation, eq. (4.2), for several cases of non-Newtonian behavior, including that for power law liquids. In one dimensional form, the constitutive relation for a power law liquid may be written as

$$\tau = \hat{K} \gamma^m \tag{4.4}$$

where both $\hat{K}$ and m are constants. The viscometer response for such liquid a may be determined by substituting eq. (4.4) into eq. (4.2) and integrating. Schonblom found the resulting response to be

$$1/t = \frac{d_m^M \, \Gamma(M+\tfrac{1}{2})}{2^{M-2}\sqrt{\pi} \; al_t L^{M-2} M\hat{K}^{1/m} \, \Gamma(M+1)} \, (\hat{P})^{1/m} \tag{4.5}$$

where $\Gamma(M+1/2)$ and $\Gamma(M+1)$ are Gamma functions with $M=(1+2m)/m$ and where the other variables are as previously defined. Thus, the viscometer response in terms of the measurable variables of applied load $\hat{P}$ and fall time t should also follow a power law type behavior. It may also be noted that for the case where $m=1$, the Newtonian solution, eq. (4.3), is recovered (with $\hat{K}$ becoming the shear viscosity coefficient).

For viscometer measurements which do not follow a power law response, Schonblom devised another more general procedure to determine the shear stress-strain rate relationship. It consisted of first determining the functional relationship between $\hat{P}$ and t, and then using it to solve eq. (4.2). For the details of this procedure, the reader is referred to Schonblom's dissertation. For the low additive concentration solutions used in this dissertation, it is expected that the laminar shear flow behavior exhibited in the viscometer will be nearly Newtonian (for the deformation rates to be examined) and that either eq. (4.1) or (4.4) should be adequate to describe shear behavior.

Viscometer Calibration

In order to use either eqs. (4.1), (4.3), or (4.5), the viscometer needs to be calibrated with a fluid of known viscosity to determine either the constant K for

use with eq. (4.1) or to determine the effective length L for use with eqs. (4.3) and (4.5).

Before determination of these calibration constants, it is necessary to discuss two limitations of the Hoppler Rheo-Viscometer. First, previous investigators (Lindgren, 1957; Schonblom, 1974) have noticed the presence of frictional resistance in the main ball bearing of the balance arm. This resistance reduces the effective load on the sphere and, if not corrected for, manifests itself as an apparent decrease in the calibration constant K for decreasing loads. Lindgren (1957) suggested that the true value of the calibration constant should be that which was associated with an infinite load. Schonblom (1974) followed this idea and determined that the bearing friction may be adequately accounted for by replacing the applied loading on the viscometer sphere with an effective load, $(\hat{P}-\hat{P}_f)$, where $\hat{P}_f$ is a constant representing the amount of frictional resistance. Thus, for more accurate representation of the true loads on the viscometer sphere, the effective load $(\hat{P}-\hat{P}_f)$ should be used in place of $\hat{P}$ in eqs. (4.1)-(4.5).

The resistance load, $\hat{P}_f$, may easily be determined through measurements made with a Newtonian liquid. After replacing the applied load, $\hat{P}$, with the effective loading $(\hat{P}-\hat{P}_f)$ in eq. (4.1) and

rearranging, one finds

$$\hat{P}t = \hat{P}_f t + (\mu/K) \qquad\qquad (4.6)$$

Thus, the frictional resistance load equals the slope of the line formed when the viscometer measurements are presented as a plot of $\hat{P}t$ versus t.

The second limitation on the use of this viscometer concerns flow transition within it. Lindgren (1957) noticed that when calibrating the instrument with distilled water, that at loads above a certain level, an abrupt lowering of the calibration constant occurred. Along with lower values for the calibration constant, greater deviations between repeated measurements were also noticed. Lindgren concluded that this phenomenon was almost certainly caused by turbulence in the measuring vessel. Schonblom (1974) also encountered this problem and further suggested that this phenomenon was associated with the viscometer sphere separating from the cylinder wall. After examination of this phenomenon, Schonblom concluded that transition occurs at

$$\hat{P}/\mu^2 \cong 1.52 \ m^2/Ns^2 \qquad\qquad (4.7)$$

Thus, use of the viscometer should be restricted to loads low enough so that the above criterion, eq. (4.7), is not exceeded.

The viscometer calibration consisted of conducting measurements with a fluid of known viscosity and using the results to determine the frictional resistance, $\hat{P}_f$, the general calibration constant, K, and the effective length, L. Distilled water was used as the calibration liquid with two separate sets of measurements being conducted at 20.7 and 24.7 ^{O}C. All measurements were made with a viscometer sphere of 1.596 cm in diameter and an outer measuring vessel of 1.603 cm in diameter. For each set of measurements, eight loads ranging from 245 N/m^2 to 1470 N/m^2 were applied, with at least two runs being made for each load.[1]

Determinations of the frictional resistance load, $\hat{P}_f$, were calculated to be 48.7 and 45.2 N/m^2 for the measurements made at 20.7 and 24.7 ^{O}C, respectively. An average value of 47 N/m^2 was then used to calculate the other calibration constants K and L. After determining K for each of the various loadings and averaging, the mean K value was found to be 5.80×10^{-8}, with the corresponding effective length being equal to 0.129 cm. With the exception of the lowest loading, all values of K were found to be within

---

[1] Some additional loads ranging up to 6860 N/m^2 were also applied, but whose results were not used in the calibration calculations. These measurements were only used to verify eq. (4.7). Treatment of these additional calculations is presented in Appendix B.

0.35% of the mean value. For further details of this calibration and for a listing of the experimental data, the reader is referred to Appendix B.

Experimental Procedure

First, polymer solution flow through the main experiment pipe at the desired additive concentration was established. Test samples for the viscometer measurements were then taken from the main experiment pipe (at the valve located just upstream of the conical channel set-up, with these channels being temporarily removed to facilitate access to this valve) and immediately transferred to the viscometer. Various loads were systematically applied to the viscometer sphere and resulting fall times were recorded.

During this process, the flow in the main experiment pipe was being conducted at a Reynolds number of $\bar{U}D/\nu$ =8000, and the mixing rate was set at either 10 or 30 rps.

For each test sample, eleven loads ranging from 245 N/m^2 to 2970 N/m^2 were applied, with two runs being made for each load. Between measurements on different samples, the viscometer sphere and measuring vessel were rinsed with alcohol and distilled water, with care being taken not to contaminate the surfaces with fingerprints.

Analytical Procedure

The viscometer measurements were evaluated using two procedures. First, shear stress-strain rate relationships were determined, following Schonblom's analysis, by using eqs. (4.4) and (4.5). Secondly, the viscometer measurements were evaluated by direct comparison of fall times with those for tap water (the solvent) at similar loading conditions.

In the first case, the experimental fluids were assumed to follow a power law response of the form of eq. (4.4). After calculating the average fall time, t, for each load, a linear least squares fit between $\log(1/t)$ and $\log(\hat{P}-\hat{P}_f)$ was determined for each set of measurements.[2] These least squares fits were expressed in the same form as eq. (4.5), and then, by eliminating the fall time between each of these equations and eq. (4.5), the power law constants $\hat{K}$ and m were determined.

In the second case, the relative increases in fall time, t_p/t_w (where t_p is the average measured fall time in the polymer solution and t_w is the corresponding fall time for water, as determined from the viscometer calibration) were calculated for each loading.

---

[2] To avoid transition effects, only measurements for applied loads of less than 1470 N/m^2 were used in the least squares analysis.

Experimental Results

The viscometer measurements may be found in Appendix C.

The results of the viscometer measurements, as analyzed by following Schonblom's procedure, are tabulated in Table 4.1. These results are presented as the power law constants $\hat{K}$ and m, estimated solution viscosities for a strain rate of 10,000 1/s, and the ratios of these viscosities to their solvent values at this strain rate. The solution viscosities, taken as stress to strain rate ratios, were determined using the power law model, eq. (4.4), with the appropriate constants.

In the determination of the power law constants, the applied viscometer loads ranged from 245 to 1470 N/m^2, and after accounting for frictional resistance, these loads effectively ranged from 199 to 1426 N/m^2. For this range of loads, the average wall shear stresses were calculated (by use of force balances across an annular fluid element) to have ranged from 3 to 19 N/m^2. Thus, the corresponding average strain rates encountered during the viscometer measurements ranged from about 3000 to 19,000 1/s. The results presented in Table 4.1 should be valid for over these ranges of shear stresses and strain rates.

From the results presented in Table 4.1, it can be seen that for laminar shear flow and for over the range

Table 4.1. Results of shear viscosity measurements expressed in terms of the power law constants $\hat{K}$ and m, including estimates of the solution viscosity (μ_p) and the ratio of solution to solvent viscosity (μ_p/μ_w) at a strain rate of 10,000 1/s. The test samples were maintained at temperatures of 24.7, 21.3, and 20.7 °C (each within ±0.06 °C) for the Separan AP-273, Separan AP-30, and Polyox WSR-301 runs, respectively.

Additive	Concentration (ppm)	Mixing Speed (rps)	Power Law Constants $\hat{K}$	Power Law Constants m	μ_p (N-s/m²)	(μ_p/μ_w) @ 10,000 1/s
Separan AP-273	45	10	.00118	.983	.00101	1.12
	30	10	.00108	.988	.00097	1.08
	20	10	.00090	1.005	.00094	1.04
	15	10	.00088	1.004	.00091	1.01
	15	30	.00083	1.012	.00093	1.03
	5	30	.00089	1.003	.00091	1.01
	0		.00086	1.005	.00090	1.00
Separan AP-30	20	10	.00134	.971	.00103	1.04
	10	10	.00121	.981	.00102	1.03
	5	10	.00105	.994	.00099	1.00
	0		.00104	.995	.00099	1.00
Polyox WSR-301	30	10	.00102	.999	.00101	1.02
	20	10	.00104	.996	.00100	1.01
	0		.00102	.997	.00099	1.00

of deformation rates studied that (1) the experimental solutions behaved in a Newtonian, or nearly Newtonian manner, and that (2) the solution shear viscosities were only marginally increased as a result of polymer addition at the concentration levels studied. Specifically, the 30 and 45 ppm Separan AP-273 solutions and the 10 and 20 ppm Separan AP-30 solutions demonstrated slight shear-thinning behavior, while the remaining solutions exhibited essentially Newtonian behavior.

Further, for each set of measurements, the degree of non-Newtonian behavior and the level of viscosity were found to decrease with concentration. As an example of the degree of non-Newtonian behavior and the level of viscosity measured, consider the results from the 45 ppm Separan solution. This solution exhibited the highest relative viscosity, having a 12% increase over the solvent viscosity at a strain rate of 10,000 l/s. As for its shear-thinning ability, its viscosity was found to decrease about 3% as the strain rate was increased from 3000 to 10,000 l/s.

In Table 4.2, the results from the direct comparisons of the behavior of the polymer solutions with that for their solvents are presented. For each loading condition, the ratios of the sphere fall time in the polymer solution to that for the solvent are listed. It can be seen for each solution, that these relative

Table 4.2. Direct comparison of polymer solution shear viscometer measurements with solvent behavior. Relative increases in fall time (t_p/t_w) are listed for each viscometer loading condition. The test samples were maintained at temperatures of 24.7, 21.3, and 20.7 °C (each within ±0.06 °C) for the Separan AP-273, Separan AP-30, and Polyox WSR-301 runs, respectively.

Additive	Conc.	Mixing Speed	Ratio of viscometer sphere fall times in the polymer solutions to that in water for effective loads of							
	(ppm)	(rps)	199	321	445	568	689	934	1179	1426 N/m²
Separan AP-273	45	10	1.14	1.13	1.11	1.11	1.11	1.11	1.10	1.09
	30	10	1.09	1.09	1.08	1.08	1.08	1.07	1.07	1.05
	20	10	1.03	1.04	1.04	1.04	1.04	1.04	1.04	1.03
	15	10	1.02	1.02	1.02	1.02	1.02	1.02	1.02	1.01
	15	30	1.00	1.02	1.02	1.03	1.03	1.03	1.03	1.02
	5	30	1.01	1.01	1.00	1.01	1.01	1.01	1.01	1.01
Separan AP-30	20	10	1.08	1.05	1.04	1.04	1.04	1.04	1.03	1.03
	10	10	1.04	1.03	1.02	1.02	1.03	1.02	1.02	1.01
	5	10	1.02	1.00	1.00	1.01	1.01	1.01	1.01	1.01
Polyox WSR-301	30	10	1.02	1.03	1.02	1.02	1.02	1.02	1.02	1.02
	20	10	1.02	1.03	1.01	1.01	1.01	1.02	1.01	1.02

increases in fall time are constant or decrease only slightly with increasing loads. This again indicates that only slight shear-thinning effects were occurring. Further, since the fall times were increased by only a few per cent, it may again be concluded that the solution shear viscosities were nearly the same as that for their solvents.

The results presented in Tables 4.1 and 4.2 are in general agreement with the expected behavior for dilute polymer solutions. For example, Darby (1970) measured the behavior of three polyacrylamide solutions for concentrations of 100, 200, and 500 ppm. These solutions were also found to be shear-thinning and approached Newtonian behavior for strain rates greater than about 10,000 1/s. However, Darby's results also illustrate that the present results can not be extrapolated to low strain rates. From nearly constant levels of apparent viscosity at high strain rates, his polyacrylamide solutions exhibited rapid decreases in viscosity as the strain rate was decreased from about 1000 1/s to 0.01 1/s, and then, for further decreases in strain rate, the apparent viscosities started to approach constant levels again. Such behavior can not possibly be predicted from a power law model determined from high strain rate data. Hence, the results reported in Tables 4.1 and 4.2 should not be extrapolated to lower strain rates.

Comments on the Viscometer Flow Analysis

Lastly, some comments on the viscometric flow analysis developed by Schonblom (1974) should be made. In his analysis, the flow was effectively modeled as steady flow through an eccentric annulus. Schonblom discussed the assumptions involved in this model and concluded that it would produce satisfactory results. However, it should be mentioned that such a model has yet to be experimentally verified for non-Newtonian flow. To verify Schonblom's model, results using his analysis should be experimentally compared with those obtained using a more widely accepted procedure for determining the high strain rate response of non-Newtonian liquids (e.g., capillary viscometry).

However, despite such a lack of model verification, the results and conclusions presented for the present series of experiments should still be valid. First, the majority of the solutions studied responded in a Newtonian manner and Schonblom's analysis accurately predicts the response for Newtonian liquids. For the remaining solutions, which exhibited only slight shear-thinning effects, it may be noted that Schonblom's power law analysis does reduce to the Newtonian result. Hence, it seems reasonable that the power law analysis can be used to determine slight non-Newtonian behavior. Further, even though the accuracy of the non-Newtonian

flow analysis is not known, the basic conclusions of the analysis are still valid, since the same conclusions were also arrived at through direct comparison of the responses of the polymer solutions to their corresponding solvent responses (without using Schonblom´s model).

CHAPTER V
DRAG REDUCTION MEASUREMENTS

In this investigation, drag reduction was determined from observations of flow rate and pressure drop in turbulent pipe flow. The polymer test solutions, which were used on a single-pass basis, were prepared "on-the-fly" by the injection of a concentrated master solution into the main flow at a mixer located just upstream of the experiment pipe. For a detailed description of the experimental set-up, the reader is referred to Chapter III.

Customarily, drag reduction has been quantified by the comparison of polymer solution and solvent friction coefficients (f_p and f_s respectively), which are evaluated at similar Reynolds numbers, R. More specifically,

$$\text{\% drag reduction} \quad 100(1-f_p/f_s)_{R=const.} \quad (5.1)$$

In this dissertation, this definition of the per cent drag reduction will also be referred to as the relative drag reduction. Two sets of drag reduction measurements are reported in this chapter. In the first set, friction

93

coefficients were determined for each test solution (of particular additive type, concentration, and mixing condition) for a series of different Reynolds number flows. In the second set, the flow was kept at a constant Reynolds number and the friction coefficients were determined for solutions (of a particular additive type and mixing condition) at various additive concentrations.

The use of turbulent pipe flow measurements to characterize the drag-reducing abilities of polymer solutions has been widely used. The gross flow measurements of flow rate and pressure drop can be conducted without intrusive probes and measurements for over a wide range of flow conditions can usually be quickly and easily made. To help obtain consistent reproducible results, the solutions in this investigation were used on a single-pass basis. Low concentration polymer solutions are often susceptible to degradation by shearing forces and a repeated recycling of them through a pipe would likely result in a lowering of their drag-reducing abilities. The use of an in-line injection technique to prepare the test solutions was also helpful in obtaining consistent results. By using a single master solution (for each additive), each of the test solutions was subjected to nearly identical preparation procedures. This avoided possible inconsistencies due to

variable solution preparation and handling procedures. A further advantage of using an in-line injection technique was that it allowed concentration effects to be easily examined, since the additive concentrations could be varied while holding other flow conditions constant.

Water Measurements

Before reporting the polymer solution measurements, the results of some experimental runs conducted with tap water (the solvent in all cases) are presented.

Measurements were conducted with tap water to check the operation of the equipment and to provide reference information on the solvent behavior of the test solutions.

Prior to these measurements, the flow meter and pressure transducers were individually calibrated. The water measurements then consisted of taking flow rate and pressure drop readings for over the range of flow rates that could be obtained in the system.

The results of three separate sets of measurements are presented in Figs. 5.1 and 5.2 for the upstream and downstream measuring sections respectively. These results are presented in the standard double logarithmic coordinates of friction factor, $f=(2D/l) \cdot (\Delta p/ \rho \bar{U}^2)$, versus Reynolds number, $R=\bar{U}D/\nu$. Here, D is the pipe diameter, $\bar{U}$ is the mean flow velocity, Δp is the
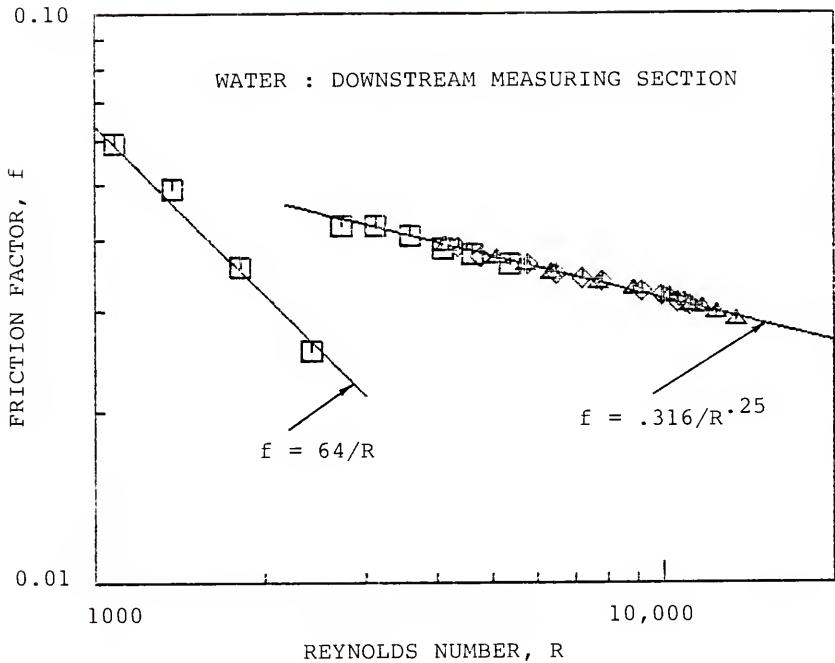
Fig. 5.1. The friction factor as a function of the Reynolds number for water flow through a pipe of diameter D=16 mm for the downstream measuring section (135D from the inlet). These measurements were conducted on three separate occasions at three different temperatures: 23.3 ^{O}C (▱), 21.6 ^{O}C (△), and 21.2 ^{O}C (◇).

0.10

WATER : UPSTREAM MEASURING SECTION

FRICTION FACTOR, f

$f = .316/R^{.25}$

$f = 64/R$

0.01

1000

10,000

REYNOLDS NUMBER, R

Fig. 5.2.   The friction factor as a function of the
Reynolds number for water flow through a pipe
of diameter D=16 mm for the upstream measuring
section (80D from the inlet). These
measurements were conducted on three separate
occasions at three different temperatures:
23.3 °C (□), 21.6 °C (△), and 21.2 °C (◇).

pressure drop along the pipe measuring section of length l, ρ is the mass density, and ν is the kinematic viscosity. For reference purposes, curves are presented for fully developed Poiseuille flow, $f=64/R$, and for smooth turbulent flow as represented by the Blasius equation, $f=.316/R^{.25}$. Least squares fits (for R>4000) yielded $f=.2495/R^{.2239}$ for data associated with the upstream measuring section and $f=.2862/R^{.2394}$ for the downstream measuring section.

It can be noticed that there is good agreement between the experimental values and the Blasius relation for both the upstream and downstream measuring sections. At a Reynolds numbers of 4000, the least squares fits of the experimental data from both measuring sections give friction factors that are about 1% less than those given by the Blasius relation and this difference decreases for increasing Reynolds number. Further, the variation of the experimental results from the least squares fits is less than 1% for most of the data points. For example, 80% of the measured points at the downstream section were within $\pm$1% of the least squares fit (with all of the remaining points being within $\pm$2% of the least squares fit).

For use later in this chapter, a least squares fit in the semi-logarithmic friction law coordinates of $1/f^{1/2}$, $f^{1/2}R$ for the water measurements from the

downstream measuring section is

$$1/f^{1/2} = 1.73\log(f^{1/2}R) + 0.01 \qquad (5.2)$$

for $500 < (f^{1/2}R) < 2200$.

Polymer Solution Measurements for Varying Reynolds Number

Goal

The goal of this set of polymer solution measurements was to provide a general quantitative description of the drag-reducing abilities of the test solutions in order to provide a basis for correlation of these abilities with their viscoelastic properties.

Scope

In this set of experiments, friction coefficients were determined for the polymer test solutions as a function of Reynolds number for Reynolds numbers ranging from 3000 to 14,000. The test solutions were examined for additive concentrations at 1, 2, 5, 10, 15, 20, 30, and 45 ppm for the Separan AP-273 solutions; at 5, 10, and 20 ppm for the Separan AP-30 solutions; and at 20 and 30 ppm for the Polyox WSR-301 solutions. (For a description of these additives and of solution preparation procedures, the reader is referred to Chapter III).

Two sets of mixing conditions were also examined. Initially, all test solutions were conducted with the rotational mixer operating at 10 revolutions per second (rps). From the previous investigations of Stenberg et al. (1977a, 1977b) and Inge et al. (1979) in which a similar set-up and mixer were employed, it was found that the effect of mixing at 10 rps was to disperse the polymer in the flow more evenly than without mixing. This tended to remove "irregular" data points with no loss of solution drag-reducing ability. For the second set of mixing conditions, the mixer was run at 30 rps. This speed was sufficient to introduce degradation effects (viz., loss of drag-reducing ability). Measurements were conducted with the mixer operating at 30 rps for the Separan AP-273 solutions of 5, 10, 15, and 20 ppm.

Experimental Procedure

Prior to the experimental measurements, the peristaltic injection pump was calibrated for each master solution. This calibration was then rechecked each day that polymer solution measurements were conducted. Further, immediately before and after each run, several measurements were made with tap water to check the operation of the equipment.

The polymer solution measurements consisted of setting the main flow rate, followed by adjusting the peristaltic pump to inject the appropriate amount of additive (to maintain the desired concentration), and then taking flow rate and pressure drop readings as soon as these readings stabilized (usually in a minute or two). Typically, the flow rate was then increased in a small increment and the above steps were repeated. After conducting a series of measurements by systematically increasing the flow rate, several data points were then taken at random flow rates. The only difference ever noticed between taking the data in a random order as opposed to a systematic order was that it took longer for the random points to achieve stable readings. During each run, the mixer was kept at a constant rotational speed, which was continually monitored with an electromagnetic tachometer.

Analytical Procedure

The gross flow measurements of pressure drop and flow rate can be used to examine drag reduction in a variety of ways. In this investigation, the experimental measurements were used to calculate friction coefficients as a function of Reynolds number, to determine the relative drag reduction as a function of a characteristic flow time scale, and to examine the flow structure using the semi-logarithmic friction law parameters.

Friction coefficients and Reynolds numbers were determined in the same manner as that used for the water measurements, with solvent values being used for the viscosities in the Reynolds number determinations.

Presenting the experimental data in the form of friction coefficients as a function of Reynolds number is convenient for the comparison of the data with the well known Newtonian behavior. However, it has been found that these dimensionless variables are not sufficient to completely describe polymer solution behavior. Often, a "diameter effect" can be noticed, where a different f-R relationship is observed depending on the diameter of the pipe. In particular, "onset" usually occurs at increasing Reynolds numbers for increases in pipe diameter. As mentioned in Chapter II, most investigators feel that "onset" will occur when some time scale of the turbulent motions is of the same order of magnitude as some characteristic time scale of the polymer molecules. This suggests that an appropriate manner of examining this phenomenon would be to determine the relative drag reduction as a function of either the characteristic time scale, ν/u_*^2, of the turbulent motions near the wall or of a ratio of this flow time scale to a molecular time scale. At this point in this investigation, the relative drag reduction was determined as a function of the turbulent time scale ν/u_*^2. In computing these time

scales, solvent values were used for the kinematic viscosities and a force balance along the pipe measuring section, $(\rho\, u_*^2)\cdot\pi Dl = \Delta p(\pi/4)D^2$, was used to calculate the square of the friction velocities.

Investigators have also found the semi-logarithmic representation of $f^{-1/2}$ versus $\log(f^{1/2}R)$, useful for presenting and evaluating gross flow drag reduction measurements. In this formulation, the drag reduction trajectories after onset are often well approximated by straight lines, with the slopes of these lines being independent of pipe diameter (Virk, 1975). Investigators (Virk, 1975; Berman, 1977b, 1978) have found the linear relationship between these parameters useful for estimating "onset" conditions and for obtaining information on the increases in the buffer layer thickness of the polymer solutions. Further, since the slopes of the drag reduction trajectories are independent of pipe diameter, drag reduction may often be completely described by specifying only two parameters: a slope parameter and an "onset" parameter.

The estimates of the "onset" conditions may be determined from the coordinates of the intersections of the drag reduction and solvent trajectories. These coordinates can then be expressed in terms of an appropriate "onset" parameter, for example, as a multiple of the turbulent time scale ν/u_*^2.

The increases in buffer layer thickness may be determined using the following analysis. First, consider the logarithmic portion of the turbulent velocity profile for solvent (Newtonian) flow in a smooth pipe. This may be expressed as

$$u_s^+ = A \log(y^+) + B \qquad (5.3)$$

where (as previously described in Chapter II) u_s^+ is the dimensionless velocity of the solvent $(u_s^+ = U/u_*)$, y^+ is the dimensionless distance from the wall $(y^+ = yu_*/\nu)$, $U = U(y)$ is the average flow velocity at a distance y from the wall, u_* is the friction velocity, and A and B are the constants 2.5 and 5.6. Integrating this relation over the pipe radius (neglecting the wall and buffer layers), dividing by the cross sectional area, and then rewriting in terms of friction coefficients and Reynolds numbers yields the equation

$$1/f_s^{1/2} = \hat{A}_s \log(f_s^{1/2}R) + \hat{B}_s \qquad (5.4)$$

where $\hat{A}_s$ and $\hat{B}_s$ are constants that have been found experimentally to be 2.0 and −0.8 and where the subscript s again denotes solvent (Newtonian) conditions.

For polymer solution flow, the logarithmic velocity profile is displaced to higher velocity levels and may be written as

$$u_p^+ = u_s^+ + \Delta B \qquad (5.5)$$

where ΔB is the increase in the buffer layer thickness and where the subscript p denotes polymer solution conditions. After, integrating and manipulating this equation in a similar manner as for the solvent case, the friction relation for polymer solution flow becomes

$$1/f_p^{1/2} = \hat{A}_s \log(f_p^{1/2}R) + \hat{B}_s + \Delta B/8^{1/2} \qquad (5.6)$$

By subtracting eq. (5.4) from eq. (5.6) (for similar $f^{1/2}R$ values for both the solvent and solution) and then rearranging; the increase in buffer layer thickness is found to be

$$\Delta B = (1/f_p^{1/2} - 1/f_s^{1/2})/8^{1/2} \qquad (5.7)$$

This quantity may be determined from the experimental measurements in the following manner. First, it is assumed that the drag reduction trajectories can be expressed as

$$f^{-1/2} = \hat{A}_p \log(f^{1/2}R) + \hat{B}_p \qquad (5.8)$$

where $\hat{A}_p$ and $\hat{B}_p$ are constants. Subtraction of eq. (5.4) from this expression yields

$$(1/f_p^{1/2}-1/f_s^{1/2}) = (\hat{A}_p-\hat{A}_s)\log(f^{1/2}R) - (\hat{B}_p-\hat{B}_s) \qquad (5.9a)$$

Then, by expressing the constant $(\hat{B}_p-\hat{B}_s)$ in terms of "onset" values (denoted by the subscript o)

$$(\hat{B}_p-\hat{B}_s) = \delta_A \log(f^{1/2}R)_o$$

eq.(5.9a) can be rewritten as

$$(1/f_p^{1/2}-1/f_s^{1/2}) = \delta_A \log[(f_p^{1/2}R)/(f_p^{1/2}R)_o] \qquad (5.9b)$$

or, in terms of "onset" time scales, as

$$(1/f_p^{1/2}-1/f_s^{1/2}) = \delta_A \log[(\nu/u_*^2)_o/(\nu/u_*^2)] \qquad (5.9c)$$

where δ_A is the slope difference $(\hat{A}_p-\hat{A}_s)$.

Lastly, by using eq. (5.9c) to substitute for $(1/f_p^{1/2}-1/f_s^{1/2})$ in eq. (5.7), the increase in buffer layer thickness may be expressed as

$$\Delta B = \delta_A \log[(\nu/u_*^2)_o/(\nu/u_*^2)]/8^{1/2} \qquad (5.10)$$

Thus, the increases in the buffer layer thickness can be determined by using eq. (5.10) with the experimentally determined slopes of the drag reduction trajectories and "onset" time scales. It should also be noted that this anaylsis is only valid for low levels of drag reduction, where the logarithmic portion of the velocity profile is the dominant feature of this profile.

Experimental Results

For a complete presentation of the experimental results for this set of polymer solution measurements, the reader is referred to Appendix D. In this appendix, flow temperatures, flow rates, mean velocities, friction velocities, pressure drops, friction factors, Reynolds numbers, wall strain rates, relative drag reduction values, and the friction law parameters of $f^{-1/2}$ and $f^{1/2}R$ are reported for all of the measurements made during each experimental run.

In this section, the drag reducing behavior of the test solutions is examined using $f^{-1/2}$, $\log(f^{1/2}R)$ diagrams. First, to obtain a general overall view of the behavior of the test solutions, the results of some selected runs are plotted in Figs. 5.3-5.5 for measurements made at the downstream measuring section. In Fig. 5.3, the results of measurements made with Separan AP-273 solutions having additive concentrations

of 5, 15, 30, and 45 ppm are presented. In Fig. 5.4, measurements made with 5, 10, and 20 ppm Separan AP-30 solutions are shown and Polyox WSR-301 measurements at 20 and 30 ppm are presented in Fig. 5.5. These measurements were conducted using 1% master solutions with the mixer rotating at 10 rps, and with the flow temperatures at $25^{\circ}C$ for the Separan AP-273 runs and $21^{\circ}C$ for the Separan AP-30 and Polyox WSR-301 runs. For reference purposes, the curves for fully developed Poiseuille flow, $f^{-1/2}=(f^{1/2}R)/64$, and for smooth turbulent flow as represented by a least squares fit of the measurements made with tap water, eq. (5.2), are also presented. The dashed lines in these figures represent linear least squares fits of the experimental data. For a listing of the slopes and intercepts of these least squares fits and for the range of data used in each regression analysis, the reader is referred to Table 5.1.

From previous investigations (eg., see Virk (1975)), it has been found that for the majority of drag-reducing solutions, the gross flow trajectories follow Poiseuille's law for laminar flow, observe a normal transition to Newtonian turbulent flow, and then follow this turbulent curve until "onset." After "onset," $f^{-1/2}$ is found to increase linearly with $\log(f^{1/2}R)$, with the slopes of these trajectories increasing with concentration (at least until the maximum drag reduction
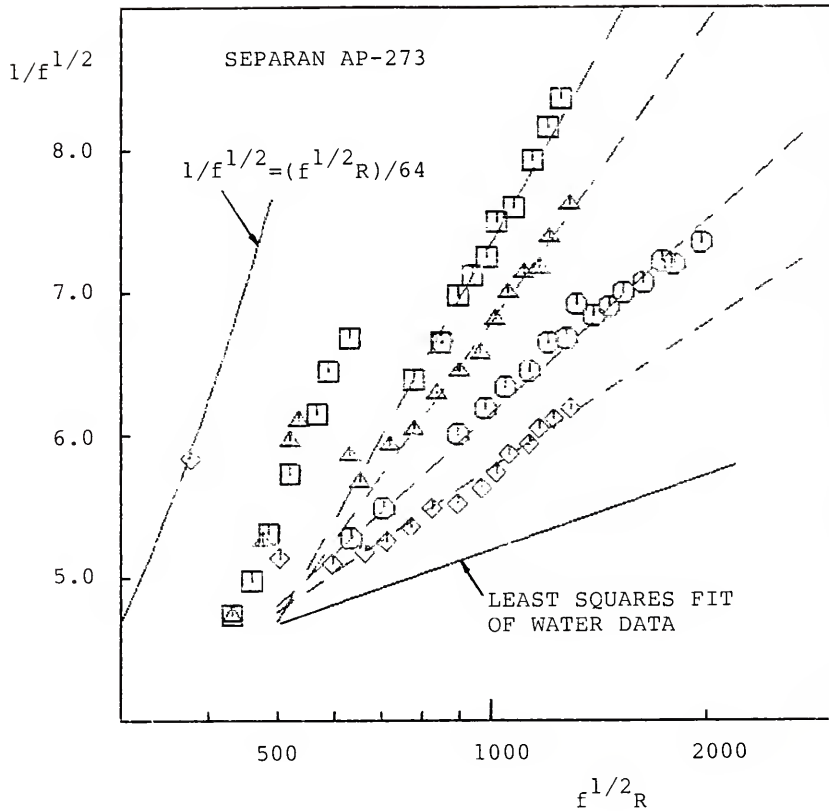
Fig. 5.3. Flow trajectories for 5 ($\diamondsuit$), 15 ($\odot$), 30 ($\triangle$), and 45 ($\square$) ppm Separan AP-273 solutions0(10 rps mixing, 1% master solution, downstream measuring section).
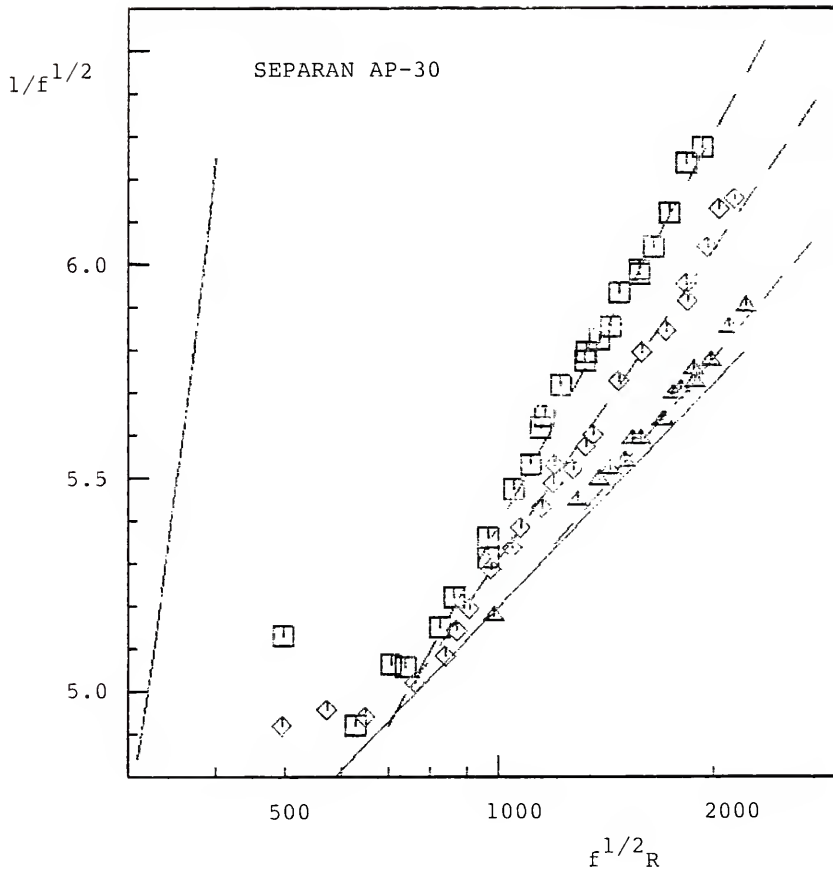
Fig. 5.4. Flow trajectories for 5 ($\triangle$), 10 ($\diamondsuit$), and 20 ($\square$) ppm Separan AP-30 solutions (10 rps mixing, 1% master solution, downstream measuring section).
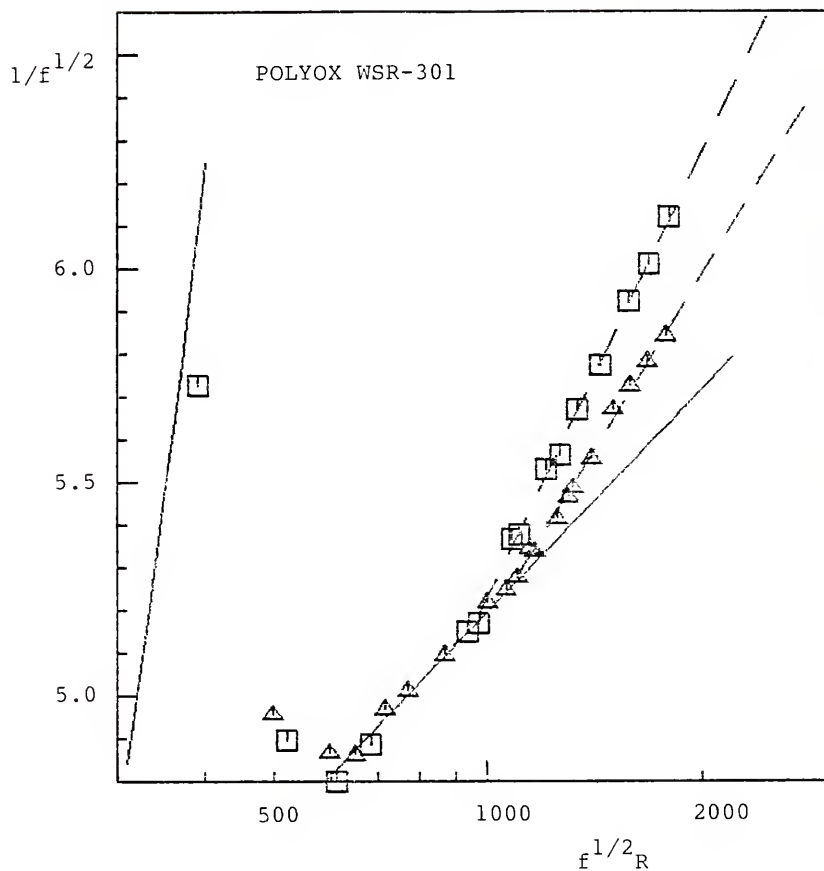
Fig. 5.5.   Flow trajectories for 20 ($\triangle$) and 30 ($\square$) ppm
Polyox WSR-301 solutions (10 rps mixing, 1%
master solution, downstream measuring section).

asymptote has been reached). However, if the concentration is sufficiently high enough, normal transition can be suppressed with the gross flow trajectories going directly from the laminar flow regime to the drag-reducing regime.

Generally, the present polymer test solutions have been found to behave as in these previous investigations. It can be seen in Figs. 5.3-5.5 that after "onset," all of the gross flow trajectories are quite well approximated by straight lines and their slopes are seen to increase with concentration. It may also be noted that the trajectories of the Polyox solutions appear to observe a normal transition and then follow the Newtonian smooth turbulent flow curve until "onset." For the Separan solutions, "onset" generally occurred at lower $f^{1/2}R$ values than for the Polyox solutions; and as can be seen in Fig. 5.3, drag reduction is even evident before the transition from laminar to Newtonian turbulent flow is complete for some of the solutions. Further, with respect to the Separan additives, it can be noted that the higher molecular weight grade polymer, Separan AP-273, is the more effective drag-reducer.

In Fig. 5.6, results are presented for 5 ppm Separan AP-273 solutions with the mixer operating at 10 and 30 rps for runs made using both 1% and 0.2% master
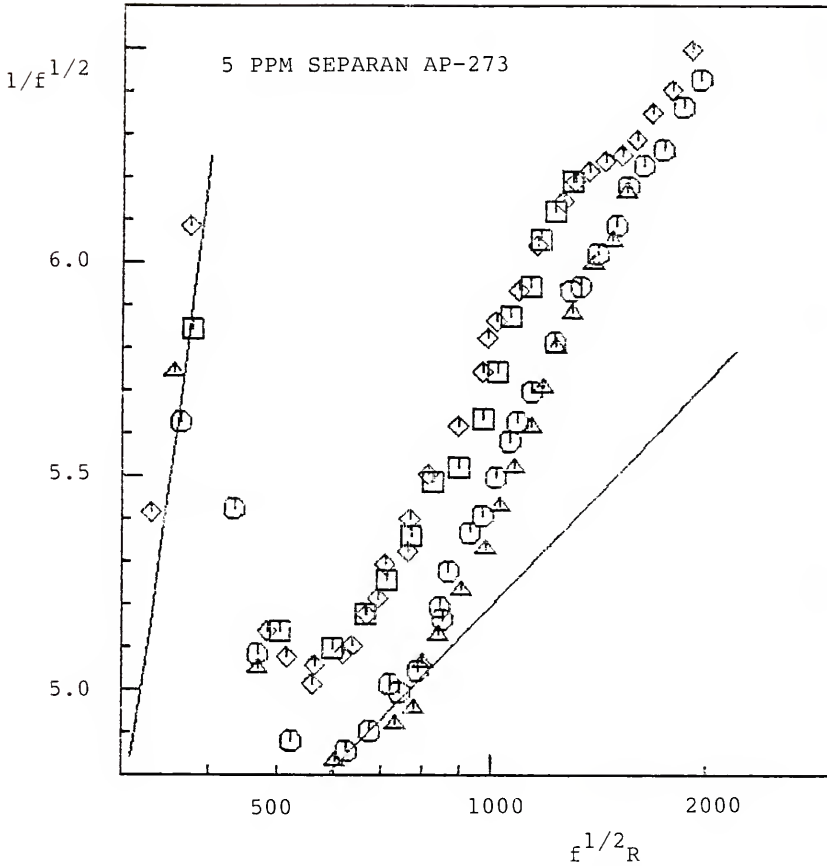
Fig. 5.6. Flow trajectories for 5 ppm Separan AP-273
solutions with 10 (□) and 30 (△) rps mixing
for a 1% master solution and with 10 (◇) and
30 (⊙) rps mixing for a 0.2% master solution,
with all results being reported for the
downstream measuring section.

solutions. These measurements were taken at the downstream measuring section and the solid lines indicate the same reference lines as in Figs. 5.3-5.5. First, it can be seen that for these solutions there is little difference between the runs made using the 1% and 0.2% master solutions. Secondly, for increases in mixing rate, decreases in drag reduction were observed with the main effect being a delay of "onset" to higher $f^{1/2}R$ values. At 10 rps, "onset" occurred during the transition process, while at 30 rps, "onset" did not occur until after the smooth turbulent curve was reached. Some slight increases in the slopes of the trajectories also occurred with the increase in mixing rate. For runs with 15 and 20 ppm Separan AP-273 solutions, similar mixing effects were also noticed.

In Fig. 5.7, results are presented for the 1 and 2 ppm Separan AP-273 solutions with the mixer operating at 10 rps. These measurements, which are again being reported for the downstream measuring section, were made using a 0.2% master solution. For both solutions, a certain low level of drag reducing behavior is noticed without any clearly defined "onset." Such behavior has also been previously observed. Berman (1980) has reported that for polyelectrolytic drag-reducing solutions (as are the Separan solutions), the gross flow trajectories do not necessarily follow the Newtonian
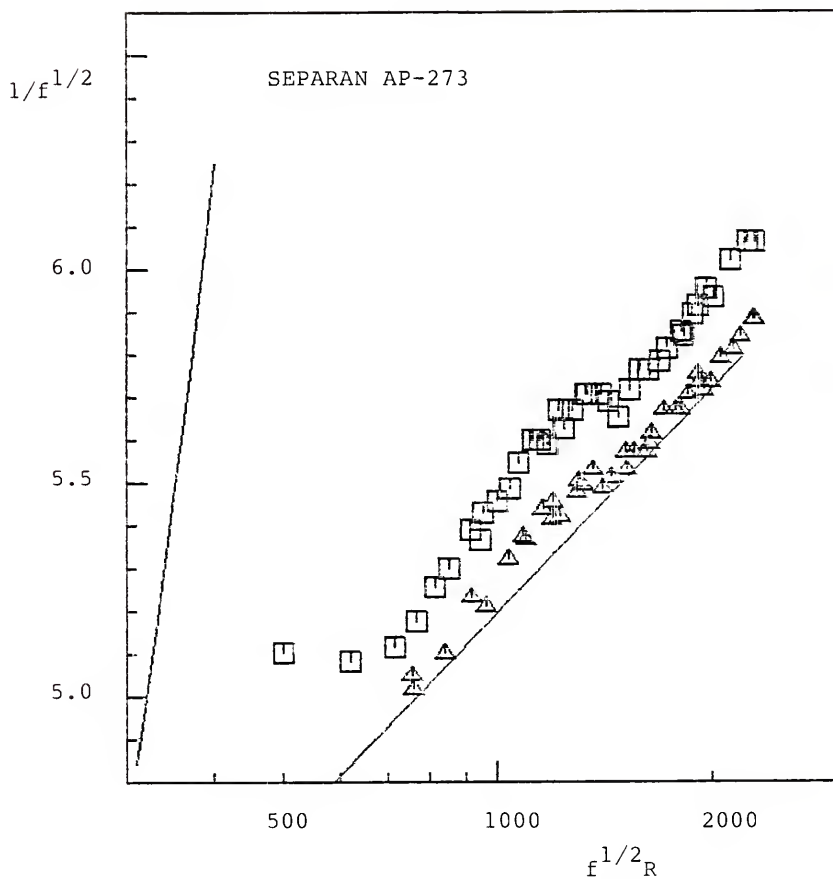
Fig. 5.7. Flow trajectories for 1 ($\triangle$) and 2 ($\square$) ppm Separan AP-273 solutions (10 rps mixing, 0.2% master solution, downstream measuring section).

turbulent flow curve, but instead, may follow a curve parallel to it (and displaced to higher $f^{-1/2}$ values). In such cases, a linear drag-reducing region is still observed at sufficiently high $f^{1/2}R$ values. For the present results, it appears that this linear region starts at about $(f^{1/2}R)=1500$; however, the overall level of drag reduction is too low to accurately determine such a trend.

All of the measurements that have been reported so far (Figs. 5.3-5.7) were for the downstream measuring section. At this point, it should be noted that no significant differences between the results from the two measuring sections were ever observed. However, some slight deviations between the results from these two sections did occur for the highest $f^{1/2}R$ values of each run. As an example, consider the results for the 5 ppm Separan Ap-273 solution (30 rps, 0.2% master solution) shown in Fig. 5.8. It can be seen that the results from both measuring sections are similar, except for $(f^{1/2}R)>1500$, where the $f^{-1/2}$ values for the upstream measurements are about 1% less than for the corresponding downstream measurements. Since these differences are of the order of the accuracy of the experiments, no conclusions are drawn about their causes.

Least squares fit lines were determined for the experimental data which formed the drag-reducing sections
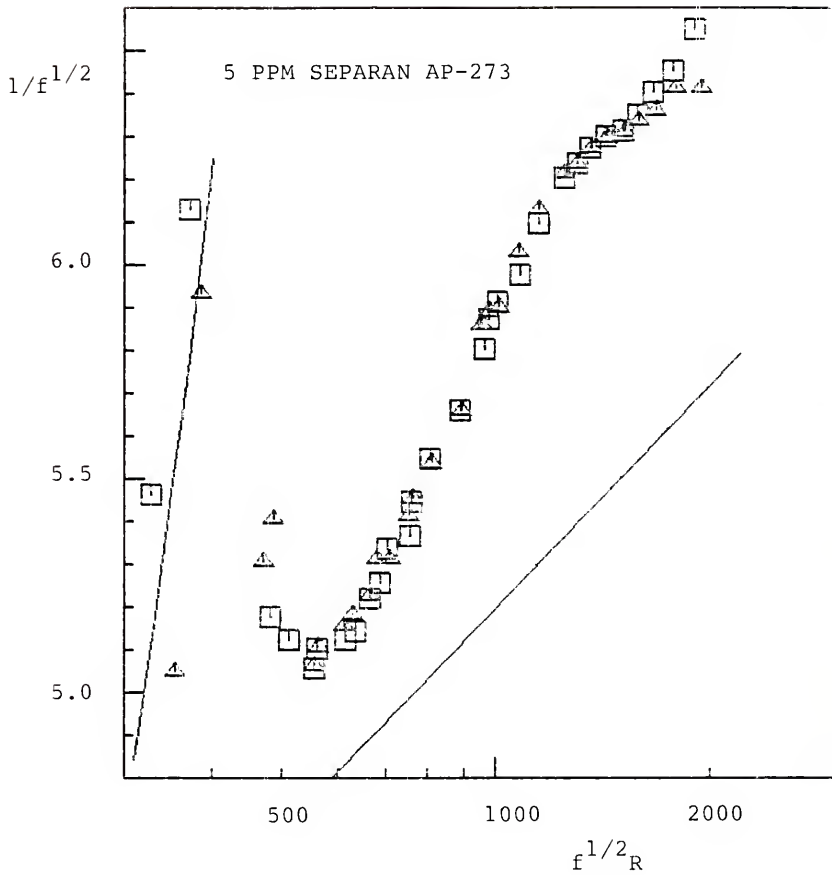
Fig. 5.8. Flow trajectories for a 5 ppm Separan AP-273 solution with 30 rps mixing and a 0.2% master solution for both the upstream ($\triangle$) and downstream ($\square$) measuring sections.

of the gross flow trajectories. More specifically, the slopes $\hat{A}_p$ and intercepts $\hat{B}_p$ were determined for drag reducing trajectories of the form of eq. (5.8). From these parameters, slope differences (from water flow) and "onset" strain rates were calculated. The slope differences (δ_A) were calculated by subtraction of the slope of the Newtonian turbulent line as determined from a least squares fit of the water measurements (cf. eq. (5.2)) from the slopes ($\hat{A}_p$) of the least squares fits of the drag reduction data. The "onset" strain rates (taken as the reciprocal of the inner turbulent time scale at "onset," ($\nu/u_*^2)_o$)), were determined from the coordinate values of the intersections of the drag reduction trajectories with the Newtonian turbulent line. For the cases where drag reduction was evident before the Newtonian turbulent line was reached, the "onset" points were determined from the intersections of extensions of the the drag reduction trajectories with the Newtonian turbulent line. Solvent values were used for the shear viscosity coefficients in these calculations. The results of these calculations are presented in Table 5.1, with the slope differences, "onset" strain rates, and the range of $f^{1/2}R$ values covered in the least squares fits of the drag-reducing data being listed.

At this point, it should be noted that the scales of motion at "onset" represent scales characteristic of the

Table 5.1. Summary of drag reduction data (downstream measuring section).

Master Solution conc.	Additive	conc. (ppm)	Mixing speed (rps)	$(u_*^2/\nu)_o$ (1/s)	δ_A	$f^{1/2}_R$ Range of Least Squares Fit
1%	Separan AP-273	45	10	111	7.10	700-1500
		30	10	111	5.22	700-1600
		20	10	75	3.57	600-1800
		15	10	98	3.57	700-2000
		10	10	†	†	†
		5	10	104	1.61	550-1500
0.2%	Separan AP-273	5	10	117	1.84	600-1300
		2	10	*	*	*
		1	10	*	*	*
1%	Separan AP-30	20	10	255	1.31	950-1950
		10	10	280	.68	900-2200
		5	10	486	.23	1350-2250
1%	Polyox WSR-301	30	10	446	1.74	1050-1850
		20	10	571	1.00	1150-1800
1%	Separan AP-273	20	30	191	5.37	700-1850
		15	30	247	3.89	750-2000
		10	30	†	†	†
		5	30	300	2.37	800-1550
0.2%	Separan AP-273	5	30	253	1.99	800-1700

* Values not determined.
† Data for the 10 ppm solutions not included due to unreliable performance of injection pump.

turbulent motions at the point where the drag reduction effect first becomes measurable and starts to noticeably increase in magnitude. As such, these "onset" scales can be used as convenient parameters for comparison purposes; however, they may not represent actual "onsets" of the phenomenon. There are two main reasons for this. First, drag reduction may be the result of some "continuous" process, in which case, a true "onset" can not be defined. Secondly, since in turbulent flows a wide variety of motions with varying time scales occur and since the polymer solutions are inhomogeneous, it is not possible from gross flow measurements to determine the precise scales of motion that are being affected.

The results listed in Table 5.1 are presented graphically in Figs. 5.9 and 5.10. First, in Fig. 5.9, the "onset" strain rates are plotted as a function of additive concentration. The solid lines, which are used for visual purposes only, connect each set of data points that were determined under similar experimental conditions (viz., similar mixing rates and master solution concentrations). It can be seen that the Separan AP-273 solutions (10 rps, 1% master solution) have the lowest "onset" strain rates and these appear to be nearly constant with respect to concentration. The other solutions exhibited greater "onset" strain rates and these are seen to decrease with increasing
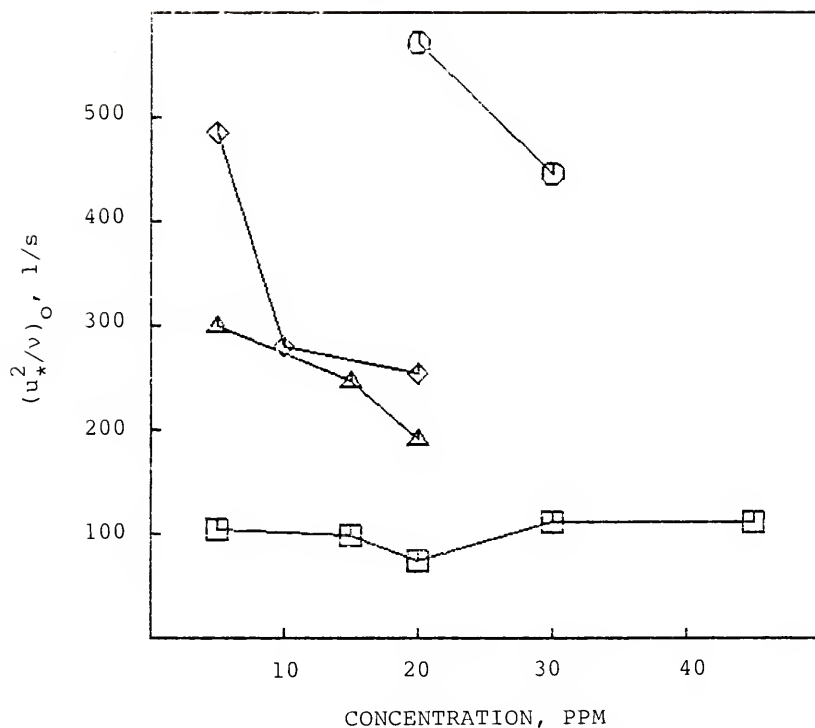
Fig. 5.9   Wall strain rate at "onset" as a function of
additive concentration.

concentration. Generally, the impression one gets is that at low concentrations, an increase in concentration will decrease the "onset" strain rate until some saturation condition is reached, after which the "onset" strain rate will be independent of concentration. Also, it can again be seen that the effect of increasing the mixing rate and of using lower molecular weight grade additives (for a given polymer) will increase the "onset" strain rate.

In Fig. 5.10, the slope difference (δ_A) is plotted as a function of concentration for the results presented in Table 5.1. The solid lines are again used to connect related data points. It can be seen that the slopes of the drag reduction trajectories increase with concentration. Both the Separan AP-30 and Polyox WSR-301 solutions exhibited nearly the same magnitudes of slope difference and the rates of increase of this difference with concentration were also found to be similar. The Separan AP-273 solutions were found to exhibit greater slope differences and the rates of increase of slope difference with concentration were also found to be greater than for the Separan AP-30 and Polyox WSR-301 solutions. With regards to the mixing of the Separan AP-273 solutions, the slope differences at the higher speed mixing, 30 rps, were found to be greater than for the mixing at 10 rps.
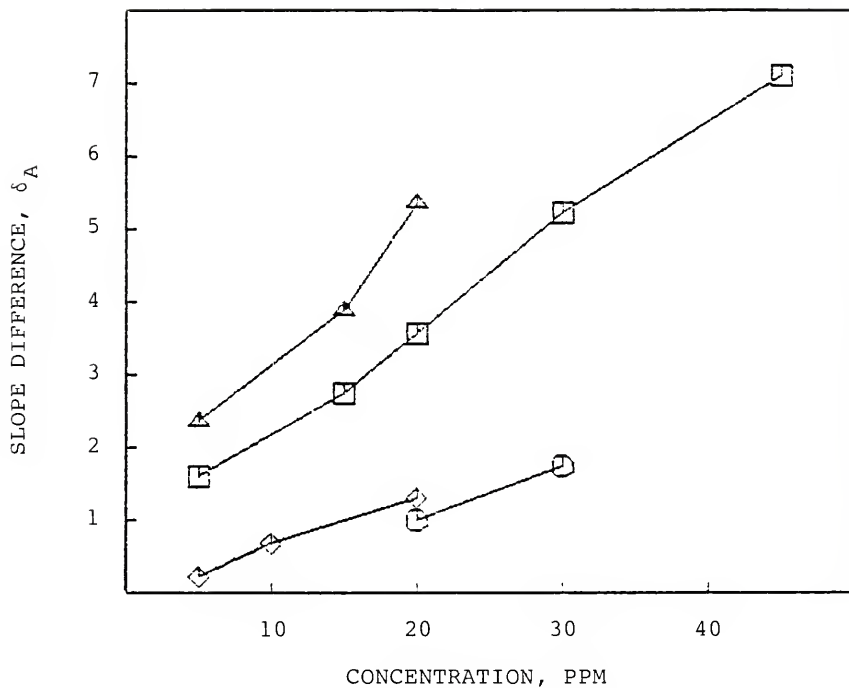
Fig. 5.10. Slope difference as a function of additive
concentration.

In summary, the goal of this set of measurements was to provide a quantitative description of the drag-reducing behavior of the test solutions in order to provide a basis for the comparison of this behavior with their viscoelastic properties. By using semi-logarithmic $1/f^{-1/2}$, $f^{1/2}R$ plots, the drag reduction trajectories have been were described by specifying slope differences (from water flow) and "onset" strain rates (cf. Table 5.1). Friction coefficients, Reynolds numbers, relative drag reduction values, and wall strain rates as shown in Appendix D have also been determined for all of the experimental measurements.

Generally, the drag-reducing behavior of the test solutions was as expected. In the semi-logarithmic $1/f^{-1/2}$, $f^{1/2}R$ diagrams, the drag reduction trajectories were found to be well approximated by straight lines, with the slopes of these lines increasing with additive concentration. The "onset" of drag reduction was found to occur at increasing flow strain rates for decreases in additive concentration, with the exception of some of the Separan runs where "onset" was independent of concentration. The main effect of increased mixing was mainly to delay "onset," with the slopes of the trajectories also increasing slightly. With regards to additive molecular weight, the higher molecular weight grade of the two Separan additives was found to be the more effective drag-reducer.

Polymer Solution Measurements for Varying Concentration at Constant Reynolds Number

Goal

This set of measurements has been conducted in order to examine the polymer solutions used in this investigation for evidence of molecular interaction during drag reduction.

Scope

In these experiments, friction coefficients were determined as a function of concentration for flows at constant Reynolds numbers. Measurements were conducted for each of the three polymers examined in the previous section for flows at several different Reynolds numbers with additive concentrations ranging from 0.2 to 70 ppm. In this section, results are reported for runs conducted at Reynolds numbers of 8,000 and 14,000. At R=8,000, measurements are reported for runs conducted with a 1% Separan AP-30 master solution and 10 rps mixing. At R=14,000, measurements made with a 1% Polyox WSR-301 master solution are examined for the mixer operating at 10 rps and 30 rps, and measurements are also reported for runs conducted with a 0.06% Separan AP-273 master solution for the mixer operating at 10 rps.

Experimental Procedure

In this set of measurements, the same experimental set-up was utilized as for the previously described polymer solution measurements. For the present measurements, an experimental run consisted of first setting the main flow rate and, without additive injection, taking pressure drop and flow rate readings. Then, the peristaltic pump was turned on and the polymer master solution was injected into the main flow at a measured rate. During this process, the main flow rate was readjusted to maintain its original value. (Since the shear viscosities of the test solutions at high strain rates did not vary very much with concentration, maintaining a constant flow rate was essentially the same as keeping the Reynolds number constant.) After the flow stabilized, the change in pressure drop from that for the solvent was recorded. The injection rate of the polymer master solution was then varied and the above steps were repeated. This entire process was continued until flow responses for over the desired concentration range were obtained.

To determine the amount of drag reduction (cf. eq. 5.1), the change in pressure drop from the corresponding solvent flow needs to be known. One method of determining this is to measure the pressure drops in both the solution and solvent flows and then subtract one from

the other.   However, at very   low   concentrations,   the
change   in   pressure drop is small compared to   the   total
pressure   drop.   Thus, any uncertainites   in   the   total
pressure   drop measurement, while being small with respect
to   this   value, can still be large when compared   to   the
change   in   pressure   drop.   To avoid   this   problem,   the
chart   recorder was set to measure the change in   pressure
drop   directly.   The   total   pressure   drop   along   the
measuring   section   was first recorded for   solvent   flow.
The   span of the chart recorder was then set to a   smaller
span   setting   and   re-zeroed   so that   the   signal   would
correspond   to a full scale reading.   Additives were   then
injected   into   the flow and the change in   pressure   drop
was   directly   recorded   for the   polymer   solution   flow.
Since   a   smaller   span was used for these   readings,   the
change   in   pressure drop caused a greater   deflection   in
the   chart   recorder   pen   and   allowed   a   more   precise
determination   of   the magnitude of this change   (than   if
total pressure drops were measured).

As for the previous polymer solution measurements,
the   calibration   of   the peristaltic injection   pump   was
checked   prior to each run.   Also, water measurements were
conducted   immediately before and after each run to   check
the operation of the equipment.

128

Analytical Procedure

"If the phenomenon of drag reduction is due to the interaction of isolated polymer molecules with the surrounding solvent rather than on interparticle effects, the drag reduction would be expected to increase linearly with concentration at least for low concentrations" (Paterson and Abernathy, p. 707, 1970).

To examine the present experimental results for evidence of molecular interaction during drag reduction, the procedures of previous investigators (Virk, 1966; Paterson and Abernathy, 1970; Berman, 1978) were followed and the ratio of drag reduction to additive concentration (the specific drag reduction) was plotted as a function of concentration. If molecular interaction is not a significant factor in drag reduction, then the specific drag reduction would be expected to approach a constant value in the limit of decreasing concentration.

Experimental Results

In Fig. 5.11, specific drag reduction has been plotted as a function of concentration for the measurements conducted at a Reynolds number of 8,000 with a 1% Separan AP-30 master solution and 10 rps mixing. In this figure, it can be seen that as the concentration is increased, the specific drag reduction increases to a maximum and then decreases with further increases in
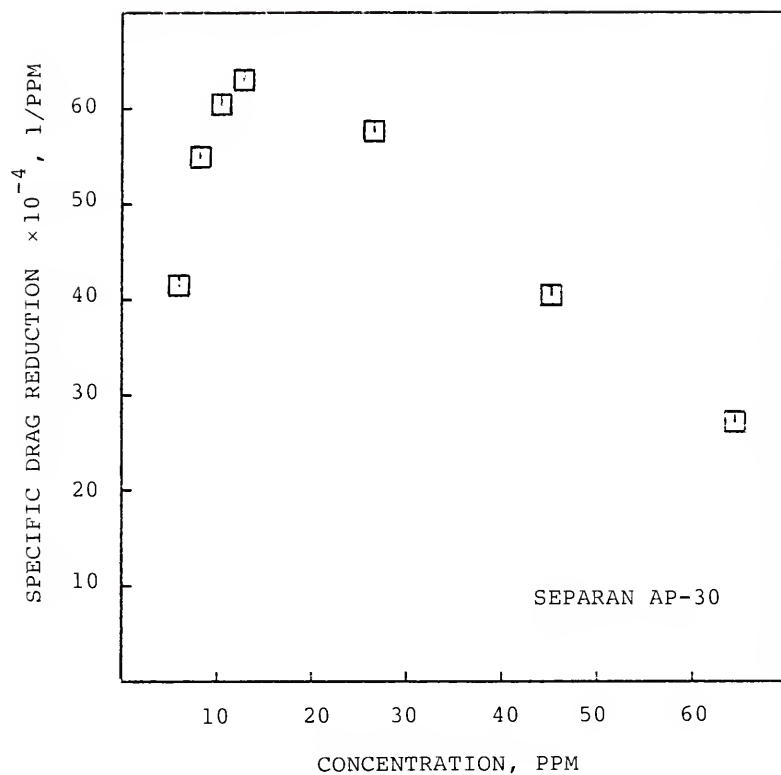
Fig. 5.11   Specific drag reduction as a function of
             additive concentration for Separan AP-30 with
             the flow being conducted at a Reynolds number
             of 8000 (1% master solution, 10 rps mixing,
             downstream measuring section).

concentration.   This   type of behavior was found   to   be
followed for all of the experimental runs.

No evidence for the existence of a constant level of
specific drag reduction in   the limit of decreasing
concentration (intrinsic drag reduction) was ever found.
In fact, for the Polyox runs, no drag reduction at all
was observed at the lowest concentrations.   As an
example, consider the results of the Polyox runs
(R=14,000; 10 and 30 rps mixing; 1% master solution)
presented in Fig. 5.12. Here, at concentrations at less
than 10 ppm, not only was drag reduction not observed,
but negative specific drag reduction values were found
due to pressure drop increases. It seems likely that
these pressure drop increases (which were of the order of
1%) were the result of shear viscosity increases and that
these viscous effects apparently dominated any drag-
reducing effects at these low concentrations.

For the Separan runs, specific drag reduction was
also found to decrease with decreasing concentration;
however, in contrast to the Polyox runs, drag reduction
was always observed no matter how low the concentration
was.   In Fig. 5.13, some low concentration Separan AP-273
results are presented (0.06% master solution, 10 rps).
It can be seen that even for concentrations as low as
0.25 ppm, drag reduction (of 0.025%) was still observed.
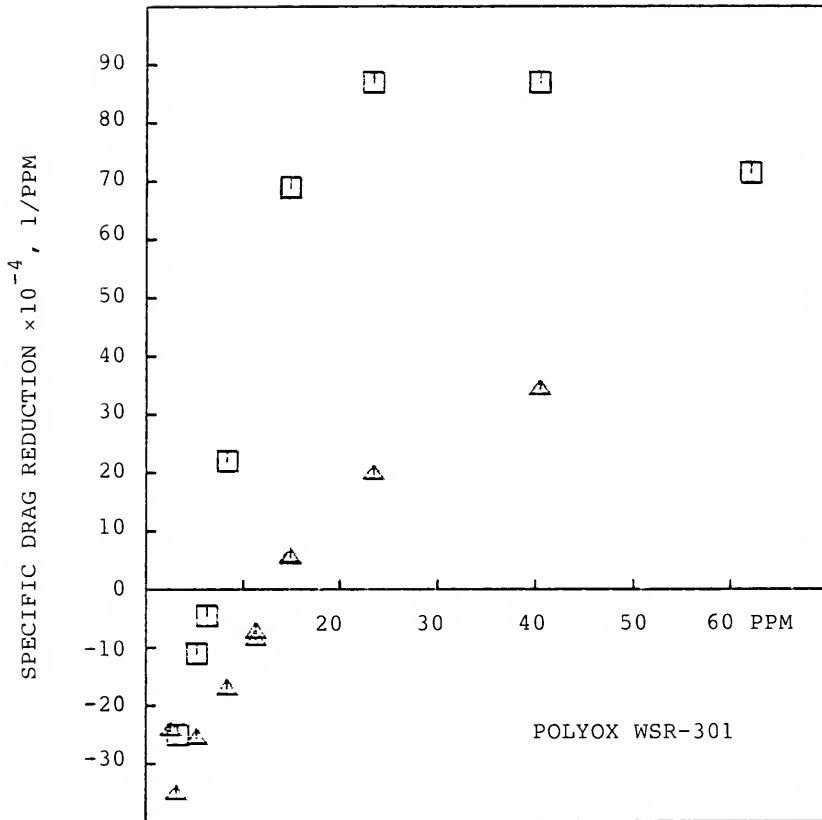
Fig. 5.12 Specific drag reduction as a function of
additive concentration for Polyox WSR-301 (1%
master solution) with the flow being conducted
at a Reynolds number of 14,000 for 10 (□) and
30 (△) rps mixing speeds.
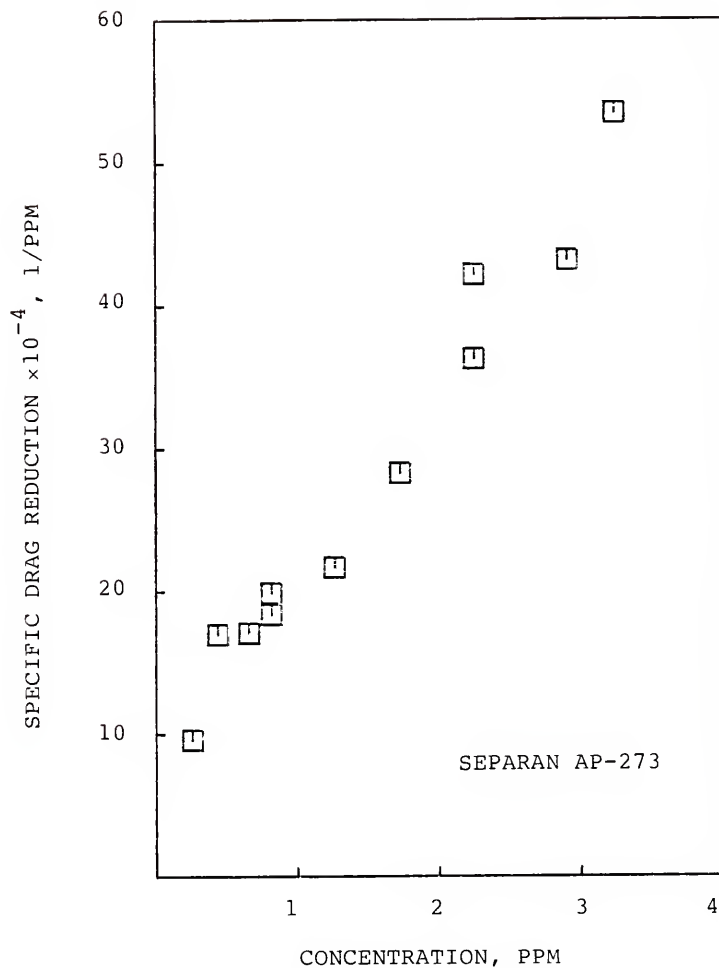
Fig. 5.13 Specific drag reduction as a function of additive concentration for Separan AP-273 with the flow being conducted at a Reynolds number of 14,000 (0.06% master solution, 10 rps, mixing speed).

In summary, specific drag reduction was found to increase with concentration at the lowest measured concentrations for each polymer examined. No evidence for the existence of a constant specific drag reduction value in the limit of decreasing concentration was ever found. Further, different types of behavior were noted for the Separan and Polyox runs. For the Polyox runs, a certain concentration was required before drag reduction effects could be noticed, while for the Separan solutions, drag reduction was always measured, no matter how low the concentration.

Discussion

These results indicate that in the present experiments, molecular interaction played a significant role in the drag reduction mechanism. Further, since different types of drag-reducing behavior were observed depending on polymer type, it may be concluded that the manner of molecular interaction can vary depending on polymer type.

The present results contradict the conclusions of Virk (1966) and Paterson and Abernathy (1970). As in the present investigation, they found the specific drag reduction to increase with decreasing concentration for sufficiently high concentrations. However, as the concentration was decreased further, they found the

specific drag reduction approached a constant value, while in the present investigation, the specific drag reduction reached a maximum and then decreased with decreasing concentration. Thus, they concluded that drag reduction was due to the interaction of isolated polymer molecules with the solvent rather than on interparticle effects, which is the opposite of the present conclusions.

To reconcile these differences, the results of some Polyox WSR-301 measurements reported by Berman (1978) will be discussed. Berman presents results for measurements conducted at similar wall strain rates for flows conducted through both 6 and 57 mm diameter pipes. At sufficiently high concentrations, the results for the two pipes were similar. Then for decreasing concentration, the specific drag reduction in the larger pipe reached a maximum (at about a concentration of 100 ppm for flow conducted at a wall strain rate of 1000 1/s) and then started to decrease. However at this point, the specific drag reduction in the smaller pipe continued to increase until, at a much lower concentration (less than 10 ppm), it also appeared to reach a maximum and started to decrease with further decreases in concentration. Further, for flows conducted at higher wall strain rates, the points of maximum specific drag reduction occurred at lower concentrations. Such results indicate that for

flows in small laboratory pipes at high flow rates, that extremely low concentrations may need to be examined before decreases in specific drag reduction (for decreases in concentration) can be observed. The measurements of both Virk (1966) and Paterson and Abernathy (1970) were conducted using small pipes (3 and 6 mm diameters, respectively). Thus, it may be that for the flow rates used in their investigations, low enough concentrations were not examined to detect such decreases in specific drag reduction.

As mentioned earlier, multimolecular structures have been observed in drag-reducing solutions (Stenborg et al., 1977b; Ouibrahim, 1977; Dunlop and Cox, 1977; James and Saringer, 1980). Of particular interest, Dunlop and Cox (1977) present electron micrographs that indicate that polyacrylamide molecules tend to form a large scale fibrous network, while polyethylene oxide molecules interact to form separate compact structures of varying sizes. The present results also indicate that the manner of molecular interaction is different in the Separan (polyacrylamide) solutions than in the Polyox (polyethylene oxide) solutions. It is tempting to combine these results and conclude that the observed differences in the drag-reducing behavior between the Separan and Polyox solutions is due to these structural differences. If this is the case, then it may be

concluded that a molecular network structure is more effective at interacting with the flow than separate, more compact molecular structures.

CHAPTER VI
EXTENSIONAL FLOW MEASUREMENTS

In this investigation, measurements of flow rate and pressure drop along conical channels have been utilized to characterize the extensional behavior of the polymer test solutions. These channels, which were designed to conduct nearly shear-free flow at high extensional strain rates, were connected to the main flow apparatus in such a manner as to allow some of the fluid that was conducted through the drag reduction experiment pipe to also be conducted through these channels. For a detailed description of the conical channels, their design considerations, and their attachment to the main flow set-up, the reader is referred to Chapter III. Reasons for selection of conical channels as rheometers to measure the extensional characteristics of the test solutions are specified in Chapter II.

Flow measurements conducted with tap water are reported first in this chapter. The results of these measurements are compared with that of the boundary layer solution for Newtonian sink flow and are also used to determine to what extent friction effects are present in the flow. Secondly, results are reported on some

preliminary experiments made with various polymer test solutions. The analytical and experimental procedures that are used to determine the extensional behavior of the test solutions are presented and the results of these measurements are compared with previous theoretical and experimental results. In the final section of this chapter, extensional flow measurements are presented for the same test solutions as being used in the drag reduction measurements.

Water Measurements

Measurements conducted with tap water provide reference information on the solvent behavior of the test solutions, and have been used to determine to what extent friction effects were present in the flow through the conical channels.

In Fig. 6.1, measurements are presented for head-discharge experiments using channels A, C, D, G, and H. In this figure, the solid lines represent head-discharge curves which were determined using the relation

$$Q = 2\pi r^2 U(1-\cos\,\theta)\{1-0.416[2\nu/(rU)]^{1/2}\frac{\sin\,\theta}{(1-\cos\,\theta)}\} \quad (6.1)$$

where Q is the flow rate, $U=(2gh)^{1/2}$ is the main-stream velocity, h is the pressure head at a distance r from the apex of the cone formed by the channel walls, θ is the
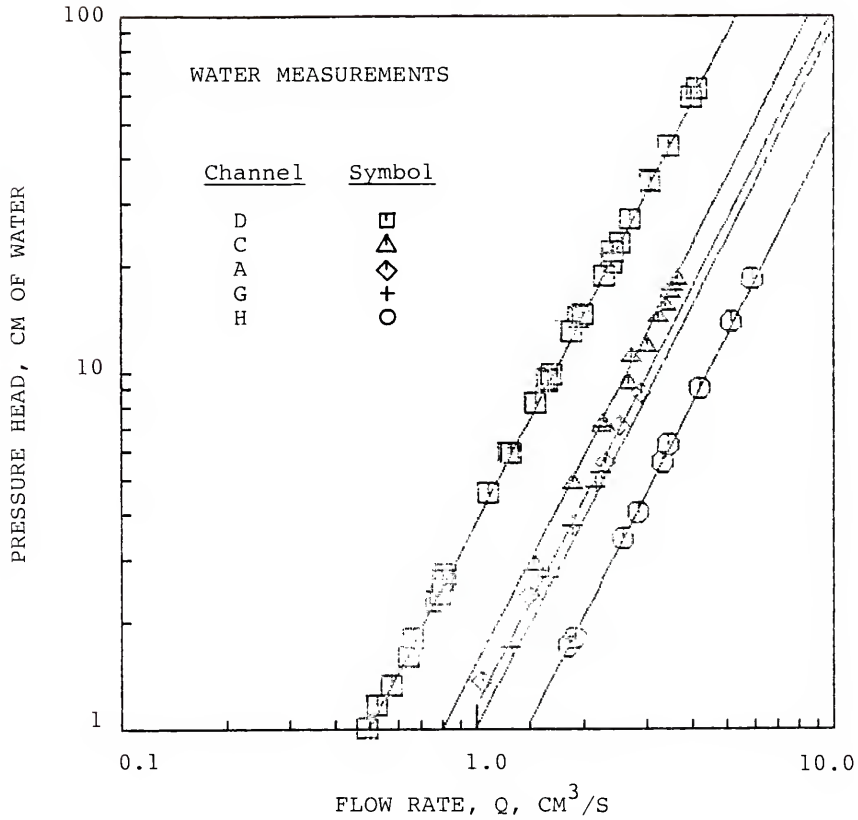
Fig. 6.1. Head-discharge measurements for water flow
through the test channels, along with
corresponding theoretical graphs (eq.(6.1))
obtained from the boundary layer solution for
steady axisymmetric flow of an incompressible
Newtonian liquid.

half angle of flow convergence, ν is the kinematic viscosity, and g is the gravitational acceleration. This general theoretical relationship has been obtained from the laminar boundary layer solution for Newtonian sink flow (Rosenhead, 1963) and the development of this expression may be found in Appendix F. It should be noted that the relationships obtained refer to the pressure head at a specific point, while the actual measurements represent "averaged" values due to pressure variation across the taps. Thus, the calculation of these graphs were made with r values representing the "pressure centers" of the taps (the points of application of single forces that would produce the same net forces and moments as the distributed pressure loadings). The radial distances of these "pressure centers" (r_p) were determined by numerically integrating the products of the pressures (as determined from the boundary layer solution) across the axial distance r over the tap areas and then dividing by the total forces exerted on the taps. The values for r_p, which were found to be constant for each channel over the whole range of flow rates used in the measurements, are presented in Table 6.1. The measured values of r at the middle of the pressure taps (r_m) are also presented in this table. Generally, the values of r associated with the centers of pressure are located further upstream of the center of each tap by distances equaling 3-5% of the tap diameters.

Table 6.1. Values of r associated with the downstream pressure taps: r_m are the measured mid-tap values; r_p represent the "pressure centers" as determined using the pressure distribution obtained from the boundary layer solution for conical sink flow with the measurements of tap geometry; and r_t are the values of r that give the best fit of the experimental data with the theoretical head-discharge relation, eq. (6.1).

Channel	r_m (cm)	r_p (cm)	r_t (cm)
A	.152	.155	.157
C	.167	.169	.169
D	.122	.125	.124
G	.115	.116	.114
H	.135	.136	.136

It can be seen in Fig. 6.1 that there is good agreement between the measured values and the behavior predicted using the boundary layer solution for Newtonian sink flow. The measured head-discharge values tend to follow the theoretical graph for each channel, with these values being displaced to either slightly higher or lower pressure heads. For channels D and G, the measured pressure heads averaged 2% and 6% greater than the predicted heads, while for channels A, C, and H, the actual heads averaged respectively 4%, 1%, and 3% less than the predicted values. These systematic deviations are likely explained by the fact that the channel dimensions were estimated to the nearest 0.005 cm, so the r_p values used in determining the theoretical values are accurate only within $\pm$.0025 cm. Such a variation in r_p would account for the observed differences. For example, by using a value of 0.114 cm for r_p for channel G (instead of 0.116 cm), the systematic difference between the theoretical and actual values was eliminated and the theoretical pressure heads were found to agree to within $\pm$2% of the measured heads. For reference purposes, the values of r (to the nearest 0.001 cm) that gave the least average deviation between the measured pressure heads and those determined using eq. (6.1) (labeled as r_t) are listed in Table 6.1. As a measure of random error in the measurements, it may be

noted that for the most extensively studied channel (D), that the majority of measured pressure heads fell within $\pm 2\%$ of the values predicted by eq. (6.1) using the r_t value listed in Table 6.1.

As discussed in Chapter III, the conical channels were designed to achieve as near to a frictionless flow as possible. To determine to what extent that the frictionless flow was obtained in the channels, consider eq. (6.1) rewritten as

$$Q_a = Q_i \left\{ 1 - \frac{C}{R^{1/2}} \right\} \qquad (6.2)$$

where Q_a is the actual flow rate, Q_i is the corresponding flow rate for inviscid flow, C is a constant dependent on channel geometry, and R is a Reynolds number, defined as $R = r(2gh)^{1/2}/\nu$. The measured pressure heads ranged from about 1 to 20 cm of water as shown in Fig. 6.1. Within this range, the ratios of the actual to the corresponding inviscid flow rates (Q_a/Q_i) were calculated using eq. (6.2). The results of these calculations, which are presented in Table 6.2, indicate that the actual flow rates were about 1% less than the flow rates would have been if the flow were completely frictionless. It may also be noted that such behavior is relatively insensitive to the level of shear viscosity. For example, a doubling of the

Table 6.2. Ratios of actual to inviscid flow rates (as
determined by eq. (6.2)) for pressure heads
at the downstream taps ($r = r_t$) being 1 and
20 cm of water.

Channel	Q_a/Q_i	
	h = 1 cm	h = 20 cm of water
A	.989	.995
C	.990	.995
D	.988	.995
G	.983	.992
H	.984	.992

viscosity in these calculations would only decrease the flow ratio (Q_a/Q_i) by about 1%. Thus, for these measurements and for the experiments conducted with the polymer solutions, which were found to have shear viscosities of less than 15% higher than their solvent values at high strain rates (cf. Chap. IV), it is likely that shear friction effects were negligible.

Measurements of the pressure head (H) occurring over the entire lengths of the channels were also conducted. From a least squares fit of the data, the overall head-discharge relation for channel D (to which reference will be made to in this chapter) was found to be $H = 2.547 \ Q^{1.767}$ for $.75 < Q < 2.6 \ cm^3/s$.

For a listing of the experimental data taken during the water flow runs, the reader is referred to Appendix G.

<u>Preliminary Polymer Solution Measurements</u>

<u>Goals</u>

The purpose of the preliminary polymer solution experiments was to gain a general understanding of the viscoelastic effects generated in the flow through the channels and to determine which channels would be the most appropriate for use in the general set of extensional flow measurements of this investigation.

Scope

In examining the general nature of the viscoelastic effects generated in the channels, three separate sets of experiments were run. First, to investigate the effects of varying channel geometry a 20 ppm Separan AP-273 solution (1% master solution, 10 rps mixing) was used with channels A, C, D, G, and H. Some additional measurements are reported for 15 and 45 ppm Separan AP-273 solutions with channels A and G. Secondly, experiments were conducted to investigate the relationship between the extra normal stresses generated in a channel with excess pressure drops occurring over the entire channel; measurements are reported for a 20 ppm Separan AP-273 solution (1% master solution, 20 rps mixing) flowing through channel D. Lastly, the degradation of viscoelastic effects with time was also examined. Here, measurements are reported for a 20 ppm Separan AP-273 solution (1% master solution, 10 rps mixing) conducted through channel F.

Experimental Procedures

Prior to each experimental run, several head-discharge measurements with water flow were recorded and compared with previous measurements in order to check the functioning of the equipment.

The first step of each of these experiments was to
establish a drag-reducing polymer solution flow through
the main experiment pipe. The same procedure was
followed as for the drag reduction flow experiments. The
main flow rate and mixer speed were set and then the
injection pump was adjusted to inject the appropriate
amount of master solution to maintain the desired
additive concentration. The calibration of the additive
injection pump was checked each day that experiments were
made.

In the experiments where the effect of varying
channel geometry was investigated, the conical channels
were attached to the main experiment pipe as shown in
Fig. 3.1. Once steady flow conditions were established
in the main experiment pipe, some of the flow was
diverted through the conical channel arrangement by
opening the needle valve which connected this arrangement
with the experiment pipe. The pressure drop along a
conical channel was measured using a strain gage
differential pressure transducer, while the flow rates
were determined by a catch and weigh technique.

The "total pressure drop" and "aging" experiments
were pursued using a separate conical channel apparatus.
Here, the channels were attached directly to a small
reservoir by flexible tubing (cf. Chapter III). After
steady polymer solution flow was established in the main

experiment pipe, some solution was transferred to this separate conical flow apparatus. The solution was collected from the same valve that connected the "in situ" conical channels to the main experiment pipe. These experiments were conducted by head-discharge measurements in the same manner as with the attached channels. In addition, the "total pressure drop" experiments were carried out by recording the pressure drop over the entire channel as determined by direct measurement of the elevation of the liquid level in the reservoir relative to that of the channel exit. In the "aging" experiment, the liquid level was maintained at a constant level in the reservoir by the continuous addition of the liquid previously collected from the main experiment pipe. Along with the head-discharge measurements, the time lapse from the moment of removal of test liquid from the main experiment pipe was also recorded.

Analytical Procedure

The results of the initial head-discharge measurements were expressed in terms of first normal stress differences and extensional strain rates for comparison with previous theoretical and experimental results. For the second set of experimental measurements, an energy balance equation was utilized to

examine the relationship between the normal stresses generated along a test channel with the excess pressure drop occurring over the entire channel. Lastly, the studies on the "aging" of the polymer solutions, i.e. the degradation of the normal stress effects, were made by observations on the changes in pressure drop for over a period of time for flows maintained at constant overall pressure heads.

Determination of extensional strain rates. From potential flow theory, the velocity field (in spherical coordinates) for frictionless sink flow through a conically shaped region is

$$u_r = \frac{-Q}{2\pi(1-\cos\theta)r^2}$$

$$u_\vartheta = u_\varphi = 0$$

(6.4)

where Q is the volumetric flow rate, Θ is the half angle of flow convergence, and u_r, u_ϑ, u_φ are the velocity components in the radial (r) and two angular (ϑ and φ) coordinate directions (a sketch of the spherical coordinate system used in this dissertation is presented in Fig. 6.2). The negative value of u_r in eq. (6.4) indicates flow toward the sink, i.e., in the negative r direction.
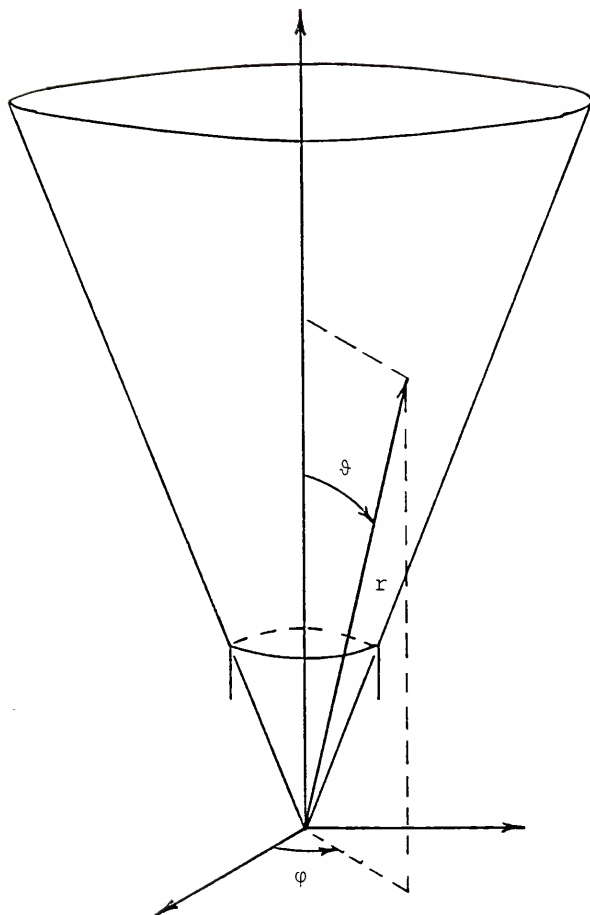
Fig. 6.2. Channel   schematic   with   spherical   coordinate
system used in dissertation.

For this flow, the components of the deformation rate tensor (D_{ij}) are

$$D_{ij} = \begin{bmatrix} \dfrac{\partial u_r}{\partial r} & 0 & 0 \\[2ex] 0 & \dfrac{u_r}{r} & 0 \\[2ex] 0 & 0 & \dfrac{u_r}{r} \end{bmatrix} \qquad (6.5a)$$

or

$$D_{ij} = \begin{bmatrix} \dfrac{Q}{\pi(1-\cos\theta)r^3} & 0 & 0 \\[3ex] 0 & \dfrac{-Q}{2\pi(1-\cos\theta)r^3} & 0 \\[3ex] 0 & 0 & \dfrac{-Q}{2\pi(1-\cos\theta)r^3} \end{bmatrix} \qquad (6.5b)$$

where positive values indicate stretching and negative values indicate compression.

The measurements presented in the previous section indicate that shearing effects are negligible for flow through the channels used in this investigation. It was shown that the water flow rates were typically only about 1% less than if the flows were completely frictionless (for a given pressure head). Further, due to the design of the channels, this behavior was relative insensitive to shear viscosity levels. For example, a liquid with

twice the shear viscosity of water should flow at a rate about 2% less than the flow rate of a frictionless fluid. It was assumed that the equations for frictionless sink flow could also be used to specify velocity and rate of deformation of polymer solution flow through the channels. In this dissertation, the extensional strain rate is determined as the radial component of the deformation rate tensor (D_{rr}) listed in eqs. (6.5)

$$D_{rr}(=D_{11}) = \frac{Q}{\pi(1-\cos\Theta)r^3}$$ (6.6)

The use of this equation implies an assumption that the presence of extra normal stresses by themselves will not alter the velocity profile. This seems to be a reasonable assumption for low concentration polymer solutions based on the following reasoning. First, at low enough flow rates, such a solution should behave as its solvent would and the velocity field should be nearly uniform across a flow section (r=constant). At some point for increasing flow rates, significant extra normal stresses may occur. Provided that the solution is sufficiently homogeneous, these extra stresses should also be uniform across a flow section in response to the uniform flow field. As a result, no imbalance in stresses is likely to exist which could cause a change in the velocity profile. Further, the uniform velocity

profile is likely to be stable, since any local change in the velocity should cause a change in the extra stresses which will tend to resist the velocity change. In the case of inhomogeneous solutions, stress imbalances are more likely to occur, possible secondary flows may result, and eq. (6.6) would no longer be valid. Lastly, of interest to this analysis is that James and Saringer (1980) have reported that polymer solution flows through conical channels remain free of secondary motions up to much higher flow rates than do flows through other channels of various shapes, but of comparable exit dimensions. This agrees with the above assessment made on the stability of polymer solution flows through a conical channel.

Determination of first normal stress differences.

The first normal stress differences were determined using two different methods. In the first method, these differences were determined from direct comparison of the differences in pressure drop for polymer solution flows to that for water flows at the same flow rates (for a given channel). Consider the constitutive equation describing the stress field for an incompressible Newtonian fluid,

$$T_{ij} = -P\delta_{ij} + 2\mu D_{ij} \qquad (6.7)$$

where $-P$ is the trace of the stress tensor T_{ij}, δ_{ij} is the Kronecker delta, and μ and D_{ij} are again the shear viscosity coefficient and deformation rate tensor. If this fluid contains dissolved or suspended material, an additional stress T'_{ij} may be generated, and for this case, the constitutive equation may be expressed (Batchelor, 1970; James and Saringer, 1980) as

$$T_{ij} = -P\delta_{ij} + 2\mu D_{ij} + T'_{ij} \qquad (6.8)$$

Further, James and Saringer suggest diagonal components of T_{ij} so that

$$T_{rr} = -P + 2\mu\frac{du_r}{dr} + \frac{2}{3} T'_{rr}$$

$$T_{\vartheta\vartheta} = -P + 2\mu\frac{u_r}{r} - \frac{1}{3} T'_{rr} \qquad (6.9)$$

$$T_{\varphi\varphi} = -P + 2\mu\frac{u_r}{r} - \frac{1}{3} T'_{rr}$$

This formulation is motivated by the fact that it still allows the trace of the stress tensor to equal $-P$.

Using eqs. (6.9), the first normal stress difference N may now be written as

$$N(r) = [T_{rr}(r) - T_{\vartheta\vartheta}(r)] = 2\mu(\frac{du_r}{dr} - \frac{u_r}{r}) + T'_{rr}(r) \qquad (6.10)$$

where it may be noted that for the case of no additional stresses and a velocity field described by eq. (6.4), that this equation reduces to Trouton's equation, $N = 3\mu D_{rr}$. For the present investigation, large normal stresses (of the order of 100 to 1000 Pa) should occur for the expected extensional strain rates of an order of magnitude of 1000 1/s in the channels, and hence, eq. (6.10) may be approximated as

$$N(r) \cong T'_{rr}(r) \tag{6.11a}$$

At such strain rates, the viscous term will be negligible (of the order of 3 Pa).

The stress component $T_{\vartheta\vartheta}$ in eq. (6.9) is equal in magnitude but of opposite sign to the pressure that would be measured at a tap. Thus, for polymer solution flow, the measured pressure drop from a point far enough upstream (say $r=r_0$), where no significant extra normal stresses exist, to a point in the channel ($r=r_1$) will consist of the drop in isotropic pressure minus $\frac{1}{3}T'_{rr}(r_1)$ (neglecting the viscous terms). For water flow, the measured pressure drop will (after again neglecting the small viscous effects) consist of just this isotropic pressure drop. If the changes in isotropic pressure between the taps for both the polymer solution and water flow are equal at a given flow rate,

then the measured pressure drop in the polymer solution flow should be less than that for the water flow by $\frac{1}{3}T'_{rr}(r_1)$. Hence, the first normal stress differences N at the downstream tap may be obtained using the relation

$$N(r_1) \cong T'_{rr}(r_1) = 3[(\Delta p)_p - (\Delta p)_w]_{Q=const.} \qquad (6.11b)$$

where p is the pressure that is recorded at the taps, $(\Delta p) = p(r_1) - p(r_0)$, and where the subscripts p and w indicate polymer solution and water flow respectively.

A second method for determining first normal stress differences is to utilize an integrated form of the equations of motion for frictionless sink flow. In spherical coordinates and for steady sink flow, the radial (r) component of Cauchy's equation of motion may be written as

$$\rho u_r \frac{\partial u_r}{\partial r} = \{ \frac{1}{r^2} \frac{\partial}{\partial r}(r^2 T_{rr}) - \frac{1}{r}(T_{\vartheta\vartheta} + T_{\varphi\varphi})\} \qquad (6.12)$$

where T_{rr}, $T_{\vartheta\vartheta}$, and $T_{\varphi\varphi}$ are components of the stress tensor and u_r is again the radial flow velocity. After assuming $T_{\vartheta\vartheta} = T_{\varphi\varphi}$ (based on flow symmetry), differentiating the radial stress term, multiplying each side of the equation by r^2, and rearranging, one

obtains

$$r^2 \frac{dT}{dr}rr + 2rT_{rr} = \rho r^2 u_r \frac{du}{dr}r + 2rT_{\vartheta\vartheta} \qquad (6.13)$$

where the partial derivatives have been replaced with total derivatives, since at a given flow rate T_{rr} and u_r are only functions of r.

Substitution for u_r in eq. (6.13) by eq. (6.4) and then integrating with respect to r from some upstream location r_0 to a downstream location r_1 yields

$$r_1^2 T_{rr}(r_1) - r_0^2 T_{rr}(r_0) = \rho \frac{-Q}{2\pi(1-\cos\theta)} [u_r(r_1) - u_r(r_0)]$$

$$+ [r_1^2 T_{\vartheta\vartheta}(r_1) - r_0^2 T_{\vartheta\vartheta}(r_0)$$

$$- \int_{T_{\vartheta\vartheta}(r_0)}^{T_{\vartheta\vartheta}(r_1)} r^2 \, dT_{\vartheta\vartheta} \qquad (6.14)$$

(In obtaining this equation, the left hand side of eq. (6.13) was first expressed as a total differential before integration and the stress term on the right hand side has been integrated by parts.)

For an initial location r_0 far enough upstream, $u_r(r_0)$ will be of negligible value and $T_{\vartheta\vartheta}(r_0)$ will equal $T_{rr}(r_0)$. For these conditions, eq. (6.14)

simplifies to

$$N(r_1) = [T_{rr} - T_{\vartheta\vartheta}]_{r=r_1}$$

$$= \rho u_r^2(r_1) - \frac{1}{r_1^2} \int_{T_{\vartheta\vartheta}(r_0)}^{T_{\vartheta\vartheta}(r_1)} r^2 \, dT_{\vartheta\vartheta} \qquad (6.15)$$

where $N(r_1)$ is the first normal stress difference at $r=r_1$.

From measurements of $T_{\vartheta\vartheta}$ as a function of r, the integral in eq. (6.15) may be calculated, and hence, first normal stress differences can be obtained. Unfortunately, this integral has not been evaluated since the pressure measurements were made for only one set of pressure taps per channel. However, through examination of some special cases, estimates of the first normal stress differences can still be determined.

For instance, for frictionless flow $dT_{\vartheta\vartheta}$ will equal $d\ \rho(u^2/2)$ and eq. (6.15) yields $N(r_1) = 0$. Another special case is obtained if $T_{\vartheta\vartheta}$ were to remain constant. In this case, there would be no contribution from the integral in eq. (6.15) and $N(r_1) = \rho u_r^2(r_1)$. Further, consider the case where $\Delta T = [T_{\vartheta\vartheta}(r_1) - T_{\vartheta\vartheta}(r_0)] = 0$. A most likely manner in which this may occur is as follows. Starting from a point far upstream of the channel exit, $T_{\vartheta\vartheta}$ should

increase with decreasing r as for solvent flow. At some point, the extra normal stresses may become of sufficient magnitude to cause $T_{\vartheta\vartheta}$ to start to increase with further decreases in r. This increase in pressure may offset any previous decreases, thus leading to no net change in pressure between the taps. If this is the case, the contribution of the integral in eq. (6.15) will be of a positive value and the first normal stress differences will be less than $\rho u_r^2(r_1)$. For the present investigation, only those flows were examined where positive measured pressure drops occurred $(\Delta T_{\vartheta\vartheta} \geq 0)$. Thus, all measured first normal stress differences should be within the range of values covered for the above special cases, or, $0 \leq N(r_1) < \rho u_r^2(r_1)$.

As a first approximation for determining the normal stress differences, it was assumed that they would vary linearly with pressure drop $(\Delta T_{\vartheta\vartheta})$ according to the relation

$$N(r_1) = \rho u_r^2(r_1) - 2\Delta T_{\vartheta\vartheta} \qquad (6.16)$$

This equation satisfies the two special cases discussed above of $N(r_1)=0$ for $\Delta T_{\vartheta\vartheta} = \rho u_r^2(r_1)/2$, and $N(r_1)= \rho u_r^2(r_1)$ for $T_{\vartheta\vartheta}$ being constant.

Energy balance. Many dilute polymer solutions
exhibit significantly larger pressure drops when flowing
through a contraction than that observed for flows of
their solvents at the same flow rates (eg., see Giles,
1969; Metzner et al., 1969; Balakrishnan, 1976; James and
Saringer, 1980, 1982; Fruman and Barigah, 1982). The
occurrence of such excess pressure drops has been
attributed to solution viscoelasticity and attempts have
been made to use measurements of these pressure changes
to determine extensional viscosities (Fruman and Barigah,
1982). However, normal stress mechanisms and the
relationship between these stresses and the excess
pressure drops are not well understood. The purpose of
the second set of preliminary experiments was to
determine if excess pressure drops would indeed occur,
and if so, to examine the possible correlations between
them and the normal stresses that were generated in the
channels.

Such an examination was made by considering the
energy balance for flow through a conical channel. These
considerations make it possible to obtain both a general
qualitiative view of the energy transfer that occurs in a
channel, and also to quantitatively predict the magnitude
of the excess pressure drop as a function of the normal
stresses generated in the channel.

First, consider flow through the control volume
pictured in Fig. 6.3. The rate of change of stored
energy (dE/dt) in the control volume will equal the net
rate of energy flux through the control volume plus the
rate of change of energy inside the volume, or

$$\frac{dE}{dt} = \frac{\partial}{\partial t} \int_V \rho e dV + \int_S \rho e u_i n_i dS \qquad (6.18)$$

where e is energy per unit mass, ρ is mass density, u_i
are the velocity components, n_i are unit vectors normal
to the surfaces of the control volume, and where S is the
closed imagined surface of the region of volume V.

By using the first law of thermodynamics, the rate
of change of energy in a system will also equal the rate
of change of heat added to the system (dQ_H/dt) minus
the rate of work done by the system (dW/dt) on the
surroundings. Hence, after further assuming steady flow,
eq. (6.18) may be written as

$$\frac{dE}{dt} = \frac{dQ_H}{dt} - \frac{dW}{dt} = \int_S \rho e u_i n_i dS \qquad (6.19)$$

The work done by the system on the surroundings
consists of two parts, one, where work is done on an
element in the flow and mechanically transferred out of
the flow (shaft work), and secondly, where work is done
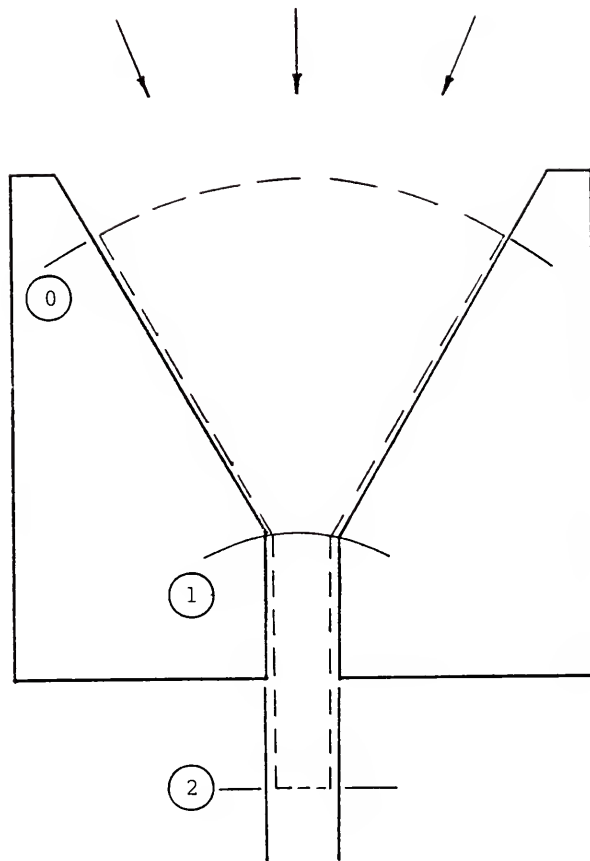
Fig. 6.3. Control volume for energy transfer analysis.

by the stresses in the fluid acting at the boundaries of the system. For the present situation, there is not any shaft work being done, and hence, the rate of work done will be due to the stresses alone, or

$$\frac{dW}{dt} = -\int_S u_i T_{ij} n_j dS \tag{6.20}$$

The closed surface S of the control volume V consists of the physical boundaries of the flow region and of imagined surfaces which are normal to the direction of the flow. Hence, only normal stresses contribute to the rate of work being done in eq. (6.20).

Before further evaluation of eq. (6.19), it must also be noted that the energy per unit mass of the system may be expressed as the sum of kinetic (e_k), potential (e_p), and internal energies (e_u), or

$$e = e_k + e_p + e_u = \rho (\frac{u}{2})^2 + gz + e_u \tag{6.21}$$

where z is the local elevation of the fluid, u is the fluid velocity, and ρ and g are again the mass density and gravitational acceleration, respectively. In this analysis, the internal energy e_u was defined as any remaining energy that was not associated with either one of the above formulations for the kinetic or potential

energies, and hence, was taken as including any possible energy stored in the polymer.

The transfer of energy in the control volume has been evaluated using eq. (6.19) for a flow region extending from cross-section 0 (a cross-section which is normal to the flow and located upstream of the channel exit) to section 1 (a normal cross-section at the end of the conic section of the channel) and for a region extending from cross-section 1 to cross-section 2 (a normal cross-section located downstream of the channel). Evaluations have been made for both water and polymer solution flows, and the differences in energy transfer have been examined in order to determine possible causes for the excess pressure drops of the polymer solution flows.

Substituting eqs. (6.20) and (6.21) into eq. (6.19) and integrating from cross-section 0 to 1, one obtains

$$\frac{dQ_H}{dt} - [(T_{rr})_1 - (T_{rr})_0]Q = [K_e \frac{u^2}{2} + gz + e_u]_1 \rho Q$$

$$- [K_e \frac{u^2}{2} + gz + e_u]_0 \rho Q \quad (6.22)$$

where the values of T_{rr}, u, z, and e_u now represent averaged values of the stresses, velocities, local elevations, and internal energies per unit mass, respectively. The kinetic energy flux correction factor

(K_e) was introduced since the average of the kinetic energy does not in general equal the kinetic energy of the average velocity (Daily and Harleman, 1973). The subscripts 0 and 1 in eq. (6.22) refer to the cross-sections over which the integrals have been evaluated.

The radial stress T_{rr} may be divided into isotropic $(-P)$ and deviatoric components (τ_{rr}) as

$$T_{rr} = -P + \tau_{rr} \qquad (6.23)$$

The deviatoric stress components can not be sustained in water flow, and hence, the radial stresses are equal to just the isotropic components. For polymer solution flow, deviatoric stresses can be sustained; however, section 0 was selected far enough upstream so that the deformation rate was too low to generate any significant deviatoric stress levels. Thus, the deviatoric stresses are included in the energy balance for polymer solution flow at section 1, but are neglected at section 0.

After utilizing eq. (6.23), the energy balance (eq. (6.22)) for water flow becomes

$$\frac{1}{\rho}[P_0 - P_1]_w = \{[\Delta(K_e \frac{u^2}{2})]_w + [g\Delta z] + [\Delta e_u]_w$$

$$+ [h_1]_w \}_{0-1} \qquad (6.24)$$

and for the polymer solution flow,

$$\frac{1}{\rho}[P_0 - P_1 + (\tau_{rr})_1]_p = \{[\Delta(K_e \frac{u^2}{2})]_p + [g\Delta z] + [\Delta e_u]_p$$

$$+ [h_1]_p \}_{0-1} \qquad (6.25)$$

where h_1 is the heat transferred from the system (heat loss) per unit mass and where (Δ) indicates the subtraction of upstream values from downstream values (eg., $(\Delta z)=(z_1-z_0)$).

The terms in eqs. (6.24) and (6.25) have been arranged so that the left hand sides of the equations represent the work done on the fluid in the control volume, while the right hand side terms represent any net increases in energy (kinetic, potential, and internal) plus any heat lost by the system. It may also be noted that each of the terms in these equations (work, energy, and heat) are expressed per unit mass.

The average velocities at both sections will be the same for both the polymer solution and water flows at the same flow rates. Further, as discussed previously, the velocity fields at each section are expected to be the same for both water and polymer solution flow. Thus, there should not be any significant difference in kinetic energy between the two flows at either cross-section. Based on this assumption, the subtraction of eq. (6.24)

from eq. (6.25) yields

$$\frac{1}{\rho}\{[P_0 - P_1 + (\tau_{rr})_1]_p - [P_0 - P_1]_w\} = [\Delta(e_u)_p - \Delta(e_u)_w]_{0-1}$$

$$+ [(h_1)_p - (h_1)_w]_{0-1} \qquad (6.26)$$

Here, we see that when compared to the water flow system, any additional work done on the fluid in the control volume of the polymer solution flow will result in additional increases in internal energy in the system and/or additional heat lost from the system.

A manner in which this energy may be transferred is as follows. As the fluid travels along the channel, the polymer along with the rest of the fluid will be stretched. At some point, the polymer will start to offer significantly increased resistance to the stretching and additional work will be required to keep the flow moving at the same flow rate. Further, as the stretching of the polymer increases, its energy should also be increasing. Since the only differences between the polymer solution and water flow are due to the stretching of the polymer, and since the stresses that are associated with polymer stretching are the deviatoric stresses, it seems reasonable to assume that the additional increases in internal energy should equal the

work done by the deviatoric stresses, or

$$(\frac{\tau_{rr}}{\rho})_1 = [\Delta(e_u)_p - \Delta(e_u)_w]_{0-1} \tag{6.27}$$

Further, as a result of the stretching of the polymer, some additional heat may be lost from the system other than that would normally occur for water flow. By subtracting eq. (6.27) from eq. (6.26), it can seen that this additional heat loss will be balanced by a corresponding amount of additional loss of isotropic pressure in the polymer solution, or

$$[(h_1)_p - (h_1)_w]_{0-1} = \frac{1}{\rho}\{[P_0 - P_1]_p - [P_0 - P_1]_w\} \tag{6.28}$$

Now, consider the flow from cross-section 1 (the end of the conic section) to cross-section 2 (at a location in the jet downstream of the channel). Immediately after passing section 1, the flow will experience an abrupt decrease in the rate of extensional deformation. As a result, the polymer should relax and lose any additional energy associated with its stretched state. To examine this energy transfer, an energy balance of the water flow system was subtracted as before from that of the polymer

flow system to yield

$$\frac{1}{\rho}\{[P_1-P_2-(\tau_{rr})_1]_p - \{[P_1-P_2]\}_w \} = \{[K_e \frac{u}{2})^2]-[K_e \frac{u^2}{2}]_w \}_2$$

$$+ [\Delta(e_u)_p - \Delta(e_u)_w]_{1-2}$$

$$+ [(h_1)_p - (h_1)_w]_{1-2} \qquad (6.29)$$

It has again been assumed that the kinetic energies for both flows at cross-section 1 were the same. At cross-section 2, the flow is not constrained (by channel walls) and the kinetic energy terms are not necessarily the same. Possible differences in kinetic energy may exist since the diameters (and hence, velocities) of the issuing jets may not be the same.

A possible mechanism for the increased pressure drops now becomes apparent. The additional transfer of energy in this section should be due to the relaxation of the polymer. It may be that the polymer molecules relax in such a manner that little or no interaction with the flow will occur. First, consider the case where all of the additional internal energy in the polymer solution may be transferred to heat with no effect on the kinetic energy of the flow. In such a case, no additional work will be done on the flow (i.e., the left hand side of eq. (6.29) will be equal to zero) and an additional pressure

drop will occur that will be of the same magnitude as the extra stresses (τ_{rr}) that were present in the flow when the relaxation process started, that is

$$[P_1-P_2]_p - [P_1-P_2]_w = (\tau_{rr})_1 \qquad (6.30)$$

Such lack of interaction between the polymer molecules and the main flow might be expected if the molecules were to relax at a much higher frequency than that of any motion in the flow. In such a case, couplings of motions which would allow energy transfer from the polymer molecules back to the flow are not likely to occur.

Realistically, some interaction between relaxing polymer molecules and the flow should take place. To consider the energy transfer for this case, eq. (6.29) may be rewritten as

$$[\Delta(e_u)_w - \Delta(e_u)_p]_{1-2} = \{[K_e \frac{u^2}{2}]_p - [K_e \frac{u^2}{2}]_w\}_2$$

$$+ [(h_1)_p - (h_1)_w]_{1-2}$$

$$- \frac{1}{\rho}\{[P_1-P_2-(\dot{\tau}_{rr})_1]_p - \{[P_1-P_2]_w\} \qquad (6.31)$$

For a tensile radial extra stress (positive ($\tau_{rr})_1$),

the left hand side of this equation is a positive
quantity (assuming no permanent change in internal energy
has occurred between cross-sections 0 and 2 in either the
polymer solution or water flow system) and may be
interpreted as the additional energy released by the
polymer molecules. If polymer-flow interaction were to
occur during the relaxation process, then it appears that
it may be possible that the energy released by the
molecules may be transferred to increased kinetic energy
in the flow as well as to heat with still no additional
work being done on the flow. However, for polymer
solutions which exhibit excess pressure drops, this is
not the case. Jets of such solutions issuing from a tube
or contraction are known to swell. Thus, the kinetic
energy in their jets should be less, not greater, than
for their solvents at similar flow rates. To balance
these relative decreases in kinetic energy, it can be
seen from eq. (6.31) that there must be either increased
additional heat loss or that less additional work will be
done on the flow. If it is assumed that the additional
heat loss can not be greater than the amount of energy
being released by the polymer molecules, then the
decrease in kinetic energy will result in less additional
work being done on the fluid, or

$$[P_1 - P_2]_p - [P_1 - P_2]_w < (\tau_{rr})_1 \tag{6.32}$$

Thus, the maximum additional increase in isotropic pressure drop due to the presence of the polymer molecules from section 1 to 2 should be that given by eq. (6.30).

To determine the total excess pressure drop (e.p.d.) occurring over the entire channel, the excess pressure drops from section 0 to 1 and from section 1 to 2 need to be added together, or

$$
\text{e.p.d.} = \{[T_{\vartheta\vartheta}(r_1)-T_{\vartheta\vartheta}(r_0)] - [T_{\vartheta\vartheta}(r_1)-T_{\vartheta\vartheta}(r_0)]_w\}_p
$$

$$
+\{[T_{\vartheta\vartheta}(r_2)-T_{\vartheta\vartheta}(r_1)]_p - [T_{\vartheta\vartheta}(r_2)-T_{\vartheta\vartheta}(r_1)]_w\} \quad (6.33)
$$

After expressing the stresses in terms of isotropic and deviatoric components, this becomes

$$
\text{e.p.d.} = \{[-P_1+(\tau_{\vartheta\vartheta})_1)+P_0]_p -[(-P_1+P_0)]_w\}
$$

$$
+ \{[-P_2+P_1-(\tau_{\vartheta\vartheta})_1)]_p -[-P_2+P_1)]_w\}
$$

$$
= [(P_0-P_1)_p -(P_0-P_1)_w] + [(P_1-P_2)_p -(P_1-P_2)_w] \quad (6.34)
$$

For the limiting case when all the additional internal energy in the polymer solution is transferred to heat (eq. (6.30)), and when any changes in isotropic pressure from polymer solution to water flow in the conic section

of the channel are negligible when compared to this heat loss, the excess pressure drop will be

$$\text{excess pressure} \atop \text{drop} = \tau_{rr}(r_1) \cong \frac{2}{3} N(r_1) \qquad (6.35)$$

Here eqs. (6.23), (6.9), and (6.11a) have been used to express the radial deviatoric stress in terms of the first normal stress difference $N(r_1)$.

To determine the excess pressure drop using eq. (6.35), the first normal stress difference (or τ_{rr}) at the end of the conic section needs to be known. The measurements determine the first normal stress differences at the downsteam tap as previously discussed. If it is known how the stress differences vary with the radial distance r, then the measured stress differences at the tap can be used to calculate the stress differences at the end of the conic section, and hence, the excess pressure drops.

The change of the first normal stress difference with the radial distance may be determined by again examining the radial component of the equations of motion for steady sink flow of a viscoelastic liquid (eq. (6.12)). After assuming that $T_{\vartheta\vartheta} = T_{\varphi\varphi}$ (based on flow symmetry), rearranging and substituting for $N(=T_{rr}-T_{\vartheta\vartheta})$, followed by integration from some upstream location r_0

to some downstream location r_1 in the conic section of the channel, eq. (6.12) may be expressed as

$$[\frac{\rho u_r^2}{2} + P]_{r_0}^{r_1} = \frac{2}{3} \int_{r_0}^{r_1} (\frac{\partial N}{\partial r} + \frac{3N}{r})dr \qquad (6.36)$$

If the isotropic pressure drop in the polymer solution flow is the same as for water flow (an assumption consistent with the derivation of eq. (6.35)), then the left hand side of eq. (6.36) will equal zero. To satisfy this condition, the integrand of the term on the right hand side of eq. (6.36) must also equal zero. Solving the resulting partial differential equation yields

$$N(r) = Gr^{-3} \qquad (6.37)$$

where G is a function independent of r (but which may vary with flow rate). Thus, the first normal stress difference at the end of the conic section $(r=r_e)$ can be determined from the normal stress differences determined at the tap $(r=r_N)$ by the equation

$$N(r_e) = (\frac{r_N}{r_e})^3 N(r_N) \qquad (6.38)$$

By substituting eq. (6.38) into eq. (6.35), the excess

pressure drop becomes

$$\text{excess pressure drop} = \frac{2}{3}\left(\frac{r_N}{r_e}\right)^3 N(r_N) \qquad (6.39)$$

In using eq. (6.39), the values of $N(r_N)$ were calculated through use of eq. (6.11b) with the measured pressure drops channels. Actual excess pressure drops were determined by subtraction of the overall pressure heads for water flows from that for the polymer solution flows. The overall pressure heads for water flow were determined from a least squares fit of previously measured water data (see the section on water measurements).

Aging analysis. As mentioned previously, the measurements on "aging" consisted of transferring polymer solution from the main experiment pipe to a separate reservoir/conical channel apparatus, and then, conducting flow rate and pressure drop measurements (from the upstream tap to the tap in the conic section of the channel) while maintaining a constant pressure head over the entire channel. The purpose of this experiment was to examine the flow for any change in the magnitude of the extra normal stress effects and to use these observations to infer relations between the structure of the polymer molecules in the flow and these effects.

It is likely that extramolecular structures were present in the test solutions. First, these solutions were freshly prepared from concentrated master solutions. It would be unrealistic to assume that the intertangled network of polymer molecules in the master solutions would completely disentangle in the short time that it took for the flow to pass through the experiment pipe. Further, the existence of polymer agglomerations in the flow through the main experiment pipe was confirmed using drag reduction measurements (cf. Chapter V). In the present separate reservoir arrangement, the solution was relatively quiescient and no shearing forces were expected to exist which could cause scission of the molecules. The only change in solution properties was likely to be due to continued disentanglement of the polymer molecules seeking some equilbrium state. Thus, any changes in the magnitudes of the viscoelastic effects with time are likely to be the result of the disentanglement of extramolecular structures. From examination of the flows for changes in the magnitude of the extra normal stress effects, the "aging" measurements have been used to obtain a qualitative view of the relationship between the presence of the extramolecular structures and solution viscoelasticity.

Experimental Results

In this section, the results of the preliminary polymer solution experiments are presented. The discussion of these results will be postponed until all of the preliminary tests have been reported.

In Figs. 6.4, 6.5, 6.6, and 6.7, graphs of first normal stress difference as a function of extensional strain rate are presented for flow of a 20 ppm Separan AP-273 solution (1% master solution, 10 rps mixing) through channels A, C, D, and G, respectively. In each figure, results are plotted for normal stresses determined using both eqs. (6.11b) and (6.16). For reference purposes, dashed lines are presented in each figure which indicate $N = \rho u_r^2$.

It should be noted that since the extensional strain rates varied across the downstream pressure taps, the first normal stress differences presented in these figures represent "averaged" values. In Figs. 6.4-6.7 each first normal stress difference has been expressed as a function of a single representative extensional strain rate.

In eq. (6.11b), the first normal stress differences are expressed in terms of differences in pressure drop from polymer solution to water flow. These differences in pressure drop have been treated as stresses acting across the pressure taps, and representative extensional
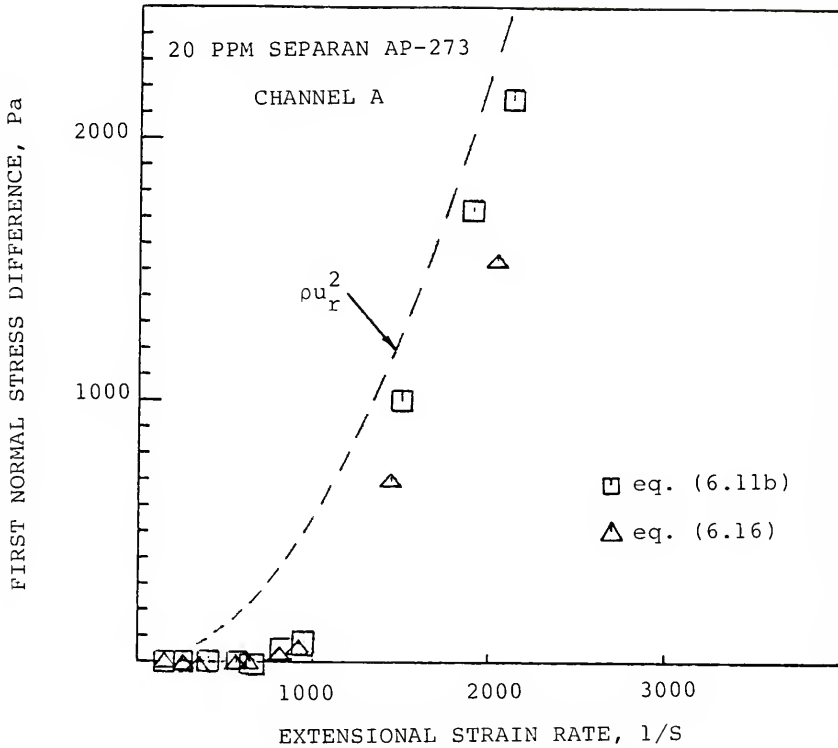
Fig. 6.4. Dependence of first normal stress difference on extensional strain rate for flow of a 20 ppm Separan AP-273 solution (1% master solution, 10 rps mixing, Reynolds number of 14,000 in the main pipe, 24 °C) through channel A.
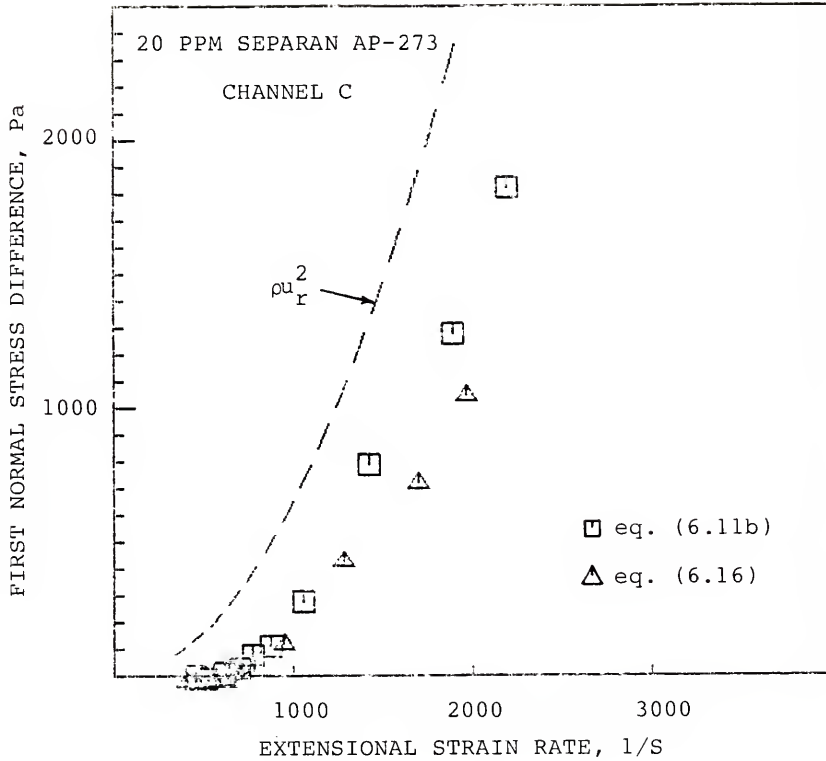
Fig. 6.5. Dependence of first normal stress difference on extensional strain rate for flow of a 20 ppm Separan AP-273 solution (1% master solution, 10 rps mixing, Reynolds number of 14,000 in the main pipe) through channel C.
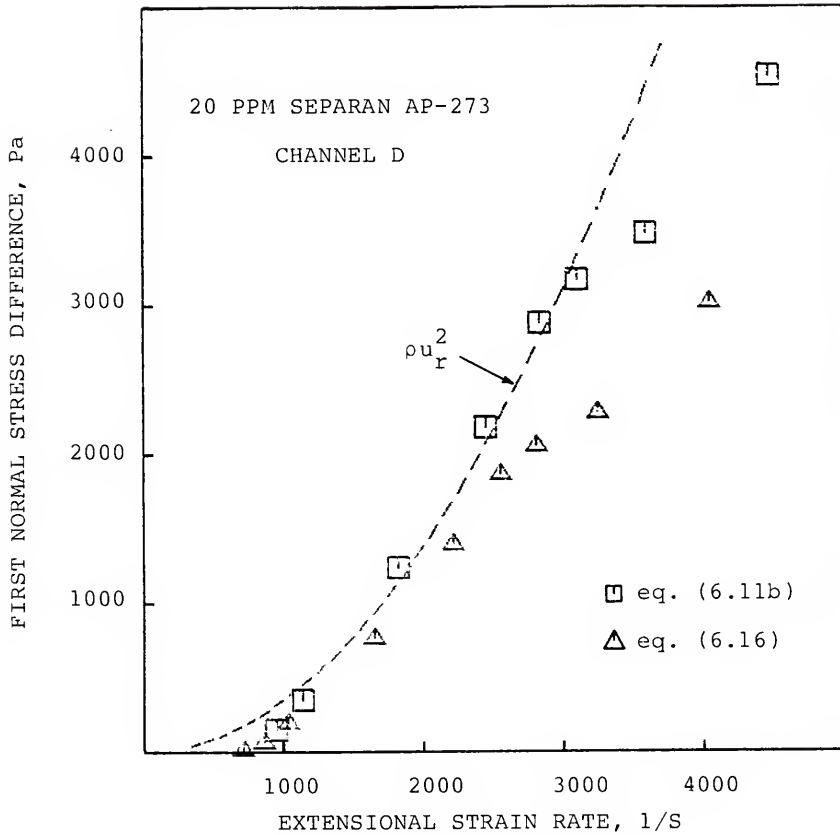
Fig. 6.6. Dependence of first normal stress difference on extensional strain rate for flow of a 20 ppm Separan AP-273 solution (1% master solution, 10 rps mixing, Reynolds number of 14,000 in the main pipe, 24 ^{o}C) through channel D.
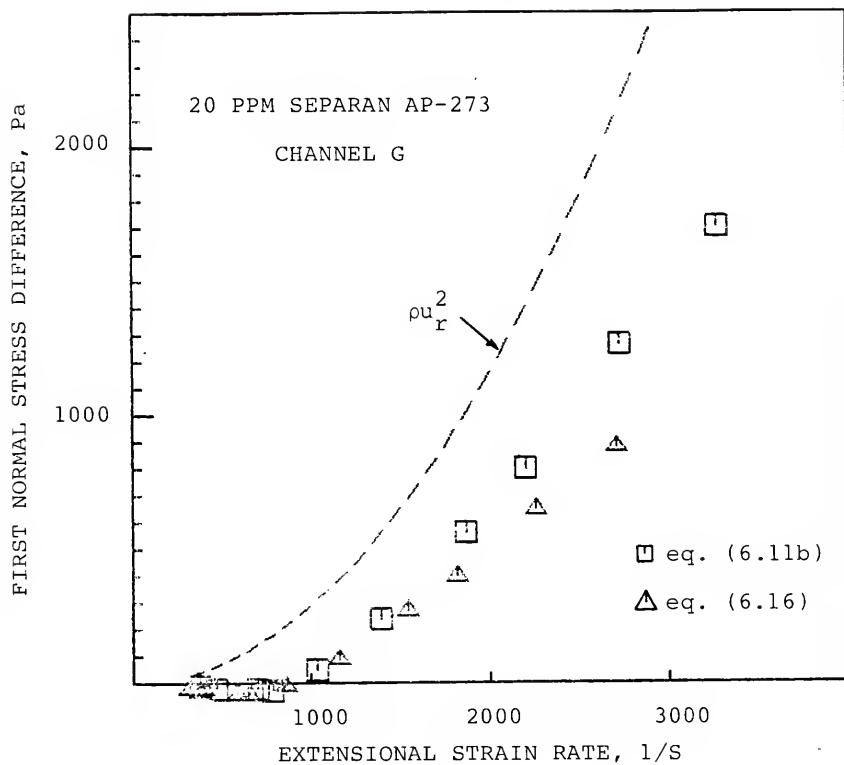
Fig. 6.7. Dependence of first normal stress difference on extensional strain rate for flow of a 20 ppm Separan AP-273 solution (1% master solution, 10 rps mixing, Reynolds number of 14,000 in the main pipe, 24 ^{o}C) through channel G.

strain rates associated with these differences have been determined as the strain rates at the locations of single forces that would produce the same net forces and moments as produced by these distributed stresses. Estimates of the locations of these lines of action have been determined (see Appendix H) to be at values of r of about 3% less than the r values at the centers of the pressure taps. These estimates (labeled as r_N and listed in Table 6.3) have been used in eq. (6.6) to determine the extensional strain rates for the normal stress differences determined by eq. (6.11b) for the data presented in Figs. 6.4-6.7.

In eq. (6.16), the first normal stress differences in part are expressed in terms of radial stresses occurring at the taps. The representative extensional strain rates associated with these differences may be determined as those associated with the lines of action of the resultant forces exerted by the radial stresses on the taps during the polymer solution flows. However, the last step in the derivation of eq. (6.16) includes an approximation in which the normal stress differences are expressed in terms of the stresses at the taps without considering the changes in radial stress with distance r. Thus, to be consistent with this approximation, the estimates of the lines of action of the radial stresses were not made. In Figs. 6.4-6.7, the representative

extensional strain rates for the normal stress differences as calculated by eq. (6.16) have been determined as the strain rates at the centers of the downstream pressure taps (the locations of the centers of these pressure taps are listed in Table 6.1).

Comparing the results, Figs. 6.4-6.7 show that the normal stress differences determined by (6.16) tend to be about 20% smaller than those determined from eq. (6.11b) at similar extensional strain rates.

The first normal stress differences presented in Figs. 6.4-6.7 and determined by eq. (6.11b) have been replotted in Fig. 6.8 on a single graph in order to compare results from different channels. Very good agreement between the results for channels A, C, and D may be noted. However, the first normal stress differences measured using channel G were about 50% lower than those determined for the other channels at similar extensional strain rates.

One difference between channels A, C, D, and channel G is that the conical angle of channel G is 44° while the others have angles at or close to 29°. On the other hand, Fig. 6.9 shows the results of 20 ppm Separan AP-273 (1% master solution, 10 rps mixing) solution flows through channels G and H, both having similar channel angles, which illustrates that significant differences in the normal stress difference levels also can occur
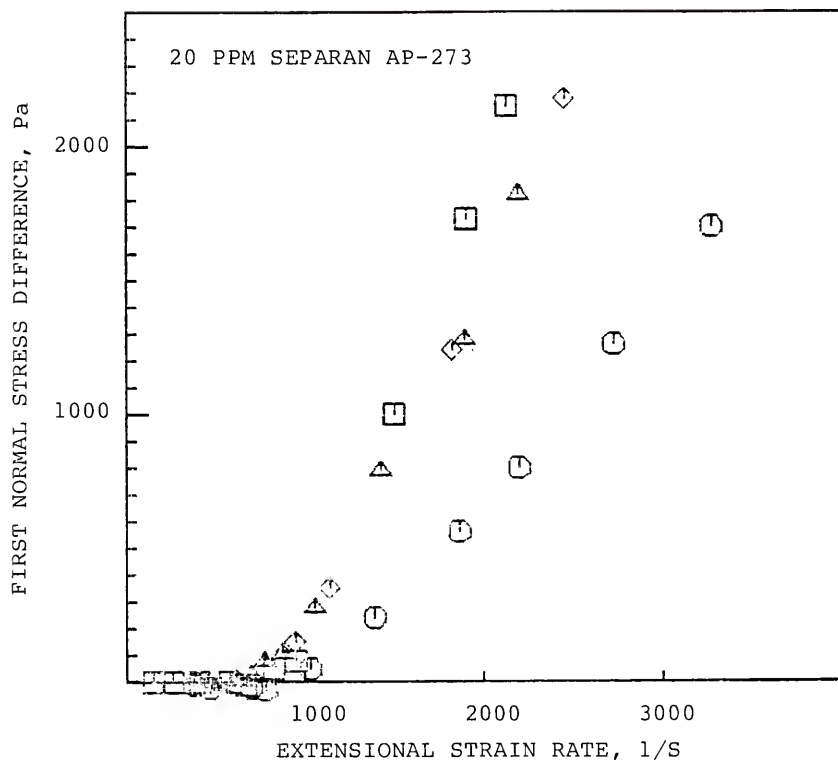
Fig. 6.8. Dependence of first normal stress difference on extensional strain rate for flow of a 20 ppm Separan AP-273 solution (1% master solution, 10 rps mixing, Reynolds number of 14,000 in the main pipe, 24 $^{\circ}$C) through channels A (⊡), C (△), D (◇), and G (⊙).
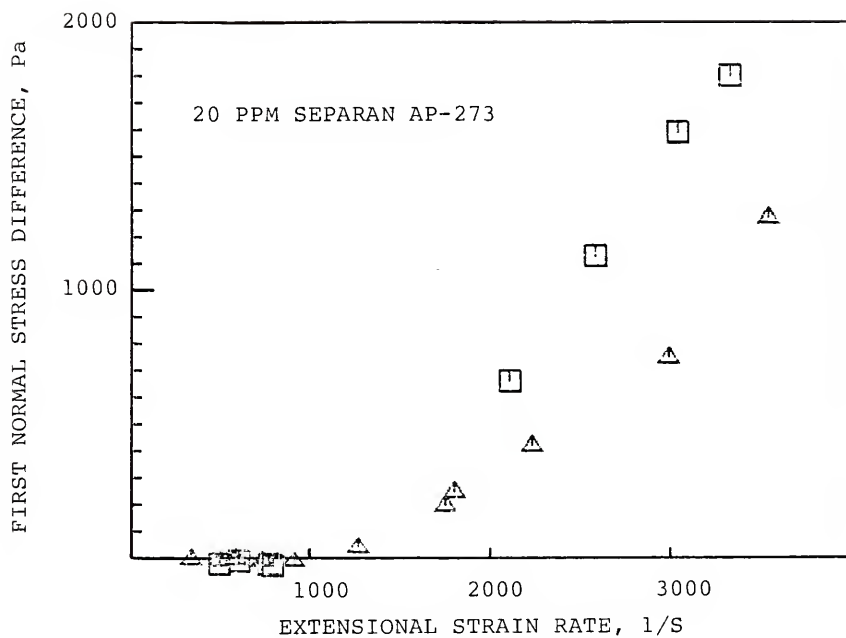
Fig. 6.9. Comparison of first normal stress differences for flow of a 20 ppm Separan AP-273 solution (1% master solution, 10 rps mixing, Reynolds number of 8,000 in the main pipe, 24 °C) through channels G (□) and H (△).

between channels of similar angles. At similar
extensional strain rates, the normal stress differences
determined from the measurements for channel H are seen
to be about 50% lower than those for channel G.

In Figs. 6.10 and 6.11, first normal stress
differences have been plotted as a function of
extensional strain rate for flows of 15 and 45 ppm
Separan AP-273 solutions (each with a 1% master solution
and 10 rps mixing) through channels A and G. It can be
seen that at similar strain rates, the normal stress
differences are greater for the 45 ppm solution and that
measurable normal stress differences occur at lower
strain rates than is the case for the 15 ppm solution.
Despite the threefold concentration difference, the
normal stress differences remained about 50% lower in
channel G than in channel A.

No secondary flows were observed to occur in these
Separan flows. From examination of the motions of both
dye and trace particles that were injected into the flow
upstream of the channels, the flow was observed to enter
the channels smoothly from all radial directions.

In Fig. 6.12, values from the total pressure drop
experiments are presented for flows of a 20 ppm Separan
AP-273 solution (1% master solution, 20 rps mixing)
through channel D. Here, the differences in pressure
drops recorded between the taps in the channel and in the
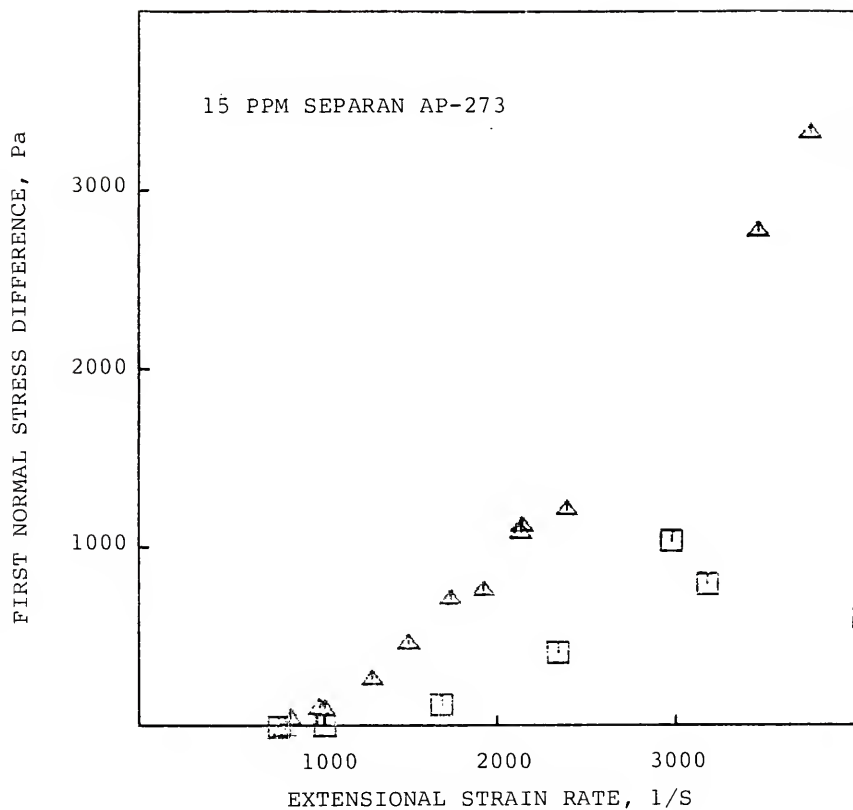
Fig. 6.10. Dependence of first normal stress difference on extensional strain rate for flow of 15 ppm Separan AP-273 solutions (1% master solution, 10 rps mixing, Reynolds number of 8000 in the main pipe, 24 °C) through channels A (△) and G (□).
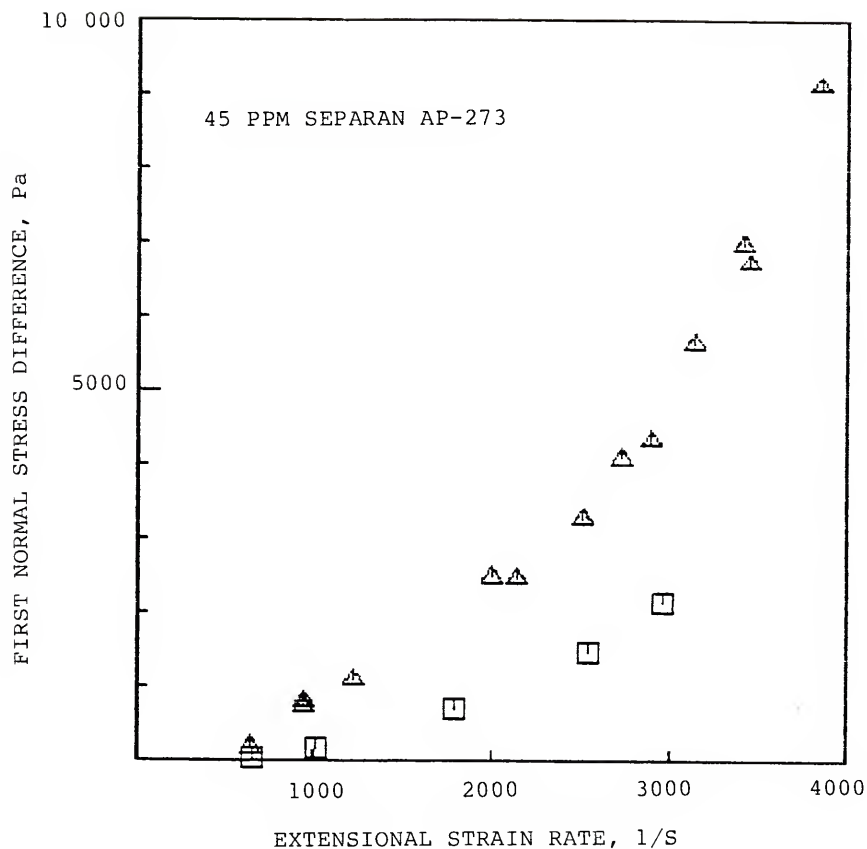
Fig. 6.11. Dependence of first normal stress difference on extensional strain rate for flow of 45 ppm Separan AP-273 solutions (1% master solution, 10 rps mixing, Reynolds number of 8000 in the main pipe, 24 °C) through channels A (△) and G (▢).

189
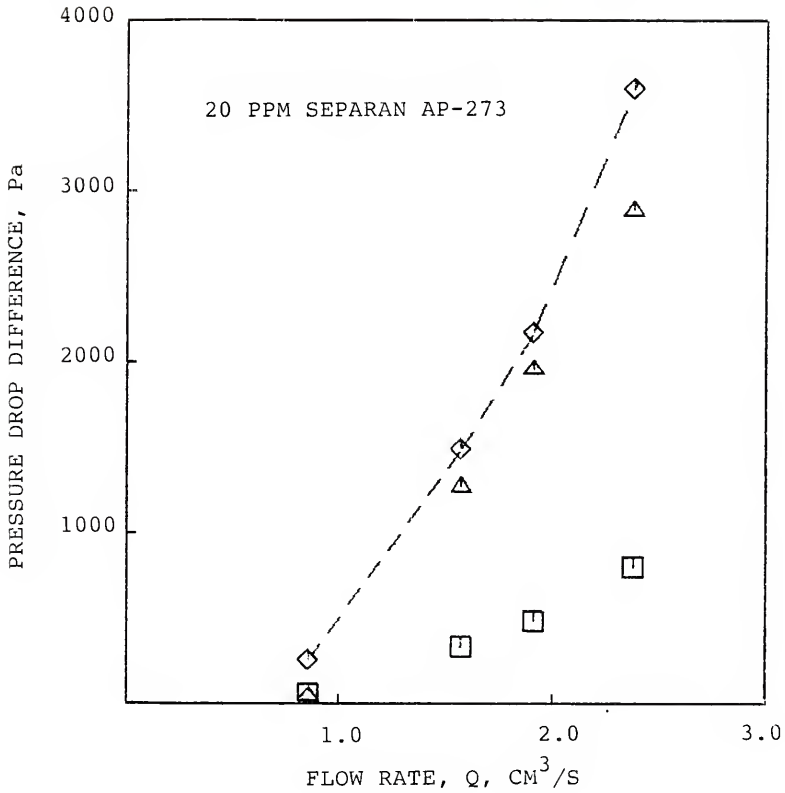
Fig. 6.12. Differences in the pressure drop recorded between taps (□) and in the overall pressure drop (△) between flows through channel D of a 20 ppm Separan AP-273 solution (1% master solution, 20 rps mixing, Reynolds number of 14,000 in the main experiment pipe, 24 °C) and of water, along with estimated differences in overall pressure drop (◇) from eq. (6.39).

pressure drops over the entire length of the channel
between polymer solution and water flow are plotted as a
function of flow rate. Both sets of measured pressure
drop differences are presented as positive values. It
should be noted, however, that the pressure drops between
the taps in the channel for the polymer solution were
less than that for water flow (at the same flow rates),
while the overall pressure drops were greater than those
occurring in corresponding water flows. In Fig. 6.12, it
can be seen that both sets of pressure drop differences
increased with flow rate, with the differences in overall
pressure drop being about 4 times as large as the
differences in pressure drop recorded between the taps.
Also presented in Fig. 6.12 are estimates of the
difference in overall pressure drop between polymer
solution and water flow as predicted by eq. (6.39). The
differences in overall pressure drop predicted by eq.
(6.39) were found to be 10-20% greater than measured
values.

In Fig. 6.13, results from the "aging" experiment
are presented. Here, the pressure drop measured between
the taps is plotted as a function of the time lapse after
removal of the solution from the main experimental flow
apparatus. The measurements plotted in this figure have
been made on the flows of a 20 ppm Separan AP-273 (1%
master solution, 10 rps mixing) through channel F, during
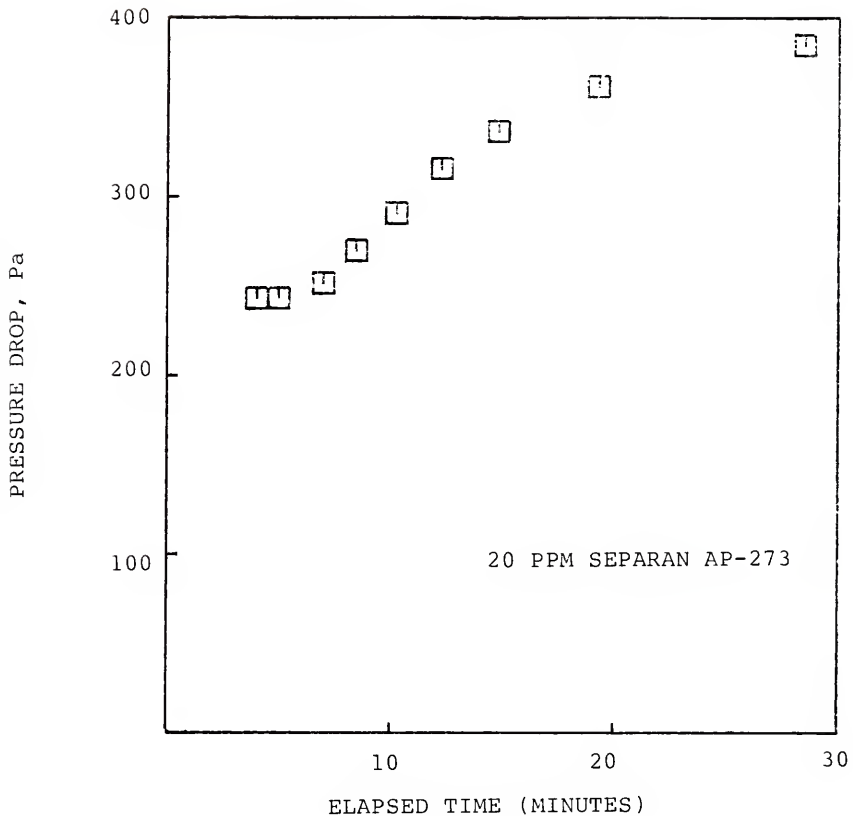
Fig. 6.13. Pressure drop between taps as a function of elapsed time from removal of solution from main experiment pipe for flow of a 20 ppm Separan AP-273 solution (1% master solution, 10 rps mixing, Reynolds number of 14,000 in the main experiment pipe, 24 $^{\circ}$C) through channel F with the overall pressure head being maintained at 4900 Pa.

which the overall pressure drop was maintained at a constant level of 4900 Pa. In Fig. 6.13, it can be seen that the pressure drop between the taps is constant initially, then increases with increased time lapse, and for large elapsed times, the pressure drop appears approach another constant value. At the start of the measurements, the flow through the channel was 1.32 cm^3/s, with the difference in pressure drop between the taps from that of water flow being 100 Pa and with the difference in overall pressure drop being 1000 Pa. After 28 minutes elapsed, the flow rate increased to 1.39 cm^3/s with the difference in pressure drop between the taps from that of water flow eliminated, while the difference in overall pressure drop decreased to 700 Pa.

In a separate "aging" experiment, the flow of a 20 ppm Separan AP-273 solution (1% master solution, 10 rps) was examined for flow through channel F, with this channel being attached to the main experiment pipe in two manners, one, where the channel was attached following 6 cm of 2.54 cm diameter tubing, and secondly, where the channel was attached using a 30 cm length of the same tubing. By using the longer tubing, the volume through which the solution had to flow before entering the channel was increased by 120 cm^3. As a result, the time between solution preparation and flow through the channel was also increased (eg., by about 4 minutes for a

flow rate of 2 cm^3/s). When compared at equal flow rates, pressure drops were found to be greater (less viscoelastic effect) for experiments conducted with the longer section of tubing than for those conducted using the shorter section for flow rates less than 2 cm^3/s, but only by very small amounts (by 10 Pa or less). No measurable differences in pressure drop were found at higher flow rates between experiments using the two different lengths of tubing.

From the preliminary experiments, it also has been observed that the level of solution viscoelasticity can be dependent on the flow rate in the main experiment pipe. Solutions which had been subject to greater flow rates in the main experiment pipe were found to exhibit slightly less viscoelastic effects. As an example, consider the results in Fig 6.14 for the flow of a 20 ppm Separan AP-273 solution (1% master solution, 10 rps mixing) through channel G for solutions which had been subject to main pipe flow at Reynolds numbers of 8000 and 11,000. At the larger measured extensional strain rates, the first normal stress differences of the solution obtained while maintaining a main pipe flow Reynolds number of 8000 are about 15% greater than those for a Reynolds number of 11,000.
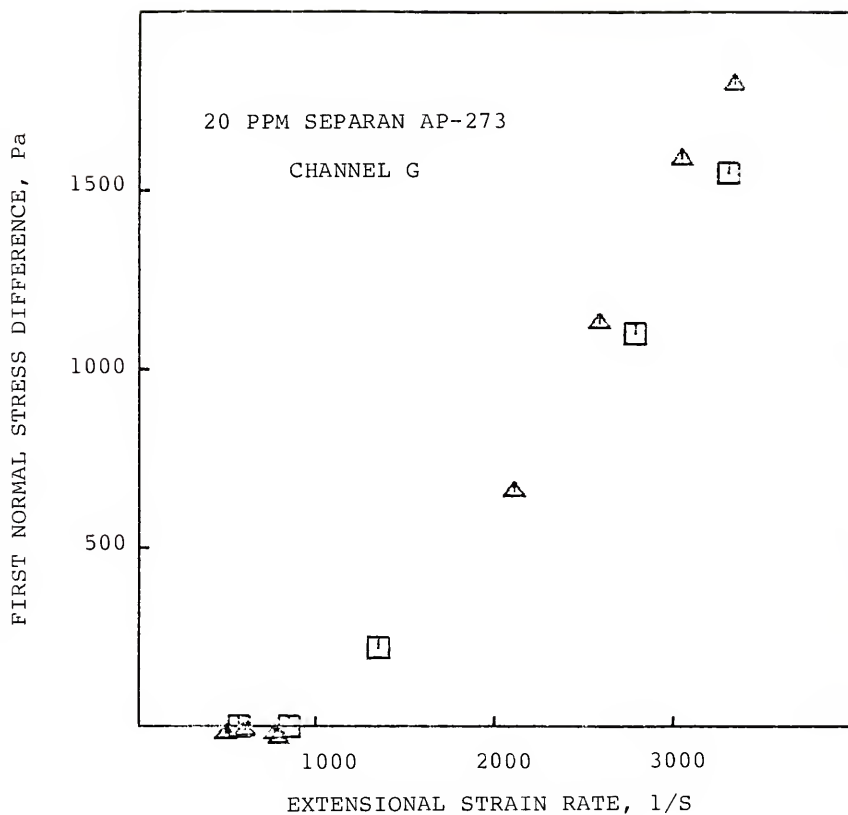
Fig. 6.14. Dependence of first normal stress difference on extensional strain rate for flow of a 20 ppm Separan AP-273 solution (1% master solution, 10 rps mixing, 24 °C) through channel D for the flow in the main experiment pipe being maintained at Reynolds numbers of 8000 (△) and 11,000 (▢).

Discussion

    Total pressure drop experiments. For the Separan
test solutions, the measured pressure drops along the
channels were found to be lower than those for water
flows of the same flow rates. In contradistinction, the
overall pressure drops for flows of these solutions were
greater than those for corresponding water flows. These
results indicate that additional normal stresses occurred
in these flows which were tensile in the radial (r)
direction and compressive in the direction normal to the
walls of the channels. Through examination of the energy
transfer in flow through the channels, it was postulated
that the additional (excess) amount of overall pressure
drop was due to the polymer molecules relaxing (upon
exiting the channels) in such a manner that little or no
interaction with the flow occurred. Estimates of the
additional overall pressure drop were made assuming that
no interaction with the flow occurred at all (all of the
additional internal energy being released to heat) and
these values were found to be only 10-20% greater than
the additional amount of overall pressure drop that
actually occurred. The general agreement of the
estimated values with the actual values was taken as
indicating that these excess pressure drops are indeed
the result of the polymer molecules relaxing with little
flow interaction. However, the fact that the estimated

values were greater than the actual values indicates that some interaction with the flow occurred, with the likely result being jet swell. As mentioned previously, with jet swell, the kinetic energies of the polymer solution jets will be lower than that for water flows at similar flow rates. Such effects will lead to less additional pressure drop than would be expected if no jet swell were to occur. If the differences between the estimated and actual additional overall pressure drops were associated only with jet swell, then it may be estimated that the jet diameters for the experiments reported in Fig. 6.12 must have increased by about 5-10%.

Aging and shear degradation. The "aging" experiments demonstrated that viscoelastic effects of the polymer solutions decreased with time from removal of the solution from the main flow pipe. Both the excess total pressure drop and the difference from water flow in pressure drop between the taps were observed to decrease with elapsed time. As discussed previously, any changes in solution properties are likely due to the disentanglement of extramolecular structures. Thus, the conclusion is that extramolecular structures can play a significant role in determining the viscoelastic properties of the Separan test solutions.

The observation that solution viscoelasticity depends on the flow rate in the main experiment pipe permits the conclusion that the viscoelastic properties of the test solutions may also degrade through shearing motions.

Comparison with simple fluid theory. Comparison of the present observations with previous theoretical results may be made by considering first the sink flow of an incompressible simple fluid. In such a fluid, the stress is determined, within an arbitrary isotropic pressure, by a functional ($\mathcal{F}$) of the history of the relative deformation gradient ($\underline{F}_t(s')$), or

$$\underline{T} = -P\underline{I} + \underset{s'=0}{\mathcal{F}} [\underline{F}_t(s)] \qquad (6.40)$$

where s' is a history parameter, $s'=t-t'$, with t being present time and t' being some reference time. Marrucci and Murch (1970) have examined a steady spherical sink flow of such a fluid as a special case of the inflation of a spherical shell (Coleman, 1968)), and they obtained the result that

$$T_{rr} - T_{\vartheta\vartheta} = N = N(\Gamma) \qquad (6.41)$$

$$T_{\vartheta\vartheta} - T_{\varphi\varphi} = 0$$

Thus, the first normal stress difference (N) for the incompressible steady sink flow of a simple fluid depends only on the local rate of the stretching (Γ).

The present experimental results do not agree with this theoretical result. At a given extensional strain rate ($D_{rr} = \Gamma$), flows of the same solution gave different levels of first normal stress differences depending on which channel was used. At a given extensional strain rate, the normal stress differences for flows through channels A, C, and D were found to be significantly larger than those for channels G and H. This was the case regardless of the procedure method followed to determine the normal stress differences (eq.(6.12) or eq. (6.16)). It is, of course, recognized that the same flow measurements were used for both methods, and that the variance in results between channels could be due to the influence of some factors unaccounted for. Such influences could possibly be the occurrence of secondary flows, unaccounted for viscous effects, and finite size hole pressure effects.

If secondary flows were to occur, then neither the use of eq. (6.6) to determine extensional strain rates, nor the methods for predicting the normal stress differences would be valid, and it is unlikely that the results from different channels would be similar. During the preliminary experiments, the flows through the

various channels were examined using dye and trace particles, and as mentioned earlier, there was no evidence of secondary flows.

The differences in pressure drop between polymer solution and water flow due to increased shear viscosity in the polymer solution were neglected in the derivation of eq. (6.11b), and all friction losses in the polymer solution flow were neglected in the derivation of eq. (6.16). Since any increased pressure drop due to viscosity would have the effect of counteracting a decrease of pressure drop due to the occurrence of additional compressive radial normal stresses, the determined normal stress differences were expected to be conservative (lower than actual values) due to the neglect of the mentioned viscous effects. Due to the design of the channels, all such viscous effects are likely to have been small, and as previously mentioned, even if the shear viscosity of the polymer solutions were twice that of water, the pressure drop in the polymer solution flow would be only about 2% greater than for corresponding water flow. The experimental data show that the changes in pressure drop in the polymer solution flow were of the same order of magnitude as for the pressure drop in water flow. Thus, any viscous effects unaccounted for are not likely to affect the results significantly, and they can not be the reason for the large variance in results between the channels.

The third factor mentioned that might lead to
different results for flows through the various channels
would be the effect of the finite size of the pressure
tap holes. In steady, low Reynolds number shear flow of
polymer solutions, pressures measured through use of taps
filled with liquid have generally been found to be
greater than for flush mounted transducers. Such effects
("hole pressure errors") have been attributed to non-zero
normal stress differences as due to hole induced
curvature of the streamlines. For the flow of
polyacrylamide solutions (0.6-3.0% by weight of Separan
AP-30, Dow Chemical Co.) through a slit die, Higashitani
and Lodge (1975) found "hole pressure errors" to be
proportional to the first normal stress differences, with
their magnitudes being about 18% of these differences.
Most other work in this area has also been conducted with
slit dies and for slow shear flows, while no "hole
pressure effects" seem to have been examined for the
extensional flows of low concentration polymer solutions.
It is not possible to determine whether "hole pressure
errors" exist or not in the present experimental
arrangement. However, if they did exist, it seems
unlikely that they would be responsible for the variance
in results between the channels. First, if it is assumed
that these errors would be proportional to the first
normal stress differences (as in shear flow) and that

there is a unique normal stress difference-extensional strain rate relationship, then at similar strain rates between channels, the magnitudes of the effects should be the same. This would lead to a constant change in the first normal stress difference for each channel (at a given extensional strain rate) and would not cause any variance in results between them. For "hole pressure errors" to account for the variance in the normal stress differences, the magnitudes of these errors would have to be the same for channels A, C, and D, but be of different magnitudes each for channels G and H. Due to the wide range of flow rates and pressures at the taps for the channels when flow conditions are compared at similar extensional strain rates, it is difficult to conceive of a relationship between the flow variables and the "hole pressure error" that would allow this to happen. Thus, while no conclusions are drawn as to whether "hole pressure errors" exist or not, it seems unlikely that if they do exist, that they would be the reason for the variance in results between the channels.

Since the occurrence of secondary flows, unaccounted for viscous effects, and "hole pressure errors" have been ruled out as factors that could cause variances in results between channels, it has been concluded that the differences in the normal stress levels between channels at similar extensional strain rates do indeed exist, and

are not artifices of the measurement and analysis procedures.

Comparison with theory for a suspension of elongated large scale particles. Before a further discussion of the experimental results, another investigation on the converging flow of low concentration polymer solutions will be described. In a study which utilized a channel similar to presently constructed channels, James and Saringer (1980) found that significant non-Newtonian stresses would occur (of the same order as the Newtonian stresses) in the flow of a 20 ppm polyethylene oxide (coagulant grade) test solution. Their findings prompted them to examine several fluid models in order to find out under what conditions such large non-Newtonian stresses could be produced. Their investigation ruled out the possibility that such large non-Newtonian stresses could be due to randomly coiled molecules with finite extension. Estimates of non-Newtonian stresses from the models that they examined were two orders of magnitude too small and they concluded that while other models of finite extension were available, that none would produce any stronger effects. They also examined Batchelor´s theory (1971) for a suspension of elongated particles to see if it could explain the occurrence of non-Newtonian stresses that would be as large as the Newtonian stresses. Batchelor´s theory has previously been

confirmed by Mewis and Metzner (1974) for suspensions of glass fibers in polybutene. Due to assumptions concerning the limits of particle size, this theory was found not to be able to predict non-Newtonian stresses of the magnitudes observed in the polymer solutions. However, it did lead James and Saringer to revise the theory in order to allow treatment of large-scale particles. An expression for the additional stresses (T_{rr}') for this revised theory was determined to be

$$T_{rr}' = \frac{\Phi}{\log(\pi/\Phi)}(\frac{l}{b})^2 g(s) \frac{du}{dr} \tag{6.42}$$

where Φ is the volume concentration, l is the half particle length, b is the effective particle radius, du/dr is the extensional strain rate, and where the function g is

$$g(s) = s^3\{ln \frac{s+2}{s-2} - \frac{s}{2} ln \frac{s^2}{s^2-4} - \frac{2}{s}\} \tag{6.43}$$

with s being the ratio r/l. This function was estimated to approach 4/3 for the case of small particles (in which case James and Saringer's equation reduces to Batchelor's result) and for the limiting large scale case of $2l$ of the order of r (the particle length $2l$ was restricted to less than r so that no particle extends past the apex of the conical channel), $g(r/l) \cong 3$.

James and Saringer concluded that the above expression can predict the magnitude of their observed non-Newtonian stresses if the aspect ratio (l/b) of the particles would be of the order of $10^{7/2}$. From the examination of electron micrographs of freeze dried samples of their polyethylene oxide test solution, they found the polymer residue to be mesh-like, with the smallest diameters of the molecular strands being estimated at about 0.1 microns. However, no ends of the molecular strands were observed and the aspect ratios of the components of the mesh were nowhere close to the magnitude of $10^{7/2}$. As a result, these investigators concluded that the polymer molecules have no inherent length scale, but rather an effective length created by the flow field. They envisoned that the polymer mesh would align itself with the flow and under these conditions, behave in a manner similar to a suspension of long aligned fibers. The effective length of the mesh was taken as being the distance from the upstream point of critical straining (the strain rate at which normal stress effects become measurable) to the exit. At their maximum observed flow rate, this distance was estimated to be of the order of the exit radius. With this value for the effective length, the aspect ratio l/b was sufficiently large enough, so that the revised Batchelor theory (eq. (6.42)) could account for the magnitude of the observed non-Newtonian stresses.

Of particular interest to the present investigation is that eq. (6.42) indicates that the normal stresses (and hence, normal stress differences) for a given solution may be dependent not only on the extensional strain rate, but also on the location of the stress measurement relative to the effective length of the mesh (r/l) and on the effective aspect ratio of the mesh (l/b), both of which can vary from channel to channel. The question that arises is, can either of these effects account for the presently observed variance in the levels of normal stress differences observed at similar extensional strain rates between the channels?

To investigate the effects of these variables on the level of normal stress differences, effective mesh lengths were estimated for flow of the 20 ppm polyacrylamide solution (Separan AP-273, Dow Chemical Co.) for flow rates such that the extensional strain rates were 2000 l/s at the downstream pressure taps for each of the channels. Following James and Saringer's suggestion, these effective lengths were taken as the distance between the location of onset of critical straining (r_o) and the exit (r_e). For the purposes of these calculations, the onset of normal stress effects was taken as occurring at an extensional strain rate of 700 l/s. This value represents the largest nominal extensional strain rate, such that the normal stress

differences determined at lower strain rates did not exceed 50 Pa for the results presented in Figs. 6.8 and 6.9. The estimated effective lengths for each of the channels are presented in Table 6.3. At an extensional strain rate of 2000 1/s for the polyacrylamide test solutions, the largest normal stress differences were observed in channel A, followed in order by channels C, D, G, and H. No correlation of this order with the estimated effective lengths was found. If the effective particle radii b may be assumed to be constant for the flow of the same solution through the different channels, then it may be concluded that the effect of variable aspect ratios l/b (as determined with the above estimated effective lengths) can not be the reason for the variance in results between the channels.

Using the estimated effective lengths, the ratios r_N/l and the values of the function g(s) were determined and these are also listed in Table 6.3. Here, the values of g(s) were found to be nearly equal for channels A, C, and D, for which nearly the same normal stress difference levels at 2000 1/s were obtained. For channels G and H, the values of the function g(s) are greater than for the other channels, and as such, would lead one to expect larger normal stress differences in these channels (than in channels A, C, and D). However, lower normal stress normal stress differences were

Table 6.3.   Estimated effective lengths of polymer mesh and values of g(s) (eq. (6.43)) for extensional strain rates at the downstream taps being 2000 1/s. Also listed are the radial distances at the end of the conical sections of the channels (r_e) and at the pressure taps (r_N).

| Channel | r_e (cm) | r_N (cm) | For Extensional Strain rates of 2000 1/s at the downstream taps ($r=r_N$) | | | | |
			r_o (cm)	Effective Length (r_o-r_e) (cm)	l (cm)	$s=r_N/l$	$g(s)$
A	.120	.150	.213	.093	.047	3.19	1.62
C	.120	.162	.230	.110	.055	2.95	1.67
D	.090	.118	.167	.077	.039	3.03	1.64
G	.070	.108	.153	.083	.042	2.57	1.83
H	.075	.130	.184	.109	.055	2.36	1.90

observed in these channels than for the other channels. Hence, while the function g(s) may affect the level of measured normal stress difference, it also is not likely that it is the reason for the observed variance in results between the channels.

Several assumptions have been made in the estimation of the effects of the aspect ratio and the function g(s) on the level of first normal stress difference. These include postulations that the effective mesh length equals $(r_o - r_N)$, that the extensional strain rate at "onset" for the same solution is the same for each channel, and that the effective radii of the aligned strands of the mesh are constant. Whether these assumptions are valid is questionable, and as such, no definite conclusions can be drawn concerning the effects of the polymer mesh structure on the level of first normal stress differences.

Duration of stretching. Another factor that possibly might influence the level of the normal stresses measured at the tap is the length of time that the polymer molecules have been subject to critical stretching. The length of time that a particle in the flow is subject to strain rates large enough to produce measurable normal stress effects should equal the flow time, t, for that particle to travel from the point in the channel where normal stress effects first become

significant to passage by the downstream tap

$$t = \int_{r_O}^{r_N} dr/u(r) \qquad (6.44)$$

where r_O and r_N are again the values of r at the onset of measurable normal stresses in the channel and at the tap respectively. After using eq. (6.4) to express the velocity in terms of radial distance r, integrating, and rewriting in terms of extensional strain rate through use of eq. (6.6), this time becomes

$$t = \frac{2}{3}[\frac{1}{\Gamma_O} - \frac{1}{\Gamma_N}] \qquad (6.45)$$

where $\Gamma_O = D_{rr}(r_O)$ and $\Gamma_N = D_{rr}(r_N)$. Thus, for a given extensional strain rate at the tap, the duration of critical stretching depends only on the onset strain rate. If onset strain rates are taken to be the same for the flow of the same 20 ppm test solution through the channels, then the duration of critical stretching can not account for the observed variances in the levels of the first normal stress differences.

Of further interest is that the time of duration of critical stretching varies with flow rate, and approaches a constant (finite) level for increasing flow rates. As a result, the levels of normal stress difference observed at the tap at a given extensional strain rate may not

necessarily be the same as for other (non-conical flow) experiments where the duration of critical stretching will not necessarily be the same. For example, the duration of critical stretching for large extensional strain rates for two-dimensional sink flow will approach a value of $(1/2)/ \Gamma_o$, while for conical flow this limiting value is $(2/3)/ \Gamma_o$. Larger normal stress differences might be expected to occur for the conical flow than in the two-dimensional sink flow, since the flow would be subject to longer periods of critical stretching.

Strain. In an investigation on the flow of polymer thickened motor oils through nozzles profiled to yield constant average extensional deformation rates, Oliver and Ashton (1976b) found that the extra axial stresses (due to the presence of the polymer) were not directly related to the extensional strain rates in the nozzles. Instead, these investigators report that these extra stresses were strain dependent.

To determine the level of strain in the flow through the conical channels, consider two material points which are located at $r(t)$ and $r(t)+dr(t)$ at time t and which were previously located at $r(t')$ and $r(t')+dr(t')$ at some reference time t'. A measure of strain (in the radial direction) may be taken as the relative elongation (ϵ) between these points, or $\epsilon = dr(t)/dr(t')$. For steady

streamline flow, $dr(t)/u(t) = dr(t´)/u(t´)$, and therefore

$$\varepsilon = \frac{dr(t)}{dr(t´)} = \frac{u(t)}{u(t´)} \tag{6.45}$$

By substitution of eqs. (6.4) and (6.6) into eq. (6.45), the relative elongation that the fluid is subjected to from "onset" ($r=r_O$) to passage by the downstream tap ($r=r_N$) may be written as

$$\varepsilon = (\frac{r_O}{r_N})^2 = (\frac{\Gamma_N}{\Gamma_O})^{2/3} \tag{6.46}$$

For a given strain rate at the downstream tap, the relative elongation will depend only on the strain rate at "onset". From the results of the 20 ppm Separan AP-273 solution flows presented in Fig 6.8, it can be seen that "onset" occurs at nearly the same extensional strain rates for channels A, C, and D; however, "onset" in channel G might be occurring at slightly higher strain rates. Consequently, at any given strain rate the relative elongation will be less than in channels A, C, or D, and this may be the reason why lower normal stress differences are observed in channel G than in these other channels. The present experimental results are not extensive enough to accurately determine "onset" conditions, and hence, permit definite conclusions to be

made concerning the effects of relative elongation.
However, as a rough calculation, for the results
presented in Fig. 6.8, assume that "onset" occurs at a
strain rate of 700 1/s in channels A, C, and D and at
1000 1/s in channel G. For first normal stress
difference levels of 1000 Pa, which occur at strain rates
of about 1600 1/s in channels A, C, and D, and at 2400
1/s in channel G, the relative elongations as determined
by eq. (6.46) are 1.73 for channels A, C, and D, and 1.79
for channel G. Thus, the first normal stress differences
may be more dependent on the level of relative elongation
than on extensional strain rate. Additionally, it should
be noted that if "onset" strain rates are not the same
for all channels, then the duration of critical
stretching may also be an important factor in determining
the level of first normal stress difference.

General comments. Due to possible strain history
effects and due to the observed variance in results
between channels, it should be emphasized that the normal
stress-extensional strain rate relationships determined
by examining conical channel flow will not be
representative of material properties. However, since
large viscoelastic effects can be generated in these
channels and since the results for a given channel and
solution were found to be easily reproducible, these
channels appear to be useful tools for determining

relative measures of the viscoelastic characteristics of low concentration polymer solutions.

Comparison with previous experimental results.

First, this author knows of no other investigations of very low concentration polymer solutions through conical channels other than that by James and Saringer (1980, 1982). In their initial experiments (1980), head-discharge measurements for channels with taps located on the channel walls were reported for flows of one 20 ppm polyethylene oxide solution through a single channel, and hence, no direct comparisons with their results will be made. In their second investigation reported in 1982, some results were presented that are of interest to this investigation. Pressure drop measurements over the entire lengths of both a conical channel and a wedge shaped channel of similar dimensions (both with solid angles of 60° and exit dimensions of 0.1 mm) were reported for the flow of several polyethylene oxide (coagulant grade) solutions. For a 20 ppm solution, the overall pressure drop along the conical channel was reported to be 100% greater than that for water flow, while for flow through the wedge shaped channel, small if any changes occurred. For the flow of a 50 ppm solution, pressure drops that were 400% greater than that for corresponding water flow occurred, with the non-Newtonian effects exhibiting an onset at about 4000 l/s, followed

by their rapid increase in magnitude with increasing extensional strain rate. In contrast, for the flow through the wedge shaped channel, a constant increased overall pressure drop of about 10-15% was measured for extensional strain rates ranging from 2000-30,000 1/s, with no onset being observed. These results illustrate that extra normal stress effects are not dependent only on the extensional strain rate in the converging flows of low concentration polymer solutions, but may also be affected by other factors. As mentioned previously, the levels of extra normal stress effects in two dimensional sink flows might be expected to be lower than that for three dimensional sink flows due to shorter durations of critical stretching. James and Saringer's suggested explanation for the differences in their results was that the non-Newtonian stresses were dependent on the polymer forming "strands" in the flow and that for the two dimensional flow, the rate of this strand formation was lower, and as a result, less viscoelastic effects were observed.

The only other extensional flow experiments known to this author for flows of either polyacrylamide or polyethylene oxide solutions at concentrations of less than 50 ppm are those reported by Balakrishnan (1976). As mentioned in Chapter II, Balakrishnan examined the freely converging flow through orifices of several

aqueous polyacrlyamide solutions. The normal stresses measured by this investigator were greater than those determined in the present investigation. For example, at an extensional strain rate of 4000 1/s (for flows of a 20 ppm Separan AP-273 solution), Balakrishnan reports first normal stress differences which range from about 12,000 to 30,000 Pa. At a similar strain rate, first normal stress differences of only about 4000 Pa were obtained for flow through channel D in the present investigation. These differences do not necessarily reflect upon the diffferent procedures for determining the first normal stress differences, but are more likely due to use of different batches of polymer and to completely different solution preparation procedures. The drag-reducing abilities of Balakrishnan´s solutions were also considerably greater than the solutions used in the present investigation. This likely indicates that the viscoelastic properties of his solutions were indeed greater, which could account for the differences between his and the present results.

Summary

When compared to water flow, flows of polyacrylamide test solutions induced lower pressure drops along the channels, but with greater pressure drops over the entire lengths of the channels. This indicates the occurrence of additional tensile normal stresses in the direction of

motion, with additional compressive normal stresses normal to the flow direction. The experiments indicate a correlation between the additional normal stresses in the channel and the additional change in overall pressure drop. Based on energy transfer considerations, the additional change in overall pressure drop was found to be reasonably predicted by assuming the additional energy in the polymer molecules was released to heat with little flow interaction when exiting from the channels. Also, it was found that the viscoelastic characteristics of the polymer solutions were susceptible to both degradation by shearing and by "aging" mechanisms. The "aging" experiments were further interpreted as indicating that extramolecular structures played a significant role in the determination of the viscoelastic properties of the polyacrylamide test solutions.

Another result was that at similar extensional strain rates, different levels of first normal stress difference were obtained, dependent on channel geometry. These results are contrary to simple fluid theory and also could not be explained by a modified Batchelor theory which treated the solutions as suspensions of elongated large scale particles. In comparison with previous experimental results, it was noted that extra normal stress effects presented by Oliver and Ashton (1976b) and James and Saringer (1982) also were dependent

on factors other than merely the extensional strain rate. The present results indicate that the first normal stress differences generated in the conical channel flows may be dependent more on strain than on extensional strain rate.

The presently determined first normal stress differences have also been found to be lower than those reported by Balakrishnan (1976) for similar polyacrylamide solutions at similar extensional strain rates.

General Polymer Solution Measurements

Goal

The purpose of the general polymer solution measurements was to obtain relative measures of the extensional characteristics of the test solutions, in order to provide a basis for correlation of these characteristics with their drag-reducing abilities.

Scope

The same test solutions have been examined in this set of experiments as in the drag reduction experiments. With the Reynolds number being maintained at 8000 in the main experiment pipe and with the mixer operating at 10 rps, experimental runs have been conducted with 1, 2, 5, 10, 15, 20, 30, and 45 ppm Separan AP-273 solutions; with

5, 10, and 20 ppm Separan AP-30 solutions; and with 20 and 30 ppm Polyox WSR-301 solutions. Additionally, measurements have been made with the mixer operating at 30 rps for Separan AP-273 solutions of 5, 10, and 15 ppm additive concentrations.

The additives have been injected into the main flow in the same fashion as has been done in the drag reduction flow experiments. Master solutions of 1% concentration by weight have been used in the preparation of all solutions, with the exception of the Separan AP-273 solutions of 5 ppm or less, where 0.2% master solutions have been used.

In cases of additive concentrations at 10 ppm or higher of Separan AP-273, the solutions have been conducted through channel A. All of the remaining experiments, including some repeated runs with 10 and 20 ppm Separan AP-273 solutions, have been made using channel D.

The experimental flow rates ranged from about 0.2 to 4 cm^3/s (channel D), corresponding to extensional strain rates ranging from 300 to 6000 1/s at the downstream pressure tap.

Experimental Procedure

The same experimental procedure was used as described for the preliminary polymer solution measurements.

Typically, the extensional flow measurements for a given solution were conducted on the same day as the drag reduction measurements, with these runs being conducted either immediately before or after the drag reduction experiments. Further, during these runs, pressure drop in the main experiment pipe was continually monitored to ensure that the drag-reducing abilities of the test solutions were not changing.

Experimental Results

It is desirable to present the experimental results as to show the viscoelastic effects clearly, while still presenting the results so as to represent the actual measurements as closely as possible. In the analysis of the preliminary extensional flow measurements, it has been shown that the first normal stress differences may be directly determined from the differences in pressure heads from polymer solution to water flow (at equal flow rates). The results in this section consequently are being presented graphically, with the differences in pressure head (h_w-h_p) being plotted as a function of flow rate, with additional abscissa scales indicating the extensional strain rates at the downstream pressure tap $(r=r_m)$.

Extensional strain rates that are characteristic of the values where the differences in pressure head first
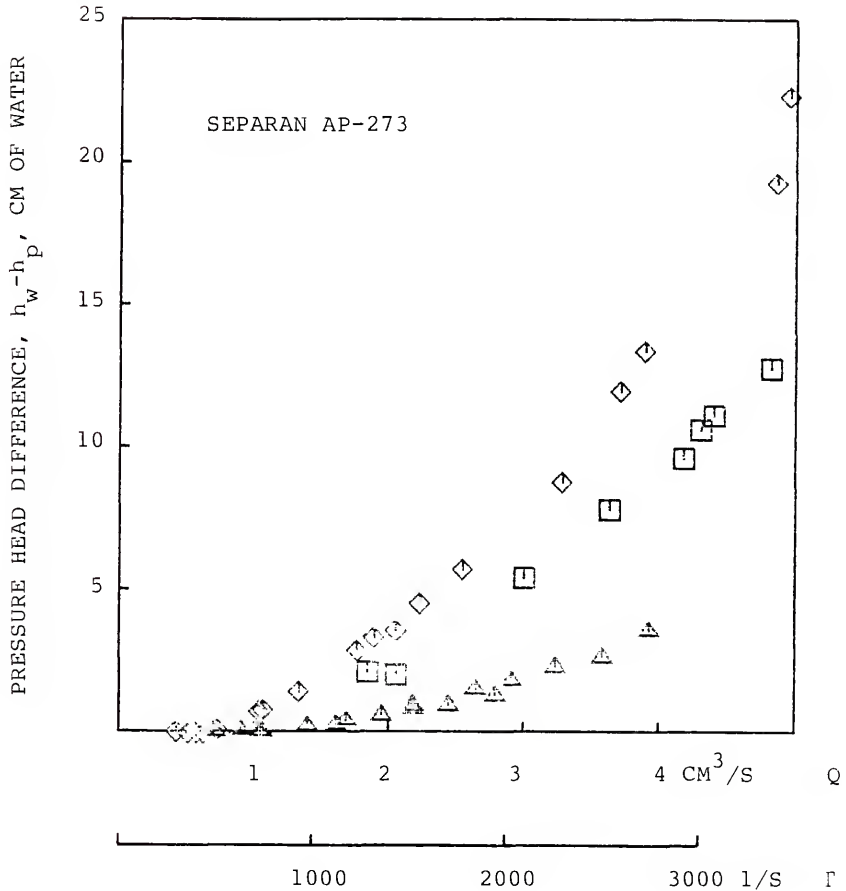
Fig. 6.15. Differences in pressure head as a function of flow rate/extensional strain rate at the downstream tap for 10 (△), 20 (▢), and 30 (◇) ppm Separan AP-273 solutions (1% master solution, 10 rps mixing, Reynolds number of 8000 in the main experiment pipe) for flow through channel A.
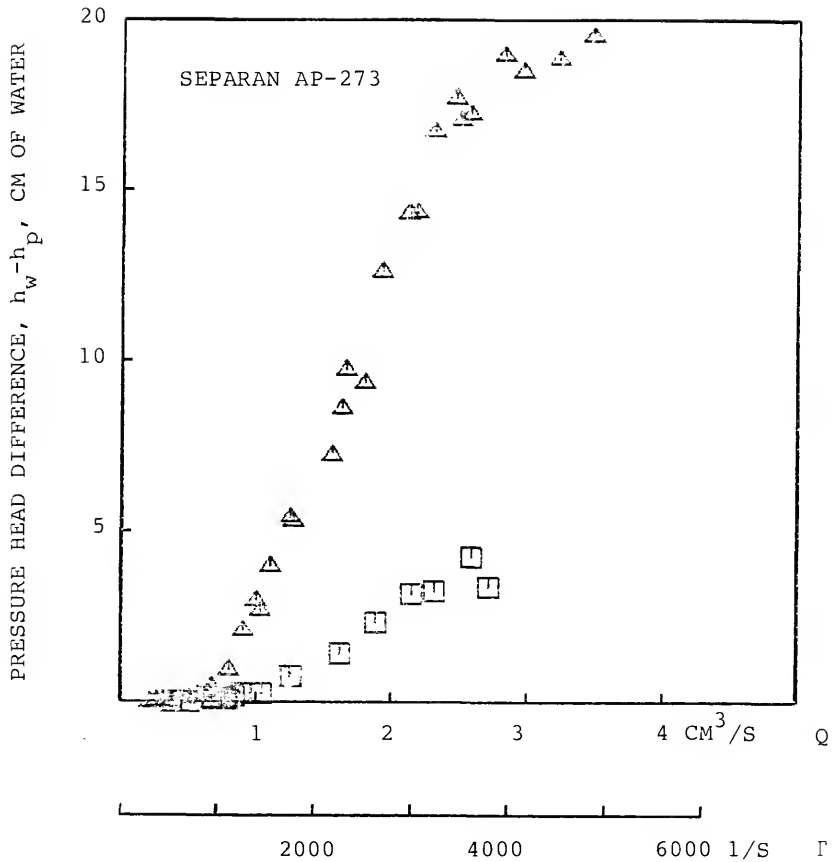
Fig. 6.16. Differences in pressure head as a function of flow rate/extensional strain rate at the downstream tap for 10 (□) and 20 (△) ppm Separan AP-273 solutions (1% master solution, 10 rps mixing, Reynolds number of 8000 in the main experiment pipe) for flow through channel D.
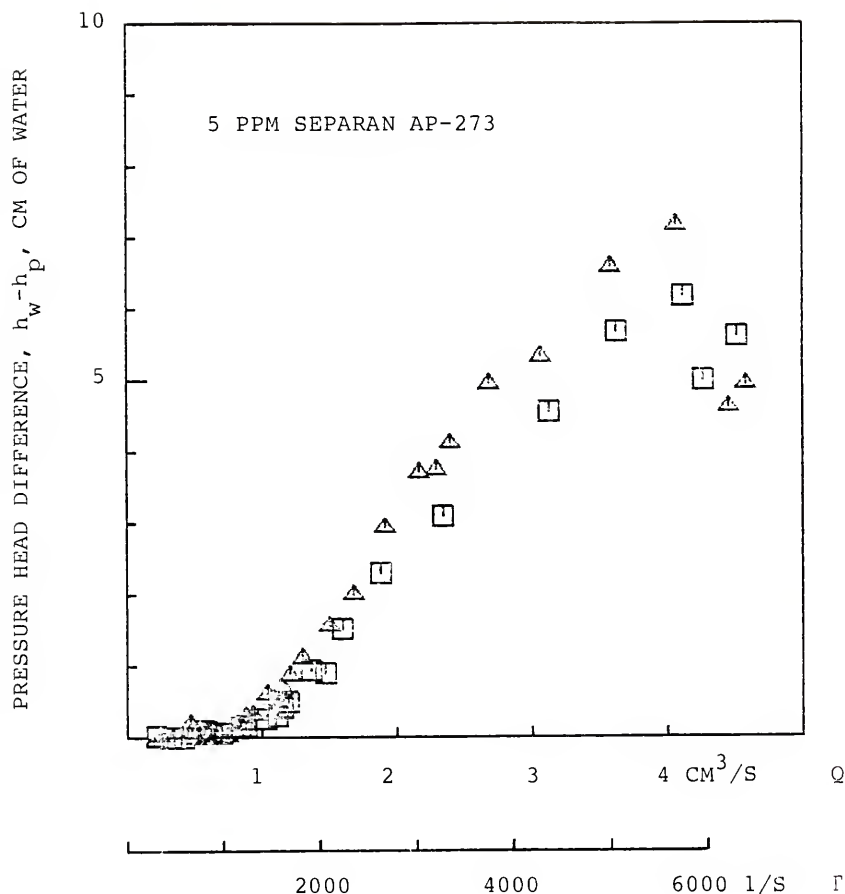
Fig. 6.17. Differences in pressure head as a function of flow rate/extensional strain rate at the downstream tap for flows through channel D for 5 ppm Separan AP-273 solutions (0.2% master solution, Reynolds number of 8000 in the main experiment pipe) for both 10 (△) and 30 (▯) rps mixing.
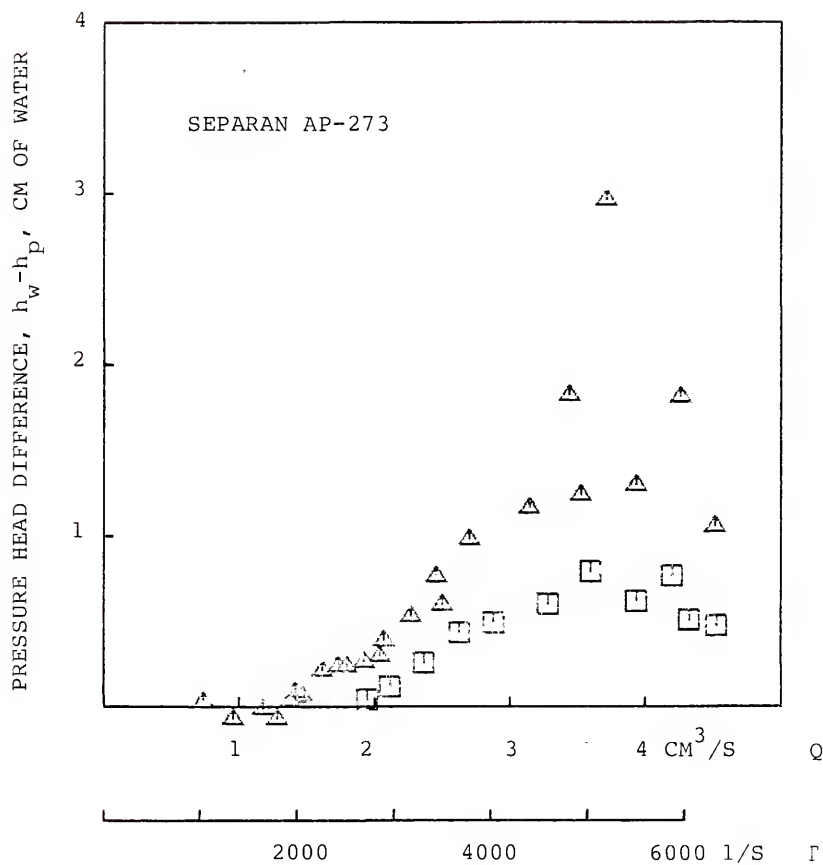
Fig. 6.18. Differences in pressure head as a function of flow rate/extensional strain rate at the downstream tap for 1 (⬜) and 2 (△) ppm Separan AP-273 solutions (0.2% master solution, 10 rps mixing, Reynolds number of 8000 in the main experiment pipe) for flow through channel D.
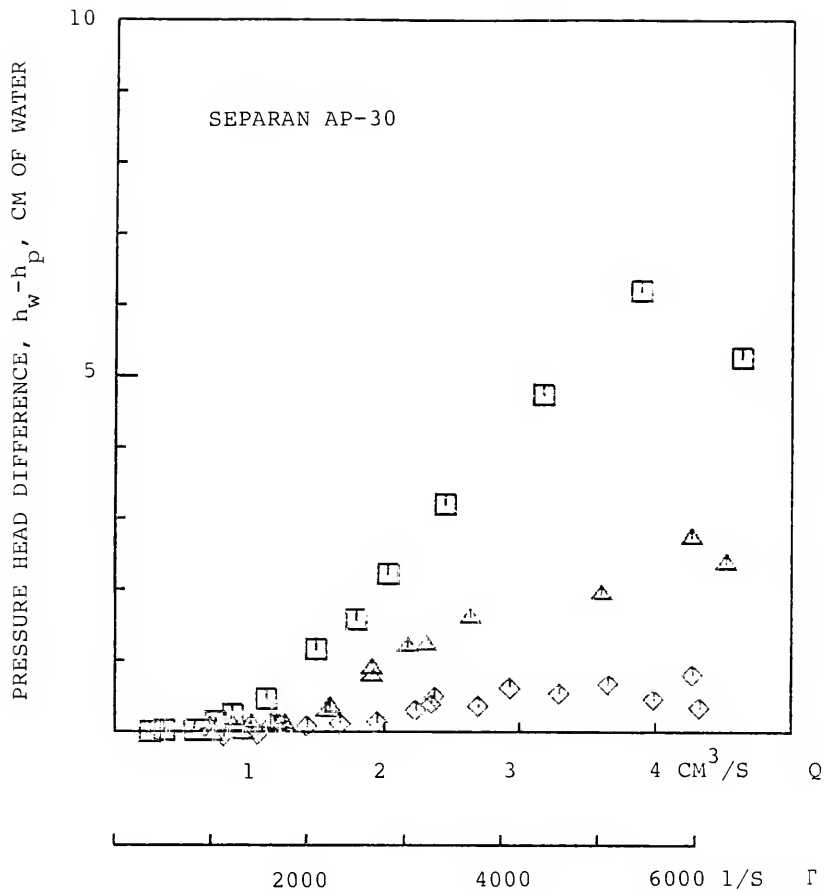
Fig. 6.19. Differences in pressure head as a function of flow rate/extensional strain rate at the downstream tap for 5 (◇), 10 (△), and 20 (⊡) ppm Separan AP-30 solutions (1% master solution, 10 rps mixing, Reynolds number of 8000 in the main experiment pipe) for flow through channel D.

become measurable have also been determined. These have been calculated by determining linear least squares fits of the pressure head difference, strain rate data points for the first few points after which the viscoelastic effects were first observed, and then, extrapolating these linear fits to zero pressure head difference to obtain the desired characteristic "onset" extensional strain rates. The least squares fits have been applied to data points for an extensional strain rate range of 1000 1/s, with the lower ends of these ranges corresponding to the data points with the lowest strain rates, above which all pressure head differences were greater than 0.2 cm of water.

In Figs. 6.15 and 6.16, results are reported for measurements on flows of Separan AP-273 solutions (1% master solution, 10 rps mixing) at additive concentrations of 10, 20, and 30 ppm for flows through channel A and of 10 and 20 ppm for flows through channel D. In Fig. 6.17, results for flows of 5 ppm Separan AP-273 solutions (0.2% master solution) are shown with the mixer operating at both 10 and 30 rps. The measurements on flows of 1 and 2 ppm Separan AP-273 solutions (0.2% master solution, 10 rps mixing, channel D) are presented in Fig. 6.18. In Fig. 6.19, data are shown for flows of 5, 10, and 20 ppm Separan AP-30 solutions (1% master solution and 10 rps mixing).

As a first observation, viscoelastic effects were observed for all of the test solutions, even at an additive concentration of only 1 ppm (Separan AP-273). With regards to the general flow behavior, no measurable differences in pressure head (from polymer solution to water flow) were observed at low flow rates for flows of the Separan solutions. Then, at some point for increasing flow rates, pressure head differences became measurable and the magnitudes of these differences were found to increase with increasing flow rate. At sufficiently high flow rates, the pressure head differences were observed to level off for many of the solutions, and at the highest measured flow rates, decreases in pressure head difference were also observed. When these decreases in pressure head difference did occur, the flow behavior was found to be more erratic than at lower flow rates.

It may also be observed that AP-273 was a much more effective additive than the lower molecular weight grade AP-30. At equal concentrations, the pressure head differences for flows of the AP-273 solutions were found to be 2-5 times as large as for the AP-30 solutions. The "onsets" occurred at lower strain rates for flows of the AP-273 solutions, and after "onset", the rates of increase of the pressure head differences were also larger than for flows of the AP-30 solutions.

With regard to in-line mixing, it was found that the higher mixing speed of 30 rps caused a decrease of the observed pressure head differences. As can be seen in Fig. 6.17 for the measurements on flows of 5 ppm Separan AP-273 solutions, increased mixing delayed the "onset" of viscoelastic effects to higher extensional strain rates.

The lower concentration Separan AP-273 solutions (5 ppm and less) were prepared using a 0.2% master solution (instead of 1% solutions used for the other experimental runs). In order to examine the influence of the concentration of the master solution upon solution viscoelasticity, measurements were carried out at an additive concentration of 5 ppm (and 30 rps mixing), while using both 1% and 0.2% master solutions. No significant differences were observed between the results of these two sets of experiments.

In Fig. 6.20, the data obtained from measurements on the flows of the Polyox WSR-301 solutions are presented. Dramatic differences are noted in comparison with observations on the flows of the Separan solutions. At a given flow rate, the pressure head in the Polyox WSR-301 solutions are observed to be greater, not less than for water flow. This difference was initially unexpected, since the polyethylene oxide results reported by James and Saringer (1980) followed the type of behavior as exhibited by the presently used Separan solutions
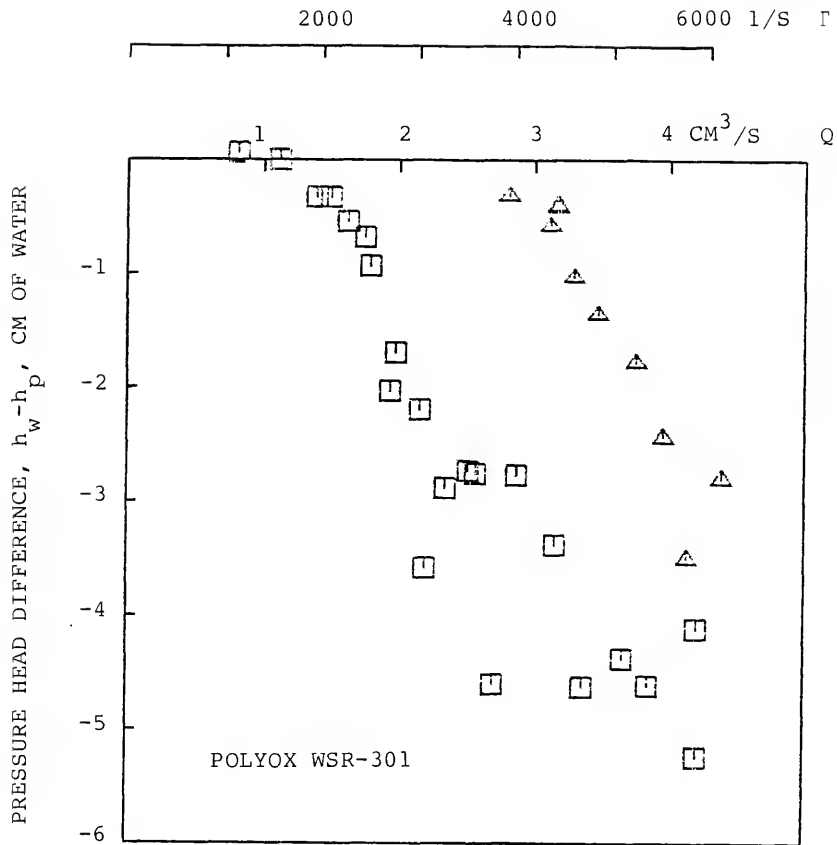
Fig. 6.20. Differences in pressure head as a function of flow rate/extensional strain rate at the downstream tap for 20 ($\triangle$) and 30 ($\square$) ppm Polyox WSR-301 solutions (1% master solution, 10 rps mixing, Reynolds number of 8000 in the main experiment pipe) for flow through channel D.
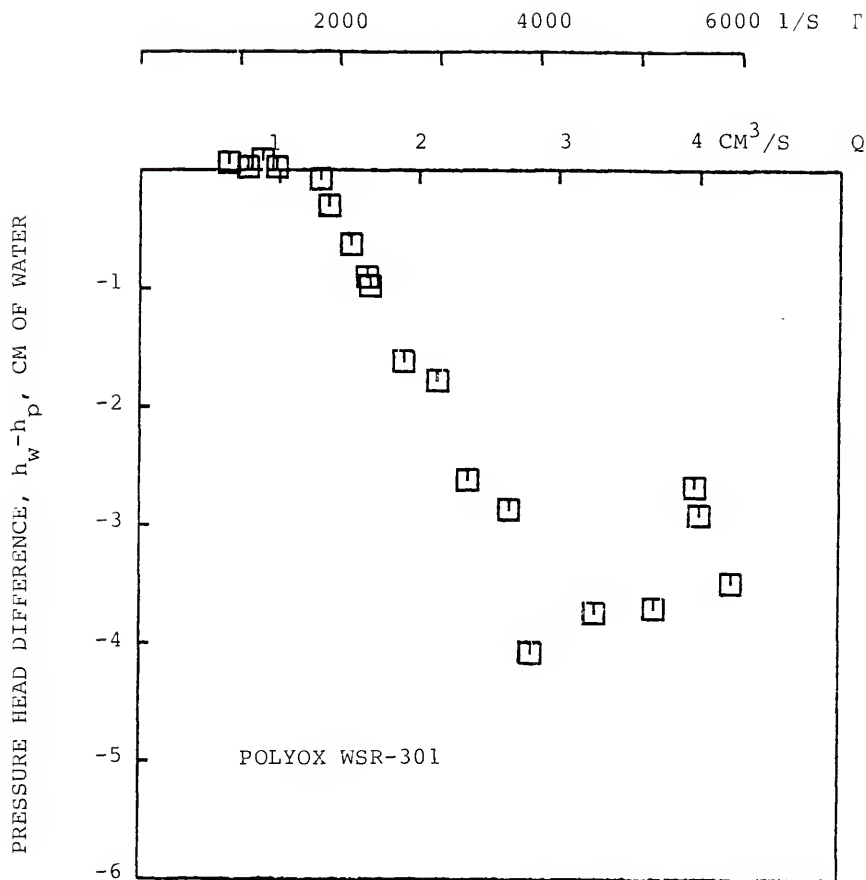
Fig. 6.21. Differences in pressure head as a function of flow rate/extensional strain rate at the downstream tap for a 30 ppm Polyox WSR-301 solutions (prepared with a different 1% master solution than for the results presented in Fig. 6.20, 10 rps mixing, main flow Reynolds number of 8000) for flow through channel D.

(i.e., measured pressure drops which were less than that for water flow at the same flow rates). To verify this result and to make sure that this behavior was not due to solution contamination and/or to some possible variation in the solution preparation procedures, a separate master solution batch was prepared and the experiments repeated. In Fig. 6.21, measurements are presented for flows of a 30 ppm Polyox solution (1% master solution, 10 rps) where a different master solution was used than for the experiments presented in Fig. 6.20. Nearly identical observations results have been recorded.

When comparing the present results with those reported by James and Saringer (1980), it should be noted their experiments were conducted using a coagulant grade of polyethylene oxide, a higher molecular weight grade of polythethylene oxide than the presently used Polyox WSR-301. In orifice flow experiments, "contrary" viscoelastic effects have also been reported for flows of aqueous solutions of each of these two different molecular weight grades of polyethylene oxide. For flow of a 30 ppm Polox WSR-301 solution, Bate (1967) reported reductions in pressure drop over an orifice (compared to water flow), while solutions made with coagulant grades of polyethylene oxide can cause increased pressure drops over orifices (eg., Giles, 1969). The energy transfer analysis previously presented with regard to the

preliminary polymer measurements showed that decreased pressure drops along a channel can be related to an increased overall pressure drop. Conversely, it might be expected that increased pressure drop along a channel would be associated with reductions in overall pressure drop[1]. Consequently, the present observations appear to agree qualitatively with the orifice flow data of Bate (1967).

Besides the "contrary" pressure effects, a difference between the Separan and Polyox flows was that "onset" occurred at higher extensional strain rates for flows of the Polyox solutions. An illustration of this may be found in Fig. 6.22, where extensional strain rates at "onset" for flows of various test solutions have been plotted as a function of additive concentration. A listing of the "onset" data is given in Table 6.4. From Fig. 6.22, it may also be seen that "onset" strain rate for the Polyox solutions varies more with concentration than for the Separan solutions.

---

[1] If at similar flow rates the isotropic pressure drop is equal for both polymer solution and water flow, then a greater pressure head in the polymer solution flow indicates a negative value for the extra stress τ_{rr} at the pressure tap. If a mechanism exists where little or no additional work (compared to water flow) is done on the polymer solution as it exits the conic section of the channel, then a negative value of the extra stress τ_{rr} indicates that a reduction in pressure drop will occur (cf. eq. (6.30)).
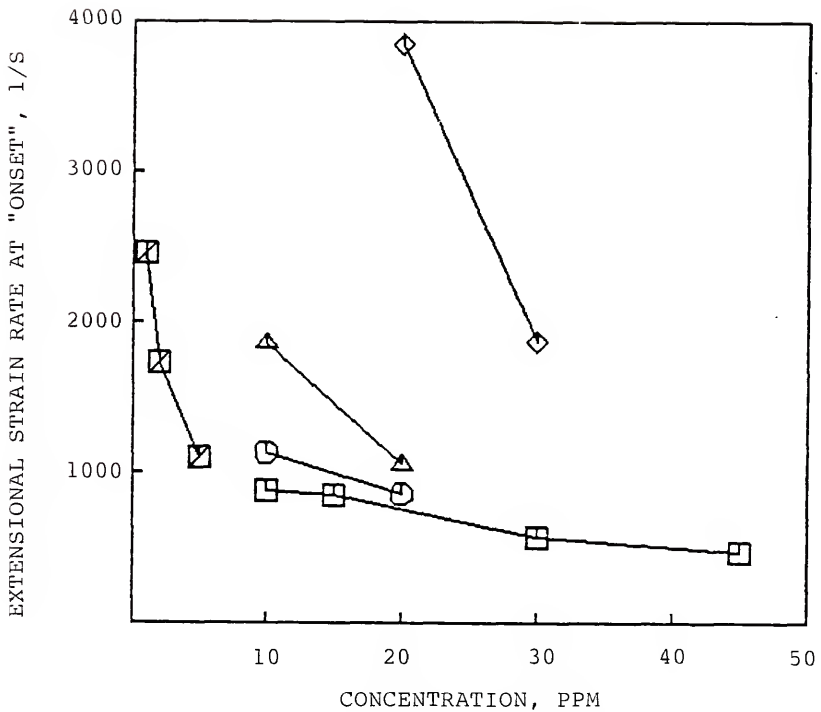
Fig. 6.22. Extensional strain rate at "onset" as a function of additive concentration, each experiment being conducted with 10 rps mixing and with a Reynolds number of 8000 for the flow in the main experiment pipe.

Table 6.4. Summary of "onset" data for extensional flows.

Channel	Master Solution conc.	Additive	conc. (ppm)	Mixing speed (rps)	Extensional Strain Rate at "onset" (1/s)	Slope of Fit (cm s)	Strain Rate Range of Fit (1/s)
A	1%	Separan AP-273	45	10	467	.00580	610-1150
			30	10	567	.00433	710-1540
			20	10	*	*	*
			15	10	854	.00282	950-1820
			10	10	883	.00145	1020-1850
D	1%	Separan AP-273	20	10	860	.00563	790-1780
			10	10	1134	.00123	1240-2260
D	0.2%	Separan AP-273	5	10	1100	.00152	1300-2110
			2	10	1730	.00039	2260-3180
			1	10	2461	.00039	3310-3810
D	1%	Separan AP-30	20	10	1056	.00108	1220-2100
			10	10	1863	.00099	2190-3030
			5	10	*	*	*
D	1%	Polyox WSR-301	30	10	1869	.00161	1940-2770
			20	10	3848	.00115	3920-4862
A	1%	Separan AP-273	15	30	928	.00228	1315-2010
			10	30	1000	.00110	900-1420
D	1%	Separan AP-273	5	30	1446	.00154	1650-2350
	0.2%		5	30	1330	.00153	1440-2240

* Values not determined.

Briefly summarizing the results from the general extensional flow measurements, it is to be noted that viscoelastic effects were observed in all of the examined test solutions. Flows of the Separan solutions induced lower pressure drops along the channels than did water flows at the same flow rates, and the higher molecular weight grade of the two Separan additives produced the greater viscoelastic effects. Increased additive concentration lowered the "onset" extensional strain rate and increased the rate of increase of pressure head difference with extensional strain rate. Increased mixing lowered the magnitude of the viscoelastic effects by delaying "onset" to higher extensional strain rates. Flows of the Polyox solutions induced greater pressure drops along the channels than did water flow at the same flow rates. Furthermore, the extensional strain rates at "onset" were greater, and a greater dependence of "onset" strain rate on concentration was observed on flows of Polyox solutions than for the Separan solutions.

COMPARISON OF DRAG REDUCTION, EXTENSIONAL FLOW,
AND SHEAR VISCOSITY MEASUREMENTS

Shear viscosity, drag reduction, and extensional
flow measurements have been conducted for a series of low
concentration polymer solutions. In this chapter, the
results of these measurements are examined for possible
correlations.

Shear viscosities have been determined for aqueous
polyacrylamide solutions at additive concentrations of 5,
15, 20, 30, and 45 ppm with Separan AP-273 (Dow Chemical
Co.), at additive concentrations of 5, 10, and 20 ppm
with Separan AP-30 (Dow Chemical Co.), and for aqueous
polyethylene oxide solutions at additive concentrations
of 20 and 30 ppm (Polyox WSR-301, Union Carbide Corp.).
For shear strain rates ranging from about 3000 to 19,000
1/s, it was found that

(1) these test solutions behave in a Newtonian, or nearly
    Newtonian manner for laminar flow conditions; and
    that

(2) the solution shear viscosities are only marginally
    increased as a result of polymer addition.

In both the extensional flow and drag reduction
measurements, significant non-Newtonian effects were

235

observed.   Further, lower pressure heads often   occurred in   the extensional flows of the polyacrylamide   solutions than   would be expected for inviscid flow at the same flow rates.   It was also noted that it is not likely   that   a purely   viscous   mechanism   can explain   the   simultaneous occurrence   of decreasing pressure heads along the conical channels,   with   the   increase in pressure drop   over   the entire   lengths of the channels (as observed for flows   of the   polyacrylamide solutions).   Consequently, it has been concluded   that the non-Newtonian behavior observed in the extensional   flows   as well as in the drag-reducing   flows are not caused by purely viscous effects.

In comparing the results of the drag reduction with the extensional flow experiments, similarities in the non-Newtonian   effects   in each of the experiments   have   been found.   Measurable   non-Newtonian   behavior   has   been observed   for   all of the test solutions in both   sets   of experiments   and the solutions which exhibited the greater levels   of   drag reduction exhibited greater extra   normal stress   effects   in   the   extensional   flows.   More specifically,   drag   reduction correlated well with   extra normal   stress   effects   for   over   the   entire   range   of additive   types, molecular weight grades,   concentrations, and mixing conditions that were investigated.

With regards to additive type, the solutions prepared   with   the   polyacrylamide   additives   were   more

effective drag-reducers and exhibited greater magnitudes of extra normal stress effects in the extensional flows than did the polyethylene oxide solutions. Also, "onset" occurred at lower strain rates in flows of the polyacrylamide solutions than in flows of the polyethylene oxide solutions in both the drag reduction and extensional flow experiments.

Since specific drag reduction has been found to decrease with decreasing concentrations at low concentrations, it was concluded that molecular interactions played a significant role in the drag reduction mechanism. The extensional flow "aging" measurements (conducted with polyacrylamide solutions) indicate that extramolecular structures also play a significant role in generating non-Newtonian normal stress effects. Furthermore, the drag-reducing experiments as well as the extensional flow experiments clearly indicate two distinct types of non-Newtonian behavior between flows of the polyacrylamide and polyethylene oxide solutions.

With regards to the effect of the two different molecular weight grades of polyacrylamide that were examined, greater non-Newtonian effects were noticed for solutions prepared with the higher molecular weight additive in both the drag reduction and extensional flow experiments. The "onset" of non-Newtonian behavior

occurred at lower strain rates, and after "onset", the rate of increase of the non-Newtonian effects were greater for the higher molecular weight (Separan AP-273) solutions than for the lower molecular weight (Separan AP-30) solutions of similar concentrations.

Similarities were also observed in the concentration dependence of the non-Newtonian effects generated in the drag reduction and extensional flow experiments. In both sets of experiments, the "onset" strain rates for flow of the Separan AP-273 solutions of greater than 10 ppm varied less with concentration than they did for flow of either the Separan AP-30 or Polyox WSR-301 solutions. Again, after "onset" in both sets of experiments, a greater increase of the non-Newtonian effects with concentration was found for the AP-273 solutions than for either of the other two sets of solutions (both of which exhibited nearly the same rates of increase in each set of experiments).

In both the drag reduction and extensional flow experiments, increasing the mixing speed from 10 to 30 rps decreased the the non-Newtonian effects.

Comparisons of the drag-reducing abilities of the polymer test solutions with their extensional characteristics are illustrated in Figs. 7.1-7.5 by plotting the increase in the buffer layer thickness (ΔB) of the non-dimensional mean velocity profile in the drag-

reducing pipe flows as a function of a multiple of the wall strain rate ($5u_*^2/\nu$), together with graphs of extensional viscosity versus extensional strain rate. The increase in the buffer layer thickness of the velocity profile has been determined by using eq. (5.7)

$$\Delta B = (1/f_p^{1/2} - 1/f_s^{1/2})/8^{1/2} \tag{5.7}$$

This equation has been evaluated separately for each set of data points (flow rate, pressure drop) with the friction law coordinate $1/f_s^{1/2}$ for the solvent flow being determined from a least squares fit of the water measurements (cf. Chapter V). For purposes of comparison, the strain rates characteristic of the drag-reducing flows are measured in $5u_*^2/\nu$ (instead of just u_*^2/ν, since for many of the test solutions the "onset" of drag reduction was found to occur at wall strain rates of about one-fifth of the strain rates at "onset" of non-Newtonian effects in the extensional flows). The extensional viscosities (η_e) have been determined as the absolute value of the first normal stress difference (as specified in eq. 6.11b) divided by the extensional strain rate (as specified in eq. (6.6)) at the center of the downstream pressure tap, $\Gamma = D_{rr}(r_m)$.
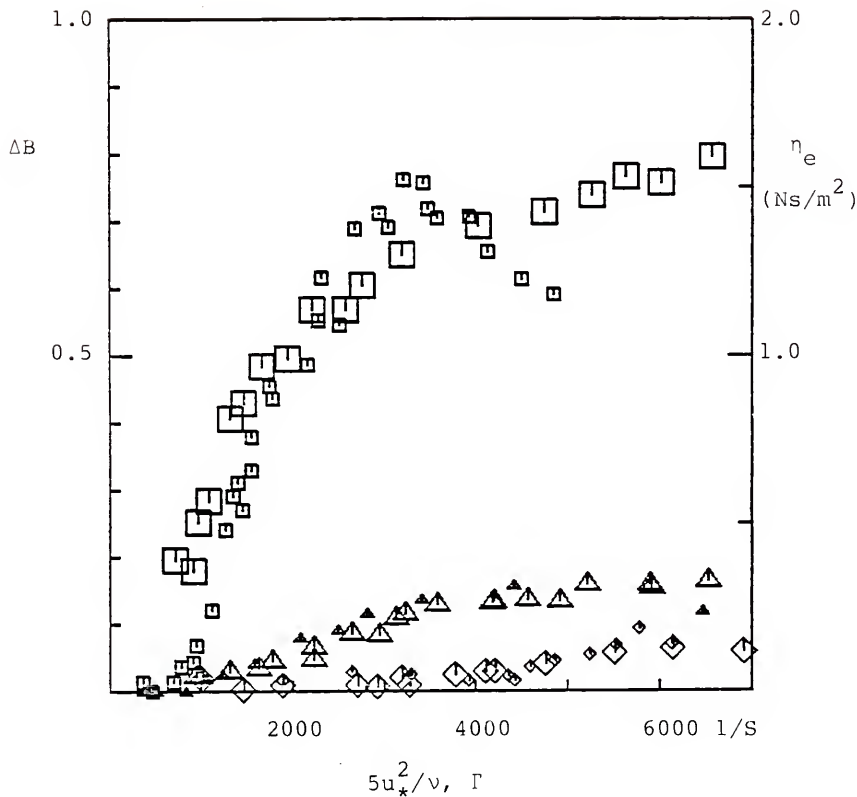
Fig. 7.1. Comparison of increased buffer layer thickness (ΔB) with extensional viscosity (η_e) for 20 ppm Separan AP-273 (⬓), 20 ppm Separan AP-30 (△), and 20 ppm Polyox WSR-301 (◇) solution flow (1% master solutions, 10 rps mixing). The larger size of each type of symbol represents $5u_*^2/\nu$, ΔB data points, while the smaller sized symbols represent Γ, η_e data points.
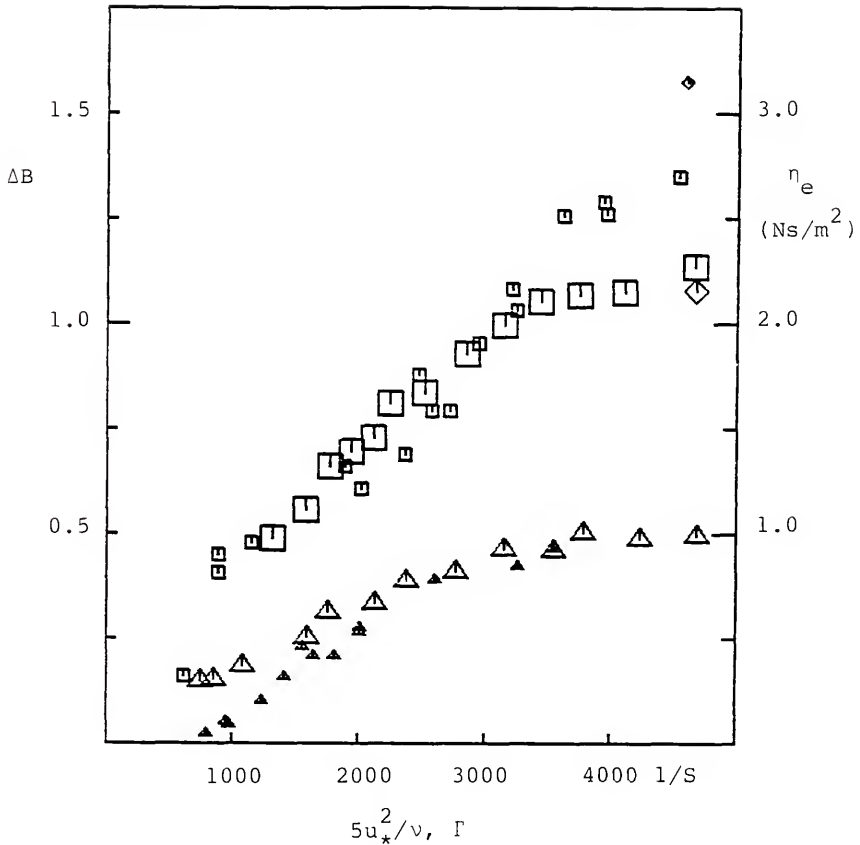
Fig. 7.2. Comparison of increased buffer layer thickness
(ΔB) with extensional viscosity (η_e) for 15
($\triangle$) and 45 ($\square$) ppm Separan   AP-273
solutions (1% master solution, 10   rps
mixing). Also presented are a pair   of
data   points   ($\diamondsuit$)   estimated   from
Balakrishnan´s (1976) measurements on flow of
a 10 ppm Separan AP-273 solution. The larger
size of each type of symbol represents
$5u_\star^2/\nu$, ΔB data points, while the smaller
sized symbols represent Γ, η_e data points.
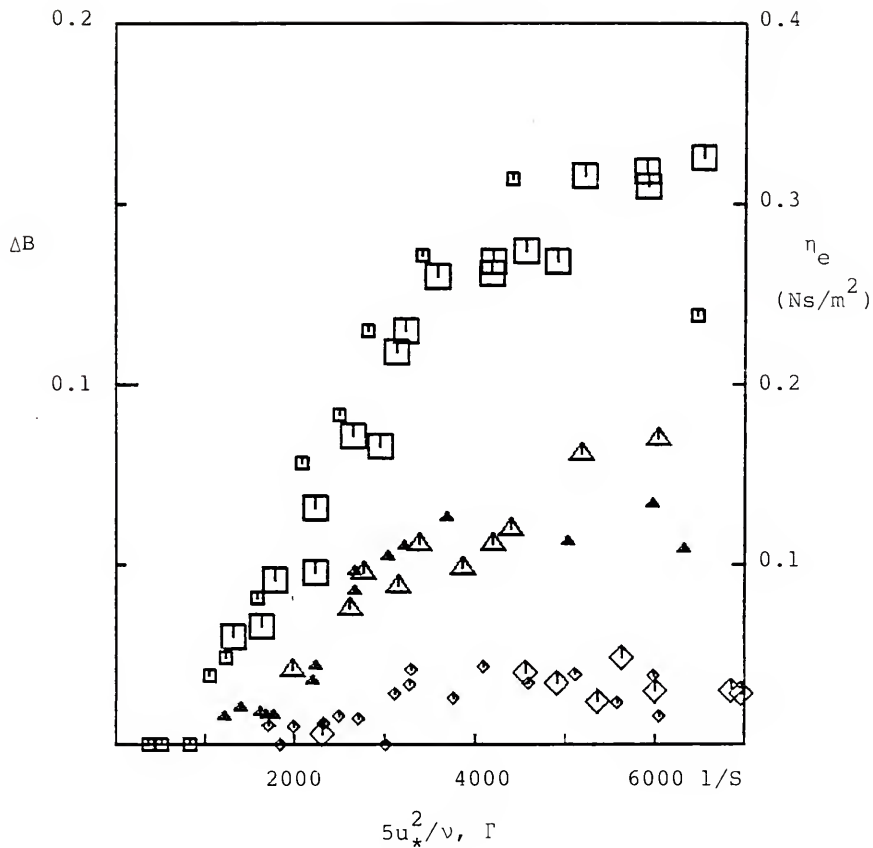
Fig. 7.3. Comparison of increased buffer layer thickness (ΔB) with extensional viscosity (η_e) for 5 (◇), 10 (△), and 20 (☐) ppm Separan AP-30 solution flow (1% master solution, 10 rps mixing). The larger size of each type of symbol represents $5u_*^2/\nu$, ΔB data points, while the smaller sized symbols represent Γ, η_e data points.
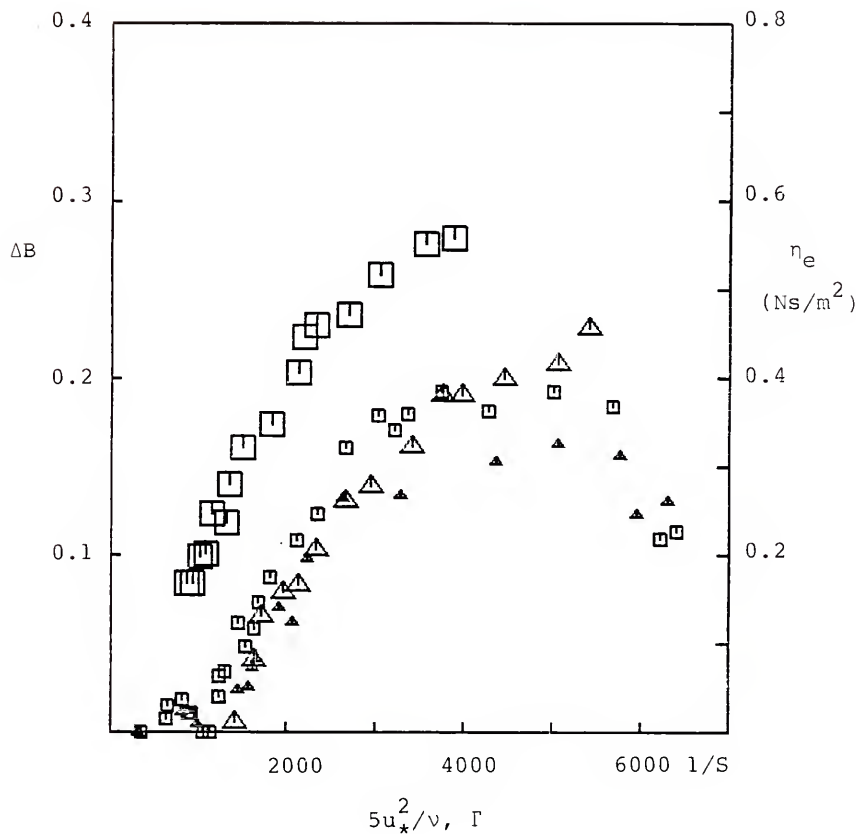
Fig. 7.4. Comparison of increased buffer layer thickness (ΔB) with extensional viscosity (η_e) for 5 ppm Separan AP-273 solution flow (0.2% master solution) for both 10 (⊡) and 30 (▲) rps mixing speeds. The larger size of each type of symbol represents $5u_*^2/\nu$, ΔB data points, while the smaller sized symbols represent Γ , η_e data points.
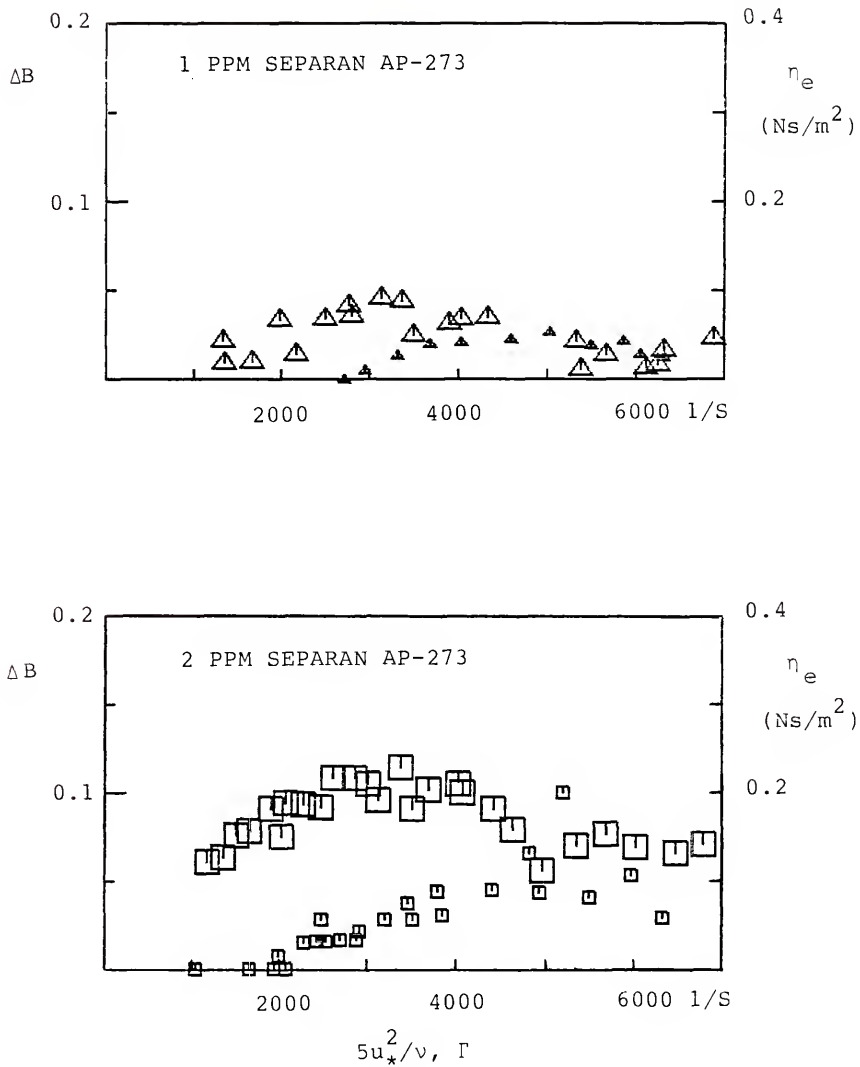
Fig. 7.5.   Comparison   of increased buffer layer thickness
(ΔB) with   extensional   viscosity (η_e)   for
1 ($\triangle$) and 2 ($\square$) ppm Separan AP-273   solution
flow (0.2%   master solution, 10   rps   mixing).
The   larger size of   each   type of symbol
represents $5u_*^2/\nu$, ΔB data   points,   while
the   smaller sized symbols represent Γ, η_e
data points.

Figure 7.1 illustrates the results for solutions of the same concentration (20 ppm) for each of the three additives, Separan AP-273, Separan AP-30, and Polyox WSR-301 (1% master solutions, 10 rps mixing). In Fig. 7.2, evaluated data are presented for flows of 15 and 45 ppm Separan AP-273 solutions, while Fig. 7.3 contains data for 5, 10, and 20 ppm Separan AP-30 solution flows (all for 1% master solutions and 10 rps mixing). Regardless of the additive type or concentration, there is a very good correlation of the increase in the buffer layer thickness with the level of extensional viscosity, both of which vary in magnitude by more than a factor of 10 over the entire range of strain rates considered.

In Fig. 7.4, data are presented for flow of 5 ppm Separan AP-273 solutions (0.2% master solution) for mixing speeds at both 10 and 30 rps. An increased buffer layer thickness is observed to correlate well with the extensional viscosity for the run with 30 rps mixing; however, the results at the lower mixing speed are not as well correlated. In fact, the extensional viscosities for this (10 rps) run appear to correlate better with the increase in buffer layer thickness with for the data for the 30 rps mixing speed. Water tests conducted before and after each run (for both experiments) confirmed that the equipment was operating properly. Also, the pressure drops recorded at the upstream tap during the extensional

runs, indicate that the same level of drag reduction was being maintained in the main pipe flow as during the drag reduction run. A possible explanation for these deviating observations may be that after passing through the measuring section of the main experiment pipe and before passing through the conical channel, that the solution with 10 rps mixing was being degraded relatively more than the 30 rps solution. Before reaching the conical channel, the test solutions have to pass through a needle valve, which may introduce sufficient shearing conditions to further degrade the viscoelastic properties of a weak solution. It is possible and likely that the flow with the mixing speed set at 10 rps was degraded some additional amount by passage of the flow through this valve, while for the flow with 30 rps mixing, which had already been subject to some more intense shearing motions in the mixer, was not as affected by the shearing in the flow through this valve. The extensional viscosities for flow of the 1 and 2 ppm Separan AP-273 solutions (10 rps mixing, 0.2% master solution) shown in Fig. 7.5 are also somewhat lower than would be expected based on the increase in buffer layer thickness of the other solutions examined in the present investigation.

Whether or not the differences in the 1, 2, and 5 ppm results can be explained, it should be noted that when compared with the entire range of results, these

differences are not very significant. It is not that the data for these runs are correlated, but that they are not as remarkably correlated as for the other solutions. Further, of all of the examined results, the 5 ppm, 10 rps run represents the "worst" case, that is, the case where the largest consistent difference was observed between the increases in buffer layer thickness and extensional viscosities (as compared using the relative scales in Figs. 7.1-7.5). As such, it may be concluded that the drag-reducing abilities of the test solutions are well correlated with their extensional characteristics. Consequently, these results support the theories which postulate that drag reduction results from turbulence suppression due to increased resistance to extensional motions.

Balakrishnan (1976) has reported both drag reduction and extensional flow measurements for some polyacrylamide solutions. In general, his drag reduction measurements have not been conducted with solutions of the same concentrations as for his extensional flow experiments. Hence, direct comparison with these results can not be made. The one exception is that both drag reduction and extensional flow measurements have been reported for a 10 ppm Separan AP-273 solution. By estimating values from graphically presented data, an extensional strain rate of 4600 1/s (the lowest measured strain rate for this run)

seems to correspond to an extensional viscosity of 3.15 Ns/m^2 and that the increase in buffer layer thickness ΔB was equal to 1.1 (for $5u_*^2/\nu$ being 4600 1/s). Separately, the magnitude of these parameters were much greater than observed for runs conducted with the Separan AP-273 solutions at this concentration level in the present investigation. (This is likely due to use of different batches of polymer, to different solution preparation procedures, and to the use of in-line mixing, which was not used in Balakrishnan´s investigation.) However, relative to the measured level of drag reduction, this extensional viscosity was not much greater than would be expected based on the present results. In the present investigation, an increase in buffer layer thickness of 1.1 is also observed for $5u_*^2/\nu$ being 4600 1/s for the 45 ppm Separan AP-273 run, with the corresponding extensional viscosity being 2.7 (compared to 3.15 for Balakrishnan´s 10 ppm solution). This comparison is also shown in Fig. 7.2, in which the pair of data points that have been estimated from Balakrishnan´s measurements are presented along with the present 45 ppm Separan AP-273 results. Since the extensional viscosities determined in either investigation are not representative of material properties, an exact correlation of the results between the two investigations may not necessarily be expected.

However, since the extensional viscosity determined from Balakrishnan's data is of the same magnitude as would be expected based on the results of the present investigation, this comparison was taken as supporting the conclusion, that the drag-reducing abilities of low concentration polymer solutions are related to their extensional properties.

To the best of the author's knowledge, there are no other experimental investigations where both the drag-reducing abilities and extensional characteristics have been reported for similar test solutions. Presently, the results from this investigation represent the only direct comparison between the drag-reducing abilities of low concentration polymer solutions with their extensional characteristics.

CHAPTER VIII
SUMMARY, CONCLUSIONS, AND RECOMMENDATIONS
FOR FUTURE WORK

In this investigation, shear viscosity, drag reduction, and extensional flow measurements have been conducted for a series of low concentration polymer solutions. Shear viscosities were determined using a sliding ball viscometer; drag reduction was measured using a pipe flow apparatus; and the extensional behavior of the test solutions was characterized using conical channel rheometers. The experimental set-up was arranged so that some of the fluid that passed through the drag reduction pipe would also pass through the conical channel rheometers. The test solutions, which were used on a single-pass basis, were prepared "on-the-fly" by the use of concentrated master solutions. The polymer additives examined in this investigation were two molecular weight grades of a polyacrylamide, Separan AP-273 and Separan AP-30 (Dow Chemical Co.), and a polyethylene oxide, Polyox WSR-301 (Union Carbide Corp.). The solvent in all cases was filtered tap water. The Separan AP-273 solutions were examined for additive concentrations of 1, 2, 5, 10, 15, 20, 30, and 45 ppm; the Separan AP-30 solutions were examined for 5, 10, and

20 ppm additive concentrations; and for Polyox WSR-301, measurements are reported for flow of 20 and 30 ppm solutions. Additionally, additive concentrations ranging from less than 0.3 ppm to greater than 60 ppm were examined for drag reduction measurements where concentration dependence specifically was being studied. The master polymer solutions were injected into the main flow at the upstream side of an in-line rotational mixer. Most experimental runs were conducted with the mixer rotating at 10 rps, with some additional results also being reported for a 30 rps mixing speed.

The main purpose of this investigation has been to determine whether the extensional characteristics of the polymer test solutions are related to their drag-reducing abilities.

Summary of Results and Conclusions

Shear viscosities were determined for the test solutions at shear strain rates ranging from about 3000 to 19,000 1/s. It has been found that

(1) the test solutions behaved in a Newtonian, or nearly Newtonian manner for laminar flow conditions; and that

(2) the solution shear viscosities were only marginally increased as a result of polymer addition.

Specifically, the 30 and 45 ppm Separan AP-273 solutions

and the 10 and 20 ppm AP-30 solutions demonstrated slight shear-thinning behavior over the range of strain rates studied, while the remaining solutions exhibited essentially Newtonian behavior. At a shear strain rate of 10,000, the shear viscosities of the test solutions were found to be 1% to 12% greater than for water at similar temperatures.

Two sets of drag reduction measurements have been reported, one, where drag reduction has been measured for solutions maintained at a constant concentration for a series of different Reynolds number flows, and secondly, where measurements have been conducted for flow at a constant Reynolds number, but for varying concentrations. The first set of measurements has been conducted to obtain a quantitative description of the drag-reducing abilities of the test solutions (in order to provide a basis for comparison of these abilities with their extensional characteristics). The second set of measurements, which addressed concentration dependence, has been used to look for evidence of molecular interaction during drag reduction. In both sets of experiments, flow rates and pressure drops were measured for flow being conducted through a 1.6 cm diameter tube.

The drag reduction measurements made on flows at various Reynolds numbers indicate that

(1)   the slopes of the drag reduction trajectories for data plotted using semi-logarithmic friction law coordinates $(1/f^{1/2}, \quad \log \quad f^{1/2}R)$ are well approximated by straight lines and the slopes of these lines increase with increasing concentration;

(2)   "onset" of drag reduction occurs at increasing wall strain rates for decreases in additive concentration, with the exception of some of the higher concentration Separan AP-273 runs, where "onset" was observed to be nearly independent of concentration; also, the strain rates at "onset" have been observed to be greater for flow of the polyethylene oxide solutions than for flow of the polyacrylamide solutions;

(3)   increase of the speed of the in-line rotational mixer causes a decrease in the level of drag reduction, the main effect being a delay of "onset" (with little change to the slopes of the drag reduction trajectories); and

(4)   the higher molecular weight grade of the two polyacrylamide additives was observed to be the more effective drag reducer, with "onset" occurring at lower strain rates and with slopes of the drag reduction trajectories being greater.

The drag reduction measurements made on flows of constant Reynolds number, but for varying concentration, indicate that

(1) specific drag reduction (relative drag reduction divided by concentration) increases with concentration at the lowest measured concentrations for each additive type, and this result is taken to indicate that molecular interaction can play a significant role in drag reduction; and that

(2) two distinct types of drag-reducing behavior occurred: for the polyethylene oxide runs, the rate of increase of specific drag reduction was greater than for the polyacrylamide runs and a certain concentration was required before drag reduction could be measured, while for the polyacrylamide solutions, drag reduction was always measured, no matter how low the concentration was.

Since two different types of drag-reducing behavior have been observed, and since in both cases it has been determined that molecular interactions do occur, it has been suggested that two different types of extramolecular structures are present in the flows. From electron micrographs published by Dunlop and Cox (1977), polyacrylamide molecules have been shown to exist in fibrous networks, while polythethylene oxide molecules form separate compact structures of varying sizes. It

was further suggested in the present report that the observed differences in the drag-reducing behavior between the polyacrylamide and polyethylene oxide solutions might have been due to such structural differences.

A series of conical channels were constructed for extensional flow measurements. These channels, which were designed to conduct nearly shear-free flow at high deformation rates, had exit dimensions of the the order of 0.1 cm with solid angles of convergence of either 58, 59, or 88 degrees. A pair of pressure taps were drilled into each channel, one being located just upstream of the end of the conic section of the channel and the other being at the entrance of the channel.

For water flow through the channels,

(1) head-discharge measurements have been found to be in good agreement with theoretical head-discharge relationships, which have been obtained using the known boundary layer solution for axisymmetric flow of a Newtonian liquid; and

(2) over the range of the measurements, the actual flow rates have been shown to be about 1% less than if the flows were completely frictionless.

Further, from examination of the theoretical head-discharge relationships, it is noted that the shear-free behavior of the flow through the channels is relatively

insensitive to the level of shear viscosity of the liquid.

To gain an general understanding of the viscoelastic effects generated in the flow through the channels, some preliminary measurements, primarily with 20 ppm Separan AP-273 solutions, were conducted. Experiments were run in order

(1) to examine the relationship between the excess pressure drop occurring over the entire length of a channel with the additional normal stresses being generated in the channel (as compared to solvent flow);

(2) to examine the degradation of viscoelastic effects; and

(3) to investigate the effects of varying channel· geometry.

The head-discharge measurements have been expressed in terms of first normal stress differences and extensional strain rates. Two methods have been used to determine the first normal stress differences, one, in which they were determined directly from the difference in pressure heads at the downstream tap from polymer solution to water flow, and secondly, by using an equation developed from the integrated equations of motion. The extensional strain rates have been determined using equations valid for frictionless sink flow.

It has been observed for the polyacrylamide test solutions that

(1) when compared to water flow, lower pressure drop occurs along a channel, while (for the same flow) greater pressure drop occurs over the entire length of the channel;

(2) from energy balances, the additional overall pressure drops (compared to water flow) could be reasonably predicted from the measured normal stresses in the channels, by using the assumption that upon exiting from the channels, the additional energy in the polymer molecules is released to heat with little flow interaction;

(3) the viscoelastic characteristics of the test solutions are susceptible to degradation by both shearing and "aging" mechanisms, and in the latter case, it has been found that both the additional overall pressure drop and the additional normal stresses in a channel decrease with time for the flow from a small reservoir (of relatively quiescent liquid) in which the overall pressure head is maintained at a constant level; it has been argued that this effect is the result of the disentanglement of polymer molecules, indicating that extramolecular structures can play a significant role in determining viscoelastic properties; and that

(4) at equal extensional strain rates at the downstream taps, different levels of first normal stress difference have been obtained for flows of the same solutions through different channels; from dye and trace particle studies, no secondary flows were observed to occur during these experiments.

The observation listed in item (4) is contrary to expectations based on both the theory on the steady sink flow of a simple fluid and on a theory on the extensional flow of a suspension of elongated large scale molecules (a modified Batchelor theory). It was suggested that the level of first normal stress difference may be more dependent on the level of strain in the flow than on strain rate; however, the present data was not extensive enough to conclusively test this hypothesis. Despite the variability in results between channels, it is noted that for a given channel, the results are consistently and easily reproducible.

Extensional flow measurements have also been conducted using the same test solutions as have been examined for the drag reduction experiments. The purpose for these measurements was to obtain relative measures of the extensional characterisitcs of the test solutions for comparison of these characteristics with their drag-reducing abilities. From these measurements it has been

found that

(1)   two distinct types of non-Newtonian behavior occur: for flow of the polyacrylamide solutions, pressure heads at the downstream tap were lower than for water flow at similar flow rates, while the polyethylene oxide solutions induced greater pressure heads;

(2)   at low flow rates, no measurable difference in pressure head was observed for polymer solution flow in comparison to water flow, then at some point for increasing flow rates, pressure head differences became measurable and these differences increased with increasing flow rate, at sufficiently high flow rates, the differences in pressure head leveled off for further increases in flow rate, and that at the highest measured flow rates, decreases in these differences were also observed;

(3)   non-Newtonian effects were observed for all of the test solutions, provided that large enough extensional strain rates were examined;

(4)   "onset" of the non-Newtonian effects occur at increasing extensional strain rates with increasing additive concentration, and that the strain rates at "onset" have been observed to be greater for flow of the polyethylene oxide solutions than for flow of the polyacrylamide solutions;

(5)   the higher molecular weight grade of the two
      polyacrylamide additives was observed to produce the
      greater   non-Newtonian   effects,   with   "onset"
      occurring at lower strain rates and with the rate of
      increase of the magnitude of the non-Newtonian
      effects with concentration being greater; and

(6)   increase of the speed of the in-line rotational
      mixer causes a decrease in the level of the non-
      Newtonian effects.

    The responses of the test solutions in both the drag
reduction and extensional flow experiments exhibited many
similarities with regard to variation of additive type,
molecular weight grade, concentration, and mixing speed.
This has been illustrated by estimation of the increase
in buffer layer thickness of the non-dimensional mean
velocity profile (as a function of a characteristic
strain rate) of the drag-reducing pipe flow, in
comparison with estimates of the extensional viscosities
(as functions of extensional strain rate). Regardless of
additive type or concentration, a very good correlation
of the increase in buffer layer thickness has been
demonstrated with the extensional viscosity values (both
of which varied by over a factor of 10) over the entire
range of strain rates investigated.

The principal conclusions of this investigation are that

(1)   the drag-reducing abilities of low concentration polymer solutions are related to their extensional characteristics; and that

(2)   molecular interaction are likely to play a significant role in both the drag reduction mechanism and in the generation of non-Newtonian effects in extensional flows.

Recommendations for Future Work

In order to gain better understanding of the phenomenon of turbulent drag reduction, a better understanding is needed about the response behavior of low concentration polymer solutions to extensional flows.

Some observations that were unreported prior to the present investigation are that (1) that the first normal stress differences generated in a channel depend not only on extensional strain rate, but also on some other not yet identified factors, and (2) not only lower, but also greater pressure heads than for water flows at the same flow rates can be generated in the flow of polymer solutions through conical channels. A logical extension of the present work would be to conduct experiments which would further investigate these effects.

In the present report, it has been suggested that the level of first normal stress difference may be more dependent on the level of strain than on strain rate. A specific suggestion for continued work would be to investigate the influence of strain on the level of first normal stress difference. Polymer solution flow could be examined using conical channels instrumented with a series of pressure taps located along the walls, which would allow direct determination of "onset" conditions for each flow. After establishment of "onset" conditions, measures of strain could be determined as previously discussed in Chapter VI.

With regard to the flows of the polyethylene oxide solutions of the present investigation, it has been conjectured (based on energy transfer considerations) that any increased pressure drop along a channel would be associated with a decrease in the pressure drop over the entire length of the channel (relative to water flow at equal flow rates). The observations of Bate (1967) indicate that reductions in pressure drop can occur over an orifice for such solutions; however, it has yet to be established for conical channel flow whether decreased overall pressure drops are indeed related to increased pressure drop along a channel. It is suggested that it should be established as to whether such a relationship exists, and if so, work should be conducted

to provide a physical interpretation for such observations. An explanation should also be sought as to why increased pressure drops (compared to water flow at the same flow rates) may be observed along a channel in flows of polyethylene oxide solutions, but not for polyacrylamide solutions, which induce lower pressure drops.

Finally, the duration of critical stretching is likely to be a major factor in the determination of the non-Newtonian response of polymer solutions. Flows through conical channels are subject to certain finite durations of critical stretching. To obtain a more complete understanding of the response of polymer solutions to extensional flows, further work should also include examining flow through geometries in which other durations of critical stretching would occur.

APPENDIX A
LIST OF EQUIPMENT USED AND THEIR MANUFACTURERS/VENDORS

Item	Brand Name/Number (and Serial Number)	Manufacturer/Vendor
Viscometer	Hoppler Rheo-Viscometer (sn 002770)	VEB Prufgerate-Werk Medingen/Dresden, DDR
Constant temperature water circulator	Model F, No. 423	Polyscience-Haake Inc. Evanston, Ill
Flow meter	Mark V-1-SS (sn 4514)	Ramapo Instruments Co. Montville, NJ
Differential pressure transmitters	1302T (sn 1302TD11112-83-3829C)	Taylor Instruments Co. Rochester, NY
Strip chart recorders	1333J (sn 1333JA14632-9867A)	Taylor Instruments Co. Rochester, NY
	Electronik 194 (sn M9004B31001)	Honeywell, Inc. Fort Washington, Pa
Rotational mixer:		
motor	cat. no. 4559 (sn 34251)	Cole Parmer Instrument Co. Chicago, Ill
controller	Stir-Pak (cat. no. 4559-03) (sn 34250)	

Injection pump:

    motor   Masterflex pump   Cole Parmer Instrument Co.
                      (sn 34495)   Chicago, Ill

    heads   cat. nos. 7013, 7014

    tachometer   cat. no. 7598
                      (sn 55980)

DC power supply   6200B   Hewlett Packard
                    (sn 1142A05287)   Palo Alto, Ca

APPENDIX B
CALIBRATION OF THE HOPPLER VISCOMETER

In this investigation, a Hoppler Rheo-Viscometer has been used to examine the shear behavior of the polymer test solutions. A description of this viscometer is presented in Chapter III and the use of this viscometer is reported in Chapter IV. Before the viscometer measurements can be used to determine the shear stress-strain rate relationships of the polymer solutions, it is first necessary to calibrate the viscometer. As discussed in Chapter IV, viscometer calibration consists of determining the frictional resistance constant, $\hat{P}_f$, the general calibration constant, K, and the effective length, L, of the viscometer sphere. In this appendix, the procedures used to determine these constants are presented. Use of this viscometer has been restricted to loads low enough so that turbulent flow will not occur within it. Schonblom (1974) determined a criterion for the occurrence of transition to turbulent flow, eq. (4.7). A verification of this criterion is also presented in this appendix.

Calibration Measurements

Two sets of calibration measurements with distilled water have been conducted, one, at a temperature of 20.7 ^{O}C, and the other, at 24.7^{O}C. A listing of these measurements is presented in Table C.1. All measurements have been conducted with a viscometer sphere of 0.01596 m in diameter and with a measuring vessel of 0.01603 m in internal diameter.

Determination of Frictional Resistance

The presence of frictional resistance in the main ball bearing of the balance arm has been noticed by previous investigators (Lindgren, 1957; Schonblom, 1974). Schonblom determined that this resistance could be adequately modeled as a constant force acting to retard movement of the viscometer sphere. Using such a model, the viscometer response for a Newtonian liquid may be expressed as

$$\hat{P}t = \hat{P}_f t + (\mu/K) \tag{4.6}$$

where $\hat{P}$ is the force applied to the viscometer sphere sphere divided by the sphere's cross sectional area, $\hat{P}_f$ is the frictional resistance (also expressed as a force on the sphere divided by its cross sectional area), μ is the shear viscosity coefficient of the liquid

Table C.1. Viscometer calibration measurements.

Solution	: Distilled Water	Solution	: Distilled Water
Date	: 10/10/82	Date	: 12/16/82
Temperature:	24.70 ± 0.06 $^{\circ}$C	Temperature:	20.70 ± 0.06 $^{\circ}$C

$\hat{P}$ (N/m^2)	t (s)	$\hat{P}$ (N/m^2)	t (s)
246	78.74 78.04 78.07	246	87.75 86.73
368	48.78 48.55 48.46	368	53.50 53.04
492	35.24 35.09 34.94	492	38.54 38.57
615	27.49 27.55 27.46	615	30.26 30.08
736	22.62 22.72 22.64	736	24.89 24.81
981	16.71 16.77 16.72	981	18.31 18.31
1226	13.24 13.23 13.27	1226	14.58 14.38
1473	11.01 10.96 11.03	1473	11.98 12.04
1717	9.40 9.46 9.39	1717	10.35 10.21
1961	8.25 8.22 8.22	1961	8.95 9.01

Table. C.1-continued.

2942	7.13	2942	7.42
	7.11		7.47
	7.13		
3922	6.11		
	6.14		
	6.20		
	6.17		
6864	4.12		
	4.16		
	4.12		

in the viscometer, t is the time for the sphere to travel 3.00 cm, and K is a calibration constant. Thus, the frictional resistance, $\hat{P}_f$, should equal the slope of the line formed by the viscometer measurements when presented as a plot of $\hat{P}t$ versus t. In Fig. C.1, $\hat{P}t$ is plotted as a function of t for both sets of calibration measurements, where t has been taken as the averaged fall time for each loading. The dashed lines in this figure represent linear least squares fits of the data. It is shown in this figure that the data for each set of measurements describe a linear graph, each with nearly equal slopes. Hence, the frictional resistance may indeed be represented as a constant retarding force acting on the viscometer sphere. From the least squares fits, the frictional resistance has been determined to be 48.7 and 45.2 N/m^2 for the measurements made at 20.7 and 24.7 ^{o}C, respectively. For computational purposes in this dissertation, an average value of 47 N/m^2 has been used to represent the frictional resistance, $\hat{P}_f$.

Determination of Calibration Constants K and L

The calibration constant K has been determined using eq. (4.6), which after rearranging may be written as

$$K = \mu / [(\hat{P} - \hat{P}_f)t] \qquad (C.1)$$

272
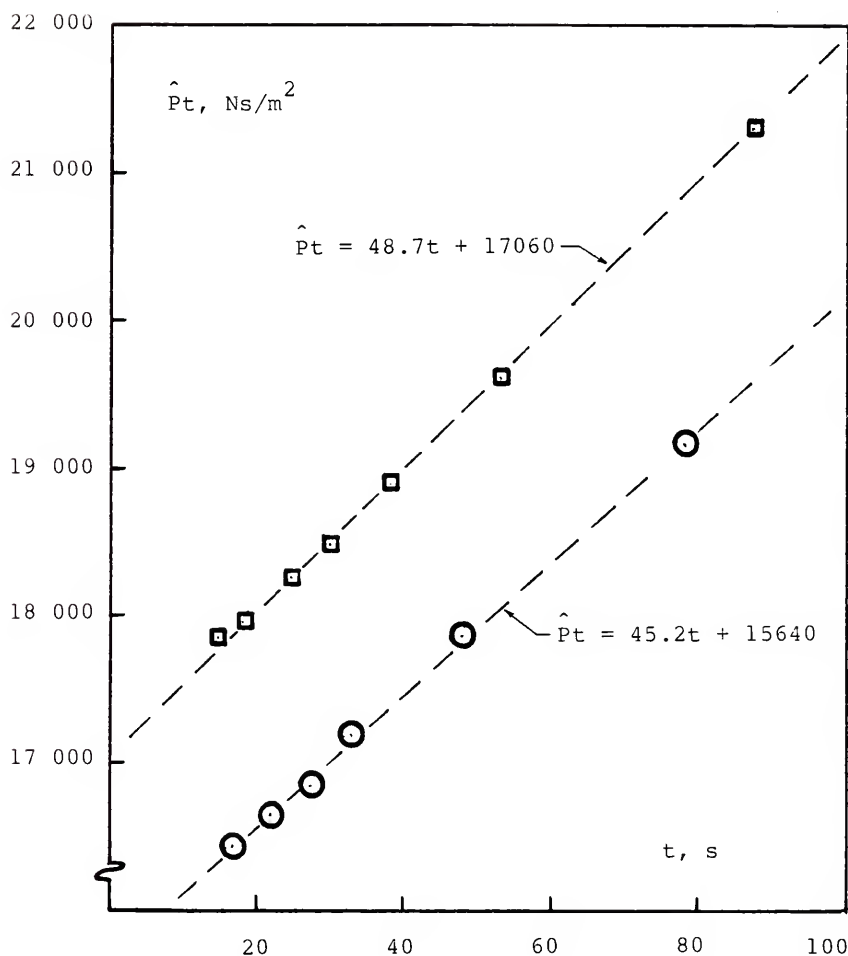
Fig. C.1. P̂t as a function of t for the shear
viscometer measurements conducted with
distilled water at 24.7 °C (⊙) and
20.7 °C (▣).

In Fig. C.2, the computed values of K are presented as a function of effective load $(\hat{P}-\hat{P}_f)$. To avoid transition effects, only data obtained for effective loads of less than or equal to 1423 N/m^2 have been examined. Along with the calculated values of K, a dashed line representing the mean of these values is indicated in this figure. This mean value is 5.80×10^{-8} (dimensionless) and all of the individual values, with the exception of the lowest loading, are within $\pm 0.35\%$ of the mean. Slightly larger deviations occur at the lowest loading; however, these values are still within about $\pm 1\%$ of the mean.

The effective length, L, of the viscometer sphere has been calculated by using eqs. (4.1) and (4.3). After eliminating the variables $\hat{P}$ and t from these two equations, L may be expressed as

$$L = 5d_m^3/96al_tK \qquad (C.2)$$

where a is the viscometer sphere radius of 0.00798 m, l_t is the 3.00 cm travel distance of the sphere, and d_m is the maximum annular width with in the viscometer measuring vessel (0.00007 m). For a value of the calibration constant K of 5.80×10^{-8}, the effective length is 0.00129 m.
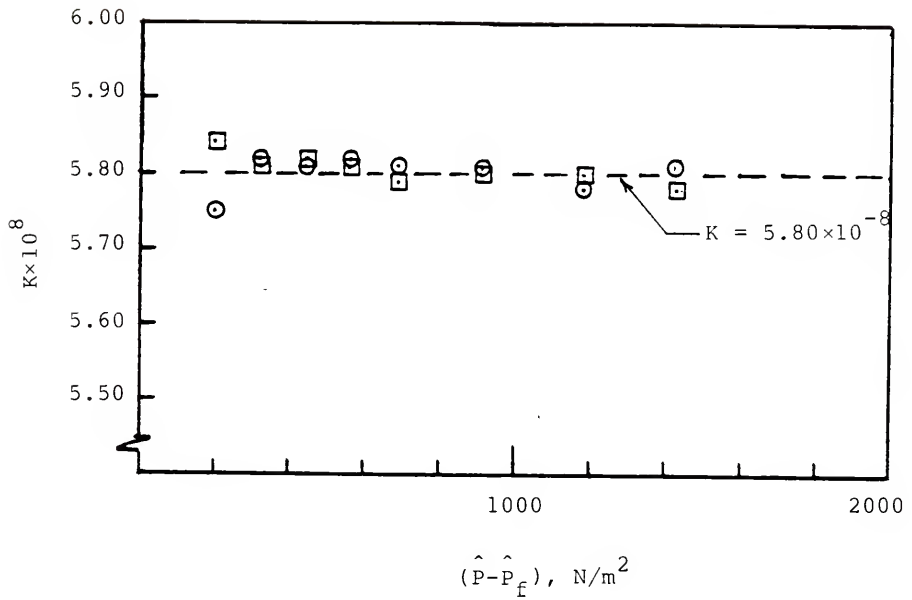
Fig. C.2. The calibration constant K as a function of effective load $(\hat{P}-\hat{P}_f)$ for the viscometer measurements conducted with distilled water at 24.7 $^{\circ}$C (▣) and 20.7 $^{\circ}$C (⊙). The dashed line represents the mean K value of 5.8×10^{-8}.

Verification of the Flow Transition Criterion

Schonblom (1974) has examined the occurrence of transition to turbulent flow within the Hoppler Rheo-Viscometer and has concluded that this phenomenon occurs at

$$\hat{P}/\mu^2 \cong 1.52 \times 10^9 \ m^2/Ns \tag{4.7}$$

To check this criterion, the values of the calibration constant have been plotted in Fig. C.3 as a function of $(\hat{P}-\hat{P}_f)/\mu^2$. An abrupt lowering of the magnitudes of these constants occur for both sets of measurements at $(\hat{P}-\hat{P}_f)$ values of about $2.0 \times 10^9 \ m^2/Ns$. It is this lowering of the values of the calibration constants that Schonblom has taken as being indicative of turbulence occurring in the flow. Thus, the flow remained laminar to somewhat greater loadings during the present investigation than in Schonblom´s investigation. For use in this disseration, Schonblom´s more conservative transtion criterion has been used.
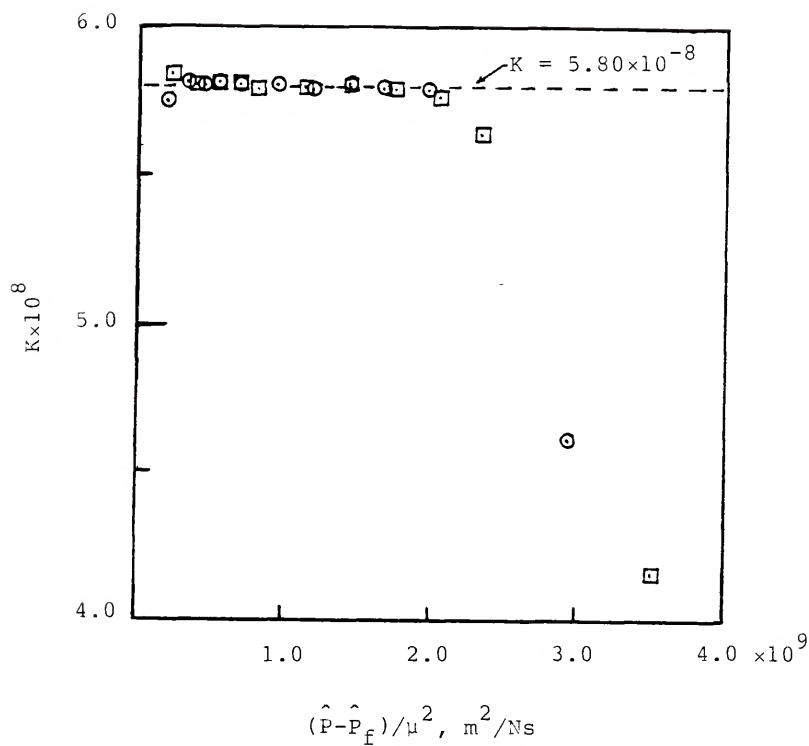
Fig. C.3. The calibration constant K as a function of $(\hat{P}-\hat{P}_f)/\mu^2$ for the viscometer measurements conducted with distilled water at 24.7 $^\circ$C (▣) and 20.7 $^\circ$C (☉). The dashed line represents the mean K value of 5.80×10^{-8}.

APPENDIX C
VISCOMETER MEASUREMENTS

This appendix contains listings of the measurements
obtained with the Hoppler Rheo-Viscometer. A
description of this instrument is presented in Chapter
III, use of this viscometer is discussed in Chapter IV,
and the calibration procedures and measurements are
reported in Appendix B. The measurements listed in this
appendix consist of the fall times, t, for each applied
load, $\hat{P}$.

All samples were obtained from the main experiment
pipe, within which polymer solution flow was being
maintained using 1% master solutions for flows at a
Reynolds number of 8000. The mixing conditions are as
listed with each set of measurements.

Additive : Separan AP-273   Additive : Separan AP-273
Conc.   : 45 ppm   Conc.   : 30 ppm
Mixing   : 10 rps   Mixing   : 10 rps
Temp.   : 24.70±0.06 ^{o}C   Temp.   : 24.70±0.06 ^{o}C

$\hat{P}$	t	$\hat{P}$	t
(N/m^2)	(s)	(N/m^2)	(s)
246	90.25	246	85.97
	89.06		85.40
368	39.19	368	52.85
	39.03		52.66
492	54.78	492	37.87
	54.85		38.02
615	30.62	615	29.65
	30.50		29.59
736	25.16	736	24.29
	25.10		24.26
981	18.36	981	17.78
	18.44		17.88
1226	14.51	1226	14.08
	14.57		14.10
1473	12.05	1473	11.61
	12.05		11.65
1717	10.33	1717	10.00
	10.33		9.91
1961	8.98	1961	8.59
	9.03		8.72
2942	6.08	2942	6.35
	6.08		6.38

Additive	: Separan AP-273
Conc.	: 15 ppm
Mixing	: 10 rps
Temp.	: 24.70±0.06 °C

$\hat{P}$ (N/m^2)	t (s)
246	78.92
	78.78
368	49.31
	49.20
492	35.72
	35.64
615	28.06
	28.08
736	23.14
	23.14
981	17.03
	17.07
1226	13.50
	13.52
1473	11.21
	11.13
1717	9.59
	9.57
1961	8.40
	8.45
2942	7.11
	7.11

Additive	: Separan AP-273
Conc.	: 15 ppm
Mixing	: 30 rps
Temp.	: 24.70±0.06 °C

$\hat{P}$ (N/m^2)	t (s)
246	79.20
	78.81
368	49.59
	49.53
492	35.83
	35.81
615	28.27
	28.22
736	23.20
	23.22
981	17.18
	17.15
1226	13.59
	13.64
1473	11.27
	11.21
1717	9.56
	9.66
1961	8.34
	8.44
2942	7.06
	6.99

Additive : Separan AP-273 Additive : Separan AP-273
Conc.   : 20 ppm   Conc.   : 5 ppm
Mixing   : 10 rps   Mixing   : 30 rps
Temp.   : 24.70±0.06 °C   Temp.   : 24.70±0.06 °C

$\hat{P}$	t	$\hat{P}$	t
(N/m^2)	(s)	(N/m^2)	(s)
246	80.84	246	80.34
	80.25		78.48
368	50.55	368	48.81
	50.58		48.72
492	36.50	492	35.22
	36.60		35.30
615	28.68	615	27.66
	28.72		27.76
736	23.61	736	22.78
	23.68		22.73
981	17.54	981	16.87
	17.34		16.79
1226	13.76	1226	13.39
	13.73		13.39
1473	11.40	1473	11.09
	11.34		11.09
1717	9.73	1717	9.55
	9.77		9.53
1961	8.47	1961	8.29
	8.52		8.35
2942	7.28	2942	7.28
	7.25		7.22

Additive	:	Separan AP-30
Conc.	:	20 ppm
Mixing	:	10 rps
Temp.	:	21.30±0.06 °C

Additive	:	Separan AP-30
Conc.	:	10 ppm
Mixing	:	10 rps
Temp.	:	21.30±0.06 °C

$\hat{P}$ (N/m^2)	t (s)	$\hat{P}$ (N/m^2)	t (s)
246	93.71 93.00	246	90.96 89.95
368	56.19 56.11	368	54.99 54.87
492	40.00 40.13	492	39.30 39.32
615	31.22 31.22	615	30.62 30.58
736	25.57 25.55	736	25.16 25.17
981	18.75 18.78	981	18.45 18.54
1226	14.78 14.80	1226	14.57 14.62
1473	12.27 12.15	1473	12.05 12.04
1717	10.45 10.41	1717	10.22 10.31
1961	9.12 9.09	1961	9.07 9.00
2942	7.43 7.52	2942	7.57 7.56

Additive : Separan AP-30
Conc.   : 5 ppm
Mixing   : 10 rps
Temp.   : 21.30$\pm$0.06 ^{o}C

$\hat{P}$	t
(N/m^2)	(s)
246	87.74
	87.85
368	53.56
	53.56
492	38.65
	38.63
615	30.26
	30.26
736	24.82
	24.83
981	18.33
	18.31
1226	14.52
	14.50
1473	12.00
	12.00
1717	10.23
	10.25
1961	8.92
	8.92
2942	7.34
	7.36

Additive	: Polyox WSR-301
Conc.	: 30 ppm
Mixing	: 10 rps
Temp.	: 20.70$\pm$0.06 $^{\circ}$C

Additive	: Polyox WSR-301
Conc.	: 20 ppm
Mixing	: 10 rps
Temp.	: 20.70$\pm$0.06 $^{\circ}$C

$\hat{P}$ (N/m^2)	t (s)	$\hat{P}$ (N/m^2)	t (s)
246	89.19	246	88.23
	88.58		87.78
368	54.61	368	54.34
	54.59		54.11
492	39.36	492	39.00
	39.22		38.84
615	30.88	615	30.49
	30.72		30.50
736	25.39	736	25.08
	25.34		25.18
981	18.72	981	18.59
	18.75		18.59
1226	14.76	1226	14.73
	14.75		14.65
1473	12.27	1473	12.19
	12.35		12.23
1717	10.42	1717	10.41
	10.56		10.44
1961	9.07	1961	9.06
	9.09		9.12
2942	7.22	2942	6.89
	7.19		6.97

PIPE FLOW MEASUREMENTS MADE ON VARIOUS
REYNOLDS NUMBER FLOWS

This appendix contains listings of measurements and evaluated data for both water and polymer solution flows conducted at various Reynolds numbers through the main experiment pipe. Measurement and data analysis procedures are reported in Chapter V.

Definitions and units of dimension of the variables listed on the following pages are

VELOCITY	Mean flow velocity, $\bar{U}$, m/s
FLOW RATE	Flow rate, Q, m^3/s
PRESSURE DROP	Pressure drop, Δp, N/m^2
FRICTION VELOCITY	Friction velocity, u_*, m/s
REYNOLDS NUMBER	Reynolds number, $R = \bar{U}D/\nu$
FRICTION FACTOR	Friction factor, $f = (2D/l) \cdot (\Delta p/\rho \bar{U}^2)$
R*ROOTF	$R(f^{1/2})$
1/ROOTF	$f^{-1/2}$
STRAIN RATE	Wall strain rate, u_*^2/ν, 1/s
DRAG REDUCTION	$100(1-f_p/f_s)$
D	Diameter, D, of experiment pipe, m
L	Length, l, of measuring section, m
TEMP	Flow temperature, $^\circ$C

284

RHO   Mass density, ρ, kg/m^3

NU   Kinematic viscosity, ν, m^2/s

RPS   Mixing speed in revolutions per
                         second

The VELOCITY and PRESSURE DROP definitions refer to
the output columns; the input data columns for these
variables refer to chart recorder readings in millivolts
and volts, respectively.

WATER ONLY, 1.6 CM TUBE : 10/21/82
DOWNSTREAM PRESSURE TAPS

PROGRAM PARAMETERS : D = 0.015970 METERS
L = 0.71 METERS
TEMP = 23.30 DEGREES CENTIGRADE

RHO = 997.47 KG PER CUBIC METER
NU = 0.00000093 SQUARE METERS PER SEC

INPUT DATA

OUTPUT

VELOCITY (MV)	PRESSURE DROP (VOLTS)	VELOCITY (M/SEC)	FLOW RATE (M**3/SEC)	PRESSURE DROP (PASCALS)	FRICTION VELOCITY (M/SEC)	REYNOLDS NUMBER	FRICTION FACTOR	R*ROOTF	1/ROOTF	STRAIN RATE (1/SEC)	DRAG REDUCTION (PERCENT)
.0038	0.009	0.063	.0000126	5.2	0.005	1083.0	0.0591	263.2	4.11	31.5	-9.93
.0060	0.012	0.080	.0000160	6.9	0.006	1371.7	0.0494	304.9	4.50	42.3	2.68
.0060	0.012	0.080	.0000160	6.9	0.006	1371.7	0.0494	304.9	4.50	42.3	2.68
.0102	0.015	0.105	.0000210	8.7	0.007	1805.1	0.0358	341.6	5.28	53.1	24.68
.0178	0.019	0.140	.0000280	11.1	0.008	2407.8	0.0256	385.1	6.25	67.5	42.36
.0226	0.040	0.158	.0000317	23.4	0.012	2724.4	0.0423	560.5	4.86	143.0	1.74
.0296	0.053	0.182	.0000365	31.1	0.013	3132.6	0.0425	645.7	4.85	189.8	-1.97
.0386	0.067	0.209	.0000419	39.3	0.015	3593.8	0.0408	726.3	4.95	240.1	-1.31
.0500	0.083	0.239	.0000479	48.8	0.017	4108.7	0.0387	808.6	5.08	297.6	0.79
.0630	0.103	0.267	.0000539	60.5	0.019	4630.6	0.0379	901.1	5.14	369.6	0.20
.0840	0.133	0.313	.0000626	78.2	0.021	5373.9	0.0363	1024.2	5.25	477.5	0.79
.1070	0.164	0.353	0000708	96.5	0.023	6075.0	0.0351	1137.5	5.34	588.9	1.39
.1540	0.226	0.422	0000845	133.0	0.027	7257.5	0.0339	1335.5	5.43	811.9	0.61
.1780	0.256	0.453	0000907	150.7	0.029	7789.5	0.0333	1421.5	5.48	919.8	0.59
.1980	0.282	0.477	0000956	166.0	0.031	8205.4	0.0331	1492.0	5.50	1013.3	0.07
.2630	0.360	0.548	.0001098	211.9	0.035	9425.9	0.0320	1685.9	5.59	1293.8	0.04
.3060	0.412	0.590	.0001182	242.6	0.037	10149.5	0.0316	1803.7	5.63	1480.8	-0.44
.3530	0.464	0.633	.0001260	273.2	0.039	10883.2	0.0309	1914.2	5.69	1667.8	-0.04
.3780	0.489	0.654	0001311	287.9	0.040	11253.1	0.0305	1965.1	5.73	1757.7	0.59
.1620	0.136	0.433	00008647	141.4	0.028	7439.3	0.0343	1377.2	5.40	863.3	-1.18

.2410	0.190	0.525	.0001052	198.3	0.034	9032.1	0.0326	1630.8	5.54	1210.6	-0.83
.3300	0.250	0.612	.0001227	261.5	0.039	10530.8	0.0316	1872.8	5.62	1596.5	-1.47
.4140	0.300	0.684	.0001370	314.2	0.042	11764.4	0.0304	2052.7	5.73	1918.0	-0.31
4800	0.342	0.735	.0001473	358.4	0.045	12645.8	0.0301	2192.5	5.77	2188.1	-0.77
.5630	0.388	0.795	0001592	406.9	0.048	13670.4	0.0292	2336.1	5.85	2494.0	0.27

WATER ONLY, 1.6 CM TUBE : 10/21/82
UPSTREAM PRESSURE TAPS

PROGRAM PARAMETERS :   D = 0.015920 METERS
L = 0.71 METERS
TEMP = 23.30 DEGREES CENTIGRADE

RHO = 997.47 KG PER CUBIC METER
NU = 0.00000093 SQUARE METERS PER SEC

INPUT DATA

OUTPUT

VELOCITY	PRESSURE DROP	VELOCITY	FLOW RATE	PRESSURE DROP	FRICTION VELOCITY	REYNOLDS NUMBER	FRICTION FACTOR	R*ROOTF	1/ROOTF	STRAIN RATE	DRAG REDUCTION
(MV)	(VOLTS)	(M/SEC)	(M**3/SEC)	(PASCALS)	(M/SEC)					(1/SEC)	(PERCENT)
.0038	0.008	0.063	.0000126	5.2	0.005	1086.4	0.0586	263.1	4.13	31.7	-12.44
.0060	0.010	0.080	.0000160	6.4	0.006	1376.0	0.0446	290.5	4.74	38.7	9.88
.0060	0.010	0.080	.0000160	6.4	0.006	1376.0	0.0446	290.5	4.74	38.7	9.88
.0102	0.015	0.106	.0000210	9.2	0.007	1810.8	0.0373	349.8	5.18	56.1	19.76
.0178	0.020	0.141	.0000200	12.1	0.008	2415.4	0.0275	400.4	6.03	73.5	36.98
.0226	0.040	0.159	.0000317	23.5	0.012	2733.0	0.0418	558.8	4.89	143.0	1.45
.0296	0.054	0.183	.0000365	31.5	0.013	3142.4	0.0424	.47.0	4.86	191.7	-3.09
.0386	0.069	0.210	.0000417	40.1	0.015	3605.1	0.0410	.29.7	4.94	243.9	-2.76
.0500	0.086	0.240	.0000477	49.8	0.017	4121.6	0.0389	813.4	5.07	303.1	-0.65
.0630	0.107	0.271	.0000537	61.8	0.019	4645.2	0.0381	906.2	5.13	376.1	-1.01
.0840	0.138	0.314	.0000626	79.5	0.021	5390.7	0.0364	1027.9	5.24	484.0	0.22
.1070	0.170	0.356	.0000700	97.8	0.024	6094.1	0.0350	1140.0	5.35	595.3	1.29
.1540	0.238	0.425	.0000845	136.7	0.028	7280.3	0.0343	1347.6	5.40	831.8	-0.58
.1780	0.268	0.456	.0000907	153.8	0.029	7814.0	0.0335	1429.7	5.47	936.2	0.17
.1980	0.297	0.480	.0000756	170.4	0.031	8231.2	0.0334	1504.7	5.47	1037.1	-0.83
.2630	0.378	0.552	.0001098	216.7	0.035	9455.5	0.0322	1696.9	5.57	1318.9	-0.23
.3060	0.436	0.594	.0001182	249.9	0.038	10181.4	0.0320	1822.1	5.59	1520.7	-1.34
.3530	0.492	0.637	.0001268	281.9	0.040	10917.4	0.0314	1935.3	5.64	1715.5	-1.00
.3780	0.520	0.657	.0001311	297.9	0.041	11288.4	0.0311	1989.4	5.67	1812.9	-0.58
.1620	0.140	0.435	.0000867	141.7	0.028	7462.7	0.0338	1372.1	5.44	862.4	0.21

.2410	0.197	0.529	.0001052	199.8	0.034	9060.5	0.0323	1629.5	5.56	1216 2	0 30
.3300	0.261	0 616	.0001227	265.1	0.039	10563.9	0.0316	1876.8	5.63	1613 4	-0 70
4140	0.316	0.688	.0001370	321.2	0.043	11801.3	0.0306	2065.8	5.71	1954 8	-0 22
4800	0.361	0.740	.0001473	367.1	0.046	12685.6	0.0303	2208.5	5.74	2234 1	-0.75
.5630	0.414	0.800	.0001592	421.2	0.049	13713.3	0.0298	2365.5	5.80	2563 0	-0 65

WATER ONLY, 1.6 CM TUBE : 10/28/82
DOWNSTREAM PRESSURE TAPS

PROGRAM PARAMETERS : D = 0.015970 METERS
L = 0.71 METERS
TEMP = 21.60 DEGREES CENTIGRADE

RHO = 997.85 KG PER CUBIC METER
NU = 0.00000097 SQUARE METERS PER SEC

INPUT DATA

OUTPUT

VELOCITY	PRESSURE DROP	VELOCITY	FLOW RATE	PRESSURE DROP	FRICTION VELOCITY	REYNOLDS NUMBER	FRICTION FACTOR	R*ROOTF	1/ROOTF	STRAIN RATE	DRAG REDUCTION
(MV)	(VOLTS)	(M/SEC)	(M**3/SEC)	(PASCALS)	(M/SEC)					(1/SEC)	(PERCENT)
.1270	0.110	0.384	.0000770	114.1	0.025	6348.0	0.0350	1188.2	5.34	668.8	0 41
.1870	0.153	0.464	.0000930	159.4	0.030	7668.6	0.0335	1404.6	5.46	934.6	0 23
.2510	0.199	0.536	.0001073	207.9	0.034	8854.3	0.0328	1604.0	5.52	1218.8	-1 01
.3360	0.256	0.618	.0001238	267.9	0.039	10209.9	0.0318	1821.1	5.61	1571.0	-1.32
.4050	0.296	0.677	.0001356	310.1	0.042	11185.2	0.0307	1959.1	5.71	1818.2	0 14
.4440	0.321	0.708	.0001418	336.4	0.044	11698.9	0.0304	2040.7	5.73	1972.7	-0 11
.4990	0.351	0.750	.0001502	368.1	0.046	12385.7	0.0297	2134.4	5.80	2158.1	0 94
.5900	0.402	0.814	.0001630	421.8	0.049	13441.7	0.0289	2284.9	5.88	2473.3	1 71
.0550	0.093	0.251	.0000503	54.7	0.018	4148.2	0.0393	822.6	5.04	320.5	-0 95
.0820	0.133	0.309	.0000618	78.2	0.021	5100.4	0.0372	984.1	5.18	458.8	-0 41
.1030	0.163	0.347	.0000695	95.9	0.023	5730.6	0.0362	1089.6	5.26	562.4	-0 27
.1360	0.206	0.397	.0000796	121.3	0.026	6563.8	0.0348	1225.1	5.36	711.0	0 19
.2130	0.304	0.495	.0000991	179.0	0.032	8172.0	0.0332	1488.5	5.49	1049.6	-0 18
.1580	0.236	0.427	.0000856	138.9	0.028	7062.6	0.0345	1311.4	5.39	814.7	-0 53
.1950	0.280	0.474	.0000949	164.9	0.031	7827.1	0.0333	1428.5	5.48	966.7	0 45
.2640	0.364	0.547	.0001100	214.4	0.035	9075.4	0.0322	1628.9	5.57	1257.0	0 25
.2380	0.335	0.522	.0001045	197.3	0.033	8627.2	0.0328	1562.6	5.52	1156.8	-0 36
.2910	0.399	0.576	.0001154	235.0	0.036	9517.5	0.0321	1705.5	5.58	1377.9	-0 56
.3310	0.445	0.613	.0001229	262.1	0.037	10135.4	0.0316	1801.2	5.63	1536.9	-0 40
.3630	0.479	0.642	.0001285	282.1	0.040	10602.8	0.0311	1868.7	5.67	1654.3	0 17

.3860	0.501	0.661	.0001325	295 1	0.041	10925.8	0.0306	1911.2	5.72	1730 4	0 95
4030	0.517	0.675	.0001353	304.5	0.042	11158.2	0.0303	1941.5	5.75	1785.6	1 51
.4560	0.326	0.717	.0001437	341.7	0.044	11852.3	0.0301	2056.6	5.76	2003 6	0 62
.5140	0.362	0.761	.0001523	379 7	0.046	12566.2	0.0298	2167.7	5.80	2226 1	0 39
.5880	0.404	0.812	.0001627	423.9	0.049	13419.4	0.0291	2290.6	5.86	2485.6	0 93
.6120	0.413	0.828	.0001659	433.4	0.050	13684.3	0.0286	2316.1	5.91	2541 2	2.14

WATER ONLY, 1.6 CM TUBE . 10/28/02
UPSTREAM PRESSURE TAPS

PROGRAM PARAMETERS :   D = 0.015720 METERS
                       L = 0.71 METERS
                       TEMP = 21.60 DEGREES CENTIGRADE

RHO = 997.85 KG PER CUBIC METER
NU = 0.00000097 SQUARE METERS PER SEC

INPUT DATA   OUTPUT

VELOCITY	PRESSURE DROP	VELOCITY	FLOW RATE	PRESSURE DROP	FRICTION VELOCITY	REYNOLDS NUMBER	FRICTION FACTOR	R*ROOTF	1/ROOTF	STRAIN RATE	DRAG REDUCTION
(MV)	(VOLTS)	(M/SEC)	(M**3/SEC)	(PASCALS)	(M/SEC)					(1/SEC)	(PERCENT)
.1270	0.114	0.387	.0000770	115.2	0.026	6367.9	0.0348	1188.7	5.36	673.6	0 74
.1870	0.158	0.467	.0000930	160.1	0.030	7692.6	0.0332	1401.2	5.49	936.0	1 40
.2510	0.207	0.539	.0001073	210.1	0.034	8882.1	0.0327	1605.1	5.53	1228.2	-0 23
.3360	0.267	0.622	.0001238	271.3	0.039	10242.0	0.0317	1824.0	5.62	1586.0	-0 49
.4050	0.314	0.681	.0001356	319.3	0.042	11220.3	0.0311	1978.6	5.67	1866.3	-0 57
.4440	0.339	0.713	.0001418	344.8	0.044	11735.7	0.0307	2056.2	5.71	2015.4	-0 27
.4990	0.375	0.754	.0001502	381.5	0.046	12424.6	0.0303	2162.9	5.74	2230.1	-0 27
.5900	0.435	0.819	.0001630	442.8	0.050	13483.9	0.0299	2330.0	5.79	2587.9	-0 62
.0550	0.095	0.253	.0000503	55.0	0.018	4161.3	0.0389	820.9	5.07	321.3	-0 80
.0820	0.137	0.311	.0000618	79.0	0.021	5116.5	0.0370	984.1	5.20	461.7	-0 35
.1030	0.168	0.347	.0000695	96.7	0.023	5748.6	0.0359	1089.0	5.28	565.3	0 10
.1360	0.214	0.400	.0000796	123.0	0.026	6584.5	0.0348	1228.2	5.36	719.1	0.15
.2130	0.316	0.498	.0000991	181.4	0.032	8197.7	0.0331	1491.2	5.50	1060.0	0 26
.1580	0.245	0.430	.0000856	140.7	0.028	7084.8	0.0344	1313.7	5.39	822.7	0 31
.1950	0.292	0.477	.0000947	167.6	0.031	7851.7	0.0333	1433.6	5.48	979.8	0 47
.2640	0.382	0.553	.0001100	219.1	0.035	9103.9	0.0324	1639.0	5.55	1280.6	-0 03
.2380	0.349	0.525	.0001046	200.2	0.034	8654.3	0.0328	1566.8	5 52	1170.3	-0 01
.2910	0.419	0.580	.0001154	240.3	0.037	9547.4	0.0323	1716.3	5.56	1404.3	-0 80
.3310	0.467	0.617	.0001229	267.7	0.039	10167.3	0.0318	1811.7	5.61	1564.7	-0 44
.3630	0.505	0.646	.0001285	289.4	0.040	10636.1	0.0314	1883.8	5.65	1691.8	-0 24

.3860	0.532	0.665	.0001325	304.9	0.042	10960.1	0.0311	1933.4	5.67	1782.0	-0.11
.4030	0.549	0.680	.0001353	314.6	0.042	11193.3	0.0308	1964.0	5.70	1838.8	0.49
.4560	0.345	0.722	.0001437	350.9	0.045	11889.6	0.0304	2074.3	5.73	2051.2	0.28
.5140	0.384	0.765	.0001523	390.7	0.047	12605.6	0.0301	2188.8	5.76	2283.8	-0.07
.5880	0.433	0.817	.0001677	440.7	0.050	13461.6	0.0298	2324.6	5.79	2576.0	-0.45
.6120	0.446	0.833	.0001659	454.0	0.051	13727.3	0.0295	2359.3	5.82	2653.5	0.06

WATER ONLY, 1.6 CM TUBE : 10/29/82
DOWNSTREAM PRESSURE TAPS

PROGRAM PARAMETERS : D = 0.015970 METERS
L = 0.71 METERS
TEMP = 21.20 DEGREES CENTIGRADE

RHO = 997.94 KG PER CUBIC METER
NU = 0.00000098 SQUARE METERS PER SEC

OUTPUT

INPUT DATA

VELOCITY (MV)	PRESSURE DROP (VOLTS)	VELOCITY (M/SEC)	FLOW RATE (M**3/SEC)	PRESSURE DROP (PASCALS)	FRICTION VELOCITY (M/SEC)	REYNOLDS NUMBER	FRICTION FACTOR	R*ROOTF	1/ROOTF	STRAIN RATE (1/SEC)	DRAG REDUCTION (PERCENT)
.0620	0.104	0.267	.0000535	61.2	0.019	4371.6	0.0389	861.7	5.07	355.1	-1.00
.1070	0.170	0.353	.0000708	100.1	0.024	5782.9	0.0363	1102.2	5.25	581.0	-0.97
.1980	0.289	0.477	.0000956	170.2	0.031	7810.8	0.0339	1437.5	5.43	988.3	-1.17
.2760	0.383	0.561	.0001124	225.6	0.036	9186.6	0.0325	1655.0	5.55	1310.0	-0.78
.3260	0.443	0.609	.0001220	261.0	0.038	9964.9	0.0319	1780.0	5.60	1515.4	-1.03
.3920	0.516	0.666	.0001335	304.0	0.042	10903.9	0.0310	1921.1	5.68	1765.2	-0.43
.1350	0.205	0.396	.0000773	120.7	0.026	6478.2	0.0349	1210.5	5.35	700.8	0.28
.0740	0.120	0.293	.0000586	70.6	0.020	4790.7	0.0373	925.8	5.17	409.9	0.78
.4100	0.533	0.681	.0001364	314.6	0.042	11145.7	0.0307	1952.5	5.71	1823.4	0.19
.1680	0.249	0.440	.0000882	146.6	0.029	7208.5	0.0343	1334.2	5.40	851.4	-0.38
.3680	0.484	0.646	.0001274	285.1	0.040	10572.5	0.0310	1060.6	5.68	1655.7	0.54

WATER ONLY, 1.6 CM TUBE : 10/29/82
UPSTREAM PRESSURE TAPS

PROGRAM PARAMETERS : D = 0.015920 METERS
L = 0.71 METERS
TEMP = 21.20 DEGREES CENTIGRADE

RHO = 997.94 KG PER CUBIC METER
NU = 0.00000098 SQUARE METERS PER SEC

INPUT DATA

OUTPUT

VELOCITY	PRESSURE DROP	VELOCITY	FLOW RATE	PRESSURE DROP	FRICTION VELOCITY	REYNOLDS NUMBER	FRICTION FACTOR	R*ROOTF	1/ROOTF	STRAIN RATE	DRAG REDUCTION
(MV)	(VOLTS)	(M/SEC)	(M**3/SEC)	(PASCALS)	(M/SEC)					(1/SEC)	(PERCENT)
.0620	0.109	0.269	.0000535	63.0	0.019	4385.3	0.0394	870.3	5.04	364.6	-3.21
.1070	0.179	0.356	.0000708	103.0	0.024	5801.0	0.0368	1113.1	5.21	596.3	-2.71
.1980	0.304	0.480	.0000956	174.5	0.031	7835.3	0.0342	1448.7	5.41	1010.2	-2.02
.2760	0.405	0.565	.0001124	232.3	0.036	9215.4	0.0329	1671.4	5.51	1344.6	-1.79
.3260	0.469	0.613	.0001220	268.9	0.039	9996.2	0.0324	1798.3	5.56	1556.4	-1.99
.3920	0.545	0.670	.0001335	312.3	0.042	10938.1	0.0314	1938.2	5.64	1808.1	-0.96
.1350	0.211	0.398	.0000793	121.3	0.026	6498.5	0.0346	1207.9	5.38	702.3	1.13
.0740	0.122	0.295	.0000586	70.4	0.020	4805.8	0.0367	920.3	5.22	407.6	1.92
.4100	0.564	0.685	.0001364	323.2	0.043	11180.7	0.0311	1971.6	5.67	1871.0	-0.48
.1680	0.257	0.443	.0000882	147.6	0.029	7231.1	0.0340	1332.5	5.43	854.6	0.48
.3680	0.511	0.650	.0001274	292.9	0.041	10605.8	0.0313	1076.9	5.65	1695.5	-0.01

45 PPM SEPARAN AP-273, 1% MASTER SOLUTION, 10 RPS : 10/5/82

DOWNSTREAM PRESSURE TAPS

PROGRAM PARAMETERS : D = 0.015970 METERS
L = 0.71 METERS
TEMP = 25.00 DEGREES CENTIGRADE

RHO = 997.10 KG PER CUBIC METER
NU = 0.00000089 SQUARE METERS PER SEC

INPUT DATA

OUTPUT

VELOCITY	PRESSURE DROP	VELOCITY	FLOW RATE	PRESSURE DROP	FRICTION VELOCITY	REYNOLDS NUMBER	FRICTION FACTOR	R*ROOTF	1/ROOTF	STRAIN RATE	DRAG REDUCTION
(MV)	(VOLTS)	(M/SEC)	(M**3/SEC)	(PASCALS)	(M/SEC)					(1/SEC)	(PERCENT)
.0120	0.022	0.114	.0000229	12.8	0.009	2040.1	0.0446	431.0	4.73	81.4	3.34
.0150	0.025	0.128	.0000257	14.6	0.009	2289.8	0.0403	459.7	4.98	92.6	10.25
.0190	0.028	0.145	.0000290	16.4	0.010	2587.7	0.0354	486.8	5.32	103.8	18.87
.0250	0.032	0.167	.0000334	18.7	0.010	2982.5	0.0305	520.6	5.73	118.7	27.71
.0340	0.038	0.196	.0000392	22.2	0.011	3496.9	0.0264	567.7	6.16	141.1	35.06
.0400	0.041	0.213	.0000426	24.0	0.012	3803.6	0.0240	589.8	6.45	152.4	39.55
.0490	0.047	0.236	.0000474	27.5	0.012	4224.8	0.0224	631.7	6.69	174.8	42.35
.0670	0.071	0.278	.0000557	41.7	0.015	4967.1	0.0245	777.1	6.39	264.5	34.40
.0860	0.085	0.316	.0000634	49.9	0.017	5652.1	0.0226	850.5	6.65	316.8	37.41
.1060	0.095	0.352	.0000704	55.8	0.018	6283.3	0.0205	899.2	6.99	354.2	41.93
.1210	0.104	0.375	.0000751	61.1	0.019	6702.9	0.0197	941.0	7.12	387.8	43.25
.1380	0.114	0.400	.0000801	67.0	0.019	7147.5	0.0190	985.3	7.25	425.2	44.43
.1570	0.121	0.426	.0000853	71.1	0.020	7612.3	0.0178	1015.1	7.50	451.3	47.21
.1810	0.135	0.457	.0000915	79.4	0.021	8160.0	0.0173	1072.3	7.61	503.7	47.87
.2240	0.153	0.507	.0001015	90.0	0.023	9055.4	0.0159	1141.7	7.93	570.9	50.81
.2630	0.169	0.548	.0001098	99.4	0.024	9793.9	0.0150	1200.0	8.16	630.7	52.66
.3010	0.184	0.585	.0001173	108.2	0.025	10461.3	0.0143	1252.2	8.35	686.8	54.10
.3350	0.201	0.617	.0001236	118.2	0.026	11022.7	0.0141	1308.9	8.42	750.3	54.26
.3730	0.220	0.650	.0001302	129.4	0.027	11616.6	0.0139	1369.4	8.48	821.3	54.35
.4480	0.250	0.711	.0001424	147.1	0.029	12704.1	0.0132	1459.9	8.70	933.5	55.69

45 PPM SEPARAN AP-273, 1% MASTER SOLUTION, 10 RPS : 10/5/82
UPSTREAM PRESSURE TAPS

PROGRAM PARAMETERS : D = 0.015920 METERS
L = 0.71 METERS
TEMP = 25.00 DEGREES CENTIGRADE

RHO = 997.10 KG PER CUBIC METER
NU = 0.00000089 SQUARE METERS PER SEC

INPUT DATA   OUTPUT

VELOCITY	PRESSURE DROP	VELOCITY	FLOW RATE	PRESSURE DROP	FRICTION VELOCITY	REYNOLDS NUMBER	FRICTION FACTOR	R*ROOTF	1/ROOTF	STRAIN RATE	DRAG REDUCTION
(MV)	(VOLTS)	(M/SEC)	(M**3/SEC)	(PASCALS)	(M/SEC)					(1/SEC)	(PERCENT)
.0120	0.021	0.115	.0000229	12.6	0.008	2046.5	0.0433	425.9	4.81	79.9	4.31
.0150	0.025	0.127	.0000257	14.9	0.009	2297.0	0.0406	462.8	4.96	94.4	7.95
.0190	0.029	0.146	.0000290	17.2	0.010	2595.8	0.0367	497.0	5.22	108.9	14.58
.0250	0.032	0.168	.0000334	18.9	0.010	2991.9	0.0303	521.2	5.74	119.7	27.01
.0340	0.038	0.197	.0000392	22.4	0.011	3507.8	0.0261	566.4	6.19	141.4	35.01
.0400	0.043	0.214	.0000426	25.2	0.012	3815.6	0.0249	601.5	6.34	159.5	36.87
.0490	0.049	0.238	.0000474	28.6	0.013	4238.0	0.0229	641.1	6.61	181.2	40.48
.0670	0.068	0.280	.0000557	39.5	0.015	4982.8	0.0228	752.9	6.62	249.9	38.43
.0860	0.084	0.318	.0000634	48.6	0.017	5669.8	0.0217	835.6	6.79	307.7	39.72
.1060	0.098	0.354	.0000704	56.6	0.018	6303.0	0.0205	901.7	6.99	358.3	41.84
.1210	0.106	0.377	.0000751	61.2	0.019	6724.0	0.0194	937.3	7.17	387.3	43.96
.1380	0.117	0.402	.0000801	67.5	0.020	7169.9	0.0188	984.3	7.28	427.0	44.87
.1570	0.123	0.429	.0000853	70.9	0.020	7636.2	0.0175	1009.0	7.57	449.7	48.20
.1810	0.139	0.459	.0000915	80.1	0.021	8185.6	0.0172	1072.1	7.64	506.6	48.31
.2240	0.158	0.510	.0001015	90.9	0.023	9083.8	0.0158	1142.4	7.95	575.3	51.21
.2630	0.178	0.551	.0001098	102.4	0.024	9824.6	0.0152	1212.1	8.11	647.6	52.22
.3010	0.196	0.589	.0001173	112.6	0.025	10494.1	0.0147	1271.6	8.25	712.6	53.23
.3350	0.218	0.621	.0001236	125.2	0.027	11057.3	0.0147	1340.6	8.25	792.2	52.62
.3730	0.233	0.654	.0001302	133.8	0.028	11653.1	0.0141	1385.8	8.41	846.4	53.88
.4480	0.273	0.715	.0001424	156.6	0.030	12744.0	0.0138	1499.5	8.50	991.0	53.93

30 PPM SEPARAN, 10 PASS : 10/5/82

DOWNSTREAM PRESSURE TAPS

PROGRAM PARAMETERS   D = 0.015970 METERS
L = 0.71 METERS
TEMP = 25.00 DEGREES CENTIGRADE

RHO = 797.10 KG PER CUBIC METER
NU = 0.000000089 SQUARE METERS PER SEC

INPUT DATA

OUTPUT

VELOCITY	PRESSURE DROP	VELOCITY	FLOW RATE	PRESSURE DROP	FRICTION VELOCITY	REYNOLDS NUMBER	FRICTION FACTOR	R*ROOTF	1/ROOTF	STRAIN RATE	DRAG REDUCTION
(MV)	(VOLTS)	(M/SEC)	(M**3/SEC)	(PASCALS)	(M/SEC)					(1/SEC)	(PERCENT)
0120	0.022	0.114	.0000229	12.0	0.009	2040.1	0.0446	431.0	4.73	81.4	3.34
.0180	0.027	0.141	.0000282	15.8	0.009	2516.3	0.0361	477.9	5.27	100.0	17.84
.0270	0.032	0.174	.0000349	18.7	0.010	3103.7	0.0281	520.6	5.96	118.7	32.61
0300	0.034	0.183	.0000367	19.9	0.011	3277.6	0.0268	536.8	6.11	126.2	34.92
.0300	0.047	0.207	.0000415	27.5	0.012	3704.0	0.0291	631.7	5.86	174.8	27.33
.0300	0.050	0.207	.0000415	27.3	0.013	3704.0	0.0310	651.7	5.68	186.0	22.67
.0500	0.061	0.237	.0000477	35.8	0.014	4269.1	0.0284	720.1	5.93	227.1	26.46
0600	0.071	0.263	.0000526	41.7	0.015	4691.5	0.0274	777.1	6.04	264.5	27.47
0750	0.082	0.295	.0000590	48.2	0.017	5265.7	0.0252	835.3	6.30	305.6	31.61
.0910	0.096	0.326	.0000654	56.4	0.018	5832.0	0.0240	904.0	6.45	357.9	33.08
.1070	0.110	0.356	.0000714	64.6	0.019	6369.6	0.0231	967.8	6.58	410.2	34.33
1280	0.120	0.386	.0000772	70.5	0.020	6889.6	0.0215	1010.9	6.82	447.6	37.59
1470	0.130	0.412	.0000826	76.4	0.021	7371.5	0.0204	1052.3	7.01	485.0	39.97
1710	0.145	0.444	.0000890	85.3	0.022	7936.6	0.0196	1111.4	7.14	541.0	41.20
1910	0.160	0.467	.0000937	74.1	0.023	8377.2	0.0194	1167.6	7.17	591.1	40.97
2170	0.171	0.499	.0000997	100.6	0.024	8916.0	0.0183	1207.1	7.39	630.2	43.49
2640	0.194	0.549	.0001100	114.1	0.025	9812.1	0.0172	1285.8	7.63	724.2	45.82
3060	0.220	0.590	.0001182	129.4	0.027	10545.8	0.0169	1369.4	7.70	821.3	45.88
3500	0.238	0.630	.0001262	140.0	0.028	11261.0	0.0160	1424.4	7.91	888.6	47.84

3990	0 260	0 672	.0001346	153 0	0.029	12005 3	0.0154	1488 8	8.06	970 8	49.08
4590	0 288	0.719	0001439	169 5	0.031	12841 9	0.0149	1567.0	8.20	1075 5	49 90

30 PPM SEPARAN, 10 RPS : 10/5/82

UPSTREAM PRESSURE TAPS

PROGRAM PARAMETERS : D = 0.015920 METERS
                        L = 0.71 METERS
                        TEMP = 25.00 DEGREES CENTIGRADE

RHO = 777.10 KG PER CUBIC METER
NU = 0.00000087 SQUARE METERS PER SEC

INPUT DATA   OUTPUT

VELOCITY (MV)	PRESSURE DROP (VOLTS)	VELOCITY (M/SEC)	FLOW RATE (M**3/SEC)	PRESSURE DROP (PASCALS)	FRICTION VELOCITY (M/SEC)	REYNOLDS NUMBER	FRICTION FACTOR	R*ROOTF	1/ROOTF	STRAIN RATE (1/SEC)	DRAG REDUCTION (PERCENT)
.0120	0.021	0.115	.0000229	12.6	0.008	2046.5	0.0433	425.9	4.81	79.9	4.31
.0180	0.025	0.142	.0000282	14.9	0.009	2524.2	0.0336	462.8	5.45	94.4	22.15
.0270	0.031	0.175	.0000348	18.4	0.010	3113.4	0.0272	513.2	6.07	116.1	34.05
.0300	0.037	0.185	.0000367	21.8	0.011	3287.9	0.0289	559.1	5.88	137.8	28.95
.0380	0.048	0.209	.0000415	28.1	0.013	3715.6	0.0292	634.7	5.85	177.6	26.32
.0380 ·	0.048	0.209	.0000415	28.1	0.013	3715.6	0.0292	634.7	5.85	177.6	27.59
.0500	0.061	0.240	.0000479	35.5	0.014	4282.6	0.0278	713.8	6.00	224.6	28.90
.0600	0.071	0.264	.0000526	41.2	0.015	4706.2	0.0267	769.1	6.12	260.7	32.44
.0750	0.083	0.297	.0000590	48.1	0.016	5282.2	0.0247	830.6	6.36	304.1	33.61
.0910	0.098	0.328	.0000654	56.6	0.018	5850.4	0.0238	901.7	6.49	358.3	36.36
1090	0.110	0.357	.0000714	63.5	0.019	6389.6	0.0223	954.7	6.69	401.7	39.65
1200	0.120	0.380	.0000772	69.2	0.020	6911.3	0.0208	996.7	6.93	437.9	40.30
1470	0.134	0.415	.0000826	77.2	0.021	7394.6	0.0203	1052.8	7.02	488.5	41.82
1710	0.149	0.447	.0000890	85.8	0.022	7961.5	0.0194	1109.7	7.17	542.7	42.22
1910	0.163	0.472	.0000937	93.8	0.023	8403.5	0.0191	1160.2	7.24	593.3	43.55
2170	0.178	0.502	.0000997	102.4	0.024	8944.0	0.0184	1212.1	7.38	647.6	44.40
2640	0.208	0.553	.0001100	119.5	0.026	9842.9	0.0177	1309.7	7.52	756.0	45.24
3060	0.233	0.594	.0001182	133.8	0.028	10578.9	0.0172	1385.8	7.63	846.4	45.24
3300	0.258	0.634	.0001262	148.1	0.027	11296.4	0.0167	1457.9	7.75	936.8	46.06

.3990	0.286	0.676	.0001346	164.1	0.030	12043.0	0.0162	1534.6	7.85	1038.0	46.65
.4500	0.320	0.723	.0001439	183.5	0.032	12882.2	0.0159	1623.0	7.94	1160.9	47.06

20 PPM SEPARAN AP-273, 1% MASTER SOLUTION, 10 RPS : 9/27/82
DOWNSTREAM PRESSURE TAPS

PROGRAM PARAMETERS : D = 0.015970 METERS
                     L = 0.71 METERS
                     TEMP = 24.00 DEGREES CENTIGRADE

                  RHO = 997.32 KG PER CUBIC METER
                  NU = 0.00000091 SQUARE METERS PER SEC

INPUT DATA   OUTPUT

VELOCITY (MV)	PRESSURE DROP (VOLTS)	VELOCITY (M/SEC)	FLOW RATE (M**3/SEC)	PRESSURE DROP (PASCALS)	FRICTION VELOCITY (M/SEC)	REYNOLDS NUMBER	FRICTION FACTOR	R*ROOTF	1/ROOTF	STRAIN RATE (1/SEC)	DRAG REDUCTION (PERCENT)
.0120	0.017	0.114	.0000229	9.9	0.007	1995.0	0.0344	369.8	5.39	61.3	25.96
.0180	0.022	0.141	.0000282	12.8	0.009	2460.7	0.0293	421.4	5.84	79.5	33.56
.0270	0.040	0.174	.0000348	23.4	0.012	3035.1	0.0352	569.6	5.33	145.3	16.11
.0220	0.024	0.156	.0000313	14.0	0.009	2729.9	0.0260	440.3	6.20	86.9	39.58
.0340	0.050	0.196	.0000392	29.3	0.013	3419.6	0.0347	637.2	5.37	181.9	14.90
.0390	0.053	0.210	.0000421	31.1	0.013	3671.2	0.0319	656.1	5.60	192.8	20.37
.0460	0.060	0.229	.0000458	35.2	0.014	3998.5	0.0305	698.3	5.73	218.4	22.40
.0630	0.072	0.269	.0000539	42.3	0.015	4705.1	0.0264	765.2	6.15	262.3	30.03
.0730	0.081	0.291	.0000582	47.6	0.016	5077.8	0.0256	811.7	6.26	295.1	31.14
.0880	0.092	0.320	.0000641	54.1	0.018	5593.3	0.0239	865.2	6.46	335.3	34.01
.1050	0.107	0.350	.0000701	62.9	0.019	6116.1	0.0233	933.3	6.55	390.2	34.40
.1300	0.122	0.389	.0000770	71.7	0.020	6788.6	0.0216	996.7	6.81	445.0	37.74
.1540	0.142	0.422	.0000845	83.5	0.022	7374.3	0.0213	1073.4	6.86	518.1	37.34
.1720	0.152	0.445	.0000892	89.4	0.023	7783.4	0.0204	1112.7	6.99	554.6	39.00
.2090	0.175	0.490	.0000981	102.9	0.024	8560.5	0.0195	1194.1	7.17	639.7	40.60
.2490	0.204	0.534	.0001067	120.0	0.026	9325.0	0.0191	1289.3	7.23	744.6	40.42
.2820	0.221	0.567	.0001136	130.0	0.027	9909.4	0.0183	1342.0	7.38	806.8	42.00
.3440	0.260	0.625	.0001252	153.0	0.029	10919.6	0.0178	1455.7	7.50	949.3	42.48
.3950	0.289	0.669	.0001339	170.1	0.031	11682.5	0.0173	1534.9	7.61	1055.3	43.22
.4340	0.309	0.700	.0001402	181.9	0.032	12232.3	0.0168	1587.1	7.71	1128.3	44.01

4650	0.330	0.724	.0001450	194.2	0.033	12651.5	0.0168	1640.2	7.71	1205.1	43.65
5270	0.360	0.770	.0001542	211.9	0.035	13449.1	0.0162	1713.2	7.85	1314.7	44.80
5800	0.390	0.807	.0001616	229.6	0.036	14093.6	0.0160	1703.2	7.90	1424.3	44.92

20 PPM SEPARAN AP-273, 1% MASTER SOLUTION, 10 RPS : 9/27/82
UPSTREAM PRESSURE TAPS

PROGRAM PARAMETERS :   D = 0.015920 METERS
L = 0.71 METERS
TEMP = 24.00 DEGREES CENTIGRADE

RHO = 997.32 KG PER CUBIC METER
NU = 0.00000091 SQUARE METERS PER SEC

INPUT DATA

OUTPUT

VELOCITY (MV)	PRESSURE DROP (VOLTS)	VELOCITY (M/SEC)	FLOW RATE (M**3/SEC)	PRESSURE DROP (PASCALS)	FRICTION VELOCITY (M/SEC)	REYNOLDS NUMBER	FRICTION FACTOR	R*ROOTF	1/ROOTF	STRAIN RATE (1/SEC)	DRAG REDUCTION (PERCENT)
.0120	0.018	0.115	.0000229	10.9	0.008	2001.3	0.0374	387.2	5.17	67.6	17.72
.0180	0.023	0.142	.0000282	13.8	0.009	2468.4	0.0310	434.9	5.68	85.2	28.49
.0270	0.037	0.175	.0000348	21.8	0.011	3044.6	0.0322	546.7	5.57	134.7	22.13
.0220	0.026	0.157	.0000313	15.5	0.009	2738.5	0.0284	461.1	5.94	95.8	33.13
.0340	0.048	0.197	.0000392	28.1	0.013	3430.3	0.0327	620.6	5.53	173.6	18.82
.0390	0.055	0.211	.0000421	32.1	0.013	3682.7	0.0324	663.4	5.55	198.4	18.23
.0460	0.061	0.230	.0000458	35.5	0.014	4011.1	0.0303	697.9	5.75	219.6	22.23
.0630	0.075	0.271	.0000539	43.5	0.016	4719.9	0.0268	772.6	6.11	269.1	28.62
.0730	0.084	0.292	.0000582	48.6	0.017	5093.8	0.0257	817.0	6.23	300.9	30.29
.0880	0.096	0.322	.0000641	55.5	0.018	5610.9	0.0242	872.7	6.43	343.3	33.01
.1050	0.112	0.352	.0000701	64.7	0.019	6135.3	0.0236	941.9	6.51	399.9	33.42
.1300	0.130	0.391	.0000778	74.9	0.021	6809.9	0.0222	1014.0	6.72	463.5	35.88
.1540	0.148	0.425	.0000845	85.2	0.022	7397.4	0.0214	1081.4	6.84	527.1	37.05
.1720	0.161	0.448	.0000892	92.7	0.023	7807.9	0.0209	1127.6	6.92	573.1	37.02
.2070	0.186	0.493	.0000981	106.9	0.025	8587.4	0.0199	1211.4	7.09	661.5	37.37
.2490	0.221	0.537	.0001067	127.0	0.027	9354.3	0.0199	1319.8	7.09	785.2	38.19
.2820	0.237	0.571	.0001136	136.1	0.028	9940.6	0.0189	1366.5	7.27	841.8	40.52
.3440	0.281	0.629	.0001252	161.2	0.030	10953.9	0.0184	1487.4	7.36	997.3	40.69
.3950	0.316	0.673	.0001337	181.3	0.032	11719.1	0.0181	1577.0	7.43	1121.0	40.87
.4340	0.340	0.704	.0001402	195.0	0.033	12270.7	0.0178	1635.6	7.50	1205.9	41.38

.4650	0.364	0.729	.0001450	208.7	0.034	12691.3	0.0178	1692.2	7.50	1290.7	40.90
.5270	0.406	0.775	.0001542	232.7	0.036	13491.4	0.0175	1786.8	7.55	1439.2	40.88
5800	0.444	0.812	.0001616	254.4	0.038	14137.9	0.0175	1868.4	7.57	1573.5	40.52

20 PPM SEPARAN AP-273, 1% MASTER SOLUTION, 30 RPS : 9/27/82
DOWNSTREAM PRESSURE TAPS

PROGRAM PARAMETERS : D = 0.015970 METERS
L = 0.71 METERS
TEMP = 24.00 DEGREES CENTIGRADE

RHO = 997.32 KG PER CUBIC METER
NU = 0.00000091 SQUARE METERS PER SEC

INPUT DATA

OUTPUT

VELOCITY	PRESSURE DROP	VELOCITY	FLOW RATE	PRESSURE DROP	FRICTION VELOCITY	REYNOLDS NUMBER	FRICTION FACTOR	R*RC 'TF	1/ROOTF	STRAIN RATE	DRAG REDUCTION
(MV)	(VOLTS)	(M/SEC)	(M**3/SEC)	(PASCALS)	(M/SEC)					(1/SEC)	(PERCENT)
.0130	0.021	0.119	.0000238	12.2	0.008	2079.4	0.0392	411.6	5.05	75.9	14.74
.0200	0.031	0.149	.0000298	18.1	0.010	2598.6	0.0372	501.0	5.19	112.4	14.69
.0250	0.044	0.167	.0000334	25.8	0.012	2916.6	0.0420	597.5	4.88	159.9	0.96
.0320	0.054	0.190	.0000380	31.7	0.013	3314.0	0.0399	662.3	5.00	196.5	2.84
.0390	0.061	0.210	.0000421	35.8	0.014	3671.2	0.0368	704.1	5.21	222.1	8.30
.0470	0.070	0.231	.0000463	41.1	0.015	4043.3	0.0348	754.4	5.36	255.0	11.17
.0630	0.088	0.269	.0000539	51.7	0.017	4705.1	0.0323	846.2	5.56	320.7	14.43
.0800	0.101	0.305	.0000610	59.4	0.018	5324.2	0.0290	906.7	5.87	368.2	20.97
.0990	0.117	0.340	.0000681	68.8	0.020	5942.8	0.0270	976.0	6.09	426.7	24.53
.1210	0.131	0.375	.0000751	77.0	0.021	6554.8	0.0248	1032.9	6.35	477.9	28.08
.1410	0.145	0.404	.0000810	85.3	0.022	7063.4	0.0237	1086.7	6.50	529.0	30.97
.1690	0.162	0.442	.0000885	95.3	0.023	7716.8	0.0222	1148.8	6.72	591.2	33.99
.2060	0.185	0.486	.0000974	108.8	0.025	8500.3	0.0209	1227.7	6.92	675.2	36.41
.2440	0.207	0.528	.0001050	121.8	0.026	9233.1	0.0198	1298.8	7.11	755.6	38.49
.2890	0.234	0.574	.0001150	137.7	0.028	10028.9	0.0190	1301.0	7.26	854.3	39.07
.3290	0.256	0.611	.0001225	150.6	0.029	10684.4	0.0183	1444.5	7.40	934.7	41.15
.3690	0.284	0.647	.0001275	167.1	0.031	11300.3	0.0181	1521.5	7.43	1037.0	40.84
.4170	0.310	0.687	.0001375	182.5	0.032	11995.8	0.0176	1589.7	7.55	1132.0	41.87
.4170	0.348	0.687	.0001375	204.8	0.034	11995.8	0.0197	1684.4	7.12	1270.9	34.74
.5870	0.405	0.811	.0001625	238.4	0.037	14176.4	0.0164	1817.2	7.80	1479.2	43.39

20 PPM SEPARAN AP-273, 1% MASTER SOLUTION, 30 RPS : 9/27/82
UPSTREAM PRESSURE TAPS

PROGRAM PARAMETERS : D = 0.015920 METERS
L = 0.71 METERS
TEMP = 24.00 DEGREES CENTIGRADE

RHO = 977.32 KG PER CUBIC METER
NU = 0.00000091 SQUARE METERS PER SEC

INPUT DATA

OUTPUT

VELOCITY (MV)	PRESSURE DROP (VOLTS)	VELOCITY (M/SEC)	FLOW RATE (M**3/SEC)	PRESSURE DROP (PASCALS)	FRICTION VELOCITY (M/SEC)	REYNOLDS NUMBER	FRICTION FACTOR	R*ROOTF	1/ROOTF	STRAIN RATE (1/SEC)	DRAG REDUCTION (PERCENT)
.0130	0.022	0.120	.0000238	13.2	0.009	2085.9	0.0417	425.8	4.90	81.7	7.56
.0200	0.032	0.150	.0000298	18.9	0.010	2606.8	0.0382	507.6	5.12	117.1	10.86
.0250	0.043	0.168	.0000334	25.2	0.012	2925.8	0.0404	588.2	4.97	155.9	3.27
.0320	0.055	0.191	.0000380	32.1	0.013	3324.4	0.0398	663.4	5.01	198.4	1.93
.0390	0.064	0.211	.0000421	37.2	0.015	3682.7	0.0377	714.6	5.15	230.2	5.12
.0470	0.073	0.233	.0000463	42.4	0.015	4056.0	0.0353	762.4	5.32	262.0	9.02
.0630	0.088	0.271	.0000537	50.9	0.017	4719.9	0.0314	836.0	5.65	315.0	16.43
.0800	0.104	0.307	.0000610	60.1	0.018	5340.9	0.0289	907.9	5.88	371.6	20.85
.0970	0.118	0.342	.0000681	68.1	0.020	5961.5	0.0263	966.5	6.17	421.1	26.22
.1210	0.136	0.377	.0000751	78.4	0.021	6575.4	0.0249	1037.0	6.34	484.7	28.64
.1410	0.151	0.407	.0000810	86.9	0.022	7085.5	0.0238	1092.2	6.49	537.7	30.67
.1690	0.169	0.444	.0000885	97.2	0.023	7741.0	0.0223	1155.0	6.70	601.4	33.74
.2050	0.196	0.490	.0000974	112.7	0.025	8527.0	0.0213	1243.3	6.86	696.8	35.34
.2440	0.220	0.532	.0001058	126.4	0.027	9262.1	0.0202	1316.8	7.03	781.7	37.38
.2890	0.251	0.578	.0001150	144.1	0.029	10060.4	0.0195	1406.1	7.15	891.2	38.35
.3290	0.278	0.615	.0001225	157.5	0.030	10717.9	0.0191	1479.5	7.24	986.7	39.01
.3690	0.306	0.651	.0001295	175.5	0.031	11335.8	0.0187	1552.0	7.30	1085.7	39.25
.4170	0.336	0.691	.0001375	192.7	0.033	12033.5	0.0183	1626.0	7.40	1191.7	40.02
.4170	0.336	0.691	.0001375	192.7	0.033	12033.5	0.0183	1626.0	7.40	1191.7	40.02
.5870	0.457	0.816	.0001625	261.8	0.038	14221.0	0.0178	1895.5	7.50	1619.5	39.42

15 PPM SEPARAN AP-273, 1% MASTER SOLUTION, 10 RPS : 9/21/82
DOWNSTREAM PRESSURE TAPS

PROGRAM PARAMETERS : D = 0.015970 METERS
L = 0.71 METERS
TEMP = 25.20 DEGREES CENTIGRADE

RHO = 997.06 KG PER CUBIC METER
NU = 0.00000089 SQUARE METERS PER SEC

INPUT DATA

OUTPUT

VELOCITY	PRESSURE DROP	VELOCITY	FLOW RATE	PRESSURE DROP	FRICTION VELOCITY	REYNOLDS NUMBER	FRICTION FACTOR	R*ROOTF	1/ROOTF	STRAIN RATE	DRAG REDUCTION
(MV)	(VOLTS)	(M/SEC)	(M**3/SEC)	(PASCALS)	(M/SEC)					(1/SEC)	(PERCENT)
.7060	0.040	0.888	.0001778	23.4	0.012	15934.5	0.0013	585.1	27.23	149.3	95.22
.0310	0.047	0.187	.0000374	27.5	0.012	3348.4	0.0359	634.5	5.28	175.6	12.42
.0410	0.058	0.216	.0000432	34.0	0.014	3869.5	0.0332	705.2	5.49	216.9	16.15
.0490	0.072	0.236	.0000474	42.3	0.015	4243.4	0.0343	786.0	5.40	269.4	11.44
.0860	0.085	0.316	.0000634	49.9	0.017	5677.0	0.0226	854.2	6.65	318.2	37.34
.0780	0.094	0.301	.0000602	55.2	0.018	5397.3	0.0277	.78.4	6.01	352.0	24.24
.0980	0.112	0.338	.0000678	65.8	0.019	6073.7	0.0261	..0.9	6.19	419.6	26.65
1170	0.127	0.369	.0000739	74.6	0.021	6622.8	0.0249	1044.6	6.34	475.9	28.56
1420	0.148	0.406	.0000812	87.0	0.022	7279.9	0.0240	1127.9	6.45	554.7	29.50
1720	0.168	0.445	.0000892	98.8	0.024	7994.3	0.0226	1201.8	6.65	629.8	32.12
1960	0.189	0.475	.0000951	111.2	0.025	8521.0	0.0224	1274.8	6.68	708.6	31.74
2250	0.202	0.508	.0001017	118.8	0.026	9115.1	0.0209	1317.9	6.92	757.4	35.20
2460	0.226	0.530	.0001063	132.9	0.027	9521.2	0.0214	1394.1	6.83	847.5	32.85
2780	0.250	0.563	.0001128	147.1	0.029	10107.2	0.0210	1466.3	6.89	937.6	33.13
3150	0.274	0.599	.0001199	161.2	0.030	10743.3	0.0204	1535.2	7.00	1027.7	34.17
3660	0.310	0.644	.0001290	182.4	0.032	11560.3	0.0200	1633.0	7.08	1162.8	34.53
4310	0.350	0.698	.0001397	206.0	0.034	12521.3	0.0192	1735.2	7.22	1313.0	35.77
4660	0.379	0.725	.0001452	223.0	0.036	13008.0	0.0193	1805.7	7.20	1421.8	34.96
5810	0.451	0.807	.0001617	265.4	0.039	14487.7	0.0185	1969.9	7.35	1692.1	35.97

15 PPM SEPARAN AP-273, 1% MASTER SOLUTION, 10 RPS : 9/21/82
UPSTREAM PRESSURE TAPS

PROGRAM PARAMETERS : D = 0.015720 METERS
L = 0.71 METERS
TEMP = 25.20 DEGREES CENTIGRADE

RHO = 997.06 KG PER CUBIC METER
NU = 0.00000089 SQUARE METERS PER SEC

INPUT DATA

OUTPUT

VELOCITY	PRESSURE DROP	VELOCITY	FLOW RATE	PRESSURE DROP	FRICTION VELOCITY	REYNOLDS NUMBER	FRICTION FACTOR	R*ROOTF	1/ROOTF	STRAIN RATE	DRAG REDUCTION
(MV)	(VOLTS)	(M/SEC)	(M**3/SEC)	(PASCALS)	(M/SEC)					(1/SEC)	(PERCENT)
.7060	0.037	0.893	.0001778	21.8	0.011	15984.5	0.0012	561.6	28.46	138.4	95.68
.0310	0.047	0.188	.0000374	27.5	0.012	3358.9	0.0353	631.0	5.32	174.7	12.89
.0410	0.060	0.217	.0000432	34.9	0.014	3881.7	0.0336	711.2	5.46	221.9	14.41
.0490	0.070	0.238	.0000474	40.6	0.015	4256.7	0.0325	767.1	5.55	258.2	15.46
.0860	0.083	0.318	.0000634	48.1	0.016	5694.8	0.0215	834.3	6.83	305.4	40.37
.0780	0.096	0.303	.0000602	55.5	0.018	5414.3	0.0274	896.5	6.04	352.7	24.69
.0980	0.112	0.341	.0000678	64.6	0.019	6092.8	0.0252	967.5	6.30	410.8	28.87
.1170	0.130	0.371	.0000739	74.9	0.021	6643.6	0.0246	1041.7	6.38	476.1	29.30
.1420	0.151	0.408	.0000812	86.9	0.022	7302.7	0.0236	1122.0	6.51	552.4	30.66
.1720	0.172	0.448	.0000892	98.9	0.024	8019.5	0.0223	1196.9	6.70	628.6	33.18
.1960	0.196	0.478	.0000951	112.6	0.025	8547.8	0.0223	1277.2	6.69	715.8	32.07
.2250	0.212	0.511	.0001017	121.8	0.026	9143.7	0.0211	1328.0	6.89	773.9	34.84
.2460	0.236	0.534	.0001063	135.5	0.028	9551.1	0.0215	1400.8	6.82	861.0	32.90
.2780	0.262	0.567	.0001128	150.3	0.027	10139.0	0.0212	1475.6	6.87	955.5	33.04
.3150	0.291	0.602	.0001199	166.9	0.031	10777.1	0.0208	1554.8	6.93	1060.8	33.30
.3660	0.329	0.648	.0001290	180.6	0.033	11596.7	0.0203	1652.8	7.02	1198.8	33.87
.4310	0.379	0.702	.0001397	217.2	0.035	12560.6	0.0199	1773.6	7.08	1380.3	33.02
.4660	0.409	0.729	.0001452	234.3	0.036	13048.9	0.0199	1842.3	7.08	1489.3	33.33
.5810	0.500	0.812	.0001617	286.3	0.040	14533.2	0.0196	2036.4	7.14	1819.7	32.72

15 PPM SEPARAN AP-273, 1% MASTER SOLUTION, 30 RPS : 9/21/82
DOWNSTREAM PRESSURE TAPS

PROGRAM PARAMETERS :   D = 0.015970 METERS
L = 0.71 METERS
TEMP = 25.20 DEGREES CENTIGRADE

RHO = 997.06 KG PER CUBIC METER
NU = 0.00000089 SQUARE METERS PER SEC

INPUT DATA

OUTPUT

VELOCITY	PRESSURE DROP	VELOCITY	FLOW RATE	PRESSURE DROP	FRICTION VELOCITY	REYNOLDS NUMBER	FRICTION FACTOR	R*ROOTF	1/ROOTF	STRAIN RATE	DRAG REDUCTION
(MV)	(VOLTS)	(M/SEC)	(M**3/SEC)	(PASCALS)	(M/SEC)					(1/SEC)	(PERCENT)
.0210	0.040	0.152	.0000305	23.4	0.012	2737.3	0.0457	585.1	4.68	149.3	-6.18
.0310	0.058	0.187	.0000374	34.0	0.014	3348.4	0.0444	705.2	4.75	216.9	-8.17
.0190	0.030	0.145	.0000290	17.5	0.010	2599.1	0.0379	506.2	5.13	111.7	12.93
.0350	0.062	0.199	.0000398	36.4	0.014	3565.4	0.0418	729.2	4.89	231.9	-3.56
.0460	0.075	0.229	.0000458	44.0	0.016	4106.9	0.0382	802.3	5.12	280.7	2.27
.0610	0.092	0.265	.0000530	54.0	0.018	4752.6	0.0350	888.8	5.35	344.5	7.25
.0720	0.103	0.288	.0000578	60.5	0.019	5178.3	0.0330	940.6	5.51	385.8	10.69
.0930	0.122	0.330	.0000661	71.7	0.020	5920.3	0.0299	1023.8	5.78	457.1	16.40
.0830	0.112	0.311	.0000622	65.8	0.019	5573.6	0.0310	980.9	5.68	419.6	14.67
.1040	0.134	0.348	.0000690	78.8	0.021	6252.6	0.0295	1073.1	5.83	502.1	16.58
.1270	0.154	0.384	.0000769	90.5	0.023	6893.5	0.0279	1150.5	5.99	577.2	19.25
.1570	0.174	0.426	.0000853	102.3	0.024	7645.8	0.0256	1223.1	6.25	652.3	23.96
.1820	0.192	0.458	.0000917	112.9	0.025	8218.1	0.0244	1284.8	6.40	719.9	26.09
.2440	0.238	0.528	.0001058	140.0	0.028	9483.3	0.0228	1430.7	6.63	892.5	28.78
.2120	0.214	0.493	.0000980	125.9	0.027	8853.9	0.0235	1356.5	6.53	802.5	27.74
.2650	0.252	0.550	.0001102	148.3	0.029	9873.6	0.0222	1472.2	6.71	945.1	29.76
.2920	0.371	0.577	.0001155	218.3	0.035	10352.7	0.0298	1786.6	5.79	1391.8	4.84
.3160	0.291	0.599	.0001201	171.2	0.031	10760.0	0.0216	1502.1	6.80	1091.5	30.27
.3450	0.312	0.626	.0001253	183.6	0.032	11231.5	0.0213	1630.2	6.86	1170.3	30.67
.3750	0.324	0.652	.0001305	190.7	0.033	11698.3	0.0204	1669.5	7.01	1215.4	32.99

4260	0.362	0.694	.0001389	213.0	0.035	12450.1	0.0201	1764 7	7 05	1358.0	32.90
4760	0.393	0.732	.0001467	231.3	0.036	13143.7	0.0196	1838 8	7 15	1474.4	33.78
5910	0.466	0.814	.0001630	274.3	0.037	14609.0	0.0188	2002 4	7.30	1748.4	34 81
.5370	0.427	0.777	.0001556	251 3	0.038	13941.0	0.0189	1916 7	7.27	1602.0	35.14

15 PPM SEPARAN AP-273, 1% MASTER SOLUTION, 30 RPS : 9/21/82
UPSTREAM PRESSURE TAPS

PROGRAM PARAMETERS : D = 0.015920 METERS
L = 0.71 METERS
TEMP = 25.20 DEGREES CENTIGRADE

RHO = 997.06 KG PER CUBIC METER
NU = 0.00000089 SQUARE METERS PER SEC

INPUT DATA

OUTPUT

VELOCITY	PRESSURE DROP	VELOCITY	FLOW RATE	PRESSURE DROP	FRICTION VELOCITY	REYNOLDS NUMBER	FRICTION FACTOR	R*ROOTF	1/ROOTF	STRAIN RATE	DRAG REDUCTION
(MV)	(VOLTS)	(M/SEC)	(M**3/SEC)	(PASCALS)	(M/SEC)					(1/SEC)	(PERCENT)
.0210	0.034	0.153	.0000305	20.1	0.011	2745.8	0.0385	539.1	5.09	127.5	9.06
.0310	0.053	0.188	.0000374	30.9	0.013	3358.9	0.0397	669.2	5.02	196.5	2.01
.0190	0.023	0.146	.0000290	13.8	0.007	2607.3	0.0294	446.7	5.84	87.6	31.53
.0350	0.059	0.200	.0000398	34.4	0.014	3576.6	0.0389	705.3	5.07	218.3	2.64
.0460	0.073	0.230	.0000458	42.4	0.015	4119.8	0.0361	783.2	5.26	269.1	6.62
.0610	0.091	0.266	.0000530	52.6	0.017	4767.6	0.0335	873.1	5.46	334.5	10.46
.0720	0.101	0.290	.0000578	58.4	0.018	5194.6	0.0313	919.3	5.65	370.8	14.77
.0930	0.121	0.332	.0000661	67.8	0.020	5938.9	0.0287	1005.3	5.91	443.4	19.65
.0830	0.111	0.312	.0000622	64.1	0.019	5591.2	0.0297	963.2	5.80	407.1	17.88
.1040	0.133	0.386	.0000690	76.6	0.021	6272.2	0.0282	1053.5	5.95	487.0	19.91
.1270	0.155	0.386	.0000769	89.2	0.022	6915.2	0.0270	1136.6	6.08	566.9	21.60
.1570	0.180	0.429	.0000853	103.5	0.024	7669.9	0.0255	1224.3	6.26	657.7	24.33
.1820	0.198	0.461	.0000917	113.8	0.025	8243.9	0.0242	1283.7	6.42	723.1	26.82
.2440	0.244	0.532	.0001058	140.1	0.028	9513.1	0.0224	1424.2	6.68	890.1	30.14
.2120	0.220	0.496	.0000988	126.4	0.027	8881.8	0.0232	1352.7	6.57	802.9	28.81
.2650	0.261	0.554	.0001102	149.8	0.027	9904.6	0.0221	1472.8	6.72	951.8	30.45
.2920	0.282	0.580	.0001155	161.8	0.030	10385.2	0.0217	1530.7	6.78	1028.1	30.96
.3160	0.305	0.603	.0001201	174.9	0.031	10793.8	0.0217	1591.6	6.78	1111.6	30.29
.3450	0.330	0.630	.0001253	187.2	0.033	11266.7	0.0216	1655.3	6.81	1202.4	30.13
.3750	0.347	0.656	.0001305	198.9	0.034	11735.1	0.0209	1697.3	6.91	1264.1	31.67

.4260	0.391	0.698	.0001389	224.1	0.036	12489.2	0.0208	1801.4	6.93	1423.9	31.09
.4760	0.428	0.737	.0001467	245.2	0.037	13184.9	0.0204	1884.5	7.00	1558.3	31.51
.5910	0.518	0.819	.0001630	296.6	0.041	14654.9	0.0200	2072.7	7.07	1885.1	31.33
.5370	0.470	0.782	.0001556	269.2	0.039	13984.8	0.0199	1974.5	7.08	1710.8	32.27

5 PPM SEPARAN AP-273, 1% MASTER SOLUTION, 10 RPS ; 10/11/82

DOWNSTREAM PRESSURE TAPS

PROGRAM PARAMETERS :   D = 0.015970 METERS
L = 0.71 METERS
TEMP = 25.00 DEGREES CENTIGRADE

RHO = 997.10 KG PER CUBIC METER
NU = 0.00000089 SQUARE METERS PER SEC

INPUT DATA

OUTPUT

VELOCITY	PRESSURE DROP	VELOCITY	FLOW RATE	PRESSURE DROP	FRICTION VELOCITY	REYNOLDS NUMBER	FRICTION FACTOR	R*ROOTF	1/ROOTF	STRAIN RATE	DRAG REDUCTION
(MV)	(VOLTS)	(M/SEC)	(M**3/SEC)	(PASCALS)	(M/SEC)					(1/SEC)	(PERCENT)
0140	0.017	0.124	.0000248	9.9	0.007	2209.5	0.0293	378.2	5.84	62.7	35.30
0190	0.030	0.145	.0000290	17.5	0.010	2587.7	0.0379	504.0	5.13	111.2	13.03
0260	0.042	0.170	.0000341	24.6	0.012	3043.7	0.0385	597.0	5.10	156.1	8.30
0330	0.052	0.193	.0000386	30.5	0.013	3443.3	0.0373	664.6	5.18	193.5	8.53
0370	0.060	0.210	.0000421	35.2	0.014	3754.1	0.0362	714.1	5.26	223.4	9.30
0470	0.070	0.231	.0000463	41.1	0.015	4134.6	0.0348	771.6	5.36	260.7	10.68
0560	0.080	0.253	.0000507	47.0	0.016	4527.0	0.0332	825.0	5.49	298.1	12.94
0670	0.095	0.278	.0000557	55.8	0.018	4967.1	0.0328	899.2	5.52	354.2	12.16
0810	0.111	0.307	.0000614	65.2	0.019	5479.6	0.0315	972.2	5.64	414.0	13.62
0910	0.121	0.326	.0000654	71.1	0.020	5832.0	0.0303	1015.1	5.75	451.3	15.62
1040	0.132	0.348	.0000690	77.6	0.021	6225.1	0.0290	1060.3	5.87	492.5	17.92
1210	0.149	0.375	.0000751	87.6	0.022	6702.9	0.0293	1126.7	5.95	556.0	18.64
1350	0.160	0.396	.0000793	94.1	0.023	7071.1	0.0273	1167.6	6.06	597.1	20.48
1520	0.176	0.419	.0000840	103.5	0.024	7492.9	0.0267	1224.7	6.12	656.9	21.00
1730	0.195	0.447	.0000895	114.7	0.026	7981.8	0.0261	1239.1	6.19	727.9	21.68

5 PPM SEPARAN AP-273, 1% MASTER SOLUTION, 10 RPS ; 10/11/82
UPSTREAM PRESSURE TAPS

PROGRAM PARAMETERS : D = 0.015920 METERS
L = 0.71 METERS
TEMP = 25.00 DEGREES CENTIGRADE

RHO = 997.10 KG PER CUBIC METER
NU = 0.00000089 SQUARE METERS PER SEC

INPUT DATA   OUTPUT

VELOCITY	PRESSURE DROP	VELOCITY	FLOW RATE	PRESSURE DROP	FRICTION VELOCITY	REYNOLDS NUMBER	FRICTION FACTOR	R*ROOTF	1/ROOTF	STRAIN RATE	DRAG REDUCTION
(MV)	(VOLTS)	(M/SEC)	(M**3/SEC)	(PASCALS)	(M/SEC)					(1/SEC)	(PERCENT)
.0140	0.016	0.124	.0000248	9.8	0.007	2216.4	0.0286	374.7	5.92	61.9	35.73
.0170	0.027	0.146	.0000290	16.1	0.010	2595.8	0.0342	480.2	5.41	101.6	20.25
.0260	0.040	0.171	.0000341	23.5	0.012	3053.2	0.0362	580.7	5.26	148.6	12.58
.0330	0.052	0.194	.0000386	30.4	0.013	3454.1	0.0365	660.1	5.23	192.0	9.29
.0390	0.058	0.211	.0000421	33.8	0.014	3765.9	0.0342	696.3	5.41	213.7	13.41
.0470	0.068	0.233	.0000463	37.5	0.015	4147.6	0.0330	752.9	5.51	249.9	14.71
.0560	0.080	0.255	.0000507	46.4	0.016	4541.2	0.0323	815.7	5.57	293.3	14.79
.0670	0.094	0.280	.0000557	54.4	0.018	4982.8	0.0314	883.3	5.64	343.9	15.27
.0810	0.113	0.309	.0000614	65.2	0.019	5496.8	0.0310	967.5	5.68	412.6	14.61
.0910	0.119	0.328	.0000654	68.6	0.020	5850.4	0.0288	992.6	5.89	434.3	19.54
.1040	0.133	0.351	.0000698	76.6	0.021	6244.7	0.0282	1048.9	5.95	484.9	19.99
.1210	0.152	0.377	.0000751	87.5	0.022	6724.0	0.0278	1120.7	6.00	553.6	19.90
.1350	0.162	0.398	.0000793	93.2	0.023	7093.3	0.0266	1136.7	6.13	589.7	22.40
.1520	0.178	0.422	.0000840	102.4	0.024	7516.4	0.0260	1212.1	6.20	647.6	23.12
.1730	0.199	0.449	.0000895	114.4	0.025	8006.9	0.0256	1281.2	6.25	723.5	23.22

5 PPM SEPARAN AP-273, 1% MASTER SOLUTION, 30 RPS. 10/11/82
DOWNSTREAM PRESSURE TAPS

PROGRAM PARAMETERS : D = 0.015970 METERS
L = 0.71 METERS
TEMP = 25.00 DEGREES CENTIGRADE

RHO = 997.10 KG PER CUBIC METER
NU = 0.00000089 SQUARE METERS PER SEC

INPUT DATA

OUTPUT

VELOCITY	PRESSURE DROP	VELOCITY	FLOW RATE	PRESSURE DROP	FRICTION VELOCITY	REYNOLDS NUMBER	FRICTION FACTOR	R*ROOTF	1/ROOTF	STRAIN RATE	DRAG REDUCTION
(MV)	(VOLTS)	(M/SEC)	(M**3/SEC)	(PASCALS)	(M/SEC)					(1/SEC)	(PERCENT)
0120	0.015	0.114	.0000229	8.7	0.007	2040.1	0.0303	355.0	5.75	55.2	34.42
0160	0.026	0.132	.0000265	15.2	0.009	2367.5	0.0392	468.9	5.05	96.3	11.96
0240	0.043	0.163	.0000327	25.2	0.012	2920.2	0.0428	604.1	4.83	159.8	-1.00
.0360	0.063	0.202	.0000404	37.0	0.014	3601.8	0.0413	731.8	4.92	234.6	-2.46
.0410	0.071	0.216	.0000432	41.7	0.015	3852.5	0.0407	777.1	4.96	264.5	-2.61
0450	0.075	0.226	.0000453	44.0	0.016	4042.6	0.0390	798.7	5.06	279.4	0.41
.0510	0.083	0.241	.0000483	48.7	0.017	4313.1	0.0380	840.4	5.13	309.3	1.63
0610	0.096	0.265	.0000530	56.4	0.018	4731.8	0.0365	904.0	5.23	357.9	3.31
0740	0.113	0.293	.0000586	66.4	0.019	5229.2	0.0352	980.9	5.33	421.4	4.52
.0840	0.124	0.312	.0000626	72.9	0.020	5583.7	0.0339	1027.7	5.43	462.6	6.63
0940	0.135	0.332	.0000664	79.4	0.021	5925.2	0.0328	1072.3	5.53	503.7	8.42
1090	0.151	0.356	.0000714	88.8	0.022	6369.6	0.0317	1134.2	5.62	563.5	9.00
.1220	0.163	0.377	.0000754	95.9	0.023	6729.9	0.0307	1178.5	5.71	608.3	11.61
1370	0.177	0.399	.0000790	104.1	0.024	7122.1	0.0297	1220.1	5.80	660.6	13.12
1560	0.195	0.425	.0000851	114.7	0.026	7588.6	0.0289	1287.1	5.89	727.9	14.39
1880	0.225	0.465	.0000932	132.4	0.027	8312.7	0.0278	1384.9	6.00	840.0	15.85
2150	0.252	0.497	.0000995	148.3	0.029	8875.8	0.0273	1465.7	6.06	940.9	16.01
2460	0.277	0.530	.0001063	163.0	0.030	9479.4	0.0263	1536.7	6.17	1034.4	17.77

5 PPM SEPARAN AP-273, 1% MASTER SOLUTION, 30 RPS   10/11/82

UPSTREAM PRESSURE TAPS

PROGRAM PARAMETERS :   D = 0.015920 METERS
                       L = 0.71 METERS
                       TEMP = 25.00 DEGREES CENTIGRADE

RHO = 997.10 KG PER CUBIC METER
NU = 0.00000089 SQUARE METERS PER SEC

INPUT DATA

OUTPUT

VELOCITY	PRESSURE DROP	VELOCITY	FLOW RATE	PRESSURE DROP	FRICTION VELOCITY	REYNOLDS NUMBER	FRICTION FACTOR	R*ROOTF	1/ROOTF	STRAIN RATE	DRAG REDUCTION
(MV)	(VOLTS)	(M/SEC)	(M**3/SEC)	(PASCALS)	(M/SEC)					(1/SEC)	(PERCENT)
.0120	0.014	0.115	.0000229	8.6	0.007	2046.5	0.0296	352.1	5.81	54.6	34.60
.0160	0.025	0.133	.0000265	14.9	0.009	2375.0	0.0380	462.8	5.13	94.4	13.25
.0240	0.040	0.164	.0000327	23.5	0.012	2929.4	0.0393	580.7	5.04	148.6	5.91
.0360	0.060	0.203	.0000404	34.9	0.014	3613.1	0.0384	708.0	5.10	220.9	3.65
.0410	0.070	0.217	.0000432	40.6	0.015	3864.6	0.0391	763.8	5.06	257.1	0.51
.0450	0.075	0.228	.0000453	43.5	0.016	4055.3	0.0380	790.1	5.13	275.2	2.25
.0510	0.083	0.243	.0000483	48.1	0.016	4326.7	0.0369	830.6	5.21	304.1	3.71
.0610	0.097	0.266	.0000530	56.1	0.018	4746.7	0.0357	897.1	5.29	354.7	4.72
.0740	0.114	0.294	.0000586	65.8	0.019	5245.6	0.0343	971.7	5.40	416.2	6.40
.0840	0.126	0.314	.0000626	72.6	0.020	5601.2	0.0332	1021.1	5.49	457.6	8.01
.0940	0.137	0.334	.0000664	78.9	0.021	5943.8	0.0321	1064.4	5.58	499.3	10.05
.1090	0.156	0.359	.0000714	87.8	0.023	6389.1	0.0316	1135.2	5.63	568.0	10.01
.1220	0.167	0.379	.0000754	96.1	0.023	6751.1	0.0303	1174.3	5.75	607.8	12.67
.1370	0.180	0.401	.0000798	103.5	0.024	7144.5	0.0291	1218.9	5.86	654.8	14.93
.1560	0.200	0.427	.0000851	114.9	0.025	7612.4	0.0285	1284.4	5.93	727.1	15.60
.1880	0.232	0.468	.0000932	133.2	0.027	8338.8	0.0275	1382.8	6.03	842.8	16.79
.2150	0.260	0.500	.0000995	147.2	0.029	8903.7	0.0270	1463.5	6.08	944.0	17.04
.2460	0.290	0.534	.0001063	166.4	0.031	9509.2	0.0264	1545.3	6.15	1052.5	17.71

5 PPM SEPARAN AP-273, 0.2% MASTER SOLUTION, 10 RPS : 10/21/82
DOWNSTREAM PRESSURE TAPS

PROGRAM PARAMETERS : D = 0.015970 METERS
L = 0.71 METERS
TEMP = 23.30 DEGREES CENTIGRADE

RHO = 997.47 KG PER CUBIC METER
NU = 0.00000093 SQUARE METERS PER SEC

INPUT DATA

OUTPUT

VELOCITY	PRESSURE DROP	VELOCITY	FLOW RATE	PRESSURE DROP	FRICTION VELOCITY	REYNOLDS NUMBER	FRICTION FACTOR	R*ROOTF	1/ROOTF	STRAIN RATE	DRAG REDUCTION
(MV)	(VOLTS)	(M/SEC)	(M**3/SEC)	(PASCALS)	(M/SEC)					(1/SEC)	(PERCENT)
.0950	0.123	0.333	.0000668	72.3	0.020	5732.1	0.0295	984.9	5.82	441.5	18 12
.0100	0.014	0.104	.0000208	8.1	0.007	1786.7	0.0341	329.8	5.42	49.5	28.50
.0190	0.030	0.145	.0000290	17.5	0.010	2490.5	0.0379	485.0	5.14	107.0	13 85
.0240	0.040	0.163	.0000327	23.4	0.012	2810.5	0.0398	560.5	5.01	143.0	6.98
.0300	0.049	0.183	.0000367	28.7	0.013	3154.4	0.0387	620.7	5.08	175.4	6.91
.0360	0.057	0.202	.0000404	33.4	0.014	3466.5	0.0373	669.7	5.18	204.1	8.22
.0420	0.064	0.218	.0000437	37.6	0.015	3754.3	0.0357	709.8	5.29	229.3	10 41
.0510	0.075	0.241	.0000484	44.0	0.016	4151.0	0.0343	768.6	5.40	268.9	11.98
.0590	0.084	0.260	.0000521	49.3	0.017	4476.1	0.0330	813.5	5.50	301.2	13 64
.0740	0.102	0.293	.0000506	60.0	0.018	5032.7	0.0317	896.7	5.61	366.0	14 65
.0900	0.119	0.324	.0000647	70.0	0.020	5569.2	0.0303	968.7	5.75	427.1	16 66
.1020	0.130	0.345	.0000671	76.4	0.021	5934.6	0.0291	1012.5	5.86	466.7	16 58
.1210	0.150	0.375	.0000751	88.2	0.022	6451.1	0.0284	1087.8	5.93	538.6	18 07
.1430	0.170	0.407	.0000815	100.0	0.024	6999.5	0.0274	1158.1	6.04	610.5	20 34
.1740	0.199	0.448	.0000897	117.1	0.026	7703.5	0.0265	1253.1	6.15	714.8	21 22
.1920	0.216	0.470	.0000942	127.1	0.027	8083.0	0.0261	1305.6	6.19	775.9	21 42
.2120	0.236	0.493	.0000988	138.9	0.028	8483.8	0.0259	1364.8	6.22	847.9	21 15
.2380	0.262	0.522	.0001046	154.2	0.030	8977.0	0.0257	1430.1	6.24	941.4	20 75
.2670	0.292	0.552	.0001106	171.9	0.031	9495.6	0.0256	1518.3	6.25	1049.3	19 98
.2960	0.319	0.581	.0001163	187.8	0.033	9986.1	0.0253	1507.0	6.29	1146.3	19 99

3340	0.353	0.616	.0001234	207.8	0.034	10593.0	0.0248	1669.5	6.35	1268.6	20.19
3900	0.404	0.664	.0001331	237.9	0.037	11426.2	0.0244	1786.1	6.40	1452.0	20.06
.4590	0.460	0.720	.0001441	270.8	0.039	12372.5	0.0237	1905.9	6.49	1653.4	20.87
0160	0.018	0.153	0000265	10.5	0.008	2278.6	0.0270	374.7	6.08	63.9	39.87
.0210	0.034	0.167	.0000306	19.9	0.011	2622.8	0.0388	516.5	5.08	121.4	10.79
0250	0.041	0.190	.0000334	24.0	0.012	2870.4	0.0391	567.5	5.06	146.6	8.12
0320	0.052	0.210	.0000380	30.5	0.013	3261.5	0.0384	639.5	5.10	186.7	6.82
0390	0.061	0.236	.0000421	35.8	0.014	3613.1	0.0368	692.9	5.21	218.5	8.66
.0490	0.074		.0000474	43.5	0.016	4066.0	0.0353	763.4	5.33	265.3	9.94

5 PPM SEPARAN AP-273, 0.2% MASTER SOLUTION, 10 RPS : 10/21/82
UPSTREAM PRESSURE TAPS

PROGRAM PARAMETERS : D = 0.015920 METERS
L = 0.71 METERS
TEMP = 23.30 DEGREES CENTIGRADE

RHO = 997.47 KG PER CUBIC METER
NU = 0.00000093 SQUARE METERS PER SEC

INPUT DATA

OUTPUT

VELOCITY	PRESSURE DROP	VELOCITY	FLOW RATE	PRESSURE DROP	FRICTION VELOCITY	REYNOLDS NUMBER	FRICTION FACTOR	R*ROOTF	1/ROOTF	STRAIN RATE	DRAG REDUCTION
(MV)	(VOLTS)	(M/SEC)	(M**3/SEC)	(PASCALS)	(M/SEC)					(1/SEC)	(PERCENT)
.0950	0.128	0.335	.0000660	73.8	0.020	5750.1	0.0297	990.3	5.81	449.2	17.42
.0100	0.016	0.105	.0000208	9.8	0.007	1792.3	0.0405	360.5	4.97	59.5	13.22
.0190	0.029	0.146	.0000290	17.2	0.010	2498.3	0.0366	478.2	5.22	104.8	15.34
.0240	0.041	0.164	.0000327	24.1	0.012	2819.3	0.0402	565.6	4.98	146.5	4.48
.0300	0.050	0.185	.0000367	29.2	0.013	3164.3	0.0388	623.1	5.08	177.8	5.56
.0360	0.059	0.203	.0000404	34.4	0.014	3477.4	0.0378	675.7	5.15	209.1	6.07
.0420	0.067	0.220	.0000437	38.9	0.015	3766.1	0.0365	719.3	5.24	237.0	7.63
.0510	0.078	0.243	.0000484	45.2	0.016	4164.1	0.0347	775.2	5.37	275.2	10.24
.0590	0.088	0.262	.0000521	50.9	0.017	4490.2	0.0336	822.7	5.46	310.0	11.57
.0740	0.107	0.295	.0000586	61.8	0.017	5048.5	0.0322	906.2	5.57	376.1	12.87
.0900	0.122	0.326	.0000647	70.4	0.020	5586.7	0.0300	967.0	5.78	428.3	17.12
.1020	0.137	0.347	.0000671	79.0	0.021	5953.3	0.0296	1024.2	5.81	480.5	16.95
.1210	0.155	0.378	.0000751	87.2	0.022	6471.3	0.0283	1098.9	5.94	543.1	19.05
.1430	0.177	0.410	.0000815	101.8	0.024	7021.5	0.0274	1163.1	6.04	619.6	20.11
.1740	0.209	0.451	.0000897	120.1	0.026	7727.7	0.0267	1263.3	6.12	731.0	20.50
.1920	0.228	0.473	.0000942	131.0	0.027	8108.4	0.0265	1319.1	6.15	797.1	20.41
.2120	0.249	0.496	.0000988	143.0	0.028	8510.5	0.0262	1378.3	6.17	870.1	20.27
.2380	0.276	0.525	.0001046	150.4	0.030	9005.2	0.0260	1450.8	6.21	964.0	20.10
.2670	0.308	0.556	.0001106	176.7	0.032	9525.5	0.0259	1532.2	6.22	1075.4	19.34
.2960	0.338	0.584	.0001163	193.9	0.033	10017.5	0.0257	1604.9	6.24	1179.7	19.08

3340	0.377	0.620	.0001234	216.2	0.035	10626.3	0.0254	1694.6	6.27	1315.4	18.75
.3900	0.433	0.669	.0001331	248.2	0.037	11462.1	0.0251	1815.8	6.31	1510.2	18.45
.4590	0.507	0.724	.0001441	290.5	0.041	12411.3	0.0251	1764.5	6.32	1767.6	17.13
.0160	0.019	0.133	.0000265	11.5	0.008	2285.7	0.0292	390.8	5.85	70.0	33.78
.0210	0.031	0.153	.0000306	18.4	0.010	2631.1	0.0352	493.9	5.33	111.7	17.65
.0250	0.042	0.168	.0000334	24.6	0.012	2877.5	0.0395	572.2	5.03	150.0	5.81
.0320	0.053	0.191	.0000380	30.9	0.013	3271.8	0.0384	641.1	5.10	188.3	5.78
.0390	0.062	0.211	.0000421	36.1	0.014	3624.4	0.0365	692.3	5.23	219.6	8.37
.0490	0.076	0.238	.0000474	44.1	0.016	4078.8	0.0352	765.3	5.33	268.3	9.23

5 PPM SEPARAN AP-273, 0.2% MASTER SOLUTION, 30 RPS : 10/21/82
DOWNSTREAM PRESSURE TAPS

PROGRAM PARAMETERS :   D = 0.015970 METERS
                       L = 0.71 METERS
                       TEMP = 23.30 DEGREES CENTIGRADE

RHO =   997.47 KG PER CUBIC METER
NU = 0.00000093 SQUARE METERS PER SEC

INPUT DATA   OUTPUT

VELOCITY	PRESSURE DROP	VELOCITY	FLOW RATE	PRESSURE DROP	FRICTION VELOCITY	REYNOLDS NUMBER	FRICTION FACTOR	R*ROOTF	1/ROOTF	STRAIN RATE	DRAG REDUCTION
(MV)	(VOLTS)	(M/SEC)	(M**3/SEC)	(PASCALS)	(M/SEC)					(1/SEC)	(PERCENT)
.0130	0.017	0.119	.0000238	9.9	0.007	2046.5	0.0316	364.0	5.62	60.3	31.44
.0170	0.024	0.137	.0000274	14.0	0.009	2351.2	0.0340	433.3	5.43	85.5	23.88
.0200	0.035	0.149	.0000298	20.5	0.011	2557.4	0.0420	524.1	4.88	125.0	3.98
.0280	0.050	0.177	.0000355	27.3	0.013	3043.8	0.0424	627.0	4.85	179.0	-1.17
.0330	0.058	0.193	.0000306	34.0	0.014	3313.9	0.0416	675.6	4.91	207.7	-1.10
.0390	0.066	0.210	.0000421	38.7	0.015	3613.1	0.0398	720.8	5.01	236.5	1.14
.0410	0.070	0.216	.0000432	41.1	0.015	3707.8	0.0401	742.4	4.99	250.9	-0.20
.0470	0.079	0.231	.0000464	46.4	0.016	3979.3	0.0393	788.9	5.04	283.3	0.11
.0570	0.091	0.256	.0000512	53.5	0.017	4396.9	0.0371	846.8	5.19	326.4	3.44
.0730	0.110	0.291	.0000582	64.7	0.019	4997.4	0.0347	931.2	5.37	394.7	6.79
.0620	0.096	0.267	.0000535	56.4	0.018	4592.5	0.0359	869.8	5.28	344.4	5.64
.0800	0.119	0.305	.0000610	70.0	0.020	5239.9	0.0342	968.7	5.41	427.1	7.22
.0900	0.130	0.324	.0000649	76.4	0.021	5569.2	0.0331	1012.5	5.50	466.7	8.94
.1080	0.147	0.355	.0000711	87.6	0.022	6102.7	0.0316	1084.1	5.63	535.0	11.14
.1220	0.164	0.377	.0000754	96.5	0.023	6477.0	0.0308	1137.5	5.69	588.9	11.71
.1480	0.190	0.414	.0000827	111.8	0.025	7118.0	0.0296	1224.4	5.81	682.4	13.55
.1710	0.210	0.444	.0000890	123.6	0.026	7638.4	0.0284	1287.4	5.93	754.4	15.61
.1820	0.222	0.458	.0000917	130.6	0.027	7874.6	0.0283	1323.7	5.95	797.5	15.44
.2100	0.249	0.471	.0000984	146.5	0.029	8444.7	0.0276	1401.9	6.02	894.6	16.12
.2440	0.282	0.528	.0001059	166.0	0.031	9086.9	0.0270	1472.0	6.09	1013.3	16.50

.2690	0.302	0.554	.0001110	177.8	0.032	9530.3	0.0262	1544.1	6.17	1085.2	17.77
.3040	0.334	0.588	.0001179	196.6	0.033	10117.1	0.0258	1623.9	6.23	1200.3	18.13
.3500	0.380	0.630	.0001262	223.7	0.036	10837.9	0.0255	1732.2	6.26	1365.7	17.48
.4140	0.433	0.684	.0001370	254.9	0.038	11764.4	0.0247	1849.1	6.36	1556.3	18.60
.4730	0.484	0.730	.0001463	285.0	0.040	12555.4	0.0242	1955.0	6.42	1739.7	18.86
.0174	0.028	0.138	.0000277	16.4	0.010	2379.6	0.0387	468.4	5.08	99.9	12.91
.0410	0.070	0.216	.0000432	41.1	0.015	3707.8	0.0401	742.4	4.99	250.9	-0.20
0570	0.092	0.256	.0000512	54.1	0.018	4396.9	0.0375	851.5	5.16	330.0	2.38
1010	0.142	0.343	.0000688	83.5	0.022	5906.2	0.0321	1058.3	5.58	509.8	10.30

5 PPM SEPARAN AP-273, 0.2% MASTER SOLUTION, 30 RPS : 10/21/82

UPSTREAM PRESSURE TAPS

PROGRAM PARAMETERS : D = 0.015920 METERS
                      L = 0.71 METERS
                      TEMP = 23.30 DEGREES CENTIGRADE

RHO = 997.47 KG PER CUBIC METER
NU = 0.00000093 SQUARE METERS PER SEC

INPUT DATA

OUTPUT

VELOCITY PRESSURE DROP	VELOCITY	FLOW RATE	PRESSURE DROP	FRICTION VELOCITY	REYNOLDS NUMBER	FRICTION FACTOR	R*ROOTF	1/ROOTF	STRAIN RATE	DRAG REDUCTION
(MV)	(M/SEC)	(M**3/SEC)	(PASCALS)	(M/SEC)					(1/SEC)	(PERCENT)
.0130	0.120	.0000238	9.2	0.007	2052.9	0.0290	349.8	5.87	56.1	35.80
.0170	0.138	.0000274	13.8	0.009	2358.6	0.0329	428.0	5.51	83.9	24.91
.0200	0.150	.0000298	19.5	0.010	2565.5	0.0394	509.0	5.04	118.7	8.51
.0280	0.178	.0000355	28.6	0.013	3053.4	0.0408	616.9	4.95	174.3	1.35
.0330	0.194	.0000386	33.8	0.014	3324.3	0.0406	670.1	4.96	205.6	-0.06
.0390	0.211	.0000421	38.4	0.015	3624.4	0.0388	714.0	5.08	233.5	2.57
.0410	0.217	.0000432	41.2	0.015	3719.4	0.0396	740.1	5.03	250.9	0.01
.0470	0.233	.0000464	46.4	0.016	3991.8	0.0387	784.9	5.09	282.2	0.80
.0570	0.257	.0000512	53.8	0.017	4410.8	0.0367	845.5	5.22	327.4	3.60
.0730	0.292	.0000582	65.2	0.019	5013.1	0.0345	931.0	5.30	397.0	6.88
.0620	0.269	.0000535	57.8	0.018	4606.9	0.0362	876.3	5.26	351.8	4.13
.0800	0.307	.0000610	71.0	0.020	5256.4	0.0341	970.9	5.41	431.8	6.90
.0900	0.326	.0000649	77.2	0.021	5586.7	0.0329	1013.0	5.51	470.0	9.04
.1080	0.357	.0000711	88.7	0.022	6121.8	0.0314	1015.4	5.64	539.6	11.24
.1220	0.379	.0000754	98.4	0.024	6497.4	0.0310	1143.3	5.68	598.8	11.39
.1480	0.417	.0000829	117.8	0.026	7140.4	0.0307	1251.2	5.71	717.0	10.26
.1710	0.447	.0000890	126.4	0.027	7662.4	0.0286	1295.9	5.91	769.2	15.07
.1820	0.461	.0000917	133.8	0.028	7899.3	0.0295	1333.5	5.92	814.4	14.81
.2100	0.494	.0000984	149.3	0.029	8471.2	0.0276	1408.2	6.02	908.4	16.08
.2440	0.532	.0001059	169.3	0.031	9115.4	0.0271	1499.7	6.08	1030.1	16.45

Note: the (VOLTS) column values (0.015, 0.023, 0.033, 0.049, 0.058, 0.066, 0.071, 0.080, 0.093, 0.113, 0.100, 0.123, 0.134, 0.154, 0.171, 0.205, 0.220, 0.233, 0.260, 0.295) correspond to the PRESSURE DROP (VOLTS) readings.

.2690	0.318	0.558	.0001110	182.4	0.032	9560.2	0.0265	1556.8	6.14	1110.1	17.26
.3040	0.355	0.592	.0001179	203.6	0.034	10148.9	0.0263	1644.6	6.17	1238.9	16.97
.3500	0.403	0.634	.0001262	231.0	0.036	10871.9	0.0260	1751.9	6.21	1405.9	16.62
4140	0.463	0.688	.0001370	265.3	0.039	11801.3	0.0253	1877.5	6.29	1614.6	17.22
.4730	0.522	0.735	.0001463	299.0	0.041	12594.9	0.0250	1993.2	6.32	1819.8	16.88
0174	0.022	0.139	.0000277	13.2	0.009	2387.1	0.0308	419.0	5.70	80.4	29.55
0410	0.070	0.217	.0000432	40.7	0.015	3719.4	0.0390	734.9	5.06	247.4	1.40
0570	0.092	0.257	.0000512	53.2	0.017	4410.8	0.0364	840.9	5.24	323.9	4.62
.1010	0.144	0.346	.0000688	83.0	0.022	5924.7	0.0314	1049.8	5.64	504.8	11.99

2 PPM SEPARAN AP-273, 0.2% MASTER SOLUTION, 10 RPS : 10/22/81
DOWNSTREAM PRESSURE TAPS

PROGRAM PARAMETERS : D = 0.015970 METERS
L = 0.71 METERS
TEMP = 23.30 DEGREES CENTIGRADE

RHO = 997.47 KG PER CUBIC METER
NU = 0.00000093 SQUARE METERS PER SEC

INPUT DATA

OUTPUT

| VELOCITY | PRESSURE DROP | VELOCITY | FLOW RATE | PRESSURE DROP | FRICTION VELOCITY | REYNOLDS NUMBER | FRICTION FACTOR | R*ROOTF | 1/ROOTF | STRAIN RATE | DRAG REDUCTION |
(MV)	(VOLTS)	(M/SEC)	(M**3/SEC)	(PASCALS)	(M/SEC)					(1/SEC)	(PERCENT)
.0200	0.032	0.149	.0000290	18.7	0.010	2557.4	0.0384	501.0	5.10	114.2	12.26
.0300	0.049	0.183	.0000367	28.7	0.013	3154.4	0.0387	620.7	5.08	175.4	6.91
.0400	0.065	0.213	.0000426	38.2	0.015	3660.7	0.0382	715.3	5.12	232.9	4.87
.0470	0.075	0.231	.0000464	44.0	0.016	3979.3	0.0373	768.6	5.18	268.9	5.18
.0540	0.084	0.249	.0000498	49.3	0.017	4275.6	0.0362	813.5	5.26	301.2	6.39
.0600	0.092	0.263	.0000526	54.1	0.018	4515.2	0.0356	851.5	5.30	330.0	6.84
.0710	0.106	0.286	.0000574	62.3	0.019	4926.1	0.0344	914.1	5.39	380.4	7.89
.0780	0.115	0.301	.0000602	67.6	0.020	5171.7	0.0339	952.2	5.43	412.7	8.25
.0860	0.126	0.316	.0000634	74.1	0.020	5439.7	0.0336	996.8	5.46	452.3	8.02
.1020	0.145	0.345	.0000671	85.3	0.022	5934.6	0.0325	1069.5	5.55	520.6	9.17
.1140	0.159	0.364	.0000730	93.5	0.023	6266.0	0.0319	1120.0	5.59	571.0	9.47
.1250	0.174	0.381	.0000764	102.4	0.024	6554.3	0.0320	1171.7	5.59	624.9	8.47
.1390	0.188	0.401	.0000804	110.6	0.025	6903.2	0.0311	1218.0	5.67	675.2	9.72
.1520	0.205	0.419	.0000840	120.6	0.026	7211.3	0.0311	1271.9	5.67	736.4	8.84
.1700	0.226	0.443	.0000887	133.0	0.027	7616.5	0.0307	1335.5	5.70	811.9	8.71
.1860	0.246	0.463	.0000927	144.8	0.029	7958.6	0.0307	1393.5	5.71	883.8	8.02
.1940	0.258	0.472	.0000946	151.9	0.029	8124.0	0.0309	1427.1	5.69	927.0	6.96
.2050	0.276	0.485	.0000972	162.5	0.030	8345.8	0.0313	1476.0	5.65	991.7	5.07
.2270	0.298	0.510	.0001022	175.4	0.032	8771.9	0.0306	1533.8	5.72	1070.8	6.10
.2450	0.316	0.529	.0001061	186.0	0.032	9105.0	0.0301	1579.5	5.76	1135.6	6.75

.2600	0.335	0.545	.0001092	197.2	0.033	9373.2	0.0301	16.43	5.76	1203.9	6.07
.2920	0.360	0.567	.0001136	211.9	0.035	9752.6	0.0299	1685.9	5.78	1293.8	5.86
.2990	0.378	0.584	.0001169	222.5	0.036	10035.4	0.0296	1727.6	5.81	1358.5	6.00
.3320	0.413	0.614	.0001230	243.2	0.037	10562.0	0.0292	1805.9	5.85	1484.4	6.14
.3640	0.445	0.642	.0001287	262.0	0.039	11047.5	0.0288	1874.5	5.89	1599.5	6.56
.4080	0.488	0.679	.0001361	287.3	0.040	11680.8	0.0282	1963.1	5.95	1754.1	7.10
.3390	0.238	0.621	.0001243	248.9	0.038	10670.2	0.0293	1827.0	5.84	1519.3	5.64
.3810	0.260	0.657	.0001316	272.1	0.039	11296.6	0.0286	1910.1	5.91	1660.8	6.71
.4270	0.288	0.695	.0001391	301.6	0.041	11943.4	0.0284	2011.0	5.94	1840.9	6.25
.4920	0.322	0.744	.0001491	337.4	0.044	12799.3	0.0276	2127.1	6.02	2059.5	7.15
.5580	0.358	0.792	.0001586	375.3	0.046	13611.0	0.0272	2243.5	6.07	2291.0	7.31
.5830	0.374	0.809	.0001620	392.2	0.047	13905.5	0.0272	2293.3	6.06	2393.9	6.72
.0750	0.113	0.295	.0000590	66.4	0.019	5067.8	0.0347	943.9	5.37	405.5	6.57
.0940	0.137	0.332	.0000664	80.6	0.021	5702.5	0.0332	1039.5	5.49	491.8	7.95
.1200	0.167	0.374	.0000748	98.2	0.024	6424.9	0.0319	1147.8	5.60	599.7	9.02
.1420	0.195	0.406	.0000813	114.7	0.026	6975.6	0.0316	1240.5	5.62	700.4	8.06
.1690	0.224	0.442	.0000885	131.8	0.027	7594.6	0.0307	1329.6	5.71	804.7	9.06

2 PPM SEPARAN AP-273, 0.2% MASTER SOLUTION, 10 RPS : 10/22/81

UPSTREAM PRESSURE TAPS

PROGRAM PARAMETERS : D = 0.015920 METERS
L = 0.71 METERS
TEMP = 23.30 DEGREES CENTIGRADE

RHO = 997.47 KG PER CUBIC METER
NU = 0.00000093 SQUARE METERS PER SEC

INPUT DATA

OUTPUT

VELOCITY	PRESSURE DROP	VELOCITY	FLOW RATE	PRESSURE DROP	FRICTION VELOCITY	REYNOLDS NUMBER	FRICTION FACTOR	R*ROOTF	1/ROOTF	STRAIN RATE	DRAG REDUCTION
(MV)	(VOLTS)	(M/SEC)	(M**3/SEC)	(PASCALS)	(M/SEC)					(1/SEC)	(PERCENT)
.0200	0.031	0.150	.0000298	18.4	0.010	2565.5	0.0371	493.9	5.19	111.7	13.88
.0300	0.050	0.185	.0000367	29.2	0.013	3164.3	0.0388	623.1	5.08	177.8	5.56
.0400	0.066	0.214	.0000426	38.4	0.015	3672.2	0.0378	714.0	5.14	233.5	4.81
.0470	0.076	0.233	.0000464	44.1	0.016	3991.8	0.0368	765.3	5.22	268.3	5.69
.0540	0.086	0.250	.0000498	49.8	0.017	4289.1	0.0360	813.4	5.27	303.1	6.22
.0600	0.095	0.264	.0000526	54.9	0.018	4529.4	0.0356	854.4	5.30	334.4	6.08
.0710	0.108	0.288	.0000574	62.4	0.019	4941.6	0.0337	910.3	5.43	379.6	8.66
.0780	0.116	0.303	.0000602	66.9	0.019	5188.0	0.0330	943.1	5.50	407.4	10.08
.0860	0.128	0.318	.0000634	73.8	0.020	5456.8	0.0329	970.3	5.51	447.2	9.37
.1020	0.148	0.347	.0000691	85.2	0.022	5953.3	0.0320	1064.2	5.59	518.7	10.33
.1140	0.166	0.367	.0000730	95.5	0.023	6285.7	0.0321	1126.6	5.58	581.4	8.75
.1250	0.177	0.384	.0000764	103.0	0.024	6574.9	0.0316	1167.6	5.62	626.6	9.21
.1390	0.195	0.404	.0000804	112.1	0.025	6924.9	0.0311	1220.4	5.67	682.2	9.84
.1520	0.211	0.422	.0000840	121.3	0.026	7234.0	0.0308	1267.3	5.70	737.9	9.76
.1700	0.235	0.446	.0000887	135.0	0.028	7640.5	0.0307	1339.1	5.71	821.4	8.85
.1860	0.255	0.466	.0000927	146.4	0.029	7983.6	0.0305	1374.7	5.72	891.0	8.55
.1940	0.268	0.475	.0000946	153.8	0.029	8149.5	0.0308	1429.7	5.70	936.2	7.35
.2050	0.288	0.488	.0000972	165.3	0.031	8372.1	0.0313	1481.8	5.65	1005.8	5.12
.2270	0.309	0.513	.0001022	177.3	0.032	8799.5	0.0304	1534.7	5.73	1078.8	6.84
.2450	0.330	0.533	.0001061	189.3	0.033	9133.6	0.0301	1585.8	5.76	1151.9	6.90

.2600	0.350	0.549	.0001092	200.7	0.034	9402.6	0.0302	1633.0	5.76	1221.5	6.24
.2820	0.378	0.571	.0001136	216.7	0.035	9783.2	0.0301	1696.9	5.77	1318.9	5.65
.2990	0.398	0.587	.0001167	228.2	0.036	10067.0	0.0299	1741.1	5.78	1388.5	5.59
.3320	0.435	0.618	.0001230	249.3	0.038	10595.1	0.0295	1820.0	5.82	1517.2	5.80
.3640	0.472	0.684	.0001287	270.5	0.039	11082.2	0.0293	1895.6	5.85	1645.9	5.65
.4080	0.519	0.624	.0001361	297.3	0.041	11717.5	0.0288	1987.5	5.90	1809.4	6.05
.3390	0.248	0.661	.0001243	251.9	0.038	10703.7	0.0292	1829.3	5.85	1532.7	6.54
.3810	0.272	0.699	.0001316	276.3	0.040	11332.1	0.0286	1916.1	5.91	1681.7	7.34
.4270	0.306	0.749	.0001391	311.0	0.042	11980.9	0.0288	2032.8	5.89	1892.7	5.53
.4920	0.344	0.797	.0001491	349.8	0.044	12839.5	0.0282	2155.7	5.96	2128.6	6.05
.5580	0.386	0.814	.0001586	392.6	0.047	13653.7	0.0280	2283.9	5.98	2389.2	5.45
.5830	0.406		.0001620	413.0	0.048	13949.1	0.0282	2342.5	5.95	2513.4	4.25
.0750	0.117	0.297	.0000590	67.5	0.020	5083.7	0.0347	947.1	5.37	410.9	5.98
.0940	0.143	0.334	.0000664	82.4	0.022	5720.4	0.0334	1046.2	5.47	501.3	6.98
.1200	0.175	0.376	.0000748	100.7	0.024	6445.1	0.0322	1156.5	5.57	612.7	8.02
.1420	0.202	0.408	.0000813	116.1	0.026	6997.5	0.0315	1242.0	5.63	706.6	8.34
.1690	0.235	0.444	.0000885	135.0	0.028	7618.5	0.0307	1339.1	5.69	821.4	8.38

1 PPM SEPARAN AP-273, 0.2% MASTER SOLUTION, 10 RPS : 10/26/82
DOWNSTREAM PRESSURE TAPS

PROGRAM PARAMETERS : D = 0.015970 METERS
L = 0.71 METERS
TEMP = 22.00 DEGREES CENTIGRADE

RHO = 997.76 KG PER CUBIC METER
NU = 0.00000096 SQUARE METERS PER SEC

INPUT DATA

OUTPUT

VELOCITY	PRESSURE DROP	VELOCITY	FLOW RATE	PRESSURE DROP	FRICTION VELOCITY	REYNOLDS NUMBER	FRICTION FACTOR	R*ROOTF	1/ROOTF	STRAIN RATE	DRAG REDUCTION
(MV)	(VOLTS)	(M/SEC)	(M**3/SEC)	(PASCALS)	(M/SEC)					(1/SEC)	(PERCENT)
.0460	0.077	0.229	.0000458	45.2	0.016	3817.9	0.0392	755.5	5.05	267.8	1.47
.0720	0.114	0.289	.0000578	67.0	0.019	4813.9	0.0365	919.7	5.23	396.9	2.91
.1050	0.159	0.350	.0000701	93.6	0.023	5839.8	0.0346	1086.4	5.38	553.9	3.57
.1320	0.193	0.391	.0000784	113.6	0.025	6530.4	0.0336	1197.1	5.46	672.5	3.83
.1620	0.232	0.433	.0000867	136.6	0.028	7217.4	0.0331	1312.6	5.50	808.5	3.05
.0460	0.078	0.229	.0000458	45.8	0.016	3817.9	0.0397	760.4	5.02	271.3	0.18
.0580	0.096	0.258	.0000517	56.4	0.018	4304.4	0.0384	843.8	5.10	334.1	0.48
.0780	0.125	0.301	.0000603	73.5	0.020	5017.5	0.0368	963.1	5.21	435.2	1.01
.0930	0.144	0.330	.0000661	84.7	0.022	5503.7	0.0353	1033.8	5.32	501.5	3.07
.1060	0.161	0.352	.0000705	94.7	0.023	5866.9	0.0347	1093.2	5.37	560.8	3.15
.1220	0.180	0.377	.0000755	105.9	0.025	6283.9	0.0338	1156.0	5.44	627.1	4.03
.1360	0.201	0.397	.0000796	118.3	0.026	6626.3	0.0340	1221.7	5.42	700.4	2.38
.1550	0.224	0.423	.0000848	131.9	0.027	7063.4	0.0333	1289.8	5.48	780.6	2.77
.1760	0.249	0.451	.0000903	146.6	0.029	7515.6	0.0327	1359.9	5.53	867.8	3.10
.1580	0.226	0.427	.0000856	133.0	0.027	7129.8	0.0330	1295.5	5.50	787.6	3.51
.1850	0.265	0.462	.0000925	156.0	0.030	7701.0	0.0332	1403.0	5.49	923.6	1.20
.1980	0.281	0.477	.0000956	165.4	0.031	7960.7	0.0329	1444.7	5.51	979.4	1.17
.2200	0.309	0.502	.0001006	181.9	0.032	8381.1	0.0327	1515.1	5.53	1077.1	0.73
.2350	0.325	0.517	.0001039	191.4	0.033	8655.5	0.0322	1553.8	5.57	1132.9	1.34
.2620	0.359	0.547	.0001076	211.4	0.035	9127.8	0.0320	1613.1	5.59	1251.5	0.74

.2980	0.395	0.583	.0001167	232.6	0.036	9720.2	0.0311	1713.1	5.67	1377.1	2.23
.3190	0.423	0.602	.0001207	247.1	0.038	10049.0	0.0311	1772.8	5.67	1474.4	1.25
.3530	0.461	0.633	.0001268	271.5	0.039	10558.6	0.0307	1850.8	5.70	1607.4	1.35
.3840	0.492	0.660	.0001321	289.8	0.041	11001.8	0.0302	1912.0	5.75	1715.5	2.07
.1280	0.190	0.386	.0000773	111.8	0.025	6433.0	0.0341	1187.8	5.42	662.0	2.79
.2210	0.306	0.504	.0001007	180.2	0.032	8399.7	0.0322	1507.7	5.57	1066.7	2.07
.2670	0.362	0.552	.0001106	213.2	0.035	9212.4	0.0317	1640.0	5.62	1262.0	1.53
.3320	0.439	0.614	.0001231	258.6	0.038	10247.0	0.0311	1806.1	5.67	1530.6	0.97
.3830	0.494	0.659	.0001319	291.0	0.041	10987.7	0.0304	1915.9	5.73	1722.5	1.45
.4150	0.300	0.685	.0001372	314.3	0.042	11427.0	0.0304	1991.2	5.74	1860.6	0.65
.4530	0.321	0.715	.0001432	336.4	0.044	11926.6	0.0298	2060.2	5.79	1991.6	1.37
.4940	0.346	0.746	.0001494	362.8	0.045	12442.2	0.0296	2139.3	5.82	2147.5	1.28
.5830	0.397	0.809	.0001620	416.5	0.049	13490.8	0.0289	2292.3	5.89	2465.7	1.70
.2550	0.198	0.540	.0001082	206.8	0.034	9007.8	0.0322	1615.2	5.58	1224.2	0.62
.3920	0.286	0.666	.0001335	299.5	0.041	11113.1	0.0306	1943.9	5.72	1773.2	0.55
.4520	0.320	0.714	.0001431	335.4	0.044	11913.8	0.0298	2056.9	5.79	1985.3	1.49
.5270	0.365	0.770	.0001542	382.8	0.047	12841.5	0.0293	2197.6	5.84	2266.1	1.47
.5800	0.396	0.807	.0001616	415.5	0.049	13456.8	0.0289	2299.4	5.88	2459.5	1.52

1 PPM SEPARAN AP-273, 0.2% MASTER SOLUTION, 10 RPS : 10/26/82
UPSTREAM PRESSURE TAPS

PROGRAM PARAMETERS : D = 0.015920 METERS
L = 0.71 METERS
TEMP = 22.00 DEGREES CENTIGRADE

RHO = 797.76 KG PER CUBIC METER
NU = 0.00000096 SQUARE METERS PER SEC

INPUT DATA

OUTPUT

VELOCITY PRESSURE DROP		VELOCITY	FLOW RATE	PRESSURE DROP	FRICTION VELOCITY	REYNOLDS NUMBER	FRICTION FACTOR	R*ROOTF	1/ROOTF	STRAIN RATE	DRAG REDUCTION
(MV)	(VOLTS)	(M/SEC)	(M**3/SEC)	(PASCALS)	(M/SEC)					(1/SEC)	(PERCENT)
.0460	0.080	0.230	.0000458	46.4	0.016	3829.9	0.0395	761.4	5.03	273.7	-0.47
.0720	0.119	0.290	.0000578	68.7	0.020	4829.0	0.0368	926.5	5.21	405.3	1.44
.1050	0.165	0.352	.0000701	95.0	0.023	5858.1	0.0346	1089.6	5.38	560.6	3.28
.1320	0.201	0.394	.0000784	115.6	0.026	6550.9	0.0337	1201.9	5.45	682.1	3.51
.1620	0.240	0.435	.0000867	137.9	0.028	7240.1	0.0329	1312.7	5.52	813.7	3.63
.0460	0.080	0.230	.0000458	46.4	0.016	3829.9	0.0395	761.4	5.03	273.7	-0.47
.0580	0.099	0.260	.0000517	57.2	0.018	4317.9	0.0384	845.9	5.10	337.8	-0.21
.0780	0.129	0.303	.0000603	74.4	0.021	5033.2	0.0367	964.3	5.22	439.1	0.80
.0930	0.149	0.332	.0000661	85.8	0.022	5520.9	0.0352	1035.8	5.33	506.6	2.89
.1060	0.169	0.354	.0000705	97.3	0.023	5885.3	0.0351	1102.6	5.34	574.1	1.76
.1220	0.187	0.379	.0000755	107.6	0.025	6303.6	0.0338	1159.5	5.44	634.8	3.84
.1360	0.209	0.400	.0000776	120.1	0.026	6647.1	0.0340	1225.4	5.42	709.1	2.25
.1550	0.234	0.426	.0000848	134.4	0.028	7085.6	0.0335	1296.3	5.47	793.4	2.35
.1760	0.260	0.453	.0000903	147.3	0.029	7539.3	0.0328	1366.1	5.52	881.2	2.87
.1580	0.237	0.430	.0000856	136.2	0.028	7152.2	0.0333	1304.5	5.48	803.5	2.74
.1850	0.279	0.465	.0000925	160.2	0.030	7725.2	0.0335	1414.9	5.46	945.3	0.22
.1980	0.295	0.480	.0000956	167.3	0.031	7985.7	0.0332	1454.7	5.49	999.3	0.55
.2200	0.325	0.506	.0001006	186.5	0.032	8407.4	0.0330	1526.6	5.51	1100.5	0.04
.2350	0.344	0.522	.0001037	177.3	0.033	8682.7	0.0327	1570.5	5.53	1164.6	0.10
.2620	0.378	0.551	.0001076	216.8	0.035	9156.4	0.0323	1646.0	5.56	1279.4	0.14

.2980	0.420	0.586	.0001167	240.8	0.037	7750.8	0.0317	1734.8	5.62	1421.1	0.80
.3190	0.450	0.606	.0001207	258.0	0.038	10080.6	0.0317	1795.5	5.61	1522.3	-0.17
.3530	0.490	0.637	.0001268	280.8	0.040	10591.8	0.0313	1873.5	5.65	1657.3	0.12
.3840	0.523	0.664	.0001321	297.7	0.041	11036.3	0.0308	1935.4	5.70	1768.7	0.92
.1280	0.198	0.388	.0000773	113.9	0.025	6453.2	0.0342	1192.9	5.41	671.9	2.37
.2210	0.319	0.507	.0001009	183.1	0.032	8426.1	0.0322	1512.5	5.57	1080.3	2.27
.2670	0.381	0.556	.0001106	218.5	0.035	9241.4	0.0320	1652.5	5.59	1287.5	0.99
.3320	0.463	0.618	.0001231	265.4	0.039	10279.2	0.0314	1.21 2	5.64	1566.2	0.45
.3830	0.526	0.663	.0001319	301.4	0.041	11022.3	0.0310	1?.0.9	5.68	1778.8	0.12
.4150	0.315	0.689	.0001372	320.3	0.043	11462.9	0.0305	2000.7	5.73	1890.2	1.01
.4530	0.338	0.719	.0001432	343.8	0.044	11964.1	0.0300	2072.7	5.77	2028.7	1.53
.4940	0.366	0.751	.0001494	372.3	0.046	12481.3	0.0299	2157.1	5.79	2197.2	1.07
.5830	0.428	0.814	.0001620	435.6	0.050	13533.1	0.0297	2333.2	5.80	2570.5	-0.24
.2550	0.203	0.543	.0001082	206.0	0.034	9036.1	0.0315	1604.7	5.63	1215.9	2.84
.3920	0.300	0.670	.0001335	305.0	0.042	11148.0	0.0307	1952.4	5.71	1799.9	0.76
.4520	0.339	0.719	.0001431	344.8	0.044	11951.2	0.0302	2075.8	5.76	2034.7	1.05
.5270	0.390	0.775	.0001542	396.8	0.047	12881.8	0.0299	2226.9	5.78	2341.7	0.32
.5800	0.426	0.812	.0001616	433.5	0.049	13499.1	0.0297	2327.7	5.80	2558.5	-0.22

20 PPM SEPARAN AP-30, 1% MASTER SOLUTION, 10 RPS : 11/11/02
DOWNSTREAM PRESSURE TAPS

PROGRAM PARAMETERS :   D = 0.015770 METERS
                       L = 0.71 METERS
                       TEMP = 21.20 DEGREES CENTIGRADE

                       RHO = 997.94 KG PER CUBIC METER
                       NU = 0.00000098 SQUARE METERS PER SEC

INPUT DATA   OUTPUT

VELOCITY	PRESSURE DROP	VELOCITY	FLOW RATE	PRESSURE DROP	FRICTION VELOCITY	REYNOLDS NUMBER	FRICTION FACTOR	R*ROOTF	1/ROOTF	STRAIN RATE	DRAG REDUCTION
(MV)	(VOLTS)	(M/SEC)	(M**3/SEC)	(PASCALS)	(M/SEC)					(1/SEC)	(PERCENT)
.0220	0.035	0.156	.0000313	20.4	0.011	2557.5	0.0380	498.3	5.13	118.8	13.21
.0420	0.070	0.218	.0000437	41.0	0.015	3573.8	0.0390	705.9	5.06	238.3	3.37
.0590	0.096	0.260	.0000522	56.3	0.018	4260.9	0.0377	827.0	5.15	327.1	2.67
.0846	0.131	0.314	.0000628	76.9	0.021	5134.3	0.0354	966.4	5.31	446.7	4.29
.1390	0.190	0.402	.0000804	111.6	0.025	6571.2	0.0314	1164.1	5.64	648.2	10.05
.0320	0.056	0.190	.0000380	32.8	0.014	3104.7	0.0413	631.1	4.92	190.5	1.04
.0460	0.077	0.229	.0000459	45.2	0.016	3746.0	0.0391	740.4	5.06	262.2	2.13
.0660	0.105	0.276	.0000553	61.6	0.019	4515.3	0.0367	865.0	5.22	357.8	3.86
.0860	0.131	0.316	.0000634	76.9	0.021	5178.1	0.0348	966.4	5.36	446.7	5.71
.1060	0.155	0.352	.0000705	91.0	0.023	5756.4	0.0334	1051.3	5.48	528.6	7.39
.1330	0.184	0.393	.0000787	108.1	0.025	6431.1	0.0317	1145.6	5.61	627.7	9.53
.1580	0.210	0.427	.0000856	123.4	0.026	6995.6	0.0306	1223.9	5.72	716.5	10.95
.1910	0.246	0.469	.0000939	144.6	0.029	7674.7	0.0298	1324.8	5.79	839.5	11.37
.1890	0.245	0.467	.0000935	144.0	0.029	7635.3	0.0300	1322.1	5.78	836.0	10.92
.2110	0.268	0.492	.0000986	157.5	0.030	8057.2	0.0295	1382.8	5.83	914.6	11.36
.2510	0.306	0.536	.0001073	179.9	0.032	8770.2	0.0284	1477.7	5.94	1044.4	12.82
.2900	0.346	0.575	.0001152	203.4	0.034	9411.3	0.0279	1571.4	5.99	1181.0	12.93
.3270	0.383	0.610	.0001222	225.1	0.036	9979.8	0.0274	1653.3	6.04	1307.4	13.07
.3710	0.421	0.649	.0001299	247.5	0.037	10614.6	0.0267	1735.5	6.12	1437.2	14.27
.4330	0.471	0.699	.0001401	276.9	0.040	11446.8	0.0257	1816.6	6.24	1608.0	16.02

.4850	0.520	0.739	.0001481	305.7	0.042	12098 8	0.0254	1926.6	6.28	1775.3	15.85
.1210	0.173	0.375	.0000752	101.6	0.024	6140.8	0.0327	1110.8	5.53	590.1	7.74
.2290	0.288	0.512	.0001026	169.3	0.031	8385.9	0.0292	1433.5	5.85	982.9	11.21
.2900	0.347	0.575	.0001152	204 0	0.034	9411.3	0.0280	1573.7	5.98	1184.4	12.67
.3860	0.434	0.661	.0001325	255.1	0.038	10822.0	0.0264	1760.0	6.15	1481.6	14.58

20 PPM SEPARAN AP-30, 1% MASTER SOLUTION, 10 RPS : 11/11/82
UPSTREAM PRESSURE TAPS

PROGRAM PARAMETERS : D = 0.015920 METERS
L = 0.71 METERS
TEMP = 21.20 DEGREES CENTIGRADE

RHO = 997.94 KG PER CUBIC METER
NU = 0.00000098 SQUARE METERS PER SEC

INPUT DATA

OUTPUT

VELOCITY	PRESSURE DROP	VELOCITY	FLOW RATE	PRESSURE DROP	FRICTION VELOCITY	REYNOLDS NUMBER	FRICTION FACTOR	R*ROOTF	1/ROOTF	STRAIN RATE	DRAG REDUCTION
(MV)	(VOLTS)	(M/SEC)	(M**3/SEC)	(PASCALS)	(M/SEC)					(1/SEC)	(PERCENT)
.0220	0.033	0.157	.0000313	19.3	0.010	2565.6	0.0352	481.5	5.33	111.6	18.13
.0420	0.073	0.220	.0000437	41.9	0.015	3585.0	0.0392	709.8	5.05	242.5	1.82
.0590	0.010	0.262	.0000522	6.3	0.006	4274.2	0.0041	274.9	15.55	36.4	89.23
.0846	0.135	0.316	.0000628	76.9	0.021	5150.4	0.0349	961.9	5.35	445.3	5.25
.1390	0.201	0.404	.0000804	114.2	0.025	6591.9	0.0316	1172.1	5.62	661.2	9.23
.0320	0.057	0.191	.0000380	32.8	0.014	3114.4	0.0407	628.5	4.96	190.1	1.16
.0460	0.080	0.230	.0000457	45.8	0.016	3757.8	0.0390	742.5	5.06	265.4	1.16
.0660	0.110	0.278	.0000553	62.8	0.019	4529.5	0.0368	869.1	5.21	363.5	2.83
.0860	0.135	0.318	.0000634	76.9	0.021	5194.4	0.0343	961.9	5.40	445.3	6.67
.1060	0.160	0.354	.0000705	91.1	0.023	5774.5	0.0328	1046.5	5.52	527.1	8.47
.1330	0.192	0.395	.0000787	109.1	0.025	6451.3	0.0315	1145.7	5.63	631.8	9.89
.1580	0.219	0.430	.0000856	124.4	0.027	7017.6	0.0304	1223.2	5.74	720.1	11.55
.1910	0.256	0.472	.0000939	145.3	0.029	7698.8	0.0295	1322.0	5.82	841.2	12.36
.1890	0.255	0.469	.0000935	144.7	0.029	7659.3	0.0297	1319.4	5.81	837.9	11.90
.2110	0.282	0.495	.0000986	160.0	0.030	8082.5	0.0295	1387.2	5.83	926.2	11.48
.2510	0.322	0.539	.0001073	192.6	0.032	8797.8	0.0284	1482.0	5.94	1057.1	13.10
.2900	0.365	0.579	.0001152	206.9	0.034	9440.9	0.0279	1577.5	5.98	1197.7	13.13
.3270	0.405	0.614	.0001222	229.5	0.036	10011.1	0.0275	1661.5	6.03	1328.6	13.17
.3710	0.451	0.653	.0001299	255.5	0.038	10647.9	0.0271	1753.0	6.07	1479.1	13.37
.4330	0.507	0.704	.0001401	287.2	0.040	11492.7	0.0262	1858.4	6.18	1662.3	14.85

4850	0.564	0.744	.0001481	319.4	0.042	12136.8	0.0261	1959.9	6.19	1848.8	14.17
.1210	0.180	0.378	.0000752	102.4	0.024	6160.1	0.0324	1109.5	5.55	592.5	8.27
.2290	0.301	0.516	.0001026	170.7	0.031	8412.3	0.0290	1433.0	5.87	988.4	12.02
.2900	0.365	0.579	.0001152	206.9	0.034	9440.9	0.0279	1577.5	5.98	1197.7	13.13
.3860	0.463	0.665	.0001325	262.3	0.038	10856.0	0.0268	1776.2	6.11	1518.4	14.07

10 PPM, SEPARAN AP-30, 1% MASTER SOLUTION, 10 RPS : 11/18/82
DOWNSTREAM PRESSURE TAPS

PROGRAM PARAMETERS : D = 0.015970 METERS
L = 0.71 METERS
TEMP = 21.30 DEGREES CENTIGRADE

RHO = 997.91 KG PER CUBIC METER
NU = 0.00000097 SQUARE METERS PER SEC

INPUT DATA

OUTPUT

VELOCITY	PRESSURE DROP	VELOCITY	FLOW RATE	PRESSURE DROP	FRICTION VELOCITY	REYNOLDS NUMBER	FRICTION FACTOR	R*ROOTF	1/ROOTF	STRAIN RATE	DRAG REDUCTION
(MV)	(VOLTS)	(M/SEC)	(M**3/SEC)	(PASCALS)	(M/SEC)					(1/SEC)	(PERCENT)
.0270	0.047	0.174	.0000348	27.1	0.012	2850.2	0.0407	575.0	4.96	157.8	4.49
.0480	0.083	0.234	.0000469	48.0	0.016	3838.6	0.0397	765.0	5.02	279.2	-0.07
.0590	0.100	0.260	.0000522	57.8	0.018	4271.0	0.0387	839.8	5.09	336.5	0.04
.0850	0.135	0.314	.0000630	78.1	0.021	5159.2	0.0358	976.1	5.29	454.6	3.18
.0990	0.155	0.340	.0000681	89.7	0.023	5580.8	0.0351	1046.0	5.34	522.1	3.17
.1244	0.187	0.380	.0000762	108.2	0.025	6239.4	0.0339	1149.1	5.43	630.0	3.99
.1584	0.229	0.428	.0000857	132.6	0.027	7021.0	0.0328	1271.8	5.52	771.7	4.46
.0200	0.035	0.149	.0000298	20.1	0.011	2440.3	0.0413	495.8	4.92	117.3	6.68
.0340	0.060	0.196	.0000372	34.6	0.014	3211.3	0.0410	650.0	4.94	201.6	1.07
.0650	0.108	0.274	.0000548	62.5	0.019	4490.5	0.0378	872.9	5.14	363.5	1.15
.0720	0.118	0.289	.0000578	69.2	0.020	4734.6	0.0371	912.5	5.19	397.3	1.58
.1070	0.164	0.353	.0000700	94.9	0.023	5796.7	0.0345	1076.0	5.39	552.4	4.17
.1410	0.204	0.404	.0000810	118.1	0.026	6633.1	0.0327	1200.3	5.53	687.4	5.95
.1760	0.249	0.451	.0000903	144.2	0.029	7391.8	0.0322	1324.2	5.57	839.2	5.11
.1370	0.201	0.399	.0000797	116.3	0.026	6540.5	0.0332	11?.?	5.49	677.3	5.01
.1865	0.261	0.464	.0000929	151.1	0.029	7604.0	0.0319	1357.8	5.60	879.7	5.37
.2310	0.308	0.515	.0001031	178.4	0.032	8441.8	0.0305	1475.1	5.72	1038.2	7.08
.2760	0.358	0.561	.0001124	207.3	0.034	9208.5	0.0298	1570.4	5.79	1206.9	7.32
.3295	0.418	0.612	.0001226	242.1	0.037	10041.0	0.0293	1718.6	5.84	1407.3	7.07
.3880	0.479	0.663	.0001328	277.4	0.040	10875.4	0.0286	1839.8	5.91	1615.0	7.46

.3900	0.474	0.665	.0001331	274.6	0.039	10902.7	0.0282	1630.2	5.96	1598.2	8.84
.4620	0.306	0.722	.0001446	315.3	0.042	11843.3	0.0274	1761.3	6.04	1835.4	9.50
.5780	0.366	0.805	.0001613	377.5	0.046	13212.7	0.0264	2146.0	6.16	2197.3	10.64
.5170	0.331	0.763	.0001528	341.2	0.044	12512.2	0.0266	2040.3	6.13	1986.2	11.09

10 PPM, SEPARAN AP-30, 1% MASTER SOLUTION, 10 RPS : 11/18/82

UPSTREAM PRESSURE TAPS

PROGRAM PARAMETERS : D = 0.015920 METERS
L = 0.71 METERS
TEMP = 21.30 DEGREES CENTIGRADE

RHO = 997.91 KG PER CUBIC METER
NU = 0.00000097 SQUARE METERS PER SEC

INPUT DATA

OUTPUT

VELOCITY	PRESSURE DROP	VELOCITY	FLOW RATE	PRESSURE DROP	FRICTION VELOCITY	REYNOLDS NUMBER	FRICTION FACTOR	R*ROOTF	1/ROOTF	STRAIN RATE	DRAG REDUCTION
(MV)	(VOLTS)	(M/SEC)	(M**3/SEC)	(PASCALS)	(M/SEC)					(1/SEC)	(PERCENT)
.0270	0.049	0.175	.0000348	27.8	0.013	2859.2	0.0411	579.6	4.93	161.3	2.14
.0480	0.085	0.235	.0000469	47.8	0.016	3850.6	0.0389	759.8	5.07	277.2	0.90
.0590	0.104	0.262	.0000522	58.3	0.018	4284.5	0.0384	839.5	5.10	338.4	-0.07
.0850	0.142	0.316	.0000630	79.4	0.021	5175.4	0.0358	979.5	5.28	460.7	2.59
.0990	0.162	0.342	.0000681	90.5	0.023	5598.3	0.0349	1045.7	5.35	525.1	3.43
.1244	0.196	0.383	.0000762	109.3	0.025	6259.0	0.0337	1149.6	5.44	634.5	4.28
.1584	0.239	0.431	.0000857	133.2	0.027	7043.1	0.0325	1268.8	5.55	772.9	5.45
.0200	0.035	0.150	.0000298	20.0	0.011	2448.0	0.0404	492.0	4.98	116.2	7.08
.0340	0.063	0.197	.0000392	35.6	0.014	3221.4	0.0414	635.6	4.91	206.4	-1.30
.0650	0.113	0.275	.0000548	63.3	0.019	4504.6	0.0377	874.7	5.15	367.3	0.61
.0720	0.123	0.290	.0000578	68.8	0.020	4749.4	0.0369	912.2	5.21	399.5	1.60
.1070	0.173	0.356	.0000708	96.6	0.023	5814.9	0.0345	1080.4	5.38	560.5	3.64
.1410	0.217	0.407	.0000810	121.0	0.026	6653.9	0.0330	1209.2	5.50	702.1	4.99
.1760	0.262	0.453	.0000903	146.0	0.029	7415.0	0.0330	1328.1	5.58	847.0	5.44
.1370	0.212	0.401	.0000799	118.2	0.026	6561.0	0.0332	1195.3	5.49	686.0	4.02
.1865	0.277	0.466	.0000929	154.3	0.030	7627.9	0.0320	1365.5	5.59	895.2	4.95
.2310	0.327	0.518	.0001031	182.0	0.032	8468.3	0.0307	1483.2	5.71	1056.2	6.86
.2760	0.381	0.565	.0001124	212.0	0.035	9237.5	0.0300	1600.6	5.77	1230.0	7.05
.3295	0.447	0.616	.0001226	248.6	0.037	10072.5	0.0296	1733.3	5.81	1442.5	6.53
.3880	0.512	0.667	.0001328	284.6	0.040	10909.5	0.0289	1854.7	5.88	1651.7	7.12

.3900	0.510	0.669	.0001331	283.5	0.040	10937.0	0.0286	1851.1	5.91	1645.3	7.89
.4620	0.326	0.727	.0001446	321.6	0.043	11880.5	0.0275	19'1.5	6.03	1866.2	9.80
.5780	0.400	0.811	.0001613	394.8	0.047	13254.2	0.0272	21'.5	6.07	2291.2	8.82
5170	0.356	0.768	.0001528	351.3	0.045	12551.5	0.0269	2060.5	6.09	2038.5	10.63

5 PPM SEPARAN AP-30, 1% MASTER SOLUTION, 10 RPS : 11/12/82
DOWNSTREAM PRESSURE TAPS

PROGRAM PARAMETERS : D = 0.015970 METERS
L = 0.71 METERS
TEMP = 21.30 DEGREES CENTIGRADE

RHO = 997.91 KG PER CUBIC METER
NU = 0.00000077 SQUARE METERS PER SEC

INPUT DATA

OUTPUT

VELOCITY	PRESSURE DROP	VELOCITY	FLOW RATE	PRESSURE DROP	FRICTION VELOCITY	REYNOLDS NUMBER	FRICTION FACTOR	R*ROOTF	1/ROOTF	STRAIN RATE	DRAG REDUCTION
(MV)	(VOLTS)	(M/SEC)	(M**3/SEC)	(PASCALS)	(M/SEC)					(1/SEC)	(PERCENT)
.1870	0.267	0.464	.0000930	157.2	0.030	7613.9	0.0331	1385.0	5.50	915.2	1.77
.2400	0.329	0.524	.0001050	193.8	0.033	8600.9	0.0320	1537.5	5.59	1127.9	2.32
.3280	0.430	0.611	.0001223	253.3	0.038	10018.6	0.0308	1757.9	5.70	1474.4	2.39
.0830	0.135	0.311	.0000622	79.4	0.021	5096.0	0.0373	984.4	5.18	462.3	-0.62
.1590	0.232	0.429	.0000857	136.6	0.028	7034.0	0.0337	1290.9	5.45	795.1	1.88
.2030	0.287	0.483	.0000968	169.0	0.031	7925.5	0.0328	1435.9	5.52	983.8	1.61
.2550	0.350	0.540	.0001082	206.1	0.034	8859.4	0.0320	1585.8	5.59	1199.9	1.36
.2980	0.400	0.583	.0001167	235.6	0.037	9560.0	0.0315	1695.4	5.64	1371.5	1.40
.3450	0.451	0.626	.0001254	265.7	0.039	10269.0	0.0307	1800.3	5.70	1546.4	1.98
.3830	0.490	0.659	.0001320	288.6	0.040	10806.7	0.0302	1876.6	5.76	1680.2	2.65
.2240	0.177	0.507	.0001015	184.7	0.032	8315.9	0.0326	1501.1	5.54	1075.1	1.20
.3030	0.229	0.588	.0001177	239.5	0.037	9638.1	0.0315	1709.4	5.64	1394.2	1.19
.3830	0.279	0.659	.0001320	292.2	0.041	10806.7	0.0305	1888.1	5.72	1700.9	1.45
.4300	0.307	0.697	.0001396	321.7	0.043	11435.3	0.0300	1981.1	5.77	1872.7	1.78
.5020	0.347	0.752	.0001506	363.9	0.045	12333.6	0.0292	2106.9	5.85	2118.1	2.76
.5720	0.387	0.801	.0001605	406.0	0.048	13145.6	0.0287	2225.7	5.91	2363.5	3.01

5 PPM SEPARAN AP-30, 1% MASTER SOLUTION, 10 RPS : 11/12/82

UPSTREAM PRESSURE TAPS

PROGRAM PARAMETERS : D = 0.015920 METERS
L = 0.71 METERS
TEMP = 21.30 DEGREES CENTIGRADE

RHO = 997.91 KG PER CUBIC METER
NU = 0.00000097 SQUARE METERS PER SEC

INPUT DATA

OUTPUT

VELOCITY	PRESSURE DROP	VELOCITY	FLOW RATE	PRESSURE DROP	FRICTION VELOCITY	REYNOLDS NUMBER	FRICTION FACTOR	R*ROOTF	1/ROOTF	STRAIN RATE	DRAG REDUCTION
(MV)	(VOLTS)	(M/SEC)	(M**3/SEC)	(PASCALS)	(M/SEC)					(1/SEC)	(PERCENT)
.1870	0.280	0.467	.0000930	159.8	0.030	7637.9	0.0331	1389 8	5.50	927.4	1.76
.2400	0.348	0.528	.0001050	198.5	0.033	8627.9	0.0322	1548 8	5.57	1151.7	1.75
.3280	0.458	0.615	.0001223	261.0	0.038	10050.1	0.0312	1776 1	5.66	1514.6	1.46
.0830	0.140	0.313	.0000622	80.2	0.021	5112.0	0.0371	744 7	5.19	465.5	-0.62
.1590	0.245	0.431	.0000859	137.9	0.028	7056.1	0.0340	1300 4	5.43	811.9	1.00
.2030	0.301	0.486	.0000968	171.8	0.031	7950.4	0.0328	1440 7	5.52	996.7	1.58
.2550	0.369	0.543	.0001082	210.4	0.034	8887.2	0.0322	1594 7	5.57	1221.0	1.17
.2980	0.425	0.586	.0001167	242.2	0.037	9590.1	0.0318	1711 1	5.60	1405.7	0.61
.3450	0.480	0.630	.0001254	273.5	0.039	10301.2	0.0312	1818 1	5.67	1587.2	1.17
.3830	0.523	0.663	.0001320	298.0	0.041	10840.6	0.0306	1897 6	5.71	1729.0	1.67
.2240	0.184	0.510	.0001015	185.6	0.032	8342.0	0.0322	1497 5	5.57	1076 8	2.48
.3030	0.242	0.591	.0001177	244.4	0.037	9668.3	0.0316	1718 6	5.63	1418.1	1.17
.3830	0.292	0.663	.0001320	295.1	0.041	10840.6	0.0303	1888 5	5.74	1712.4	2.61
.4300	0.325	0.701	.0001376	320.6	0.043	11471.2	0.0302	1992 7	5.76	1906.7	1.92
.5020	0.372	0.757	.0001506	376.2	0.046	12372.3	0.0297	2132 4	5.80	2183.3	1.81
.5720	0.419	0.806	.0001605	423.9	0.047	13186.9	0.0295	2263 5	5.83	2457.9	1.21

30 PPM POLYOX WSR-301, 1% MASTER SOLUTION, 10 RPS : 12/13/82
DOWNSTREAM PRESSURE TAPS

PROGRAM PARAMETERS : D = 0.015970 METERS
L = 0.71 METERS
TEMP = 21.10 DEGREES CENTIGRADE

RHO = 997.96 KG PER CUBIC METER
NU = 0.00000098 SQUARE METERS PER SEC

INPUT DATA   OUTPUT

VELOCITY	PRESSURE DROP	VELOCITY	FLOW RATE	PRESSURE DROP	FRICTION VELOCITY	REYNOLDS NUMBER	FRICTION FACTOR	R*ROOTF	1/ROOTF	STRAIN RATE	DRAG REDUCTION
(MV)	(VOLTS)	(M/SEC)	(M**3/SEC)	(PASCALS)	(M/SEC)					(1/SEC)	(PERCENT)
.0290	0.054	0.180	.0000361	31.1	0.013	2943.4	0.0434	613.3	4.80	180.3	-2.66
.0170	0.022	0.137	.0000274	12.6	0.008	2232.8	0.0305	390.2	5.72	73.0	32.40
.0220	0.039	0.156	.0000313	22.4	0.011	2551.4	0.0417	520.8	4.90	130.0	4.80
.0370	0.067	0.205	.0000410	38.7	0.015	3338.9	0.0419	683.4	4.89	223.9	-2.11
.0814	0.135	0.308	.0000616	78.0	0.021	5020.8	0.0374	971.0	5.17	452.0	-0.49
.1080	0.167	0.355	.0000711	96.6	0.023	5795.3	0.0347	1080.1	5.37	559.3	3.40
.1440	0.208	0.409	.0000818	120.3	0.026	6669.6	0.0327	1205.6	5.53	696.8	6.03
.1860	0.254	0.463	.0000927	146.9	0.027	7557.8	0.0311	1332.4	5.67	851.1	7.90
.0750	0.125	0.295	.0000590	72.2	0.020	4812.6	0.0377	934.2	5.15	418.5	-0.24
.1130	0.174	0.363	.0000727	100.6	0.024	5924.8	0.0346	1102.5	5.37	582.8	3.19
.1600	0.228	0.430	.0000862	131.9	0.027	7021.8	0.0323	1262.3	5.56	763.9	5.90
.2250	0.295	0.508	.0001018	170.7	0.031	8294.2	0.0300	1436.0	5.78	988.6	9.17
.2860	0.354	0.571	.0001144	204.8	0.034	9325.3	0.0285	1573.1	5.93	1186.5	11.31
.3370	0.404	0.619	.0001240	233.8	0.036	10103.5	0.0277	1680.6	6.01	1354.2	12.10
.3980	0.459	0.671	.0001345	265.6	0.039	10958.8	0.0267	1791.4	6.12	1538.6	13.44

30 PPM POLYOX WSR-301, 1% MASTER SOLUTION, 10 RP3 : 12/13/82
UPSTREAM PRESSURE TAPS

PROGRAM PARAMETERS : D = 0.015920 METERS
L = 0.71 METERS
TEMP = 21.10 DEGREES CENTIGRADE

RHO = 997.96 KG PER CUBIC METER
NU = 0.00000098 SQUARE METERS PER SEC

INPUT DATA

OUTPUT

VELOCITY	PRESSURE DROP	VELOCITY	FLOW RATE	PRESSURE DROP	FRICTION VELOCITY	REYNOLDS NUMBER	FRICTION FACTOR	R*ROOTF	1/ROOTF	STRAIN RATE	DRAG REDUCTION
(MV)	(VOLTS)	(M/SEC)	(M**3/SEC)	(PASCALS)	(M/SEC)					(1/SEC)	(PERCENT)
.0290	0.055	0.181	.0000361	30.9	0.013	2952.7	0.0424	607.8	4.86	178.2	-1 61
.0170	0.022	0.138	.0000274	12.7	0.008	2239.8	0.0303	390.1	5.74	73.4	31 63
.0220	0.036	0.157	.0000313	20.4	0.011	2559.4	0.0373	494.3	5.18	117.9	13 37
.0370	0.069	0.206	.0000410	38.6	0.015	3349.4	0.0411	679.4	4.93	222.7	-1 49
.0614	0.141	0.309	.0000616	78.2	0.021	5036.6	0.0369	967.2	5.21	451.3	0 32
.1080	0.176	0.357	.0000711	97.4	0.023	5813.5	0.0345	1079.7	5.38	562.5	3 72
.1440	0.220	0.411	.0000818	121.6	0.026	6690.6	0.0325	1206.4	5.55	702.2	6 34
.1860	0.268	0.466	.0000927	148.0	0.029	7581.5	0.0308	1331.0	5.70	854.6	8 71
.0750	0.131	0.297	.0000570	72.7	0.020	4827.7	0.0373	932.5	5.18	419.6	0 10
.1130	0.184	0.365	.0000727	101.8	0.024	5943.4	0.0345	103.9	5.38	587.9	3 24
.1600	0.240	0.433	.0000862	132.6	0.027	7043.9	0.0320	15? 8	5.59	765.7	6 79
.2250	0.315	0.511	.0001018	173.8	0.031	8320.2	0.0301	1442.5	5.77	1003.9	9 09
.2860	0.377	0.575	.0001144	207.9	0.034	9354.6	0.0284	1577.6	5.93	1200.8	11 69
.3370	0.431	0.623	.0001240	237.6	0.037	10135.2	0.0277	1686.5	6.01	1372.3	12 47
.3980	0.497	0.675	.0001345	273.9	0.039	10993.2	0.0271	1810.8	6.07	1581.9	12 66

20 PPM POLYOX WSR-301, 1% MASTER SOLUTION, 10 RPS : 12/15/82
DOWNSTREAM PRESSURE TAPS

PROGRAM PARAMETERS : D = 0.015970 METERS
L = 0.71 METERS
TEMP = 20.70 DEGREES CENTIGRADE

RHD = 798.05 KG PER CUBIC METER
NU = 0.00000099 SQUARE METERS PER SEC

INPUT DATA

OUTPUT

VELOCITY	PRESSURE DROP	VELOCITY	FLOW RATE	PRESSURE DROP	FRICTION VELOCITY	REYNOLDS NUMBER	FRICTION FACTOR	R*ROOTF	1/ROOTF	STRAIN RATE	DRAG REDUCTION
(MV)	(VOLTS)	(M/SEC)	(M**3/SEC)	(PASCALS)	(M/SEC)					(1/SEC)	(PERCENT)
.0210	0.036	0.153	.0000306	20.9	0.011	2466.9	0.0407	497.8	4.96	120.0	7.68
.0290	0.052	0.180	.0000361	30.3	0.013	2915.3	0.0422	598.9	4.87	173.7	0.42
.0338	0.061	0.195	.0000371	35.5	0.014	3155.7	0.0423	648.9	4.86	203.8	-1.67
.0500	0.086	0.239	.0000479	50.2	0.017	3864.4	0.0398	770.9	5.01	287.7	-0.45
.1010	0.162	0.344	.0000688	94.6	0.023	5555.0	0.0363	1058.8	5.25	542.7	-0.01
.1100	0.174	0.358	.0000717	101.6	0.024	5791.5	0.0359	1097.3	5.28	582.9	0.10
.1260	0.194	0.383	.0000767	113.3	0.025	6188.7	0.0351	1158.8	5.34	650.0	0.96
.1510	0.225	0.418	.0000838	131.4	0.027	6760.7	0.0341	1248.0	5.42	754.0	1.67
.1670	0.244	0.439	.0000880	142.5	0.028	7101.6	0.0335	1299.7	5.46	817.7	2.21
.0425	0.074	0.220	.0000440	43.1	0.016	3552.8	0.0405	715.0	4.97	247.5	-0.18
.0650	0.109	0.274	.0000540	63.6	0.019	4426.3	0.0385	868.2	5.10	364.9	-0.30
.0890	0.144	0.322	.0000645	84.1	0.022	5207.8	0.0367	998.1	5.22	482.3	0.43
.1230	0.189	0.378	.0000758	110.4	0.025	6116.3	0.0350	1143.7	5.35	633.2	1.49
.1720	0.249	0.446	.0000893	145.5	0.029	7204.7	0.0332	1313.0	5.49	834.5	2.70
.2010	0.283	0.481	.0000963	165.4	0.031	7774.4	0.0324	1399.8	5.55	948.6	3.27
.2415	0.325	0.526	.0001054	189.9	0.033	8503.7	0.0311	1500.2	5.67	1089.5	5.13
.2760	0.363	0.561	.0001125	212.1	0.035	9076.9	0.0305	1585.5	5.72	1216.9	5.52
.3150	0.405	0.599	.0001177	236.7	0.037	9682.2	0.0299	1674.8	5.78	1357.8	5.91
.3610	0.453	0.640	.0001232	264.8	0.037	10348.7	0.0293	1771.3	5.84	1518.8	6.39

20 PPM POLYOX WSR-301, 1% MASTER SOLUTION, 10 RPS : 12/15/82
UPSTREAM PRESSURE TAPS

PROGRAM PARAMETERS :   D = 0.015920 METERS
L = 0.71 METERS
TEMP = 20.70 DEGREES CENTIGRADE

RHO = 998.05 KG PER CUBIC METER
NU = 0.00000099 SQUARE METERS PER SEC

INPUT DATA

OUTPUT

VELOCITY	PRESSURE DROP	VELOCITY	FLOW RATE	PRESSURE DROP	FRICTION VELOCITY	REYNOLDS NUMBER	FRICTION FACTOR	R*ROOTF	1/ROOTF	STRAIN RATE	DRAG REDUCTION
(MV)	(VOLTS)	(M/SEC)	(M**3/SEC)	(PASCALS)	(M/SEC)					(1/SEC)	(PERCENT)
.0210	0.037	0.154	.0000306	21.0	0.011	2474.6	0.0402	496.1	4.99	119.9	7.36
.0290	0.053	0.181	.0000361	29.8	0.013	2924.4	0.0409	591.1	4.95	170.2	2.23
.0338	0.063	0.196	.0000391	35.3	0.014	3165.6	0.0413	643.4	4.92	201.7	-0.63
.0500	0.092	0.241	.0000479	51.2	0.017	3876.6	0.0400	775.4	5.00	292.9	-1.98
.1010	0.172	0.346	.0000688	95.2	0.023	5572.4	0.0360	1057.2	5.27	544.5	0.48
.1100	0.186	0.360	.0000717	102.9	0.024	5809.7	0.0358	1099.1	5.29	588.5	0.11
.1260	0.208	0.385	.0000767	115.0	0.025	6208.1	0.0350	1162.0	5.34	657.7	0.77
.1510	0.240	0.421	.0000838	132.6	0.027	6782.0	0.0338	1247.7	5.44	758.4	2.21
.1670	0.261	0.442	.0000880	144.2	0.029	7124.0	0.0333	1300.9	5.48	824.4	2.59
.0425	0.079	0.221	.0000440	44.1	0.016	3563.9	0.0407	719.2	4.96	252.0	-1.87
.0650	0.117	0.275	.0000548	65.0	0.019	4440.2	0.0387	873.3	5.08	371.5	-1.64
.0890	0.153	0.324	.0000645	84.8	0.022	5224.2	0.0365	997.5	5.24	484.7	0.64
.1230	0.202	0.381	.0000758	111.7	0.025	6135.5	0.0348	1145.2	5.36	638.8	1.50
.1720	0.267	0.448	.0000893	147.5	0.029	7227.4	0.0331	1315.7	5.49	843.3	2.88
.2010	0.302	0.484	.0000963	166.7	0.031	7798.9	0.0322	1399.0	5.57	953.4	4.08
.2415	0.350	0.529	.0001054	193.1	0.033	8530.4	0.0312	1505.7	5.67	1104.3	5.25
.2760	0.390	0.565	.0001125	215.1	0.035	9105.4	0.0305	1589.1	5.73	1230.2	6.00
.3150	0.439	0.603	.0001199	242.1	0.037	9712.6	0.0301	1685.7	5.76	1384.3	5.68
.3610	0.492	0.644	.0001282	271.2	0.039	10381.2	0.0295	1784.3	5.82	1551.0	6.11

APPENDIX E
PIPE FLOW MEASUREMENTS AT VARIOUS
CONCENTRATIONS FOR CONSTANT REYNOLDS NUMBER FLOWS

This appendix contains listings of the pipe flow
measurements made at various concentrations for constant
Reynolds number flows. The measurements for each
experimental run consist of the pressure drop recorded
over the downstream measuring section for water flow, and
the changes in pressure drop from this value as a
function of additive concentration. All pressure
measurements are listed as chart recorder readings in
millivolts, with decreases in pressure drop being
recorded as positive values.

During each experiment, the flow has been maintained
at a constant flow rate. Since the shear viscosities of
the test solutions do not vary very much with
concentration (cf. Chapter IV), these experiments have
been labeled as being conducted at constant Reynolds
number flows.

Additive   : Separan AP-30

Flow rate   : 92 cm^3/s

Mixing speed   : 10 rps

Master solution
 concentration   : 1%

Temperature   : 21 ^{O}C

Pressure drop,
 water flow   : 252 mv

Concentration	Decrease in pressure drop from water flow
(ppm)	(mv)
12.8	20.5
26.3	38.5
10.5	16.0
6.0	6.3
8.2	11.5
45.2	46.0
65.4	45.4

Additive   : Polyox WSR-301

Flow rate   : 161 cm^3/s

Mixing speed   : 10 rps

Master solution
 concentration   : 1%

Temperature   : 19 ^{o}C

Pressure drop,
 water flow   : 396 mv

Concentration	Decrease in pressure drop from water flow
(ppm)	(mv)
8.3	7.3
6.3	-1.1
5.2	-2.3
3.3	-3.3
14.9	43.2
23.4	80.8
40.5	140.2
62.1	175.5
84.7	204.0
2.6	-2.6
3.2	-3.8
5.2	-2.8
6.3	-1.0
8.3	8.3

Additive   : Polyox WSR-301
Flow rate   : 161 cm^3/s
Mixing speed   : 30 rps
Master solution
 concentration   : 1%
Temperature   : 19 $^{\circ}$C
Pressure drop,
 water flow   : 396 mv

Concentration	Decrease in pressure drop from water flow
(ppm)	(mv)
14.9	3.2
11.4	-3.9
2.6	-2.5
3.2	-4.5
5.2	-5.3
11.4	-3.3
8.3	-5.6
14.9	3.3
23.4	18.4
40.5	55.0

Additive   : Polyox WSR-301

Flow rate   : 92 cm^3/s

Mixing speed   : 10 rps

Master solution
 concentration : 1%

Temperature   : 21 ^{O}C

Pressure drop,
 water flow   : 247 mv

Concentration	Decrease in pressure drop from water flow
(ppm)	(mv)
23.5	55.0
9.2	16.0
14.0	38.0

Additive   : Separan AP-273

Flow rate   : 162 cm^3/s

Mixing speed   : 10 rps

Master solution
 concentration   : 0.056%

Temperature   : 19 ^oC

Pressure drop,
 water flow   : 398 mv

Concentration	Decrease in pressure drop from water flow
(ppm)	(mv)
.82	.65
1.73	1.95
2.25	3.25
2.91	5.00
3.24	6.90
.44	.30
.66	.45
.82	.60
1.27	1.10
2.25	3.80

Additive	: Separan AP-273
Flow rate	: 161 cm^3/s
Mixing speed	: 10 rps
Master solution concentration	: 1%
Temperature	: 19 ^{O}C
Pressure drop, water flow	: 398 mv

Concentration	Decrease in pressure drop from water flow
(ppm)	(mv)
3.1	20.5
4.4	39.5
6.2	59.4
8.0	81.0
14.5	135.0
22.0	166.0
30.1	212.5
57.0	245.0

Additive	:	Separan AP-273
Flow rate	:	95 cm^3/s
Mixing speed	:	10 rps
Master solution concentration	:	0.2%
Temperature	:	21 ^{o}C
Pressure drop, water flow	:	260 mv

Concentration	Decrease in pressure drop from water flow
(ppm)	(mv)
.63	3.4
1.06	8.0
1.27	10.8
.42	1.6
1.06	8.0
1.46	13.2
.42	1.7
..68	3.5
.21	.6

Additive	: Separan AP-273
Flow rate	: 92 cm^3/s
Mixing speed	: 10 rps
Master solution concentration	: 0.2%
Temperature	: 21 $^{\circ}$C
Pressure drop, water flow	: 254 mv

Concentration	Decrease in pressure drop from water flow
(ppm)	(mv)
6.4	60.0
9.1	72.0
19.4	103.0
14.0	90.0
23.3	110.0
2.9	31.9
2.2	22.0

HEAD-DISCHARGE RELATIONSHIP FOR CONICAL CHANNEL FLOW
AS DETERMINED FROM THE BOUNDARY LAYER SOLUTION FOR
INCOMPRESSIBLE AXISYMMETRIC FLUID FLOW

For steady, incompressible, axisymmetric flow of a
Newtonian liquid, the boundary layer equations may be
written as

$$u\frac{\partial u}{\partial r} + w\frac{\partial u}{\partial z} = U\frac{dU}{dr} + \nu\frac{\partial^2 u}{\partial z^2} \qquad (F.1)$$

$$\frac{\partial}{\partial r}(Ru) + \frac{\partial}{\partial z}(Rw) = 0 \qquad (F.2)$$

where u is the velocity component in the r direction, w
the velocity component in the z direction, ν is the
kinematic shear viscosity,
and U is the main-stream
velocity, which is
$U=-m/r^2$ (m>0) for the
present situation. A
coordinate definition
sketch is provided in Fig.
F.1. According to
Rosenhead (1963),
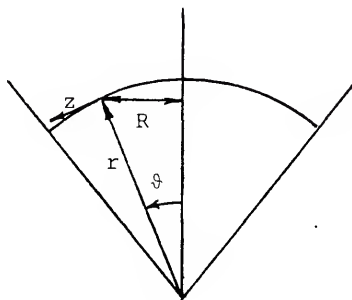
Fig. F.1. Coordinate Geometry

357

eq. (F.2) is satisfied identically by writing

$$u = Uf'(\eta)$$

$$(F.3)$$

$$w = (\frac{m\upsilon}{2r^3})^{1/2}\{f-3\eta f'\}$$

where $\qquad \eta = z(m/2\upsilon r^3)^{1/2}$

and eq. (F.1) is also satisfied provided

$$f'''-ff''+4(1-f'^2) = 0 \qquad (F.4)$$

with the boundary conditions being

$$f=f'=0 \text{ on } \eta=0$$

and $\qquad f' \to 1 \text{ as } \eta \to \infty$

The solution to eq. (F.4) is tabulated in Rosenhead (1963) as values of f' as a function of η.

To obtain the head-discharge relationship associated with this boundary layer solution, the velocity component u may be integrated across a flow section, r=constant, as

$$Q = \int_0^\Theta \int_0^{2\pi} Uf'(\eta)r^2\sin\vartheta \, d\varphi d\vartheta$$

$$= 2\pi m \int_0^\Theta [-1+(1-f'(\eta)]\sin\vartheta \, d\vartheta \qquad (F.5)$$

and after separating the integral in this equation into two terms, integrating the first and expressing the second in terms of η, one obtains

$$Q = 2\pi U r^2 (1-\cos \Theta)$$

$$- 2\pi U r^2 \left(\frac{Ur}{2\nu}\right)^{-1/2} \int [1-f'(\eta)]\sin\vartheta \, d\eta \qquad (F.6)$$

From the tabulation of $f'(\eta)$ in Rosenhead (p. 250, 1963), $f'(\eta)=1.0$ for $\eta > 3.6$, and hence, there will only be a contribution from the second term in the above equation for $0< \eta <3.6$.

The change in angle, $d\vartheta$, may be written as

$$d\vartheta = (Ur/2\nu)^{-1/2}d\eta$$

Also, $\vartheta = \Theta$ for $\eta = 0$. Thus, for sufficiently large $(Ur/2\nu)^{+1/2}$, there will be little change in ϑ across the boundary layer $(0< \eta <3.6)$, and in this region, $\sin \vartheta$ may be approximated as $\sin \Theta$. With this assumption, eq. (F.6) may be rewritten as

$$Q = 2\pi U r^2 (1-\cos \Theta)\{1-\left(\frac{Ur}{2\nu}\right)^{-1/2}\frac{\sin \Theta}{(1-\cos \Theta)} \quad [1-f'(\eta)]d\eta\} \quad (F.7)$$

The integral in this equation has been evaluated numerically using Rosenhead's values for $f'(\eta)$, and a

listing of this computation is presented in Table F.1. After substituting in this result, eq. (F.7) becomes

$$Q = 2\pi U r^2 (1-\cos\theta)\{1-0.416 \left(\frac{Ur}{2\nu}\right)^{-1/2} \frac{\sin\theta}{(1-\cos\theta)}\} \qquad (F.8)$$

The desired head-discharge relationship can then be obtained by substitution for the main-stream velocity, $U=(2gh)^{1/2}$ (according to potential flow theory).

This equation may also be expressed as

$$Q_a = Q_i \{1 - \frac{C}{R^{1/2}} \}$$

where Q_a is the actual flow rate through the conical channel, Q_i is the corresponding flow rate from potential flow theory, C is a constant, and R is a Reynolds number, which may be defined as $R=Ur/\nu$.

Table F.1. Numerical determination of $\int[1-f'(\eta)]d\eta$.

f´(η)	1-f´(η)	[1-f´(η)]	η	Δη	[1-f´(η)]Δη
.000	1.000		.0		
		.897		.1	.0897
.207	.793		.1		
		.708		.1	.0708
.377	.623		.2		
		.555		.1	.0555
.513	.487		.3		
		.434		.1	.0434
.620	.380		.4		
		.338		.1	.0338
.705	.295		.5		
		.263		.1	.0263
.770	.230		.6		
		.205		.1	.0205
.821	.179		.7		
		.160		.1	.0160
.860	.140		.8		
		.125		.1	.0125
.891	.109		.9		
		.098		.1	.0098
.914	.086		1.0		
		.070		.2	.0140
.947	.053		1.2		
		.043		.2	.0086
.967	.033		1.4		
		.027		.2	.0054
.979	.021		1.6		
		.018		.2	.0036
.986	.014		1.8		
		.012		.2	.0024
.991	.009		2.0		
		.006		.4	.0024
.996	.004		2.4		
		.003		.4	.0012
.998	.002		2.8		
		.001		.4	.0004
.999	.001		3.2		
		.000		.4	.0000
1.000	.000		3.6		

$\sum [1-f´(\eta)]\Delta\eta = .4163$

APPENDIX G
EXTENSIONAL FLOW MEASUREMENTS

This appendix contains listings of head-discharge
measurements for both water and polymer solution flows
through the conical channels.

Definitions and units of dimension of the variables
listed on the following pages are

Q   Flow rate, Q, cm^3/s

H   Pressure head measured at downstream tap,
           h, cm of water

HW   Pressure head for water flow, h_w, as
           calculated using eq. (6.1) for $r = r_t$,
           cm of water

DH   Difference in pressure heads between water
           and polymer solution flow, DH = HW - H,
           cm of water

RT   Radial distance, r_t, at downstream
           pressure tap, cm

THETA   Half angle of convergence of the conical
           channel, θ, degrees

TEMP   Temperature, $^{\circ}C$

NU   Kinematic viscosity - water, cm^2/s

362

CHANNEL A: WATER 24 C

Q (GM/S)	H (CM OF WATER)
3.620	18.33
3.520	17.58
3.470	16.83
3.230	14.35
2.710	11.11
2.250	7.26
3.360	15.47
2.660	9.37
2.230	7.07
1.850	4.90
1.450	2.91
2.990	11.86

CHANNEL C: WATER, 24 C

Q (GM/S)	H (CM OF WATER)
2.880	8.83
2.510	7.09
2.300	5.60
1.410	2.37
1.040	1.37

CHANNEL D: WATER, 24 C

Q (GM/S)	H (CM OF WATER)
0.524	1.17
0.640	1.60
0.814	2.72
0.790	2.39
0.763	2.30
0.800	2.62
0.575	1.33
0.662	1.81
0.490	1.01
1.462	8.21
1.077	4.62
1.975	14.55
1.923	14.26
1.567	9.61
1.617	9.93
1.244	5.78
1.839	13.07
1.568	9.46
1.221	5.95
2.502	23.07
2.260	18.68
3.036	34.27
3.421	43.43
3.988	59.20
2.406	21.95
2.366	20.38
2.673	26.96
3.038	34.67
4.134	62.32

CHANNEL G: WATER, 24 C

Q (GM/S)	H (CM OF WATER)
2.230	5.24
2.140	4.79
1.860	3.73
1.590	2.69
1.250	1.71

CHANNEL H: WATER, 24 C

Q (GM/S)	H (CM OF WATER)
1.880	1.81
2.570	3.42
3.320	5.62
4.220	9.06
5.910	18.30
5.170	13.91
3.440	6.30
2.830	4.06
1.800	1.71

Channel D: Water flow, 24 $^{\circ}$C

Flow rate	Pressure head over entire length of channel
(gm/s)	(cm of water)
2.549	129.
2.117	100.
1.783	70.
1.426	50.
1.107	30.
.867	20.5
.751	15.

Channel A
20 ppm Separan AP-273
1% master solution, 10 rps mixing
Reynolds number = 14000

RT = .157 cm   THETA = 29.5 degrees
TEMP = 24 deg. C   NU = 0.0090 sq. cm per sec

Q	H	HW	DH
(gm/s)	(cm)	(cm)	(cm)
1.310	2.18	2.47	.29
1.134	1.70	1.87	.17
.912	1.24	1.23	.00
.787	.92	.92	.00
.670	.68	.68	.00
.562	.50	.48	-.02
.496	.38	.38	.00
.457	.32	.33	.00
.356	.20	.20	.00
.209	.06	.07	.00
.171	.01	.05	.04
2.917	4.45	11.76	7.31
2.610	3.55	9.46	5.91
2.063	2.56	5.98	3.42

Channel C
20 ppm Separan AP-273
1% master solution, 10 rps mixing
Reynolds number = 14000

RT = .169 cm   THETA = 29 degrees
TEMP = 24 deg. C   NU = 0.0090 sq. cm per sec

Q	H	HW	DH
(gm/s)	(cm)	(cm)	(cm)
1.780	2.64	3.59	.95
1.294	1.64	1.93	.29
1.173	1.48	1.60	.12
1.039	1.21	1.26	.05
.864	.91	.89	-.02
.767	.68	.70	.02
1.465	2.07	2.46	.39
3.670	8.54	14.72	6.18
3.169	6.69	11.05	4.36
2.394	3.70	6.39	2.69

Channel D
20 ppm Separan AP-273
1% master solution, 10 rps mixing
Reynolds number = 14000

RT = .1224 cm   THETA = 29 degrees
TEMP = 24 deg. C   NU = 0.0090 sq. cm per sec

Q	H	HW	DH
(gm/s)	(cm)	(cm)	(cm)
2.890	15.56	33.08	17.52
2.320	8.33	21.51	13.18
2.006	4.40	16.19	11.79
1.830	2.88	13.53	10.65
1.587	2.20	10.25	8.05
1.181	1.20	5.77	4.57
.737	.99	2.32	1.33
.615	1.03	1.64	.61
.509	.81	1.14	.33

Channel G
20 ppm Separan AP-273
1% master solution, 10 rps mixing
Reynolds number = 14000

RT = .114 cm   THETA = 44 degrees
TEMP = 24 deg. C   NU = 0.0090 sq. cm per sec

Q	H	HW	DH
(gm/s)	(cm)	(cm)	(cm)
3.030	5.26	9.57	4.31
3.630	7.87	13.65	5.78
2.070	2.60	4.53	1.93
2.440	3.51	6.25	2.74
1.550	1.76	2.57	.81
1.150	1.27	1.44	.17
.782	.74	.68	-.06
.521	.35	.31	-.04
.422	.23	.20	-.03
.870	.91	.83	-.08

Channel G
20 ppm Separan AP-273
1% master solution, 10 rps mixing
Reynolds number = 8000

RT = .114 cm   THETA = 44 degrees
TEMP = 24 deg. C   NU = 0.0090 sq. cm per sec

Q	H	HW	DH
(gm/s)	(cm)	(cm)	(cm)
2.340	3.51	5.76	2.25
3.700	8.03	14.17	6.14
3.380	6.45	11.86	5.41
2.870	4.75	8.60	3.85
.880	.94	.85	-.09
.670	.53	.50	-.03
.550	.40	.34	-.06
.850	.84	.80	-.04
5.300	18.96	28.77	9.81
4.970	15.54	25.34	9.80
4.600	12.24	21.76	9.52

Channel H
20 ppm Separan AP-273
1% master solution, 10 rps mixing
Reynolds number = 8000

RT = .136 cm   THETA = 44 degrees
TEMP = 24 deg. C   NU = 0.0090 sq. cm per sec

Q	H	HW	DH
(gm/s)	(cm)	(cm)	(cm)
5.790	14.42	16.99	2.57
6.880	19.54	23.88	4.34
3.390	5.22	5.92	.70
1.760	1.65	1.64	.00
1.420	1.09	1.08	.00
.960	.51	.50	.00
.640	.22	.23	.00
1.130	.69	.69	.00
2.450	2.97	3.13	.16
3.480	5.39	6.24	.85
4.330	8.14	9.58	1.44

Channel G
20 ppm Separan AP-273
1% master solution, 10 rps mixing
Reynolds number = 11000

RT = .114 cm   THETA = 44 degrees
TEMP = 24 deg. C   NU = 0.0090 sq. cm per sec

Q	H	HW	DH
(gm/s)	(cm)	(cm)	(cm)
3.080	6.11	9.88	3.77
3.660	8.59	13.87	5.28
1.500	1.65	2.41	.76
.917	.90	.92	.02
.633	.45	.45	.00

Channel A
45 ppm Separan AP-273
1% master solution, 10 rps mixing
Reynolds number = 8000

RT = .157 cm   THETA = 29.5 degrees
TEMP = 24 deg. C   NU = 0.0090 sq. cm per sec

Q	H	HW	DH
(gm/s)	(cm)	(cm)	(cm)
3.983	6.90	21.64	14.74
4.743	7.60	30.50	22.90
5.785	11.02	45.08	34.06
6.618	17.02	58.75	41.73
5.756	10.02	44.63	34.61
5.287	6.70	37.76	31.06
4.698	6.20	29.93	23.73
2.753	2.02	10.50	8.48
1.679	.23	4.00	3.77
1.310	-.04	2.47	2.51
.900	.50	1.20	.70
1.308	-.30	2.47	2.77
2.948	3.60	12.00	8.40
3.465	5.30	16.47	11.17
3.761	5.40	19.34	13.94
4.315	6.10	25.33	19.23

Channel G
45 ppm Separan AP-273
1% master solution, 10 rps mixing
Reynolds number = 8000

RT = .114 cm   THETA = 44 degrees
TEMP = 24 deg. C   NU = 0.0090 sq. cm per sec

Q	H	HW	DH
(gm/s)	(cm)	(cm)	(cm)
.730	.42	.59	.17
1.140	.74	1.41	.67
1.990	1.76	4.19	2.43
2.830	3.28	8.36	5.08
3.293	3.97	11.27	7.30

Channel A
30 ppm Separan AP-273
1% master solution, 10 rps mixing
Reynolds number = 8000

RT = .157 cm   THETA = 29.5 degrees
TEMP = 24 deg. C   NU = 0.0090 sq. cm per sec

Q	H	HW	DH
(gm/s)	(cm)	(cm)	(cm)
1.942	1.44	5.31	3.87
3.893	7.37	20.70	13.33
4.862	12.77	32.02	19.25
5.651	18.73	43.04	24.31
6.384	24.05	54.73	30.68
5.631	16.40	42.74	26.34
4.958	11.00	33.28	22.28
.735	.78	.81	.03
1.071	.93	1.68	.75
2.049	2.35	5.90	3.55
2.691	5.58	10.04	4.46
3.287	8.75	14.85	6.10
3.718	6.97	18.91	11.94
2.551	3.37	9.05	5.68
1.898	1.18	5.08	3.90
2.235	2.51	6.99	4.48
1.764	1.59	4.41	2.82
1.339	1.17	2.58	1.41

1.044	.91	1.59	.68
.635	.67	.61	-.06
.579	.55	.51	-.04
.521	.46	.42	-.04
.435	.31	.30	.00

Channel A
20 ppm Separan AP-273
1% master solution, 10 rps mixing
Reynolds number = 8000

RT = .157 cm   THETA = 29.5 degrees
TEMP = 24 deg. C   NU = 0.0090 sq. cm per sec

Q	H	HW	DH
(gm/s)	(cm)	(cm)	(cm)
1.839	2.70	4.78	2.08
2.996	7.02	12.39	5.37
4.308	14.67	25.25	10.58
4.177	14.17	23.76	9.59
5.470	24.31	40.37	16.06
4.820	18.73	31.48	12.75
4.396	15.18	26.27	11.09
3.630	10.24	18.04	7.80
2.051	3.90	5.91	2.01

Channel D
20 ppm Separan AP-273
1% master solution, 10 rps mixing
Reynolds number = 8000

RT = .1244 cm   THETA = 29 degrees
TEMP = 24 deg. C   NU = 0.0090 sq. cm per sec

Q	H	HW	DH
(gm/s)	(cm)	(cm)	(cm)
.678	1.40	1.85	.45
.996	.92	3.89	2.97
1.252	.66	6.06	5.40
1.661	.77	10.51	9.74
1.923	1.38	13.98	12.60
2.114	2.51	16.82	14.31
2.304	3.21	19.90	16.69
2.458	4.90	22.59	17.69
2.567	7.38	24.59	17.21
1.800	2.93	12.29	9.36
1.555	2.01	9.24	7.23
1.033	1.51	4.18	2.67
.800	1.61	2.55	.94
.501	.96	1.04	.08
.383	.63	.62	.00
.334	.46	.48	.02
.258	.26	.29	.03
.208	.20	.19	.00

.566	1.11	1.31	.20
.652	1.43	1.72	.29
.904	1.14	3.23	2.09
1.103	.75	4.74	3.99
1.272	.961	6.25	5.29
1.632	1.56	10.15	8.59
2.182	3.57	17.90	14.33
2.496	6.23	23.28	17.05
2.816	10.54	29.48	18.94
2.962	14.09	32.55	18.46
3.224	19.62	38.44	18.82
3.471	24.94	44.44	19.50

Channel A
15 ppm Separan AP-273
1% master solution, 10 rps mixing
Reynolds number = 8000

RT = .157 cm   THETA = 29.5 degrees
TEMP = 24 deg. C   NU = 0.0090 sq. cm per sec

Q	H	HW	DH
(gm/s)	(cm)	(cm)	(cm)
1.120	1.90	1.83	-.07
1.170	1.85	1.99	.14
1.430	2.60	2.93	.33
1.800	3.70	4.58	.88
2.070	4.43	6.02	1.59
2.400	5.62	8.03	2.41
2.645	7.12	9.71	2.59
2.930	8.16	11.86	3.70
2.940	8.11	11.94	3.83
4.750	21.16	30.59	9.43
5.160	24.70	36.00	11.30
3.290	10.77	14.88	4.11

Channel G
15 ppm Separan AP-273
1% master solution, 10 rps mixing
Reynolds number = 8000

RT = .114 cm   THETA = 44 degrees
TEMP = 24 deg. C   NU = 0.0090 sq. cm per sec

Q	H	HW	DH
(gm/s)	(cm)	(cm)	(cm)
.870	.84	.83	.00
1.160	1.46	1.46	.00
1.880	3.34	3.75	.41
2.600	5.68	7.08	1.40
3.300	7.79	11.31	3.52
3.530	10.21	12.92	2.71

Channel A
15 ppm Separan AP-273
1% master solution, 30 rps mixing
Reynolds number = 8000

RT = .157 cm   THETA = 29.5 degrees
TEMP = 24 deg. C   NU = 0.0090 sq. cm per sec

Q	H	HW	DH
(gm/s)	(cm)	(cm)	(cm)
4.920	24.94	32.78	7.84
2.922	9.31	11.80	2.49
2.606	7.62	9.43	1.81
2.248	5.70	7.07	1.37
1.617	3.31	3.72	.41
3.404	12.04	15.91	3.87
4.489	20.20	27.37	7.17
.642	.53	.63	.10
1.250	2.25	2.26	.00
2.288	5.75	7.32	1.57
1.919	4.34	5.19	.85
1.497	2.99	3.20	.21
1.132	2.01	1.86	-.15
.957	1.31	1.35	.04
.810	.84	.98	.14

Channel A
10 ppm Separan AP-273
1% master solution, 10 rps mixing
Reynolds number = 8000

RT = .157 cm   THETA = 29.5 degrees
TEMP = 24 deg. C   NU = 0.0090 sq. cm per sec

Q	H	HW	DH
(qm/s)	(cm)	(cm)	(cm)
1.307	2.48	2.46	-.02
1.607	3.42	3.68	.26
1.947	4.76	5.34	.58
2.177	5.72	6.64	.92
2.441	7.37	8.30	.93
2.789	9.48	10.77	1.29
3.229	12.06	14.34	2.28
2.907	9.88	11.68	1.80
2.640	8.18	9.67	1.49
2.181	5.85	6.66	.81
3.584	14.98	17.60	2.62
4.599	23.12	28.71	5.59
3.927	17.51	21.05	3.54
1.399	2.60	2.81	.21
1.681	3.60	4.01	.41
1.064	1.64	1.65	.00
.904	1.15	1.21	.06
.718	.74	.78	.04

Channel A
10 ppm Separan AP-273
1% master solution, 30 rps mixing
Reynolds number = 8000

RT = .157 cm   THETA = 29.5 degrees
TEMP = 24 deg. C   NU = 0.0090 sq. cm per sec

Q	H	HW	DH
(gm/s)	(cm)	(cm)	(cm)
1.309	2.25	2.47	.22
1.059	1.51	1.64	.13
1.034	1.47	1.57	.10
.916	1.10	1.24	.14
.792	.85	.94	.09
1.331	2.52	2.55	.03
1.222	2.06	2.16	.10
1.590	3.52	3.60	.08
1.447	3.02	3.00	-.02
1.704	4.11	4.12	.00
1.881	4.66	4.99	.33
2.066	5.65	6.00	.35
2.290	6.72	7.33	.61
2.523	7.80	8.85	1.05
2.772	9.93	10.64	.71
3.079	11.78	13.07	1.29
3.449	14.19	16.32	2.13
3.756	16.78	19.29	2.51

4.067	19.67	22.55	2.88
4.328	21.24	25.48	4.24
4.600	25.40	28.72	3.32

Channel D
10 ppm Separan AP-273
1% master solution, 10 rps mixing
Reynolds number = 8000

RT = .1244 cm   THETA = 29 degrees
TEMP = 24 deg. C   NU = 0.0090 sq. cm per sec

Q	H	HW	DH
(gm/s)	(cm)	(cm)	(cm)
2.320	16.96	20.18	3.22
2.717	24.13	27.49	3.36
1.889	11.17	13.50	2.33
1.253	5.34	6.07	.73
1.616	8.56	9.96	1.40
2.152	14.27	17.42	3.15
2.586	20.71	24.95	4.24
.844	2.68	2.83	.15
1.042	4.00	4.25	.25
1.261	5.39	6.15	.76
.888	2.89	3.12	.23
.664	1.66	1.78	.12
.508	1.06	1.07	.00
.789	2.41	2.48	.07
.752	2.16	2.26	.10
.681	1.81	1.87	.06
.378	.62	.61	.00

Channel D
5 ppm Separan AP-273
0.2% master solution, 10 rps mixing
Reynolds number = 8000

RT = .1244 cm   THETA = 29 degrees
TEMP = 23 deg. C   NU = 0.0093 sq. cm per sec

Q	H	HW	DH
(gm/s)	(cm)	(cm)	(cm)
1.043	3.65	4.26	.61
.881	2.90	3.08	.18
1.170	4.66	5.32	.66
.936	3.14	3.46	.32
.748	2.22	2.24	.02
.628	1.51	1.60	.09
.813	2.58	2.63	.05
.585	1.30	1.40	.10
.450	.79	.85	.06
1.095	4.16	4.68	.52
1.303	5.45	6.56	1.11
1.510	7.18	8.74	1.56
1.681	8.77	10.77	2.00
1.913	10.92	13.86	2.94
2.173	14.06	17.77	3.71
2.404	17.54	21.65	4.11
2.688	22.00	26.94	4.94
.884	2.81	3.10	.29

.660	1.67	1.76	.09
.518	1.12	1.11	.00
.469	.83	.92	.09
.246	.24	.27	.03
1.209	4.81	5.67	.86
2.298	16.08	19.82	3.74
3.060	29.41	34.73	5.32
3.584	40.78	47.36	6.58
4.067	53.56	60.72	7.16
4.453	67.96	72.57	4.61
4.575	71.61	76.54	4.93

Channel D
5 ppm Separan AP-273
0.2% master solution, 30 rps mixing
Reynolds number = 8000

RT = .1244 cm   THETA = 29 degrees
TEMP = 23 deg. C   NU = 0.0093 sq. cm per sec

Q	H	HW	DH
(gm/s)	(cm)	(cm)	(cm)
1.198	5.09	5.57	.48
1.1884	11.50	5.49	-6.01
2.345	17.53	20.62	3.09
3.124	31.62	36.17	4.55
3.624	42.74	48.40	5.66
4.121	56.15	62.31	6.16
4.261	61.56	66.54	4.98
4.512	68.87	74.48	5.61
1.116	4.56	4.86	.30
1.596	8.22	9.73	1.51
1.476	7.46	8.36	.90
1.368	6.28	7.21	.93
1.154	4.78	5.18	.40
1.036	3.95	4.21	.26
.844	2.70	2.83	.13
.888	2.96	3.12	.16
.706	1.95	2.01	.06
.582	1.29	1.39	.10

.423	.77	.75	-.02
.325	.47	.46	.00
.224	.22	.22	.00

Channel D
5 ppm Separan AP-273
1% master solution, 30 rps mixing
Reynolds number = 8000

RT = .1244 cm   THETA = 29 degrees
TEMP = 25 deg. C   NU = 0.0089 sq. cm per sec

Q	H	HW	DH
(gm/s)	(cm)	(cm)	(cm)
.646	1.67	1.69	.02
.805	2.46	2.58	.12
.736	2.04	2.17	.13
.578	1.31	1.36	.05
.770	2.33	2.36	.03
.993	3.78	3.86	.08
1.267	5.60	6.20	.60
1.600	8.48	9.76	1.28
1.185	5.06	5.44	.38
1.005	4.10	3.96	-.14
.845	2.76	2.83	.07
1.277	5.93	6.29	.36
1.541	8.23	9.07	.84
1.764	10.18	11.80	1.62
1.926	12.30	14.01	1.71
2.255	16.10	19.07	2.97
2.667	21.60	26.48	4.88
2.435	19.00	22.16	3.16
2.193	15.80	18.05	2.25
2.039	13.70	15.66	1.96

Channel D
2 ppm Separan AP-273
0.2% master solution, 10 rps mixing
Reynolds number = 8000

RT = .1244 cm   THETA = 29 degrees
TEMP = 23 deg. C   NU = 0.0093 sq. cm per sec

Q	H	HW	DH
(gm/s)	(cm)	(cm)	(cm)
1.287	6.50	6.41	-.09
1.420	7.66	7.75	.09
1.619	9.76	10.01	.25
1.381	7.31	7.35	.04
1.184	5.47	5.45	-.02
.959	3.73	3.62	-.11
.739	2.16	2.19	.03
1.478	8.32	8.38	.06
1.735	11.18	11.45	.27
1.922	13.68	13.98	.30
2.275	18.81	19.44	.63
2.047	15.47	15.81	.34
2.078	15.83	16.28	.45
1.801	12.04	12.32	.28
2.710	26.21	27.37	1.16
2.502	22.71	23.41	.70
3.443	41.60	43.77	2.17
3.719	47.39	50.93	3.54

3.933	55.31	56.85	1.54
4.268	64.60	66.76	2.16
4.516	73.36	74.61	1.25
2.746	27.28	28.09	.81
2.463	21.80	22.70	.90
3.152	35.43	36.81	1.38
3.530	44.50	45.97	1.47

Channel D
1 ppm Separan AP-273
0.2% master solution, 10 rps mixing
Reynolds number = 8000

RT = .1244 cm   THETA = 29 degrees
TEMP = 22 deg. C   NU = 0.0095 sq. cm per sec

Q	H	HW	DH
(gm/s)	(cm)	(cm)	(cm)
3.286	39.27	39.97	.70
2.884	30.38	30.95	.57
2.370	20.78	21.08	.30
1.944	14.28	14.31	.03
2.113	16.72	16.84	.12
3.596	46.78	47.71	.93
4.195	63.69	64.58	.89
4.523	74.34	74.89	.55
4.324	67.96	68.54	.58
3.936	56.26	56.97	.71
2.630	25.33	25.84	.51

Channel D
20 ppm Separan AP-30
1% master solution, 10 rps mixing
Reynolds number = 8000

RT = .1244 cm   THETA = 29 degrees
TEMP = 21 deg. C   NU = 0.0097 sq. cm per sec

Q	H	HW	DH
(gm/s)	(cm)	(cm)	(cm)
3.887	49.45	55.65	6.20
2.443	19.21	22.39	3.18
2.017	13.19	15.40	2.21
3.164	32.42	37.16	4.74
4.627	73.14	78.39	5.25
1.789	10.62	12.19	1.57
1.496	7.46	8.61	1.15
1.130	4.54	4.99	.45
.749	2.12	2.26	.14
.877	2.83	3.06	.23
.591	1.42	1.43	.00
.372	.58	.59	.00
.260	.30	.30	.00

Channel D
10 ppm Separan AP-30
1% master solution, 10 rps mixing
Reynolds number = 8000

RT = .1244 cm   THETA = 29 degrees
TEMP = 21 deg. C   NU = 0.0097 sq. cm per sec

Q	H	HW	DH
(gm/s)	(cm)	(cm)	(cm)
2.301	18.70	19.92	1.22
1.570	9.17	9.45	.28
1.259	6.05	6.16	.11
1.006	3.87	3.99	.12
.702	2.09	1.99	-.10
1.199	5.49	5.60	.11
1.909	12.95	13.84	.89
2.633	24.33	25.93	1.60
.872	2.94	3.03	.09
.727	2.19	2.13	-.06
.956	3.66	3.62	-.04
1.160	5.13	5.25	.12
1.602	9.48	9.83	.35
1.903	12.97	13.75	.78
2.165	16.60	17.69	1.09
3.603	46.01	47.95	1.94
4.268	64.15	66.88	2.73
4.521	72.53	74.90	2.37

Channel D
5 ppm Separan AP-30
1% master solution, 10 rps mixing
Reynolds number = 8000

RT = .1244 cm   THETA = 29 degrees
TEMP = 21 deg. C   NU = 0.0097 sq. cm per sec

Q	H	HW	DH
(gm/s)	(cm)	(cm)	(cm)
3.990	58.13	58.58	.45
4.331	68.49	68.83	.34
3.657	48.69	49.37	.68
3.292	39.62	40.16	.54
2.929	31.32	31.94	.62
2.364	20.50	21.00	.50
4.277	66.36	67.15	.79
2.695	26.78	27.14	.36
2.344	20.28	20.65	.37
1.948	14.26	14.39	.13
1.427	7.77	7.85	.08
1.058	4.44	4.40	-.04
.806	2.67	2.60	-.07
1.329	6.82	6.84	.02
1.783	11.98	12.11	.13
2.154	17.50	17.51	.00
1.675	10.60	10.72	.12
1.232	5.82	5.91	.09
2.229	18.42	18.72	.30

Channel D
30 ppm WSR-301
1% master solution, 10 rps mixing
Reynolds number = 8000

RT = .1244 cm   THETA = 29 degrees
TEMP = 21 deg. C   NU = 0.0097 sq. cm per sec

Q	H	HW	DH
(gm/s)	(cm)	(cm)	(cm)
4.232	69.25	65.77	-3.48
3.972	60.72	58.07	-2.65
3.679	53.64	49.95	-3.69
3.266	43.28	39.54	-3.74
2.814	33.60	29.53	-4.07
2.653	29.17	26.32	-2.85
3.998	61.71	58.82	-2.89
.982	3.79	3.81	.02
.771	2.38	2.39	.00
.632	1.58	1.63	.05

Channel D
30 ppm Polyox WSR-301
1% master solution, 10 rps mixing
Reynolds number = 8000

RT = .1244 cm   THETA = 29 degrees
TEMP = 21 deg. C   NU = 0.0097 sq. cm per sec

Q	H	HW	DH
(gm/s)	(cm)	(cm)	(cm)
1.743	12.28	11.59	-.69
2.567	27.43	24.67	-2.76
3.154	40.31	36.93	-3.38
3.667	54.02	49.63	-4.39
4.206	69.10	64.98	-4.12
1.389	7.78	7.45	-.33
1.940	16.31	14.28	-2.03
2.202	21.87	18.28	-3.59
2.704	31.93	27.31	-4.62
3.368	46.63	42.00	-4.63
3.857	59.43	54.81	-4.62
4.209	70.32	65.07	-5.25
.814	2.58	2.65	.07
1.113	4.86	4.85	.00
1.494	8.93	8.59	-.34
1.976	16.50	14.80	-1.70
2.352	23.68	20.79	-2.89
1.625	10.66	10.11	-.55

1.789	13.13	12.19	-.94
2.156	19.74	17.54	-2.20
2.518	26.50	23.76	-2.74
2.873	33.53	30.76	-2.77

Channel D
20 ppm Polyox WSR-301
1% master solution, 10 rps mixing
Reynolds number = 8000

RT = .1244 cm   THETA = 29 degrees
TEMP = 21 deg. C   NU = 0.0097 sq. cm per sec

Q	H	HW	DH
(gm/s)	(cm)	(cm)	(cm)
3.478	46.10	44.74	-1.36
3.758	53.86	52.08	-1.78
3.953	59.96	57.52	-2.44
4.138	66.43	62.93	-3.50
4.386	73.36	70.56	-2.80
3.120	36.73	36.15	-.58
2.809	29.75	29.43	-.32
3.168	37.65	37.25	-.40
3.167	37.64	37.23	-.41
3.293	41.22	40.19	-1.03

Total Pressure Drop Experiment Measurements

20 ppm Separan AP-273
1% master solution, 20 rps mixing
Reynolds number = 14,000

RT = .1244 cm   THETA = 29 degrees
TEMP = 24 deg. C   NU = 0.0090 sq. cm per sec

Q	H	HW	DH	TH	TW	DT
(gm/s)	(cm)	(cm)	(cm)	(cm)	(cm)	(cm)
2.383	13.13	21.26	8.13	148	118	30
1.915	8.95	13.87	4.92	100	80	20
1.573	6.09	9.45	3.36	70	57	13
.860	2.31	2.93	.62	20	19.5	0.5

TH   is the total pressure head over the entire
     length of the channel for polymer solution flow,
     in cm of water,

TW   is the pressure head over the entire length of
     the channel for water flow, in cm of water

DT   is the difference in these values, DT = TH - TW,
     in cm of water

Q, H, HW, DH, RT, THETA, TEMP, and NU as defined
previously in this appendix.

APPENDIX H
DETERMINATION OF LINES OF ACTION
OF NORMAL STRESS DIFFERENCES

According to eq. (6.11b), the normal stress differences are three times the difference in the pressure head between polymer solution and water flows (at the same flow rates). The lines of action of these normal stress differences have been estimated by using the relation

$$r_N = \frac{\int r(h_w - h_p)dS}{\int (h_w - h_p)dS} \tag{H.1}$$

where r_N is the radial distance associated with these lines of action, r is distance from the vertex of the conical channel, h_w is the pressure head at the downstream tap for water flow, h_p is the pressure head at the downstream tap for polymer solution flow, and S represents the cross sectional area of the downstream pressure tap.

Since the pressure head difference $(h_w - h_p)$ as a function of r is initially unknown, an iterative process has been used to evaluate eq. (H.1). First, an initial value for r_N was assumed (the value for r_p being

403

used). Then, the measured pressure head differences were plotted as a function of extensional strain rate (with these strain rates being determined by eq. (6.6) using the assumed r_N value). By using a linear least squares fit, the pressure head difference as a function of strain rate (and hence, also as a function of Q and r) was estimated. This estimate was substituted into eq. (H.1) for numerical evaluation at the given flow rate to provide an improved estimate for r_N. This process was repeated until the values for r_N remained the same (to within 0.001 cm). Estimates for r_N were determined over the whole range of measured flow rates (0.5 to 5 cm^3/s).

In Fig. H.1, the resulting values of r_N are presented as a function of flow rate for measurements made with a 20 ppm Separan AP-273 solution (1% master solution, 10 rps mixing) for flow through channel D. The dashed lines in this figure represent the radial distances at the upstream (r_2) and downstream (r_1) edges of the pressure tap. Notice that as the flow rate is increased, r_N approaches a nearly constant value of about 0.119 cm, a distance being about 3% less than that for the center location of the pressure tap (or about 15% less than r_p). Similar values were obtained also for channel G (for a similar solution), with r_N being 15% less than r_p.
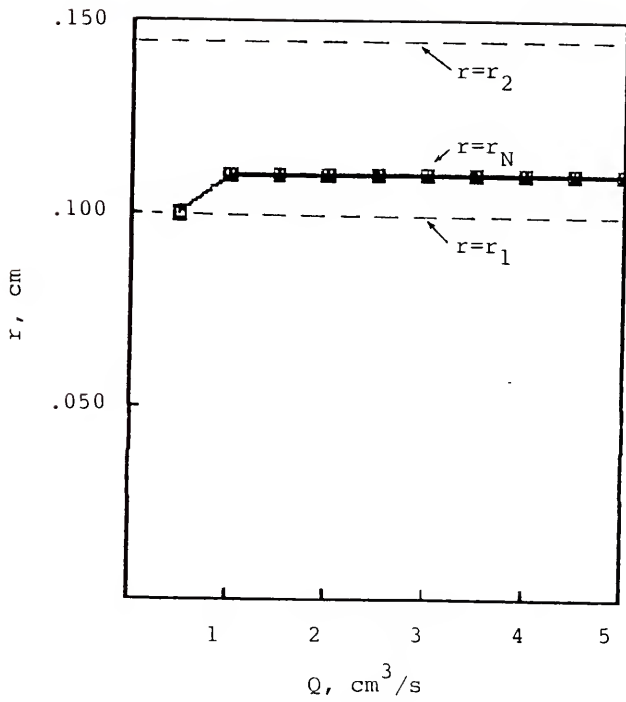
Fig. H.1.   Variation of r_N with flow rate, Q, for flow of a 20 ppm Separan AP-273 solution through channel D (1% master solution, 10 rps mixing, flow at a Reynolds number of 14,000 in the main experiment pipe, 24°C).

First normal stress differences are presented in
Fig. H.2 as a function of the extensional strain rate for
data for the flow the 20 ppm Separan AP-273 solution
through channel D, where the strain rates have been
calculated using r_N-values recorded in Fig. H.1 and
also for a constant r value of $r=0.85r_p$. Additionally,
the pressure head differences are plotted in the same
figure as a function of the extensional strain rate at
the center of the downstream pressure tap. Fig. H.2
illustrates that the variations in strain rate (between
the three sets of data) may attain values of about 10% at
any given pressure head difference.

The extensional strain rates for flows of the
Separan solutions presented in Figs. 6.4-6.12 have been
determined by using a constant r-value ($r=0.85r_p$) for
each channel. Table 6.3 contains a listing of these r-
values (labeled as $r=r_N$) for each channel.
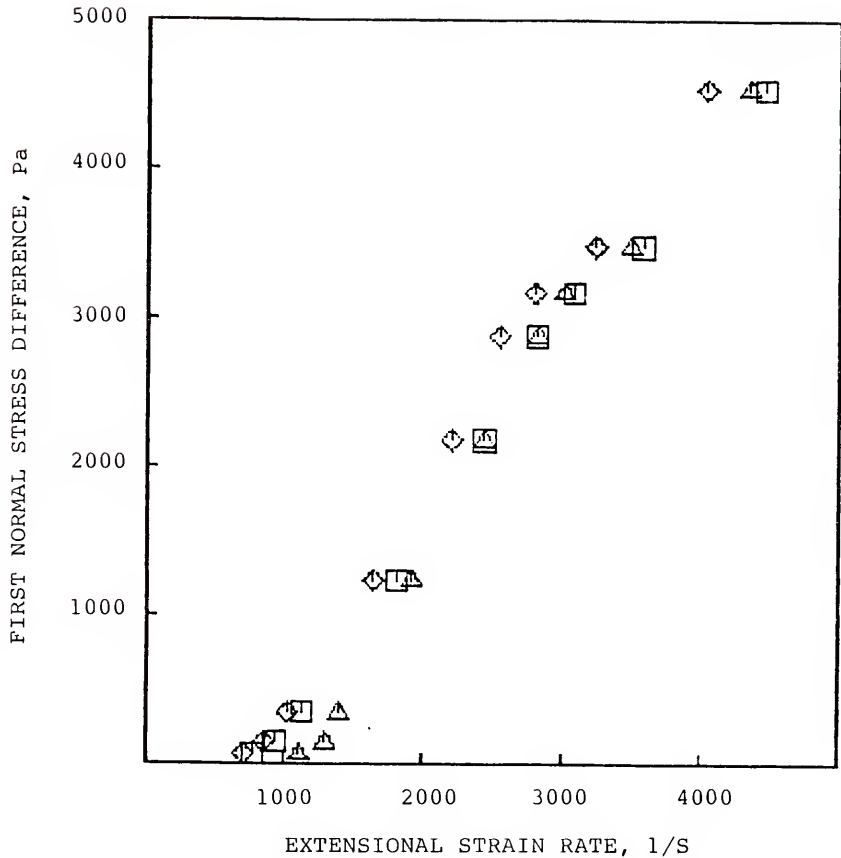
Fig. H.2.   First normal stress difference as a function of extensional strain rate, for strain rates calculated using $r=r_N$ as recorded in Fig. H.1 ($\triangle$), using $r=0.85r_p=.118$ cm ($\square$), and using the $r=r_m=.122$ cm ($\diamondsuit$), for flow of a 20 ppm Separan AP-273 solution through channel D (1% master solution, 10 rps mixing, flow at a Reynolds number of 14,000 in the main experiment pipe, 24°C).

BIBLIOGRAPHY

Acierno, D., J.N. Dalton, J.M. Rodriguez, and J.L. White, *J. Appl. Poly. Sci.*, 15, 2395 (1971).

Achia, B.U., and D.W. Thompson, *Proc. Int. Conf. Drag Reduction*, St. John's College, Cambridge, England, A2 (1974).

Agoston, G.A., W.H. Harte, H.C. Hottel, W.A. Klemm, K.J. Mysels, H.H. Pomeroy, and J. M Thompson, *Ind. Eng. Chem.*, 46, 1017 (1954).

Astarita, G., and L. Nicodemo, *Chem. Eng. J.*, 1, 57 (1970).

Balakrishnan, C., Ph.D. Dissertation, University of Florida, Gainesville, Florida (1976).

Banijamali, S., E.W. Merrill, K.A. Smith, and L.H. Peebles Jr., *AIChE J.*, 20, 824 (1974).

Bate, H.G., *Nature*, 216, 1100 (1967).

Berman, N.S., *Phys. Fluids*, 20, 715 (1977a).

Berman, N.S., *Phys. Fluids*, 20, S168 (1977b).

Berman, N.S., *Ann. Rev. Fluid Mech.*, 10, 47 (1978).

Berman, N.S., *Polym. Eng. Sci.*, 20, 451 (1980).

Bilgen, E., and P. Vasseur, *2nd Int Conf. Drag Reduction*, St. John's College, Cambridge, England, B4 (1977).

Bird, R.B., O. Hassager, and S.I. Abdel-Khalik, *AIChE J.*, 20, 1041 (1974).

Brennen, C., and G.E. Gadd, *Nature*, 215, 1368 (1967).

Bryson, A.W., V.R. Arunchalam, and G.D. Fulford, *J. Fluid Mech.*, 47, 209 (1971).

Burger, E.D., W.R. Munk, and H.A. Wahl, *J. Pet. Tech.*, 34, 377 (1982).

Cantwell, B.J., *Ann. Rev. Fluid Mech.*, 13, 457 (1981).

Chao, K.K., C.A. Child, E.A. Grens II, and M.C. Williams, AIChE J., 30, 111 (1984).

Chang, H.D., and R. Darby, J. Rheol., 27, 77 (1983).

Chang, H., and A.S. Lodge, Rheol. Acta, 10, 448 (1971).

Cogswell, F.N., J. Non-Newt. Fluid Mech., 4, 23 (1978).

Coleman, B.D., Proc. Roy. Soc., A306, 449 (1968).

Cressely, R., and R. Hocquart, VIII Int. Congress on Rheology, 2, 377 (1980).

Crowley, D.G., F.C. Frank, M.R. Mackley, and R.G. Stephenson, J. Polym. Sci. Polym. Physics Ed., 14, 1111 (1976).

Daily, J.W., and D.F. Harleman, Fluid Dynamics, Addison-Wesley, Reading, Mass. (1973).

Darby, R., Trans. Soc. Rheol., 14, 185 (1970).

Darby, R., Viscoelastic Fluids, Marcel Dekker, New York, N.Y. (1976).

Davies, G.A., and A.B. Ponter, Nature, 212, 66 (1966).

Dealy, J.M., Polym. Eng. Sci., 11, 433 (1971).

Dealy, J.M., J. Non-Newt. Fluid Mech., 4, 9 (1978).

Dodge, D.W., and A.B. Metzner, AIChE J., 5, 189 (1959).

Donohue, G.L., W.G. Tiederman, and M.M. Reischman, J. Fluid Mech., 56, 559 (1972).

Dow Chemical Co., Separan Polymers Settle Process Problems, Designed Products Dept., Midlands, Michigan (1975).

Dunlop, E.H., and L.R. Cox, Phys. Fluids, 20, S203 (1977).

duPlessis, M.P., and M. Hashish, Trans. ASME, J. Engineering for Industry, 100, 452 (1978).

Eckelman, L.D., G. Fortuna, and T.J. Hanratty, Nature Physical Science, 236, 94 (1972).

Elata, C., J. Lehrer, and A. Kahanovitz, Israel J. Tech., 4, 87 (1966).

Fabula, A.G., Trans. ASME, J. Basic Engineering, 93, 453 (1971).

Fabula, A.G., J.L. Lumley, and W. D. Taylor, in Modern Developments in the Mechanics of Continua, Academic Press, N.Y., 145 (1966).

Falco, R.E., and D.C. Wiggert, Progress in Astronautics and Aeronautics, 72, 275 (1980).

Farber, R., and J.M. Dealy, Polym. Eng. Sci., 14, 435 (1974).

Frank, F.C., A. Keller, M.R. Mackley, Polymer, 12 467 (1971).

Frank, F.C., and M.R. Mackley, J. Polym. Sci. Polym. Physics Ed., 14 1121 (1976).

Fruman, D.H., and M. Barigah, Rheol. Acta, 21, 556 (1982).

Gadd, G.E., Nature, 212, 1348 (1966).

Giles, W.B., Nature, 224, 584 (1969).

Gordon, R.J., C. Balakrishnan, and S. Pahwa, AIChE Symp. Ser. No. 130, 69, 33 (1973).

Granville, P.S., Departmental Report, David W. Taylor Naval Ship Research and Development Center, Bethesda, Md. SPD-569-04 (1976).

Granville, P.S., Departmental Report, David W. Taylor Naval Ship Research and Development Center, Bethesda, Md., 79-SPD-596-06 (1979).

Granville, P.S., Departmental Report, David W. Taylor Naval Ship Research and Development Center, Bethesda, Md., 80-SPD-569-07 (1980).

Granville, P.S., Departmental Report, David W. Taylor Naval Ship Research and Development Center, Bethesda, Md., 81-SPD-569-08 (1981).

Greene, H.L., R.F. Mostardi, and R.F. Nokes, Polymer Eng. Sci., 20, 7, 499 (1980).

Gupta, R.K., A.B. Metzner, and K.F. Wishbrun, Polym. Eng. Sci., 22, 172 (1982).

Hasegawa, T., Bulletin of JSME, 22, 54 (1978).

Han, C.D., and J.Y. Park, J. Appl. Polym. Sci., 19, 3257 (1975).

Hershey, H.C., and J.L. Zakin, Ind. Eng. Chem. Fundam., 6, 381 (1967).

Higashitani, K., and A.S. Lodge, Trans. Soc. Rheol., 19, 307 (1975).

Hinch, E.J., and C. Elata, J. Non-Newt. Fluid Mech., 5, 411 (1979).

Hoyt, J.W., Trans. ASME, J. Basic Engineering, 94, 258 (1972).

Hoyt, J.W., NUC TP433, Naval Undersea Center, San Diego, Ca (1974).

Hoyt, J.W., 2nd Int. Conf. Drag Reduction, St. John's College, Cambridge, England, Al (1977).

Hunston, D.L., and M.M. Reischman, Phys. Fluids, 18, 1626 (1975).

Inge, C., A.V. Johansson, and E.R. Lindgren, Phys. Fluids, 22, 824 (1979).

James, D.F., and J.H. Saringer, J. Fluid Mech., 97, 655 (1980).

James, D.F., and J.H. Saringer, J. Rheol., 26, 321 (1982).

Kim, O.K., R.C. Little, and R.Y. Ting, AIChE Symp. Ser., No. 130, 69, 39 (1973).

Lagerstedt, T., TRITA-MEK-79-03, Royal Institute of Technology, Dept. of Mechanics, Stockholm, Sweden (1979).

Leal, L.G., G.G. Fuller, and W.L. Olbricht, Progress in Astronautics and Aeronautics, 72, 351 (1980).

Lindgren, E.R., Ark. Fys., 12, (1957).

Little, R.C., R.J. Hansen, D.L. Hunston, O.K. Kim, R.L. Patterson, and R.Y. Ting, Ind. Eng. Chem. Fundam., 14, 283 (1975).

Lodge, A.S., Elastic Liquids, Academic Press, New York, N.Y. (1964).

Lumley, J.L., Ann. Rev. Fluid Mech., 1, 367 (1969).

Lumley, J.L., J. Polymer Sci.: Macromolecular Reviews, 7, 263 (1973).

Lyazid A., O. Scrivener, and R. Tietgen, VIII Int. Congress on Rheology, 2, 141 (1980).

Mackley, M.R., J. Non-Newt. Fluid Mech., 4, 111 (1978).

Mackley, M.R., and A. Keller, Polymer, 14 16 (1973).

Marrucci, G., and R.E. Murch, Ind. Eng. Chem. Fundam., 9, 498 (1970).

Melton, L.L., and W.T. Malone, Soc. Petr. Eng. J., 4, 56 (1964).

Merrill, E.W., K.A. Smith, H. Shin, and H.S. Mickley, Trans. Soc. Rheol., 10, 335 (1966).

Metzner, A.B., and G. Astarita, AIChE J., 13, 550 (1967).

Metzner, A.B., and A.P. Metzner, Rheol. Acta, 9, 174 (1970).

Metzner, A.B., and M. G. Park, J. Fluid Mech., 20, 291 (1964).

Metzner, A.B., E.A. Uebler, and C.F. Chan Man Fong, AIChE J., 15, 750 (1969).

Mewis, J., and A.B. Metzner, J. Fluid Mech., 62, 593 (1974).

Middleman, S., and H. Munstedt, J. Rheol., 25, 29 (1982).

Mizushina, T., and H. Usui, Phys. Fluids, 20, S100 (1977).

Morgan, D.T.G., and K. Pannell, Rheol. Acta, 11, 185 (1972).

Nicodemo, L., B. De Cindio, and L. Nicholas, J. Polym. Sci., 15, 679 (1975).

Oldaker, D.K., and W.G. Tiederman, Phys. Fluids, 20, S133 (1977).

Oldroyd, J.G., Proc. 1st Int. Congress on Rheology (1948), II, 130 North-Holland Publishing Co., Amsterdam (1949)

Oliver, D.R., and R.C. Ashton, J. Non-Newt. Fluid Mech., 1, 93, (1976a).

Oliver, D.R., and R.C. Ashton, J. Non-Newt. Fluid Mech., 2, 367, (1976b).

Oliver, D.R., and R. Bragg, Chem. Eng. J., 5, 1 (1973).

Oliver, D.R., and R. Bragg, Rheol. Acta, 13, 830 (1974).

Ouibrahim, A., 2nd Int. Conf. Drag Reduction, St. John's College, Cambridge, England, F4 (1977).

Parker, C.A., and A.M. Hedley, Nature Physical Science, 236, 136 (1972).

Paterson, R.W., and F.H. Abernathy, J. Fluid Mech., 43, 689 (1970).

Patterson, G.K., and J.L. Zakin, AIChE J., 14, 434 (1968).

Patterson, G.K., J.L. Zakin, and J.M. Rodriguez, Ind. Eng. Chem., 61, 22 (1969).

Pearson, G., and S. Middleman, AIChE J., 23, 714 (1977).

Peng, S.T.J., and R.F. Landel, J. Non-Newt. Fluid Mech., 12, 95 (1983).

Peterlin, A., Pure Appl. Chem., 12, 563 (1966).

Petrie, C.J.S., Elongational Flows, Pitman, London (1979).

Pipkin, A.C., in The Mechanics of Viscoelastic Fluids, ASME, Applied Mechanics Division, 22, 1 (1977).

Pipkin, A.C., and R.I. Tanner, in Mechanics Today, 1, 262 (1972).

Pipkin, A.C., and R.I. Tanner, Ann. Revs. Fluid Mech., 9, 13 (1977).

Powell, R.L., J. Rheol., 27, 177 (1983).

Reiner, M., Deformation and Flow, H.K. Lewis and Co., London (1949).

Reischman, M.M., and W.G. Tiederman, J. Fluid Mech., 70, 369, (1975).

Rodriguez, J.M., J.L. Zakin, and G.K. Patterson, <u>Soc. Petr. Eng. J.</u>, <u>7</u>, 325 (1967).

Rollin, A., and F.A. Seyer, <u>Can. J. Chem. Eng.</u>, <u>50</u>,714 (1972).

Rosenhead, L., <u>Laminar Boundary Layers</u>, Oxford University Press, Oxford, England (1963).

Ruckenstein, E., <u>Chem. Eng. Sci.</u>, <u>26</u>, 1075 (1971).

Ruckenstein, E., <u>J. Appl. Polym. Sci.</u>, <u>17</u>, 3239 (1973).

Savins, J.G., <u>Soc. Petrol. Eng. J.</u>, <u>4</u>, 203 (1964).

Schonblom, J.E., Ph.D. Dissertation, University of Florida, Gainesville, Florida (1974).

Schummer, P., and K.H. Tebel, <u>J. Non-Newt. Fluid Mech.</u>, <u>12</u>, 331 (1983).

Scrivener, O., C. Berner, R. Cressely, R. Hocquart, R. Sellin, and N.S. Vlachos, <u>J. Non-Newt. Fluid Mech.</u>, <u>5</u>, 475 (1979).

Sellin, R.H.J., J.W. Hoyt, and O. Scrivner, <u>J. Hydraulic Res.</u>, <u>20</u>, 29 (1982).

Seyer, F.A., and A.B. Metzner, <u>Can. J. Chem. Eng.</u>, <u>45</u>, 121 (1967).

Shaver, R.G., and E.W. Merrill, <u>AIChE J.</u>, <u>5</u>, 181 (1959).

Stenborg, L.G., T. Lagerstedt, O. Sehlen, and E.R. Lindgren, <u>Phys. Fluids</u>, <u>20</u>, 858 (1977a).

Stenborg, L.G., T. Lagerstedt, and E.R. Lindgren, <u>Phys. Fluids</u>, <u>20</u>, S276 (1977b).

Tanner, R.I., <u>AIChE J.</u>, <u>22</u>, 910 (1976).

Tanner, R.I., and R.R. Huilgol, <u>Rheol. Acta</u>, <u>14</u>, 959 (1975).

Taylor, G.I., <u>Proc. Roy. Soc.</u>, <u>A146</u>, 501 (1934).

Ting, R.Y., <u>J. Appl. Polym. Sci.</u>, <u>16</u>, 3169 (1972).

Ting, R.Y., and D.L. Hunston, <u>J. Appl. Poly. Sci.</u>, <u>21</u>, 1825 (1977).

Tordella, J.P., in _Rheology_, Academic Press, New York, N.Y., _5_, 57 (1969).

Toms, B.A., _Proc. 1st Int. Congress on Rheology (1948)_, North-Holland Publishing Co., Amsterdam, _II_, 135 (1949).

Trouton, F.T., _Proc. Royal Soc._, _A77_, 426 (1906).

Tulin, M.P., _Progress in Astronautics and Aeronautics_, _72_, 327 (1980).

Union Carbide Corp., _Chem. Eng._, _73_ (16), 36 (1966).

Virk, P.S., Sc.D. Thesis, Massachusetts Institute of Technology (1966).

Virk, P.S., _AIChE J._, _21_, 625 (1975).

Virk, P.S., E.W. Merrill, H.S. Mickely, and K.A. Smith, in _Modern Developments in the Mechanics of Continua_, Academic Press, New York, 37 (1966).

White, D.A., _J. Fluid Mech._, _28_, 195 (1967).

Winter, H.H, C.W. Macosko, and K.E. Bennett, _Rheol. Acta_, _18_, 323 (1979).

Zakin, J.L., and D.L. Hunston, _Polym. Eng. Sci._, _20_, 449 (1980a).

Zakin, J.L., and D.L. Hunston, _J. Macromol. Sci.-Phys._, _B18_, 795 (1980b).

BIOGRAPHICAL SKETCH
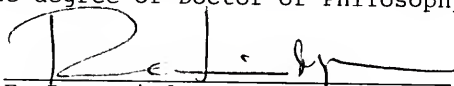
The author was born on March 22, 1952, in Madison, Wisconsin. His educational background includes a Bachelor of Science degree in civil and environmental engineering and a Master of Science degree in ocean engineering, both from the University of Wisconsin at Madison, Wisconsin. He is certified as an Engineer-In-Training, #ET-9071, by the state of Wisconsin and has also passed that state's professional engineers licensing examination.

The author is member of the Florida Alpha chapter of Tau Beta Pi, the national engineering honorary. During his stay at the University of Florida, he was also a winner of a graduate school supplemental scholarship for the 1981-82 academic year.

The author enjoys and has been active in a variety of outdoor and sporting activities. His present interests include basketball, golf, fishing, racquetball, snow skiing, and tennis. He has also received much satisfaction from being an amateur photographer and woodworker.
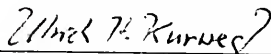
On November, 24, 1984, the author was married to the former Holly Stevens Eberly and has been happily married since.

I certify that I have read this study and that in my opinion it conforms to acceptable standards of scholarly presentation and is fully adequate, in scope and quality, as a dissertation for the degree of Doctor of Philosophy.
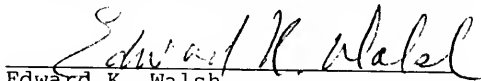
E. Rune Lindgren, Chairman
Professor of Engineering Sciences

I certify that I have read this study and that in my opinion it conforms to acceptable standards of scholarly presentation and is fully adequate, in scope and quality, as a dissertation for the degree of Doctor of Philosophy.

Ulrich H. Kurzweg
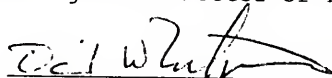Professor of Engineering Sciences

I certify that I have read this study and that in my opinion it conforms to acceptable standards of scholarly presentation and is fully adequate, in scope and quality, as a dissertation for the degree of Doctor of Philosophy.

Edward K. Walsh
Professor of Engineering Sciences

I certify that I have read this study and that in my opinion it conforms to acceptable standards of scholarly presentation and is fully adequate, in scope and quality, as a dissertation for the degree of Doctor of Philosophy.

Thomas T. Bowman
Associate Professor of Mathematics

I certify that I have read this study and that in my opinion it conforms to acceptable standards of scholarly presentation and is fully adequate, in scope and quality, as a dissertation for the degree of Doctor of Philosophy.

David W. Mikolaitis
Assistant Professor of Engineering
Sciences

This dissertation was submitted to the Graduate Faculty of the College of Engineering and to the Graduate Council, and was accepted as partial fulfillment of the requirements for the degree of Doctor of Philosophy.

May, 1985

Dean, College of Engineering

Dean for Graduate Studies and Research